Study on molecular mechanism of anti-diabetic action of *Ficus benghalensis* and *Duranta repens*

Thesis submitted to

KLE ACADEMY OF HIGHER EDUCATION AND RESEARCH
(Deemed-to-be-University)
BELAGAVI

[Declared as Deemed-to-be-University u/s3 of the UGC Act, 1956 vide Govt. of India Notification No. F.9-19/2000-U.3(A)]

Accredited 'A' Grade by NAAC (2nd cycle)
Placed in Category 'A' by MHRD (GoI)
For the award of the degree of

Doctor of Philosophy

In the Faculty of Pharmacy

By

PUKAR KHANAL M. Pharm

(Registration No: KLEU/Ph.D./18-19/DO1218014)

Under the Guidance of

Dr. B. M. Patil Ph. D.

Professor, KLE College of Pharmacy, Belagavi,
KLE Academy of Higher Education and Research, Belagavi – 590010,
Karnataka, India

2022

UNDERTAKING

I, Mr. **Pukar Khanal** hereby declare that the information and the data mentioned in my thesis entitled **"Study on molecular mechanism of anti-diabetic action of *Ficus benghalensis* and *Duranta repens*"** belongs to me and is original.

I am aware of definition of plagiarism as detailed below:

- An act or instance of using or closely imitating the language and thoughts of another author without authorization and the representation of that author's work as one's own, as by not crediting the original author.
- A piece of writing or other work reflecting such unauthorized use or imitation.
- The deliberate or reckless representation of another's words, thoughts or ideas as one's own without attribution in connection with submission of academic work, whether graded or otherwise.

I hereby declare that the thesis prepared by me is original-one and does not involve plagiarism anywhere. In case at a later stage it is found that I have indulged in plagiarism, then I am solely responsible for the same and the Institution is at liberty to take any disciplinary action against me including cancellation of dissertation or any other penalties imposed by the university.

Date:

Place: Belagavi

Mr. Pukar Khanal
Full time Ph.D. Research Scholar
Reg. No.: DO1218014
KAHER, Belagavi-590010

PLAGIARISM REPORT

KLE ACADEMY OF HIGHER EDUCATION AND RESEARCH
(Formerly known as KLE University)
(Deemed-to-be-University established u/s 3 of the UGC Act, 1956)
ಕೆ.ಎಲ್.ಇ. ಎಕ್ಯಾಡಮಿ ಆಫ್ ಹಾಯರ್ ಎಜ್ಯುಕೇಶನ ಆ್ಯಂಡ್ ರಿಸರ್ಚ್
(ಕೆ.ಎಲ್.ಇ. ವಿಶ್ವವಿದ್ಯಾಲಯವೆಂದು ಮುಂಚೆ ಗುರುತಿಸಿದ)
(ವಿ.ಧ.ಆ.ಕಲಂ 3ರಡಿ ಸ್ವಾಯತ್ತ ವಿಶ್ವವಿದ್ಯಾಲಯವೆಂದು ಸ್ಥಾಪಿಸಲ್ಪಟ್ಟಿದೆ)
Accredited 'A' Grade by NAAC (2nd Cycle) Placed in Category 'A' by MHRD (GoI)

Ref. No. KAHER/AA/21-22/D- 04022009 3rd February 2022

Sir,

The soft copy of Ph.D. research thesis of **Mr. Pukar Khanal, Faculty of Pharmacy** of **College of Pharmacy, Belagavi, KAHER**, has been submitted for anti-plagiarism check at the office of the undersigned through "Turn-it-in" package. The scan has been carried out and the scanned output reveals a match percentage of **3%** which is within the acceptable limit of 10%.

To obtain the comprehensive report of the plagiarism test, research scholar can send a mail to **diracademic@kledeemeduniversity.edu.in** along with the Registration Number, Name of the Scholar, Name of Guide/Co-guide and title of the thesis.

DIRECTOR ACADEMIC AFFAIRS Deemed-to-be University

Dr.(Mrs.) Roopa M. Bellad
Director, Academic Affairs

To,
Mr. Pukar Khanal
Full-Time Research Scholar
2018-19 Batch, Faculty of Pharmacy,
College of Pharmacy,
KAHER, **Belagavi**.

Cc to :
1. The Principal, College of Pharmacy, Belagavi
2. Dr. B. M. Patil, Prof., College of Pharmacy, Belagavi - **Guide**

JNMC Campus, Nehru Nagar, Belagavi-590 010, Karnataka, India ☎ 0831-2444444, 0831-2493777 www.kledeemeduniversity.edu.in info@kledeemeduniversity.edu.in

KLE ACADEMY OF HIGHER EDUCATION AND RESEARCH

(Deemed-to-be-University)

[Declared as Deemed-to-be-University u/s3 of the UGC Act, 1956 vide Govt. of India Notification No. F.9-19/2000-U.3(A)]

Accredited 'A' Grade by NAAC (2nd cycle)

Place in Category 'A' by MHRD (GoI)

Copyright Declaration

We hereby declare that KLE ACADEMY OF HIGHER EDUCATION AND RESEARCH (KAHER), BELAGAVI-590010, INDIA shall have the rights to preserve, use and disseminate this thesis in print or electronic format for academic/research purpose.

Mr. Pukar Khanal
Full time Ph.D. Research Scholar
Reg. No: DO1218014
KLE College of Pharmacy Belagavi
KAHER, Belagavi-590010, India.
Place: Belagavi
Date:

Prof. Dr. B. M. Patil
Department of Pharmacology
KLE College of Pharmacy Belagavi
KAHER, Belagavi-590010**,** India.
Place: Belagavi
Date:

KLE ACADEMY OF HIGHER EDUCATION AND RESEARCH

(Deemed-to-be-University)

[Declared as Deemed-to-be-University u/s3 of the UGC Act, 1956 vide Govt. of India Notification No. F.9-19/2000-U.3(A)]

Accredited 'A' Grade by NAAC (2nd cycle)

Place in Category 'A' by MHRD (GoI)

Declaration

I hereby declare that the thesis entitled "Study on molecular mechanism of anti-diabetic action of *Ficus benghalensis* and *Duranta repens*" is a bonafide and original research carried out by me under the guidance of Dr. B. M. Patil, Professor, Department of Pharmacology, KLE College of Pharmacy, Belagavi-590010. The thesis or any part of thereof has not formed the basis for the award of any degree/fellowship or similar title to any candidate of any University.

Pukar Khanal
Full time Ph.D. Research Scholar
Reg. No: DO1218014
KLE College of Pharmacy Belagavi
KAHER, Belagavi-590010
Place: Belagavi
Date:

KLE ACADEMY OF HIGHER EDUCATION AND RESEARCH

(Deemed-to-be-University)

[Declared as Deemed-to-be-University u/s3 of the UGC Act, 1956 vide Govt. of India Notification No. F.9-19/2000-U.3(A)]

Accredited 'A' Grade by NAAC (2nd cycle)

Place in Category 'A' by MHRD (GoI)

Certificate

This is to certify that the thesis entitled "Study on molecular mechanism of anti-diabetic action of *Ficus benghalensis* and *Duranta repens*" is a bonafide record of original research carried out by Mr. Pukar Khanal under the guidance of Dr. B. M. Patil, Professor, Department of Pharmacology, KLE College of Pharmacy, Belagavi-590010, India.

Place: Belagavi
Date:

Prof. Dr. M. S. Ganachari
Dean, Faculty of Pharmacy
KAHER, Belagavi-590010

KLE ACADEMY OF HIGHER EUCATION AND RESEARCH

(Deemed-to-be-University)

[Declared as Deemed-to-be-University u/s3 of the UGC Act, 1956 vide Govt. of India Notification No. F.9-19/2000-U.3(A)]

Accredited 'A' Grade by NAAC (2nd cycle)

Place in Category 'A' by MHRD (GoI)

Certificate

This is to certify that the thesis entitled "Study on molecular mechanism of anti-diabetic action of *Ficus benghalensis* and *Duranta repens*" is a bonafide record of original research carried out by Mr. Pukar Khanal for the award of degree of DOCTOR OF PHILOSOPHY IN FACULTY OF PHARMACY under my supervision and guidance.

Place: Belagavi
Date:

Signature
Prof. Dr. B. M. Patil
Professor, Department of Pharmacology
KLE College of Pharmacy Belagavi,
KAHER, Belagavi-590010, India

KLE ACADEMY OF HIGHER EDUCATION AND RESEARCH

(Deemed-to-be-University)

[Declared as Deemed-to-be-University u/s3 of the UGC Act, 1956 vide Govt. of India Notification No. F.9-19/2000-U.3(A)]

Accredited 'A' Grade by NAAC (2nd cycle)

Place in Category 'A' by MHRD (GoI)

Certificate

This is to certify that the thesis entitled "Study on molecular mechanism of anti-diabetic action of *Ficus benghalensis* and *Duranta repens*" is a bonafide record of original research carried out by Mr. Pukar Khanal under the guidance of Dr. B. M. Patil, Professor, Department of Pharmacology, KLE College of Pharmacy, Belagavi-590010.

Place: Belagavi
Date:

Signature
Prof. Dr. Sunil S. Jalalpure
Principal, KLE College of Pharmacy Belagavi,
KAHER, Belagavi-590010, India

ACKNOWLEDGEMENT

It is with great hat tip that I express my sincere gratitude to my advisor, **Prof. Dr. B. M. Patil**, for the constant support, for his patience, motivation, and immense knowledge during my Ph. D research. Having him as my advisor and mentor during my Ph. D study was a great experience. He guided me throughout the entire research and writing process.

Apart from my advisor, I'd like to thank the rest of my Ph. D committee: **Prof. Dr. P. A. Patil**, **Prof. Dr. Sunil S. Jalalpure**, and **Prof. Dr. Alka Kale**, as well as Prof. **Dr. Roopa Bellad**, Director of Academic Affairs, KAHER, and **Dr. Daksha Dixit** (Former Director of Academic Affairs, KAHER) for their insightful comments and encouragement, as well as the tricky queries that pushed me to widen my research from various perspectives.

In the last three years, I have enjoyed discussions with my colleagues (**Ms. Taaza**, **Ms. Vishakha, Ms. Rohini,** and **Mr. Prarambh**), restless nights as we worked on deadlines, and had many laughs and tears together. For their direct and indirect support in completing this study, I am also grateful to the teaching and non-teaching faculties of KLE College of Pharmacy Belagavi.

Last but not least, I want to thank my family for supporting me both mentally and emotionally during the writing of this thesis and in general.

- Pukar Khanal

ABBREVIATIONS

***ABTS*:** (2,2'-azino-bis(3-ethylbenzothiazoline-6-sulfonic acid)), ***AC50*:** Adsorption coefficient 50, ***ADP*:** Adenosine diphosphate, ***ALT*:** Alanine transaminase, ***ANOVA*:** Analysis of variance, ***AST*:** Aspartate aminotransferase, ***ATP*:** Adenosine triphosphate, ***AUC*:** Area under the curve, ***BA*:** Binding affinity, ***ChEBI*:** Chemical entities of biological interest, ***CI*:** Confidence interval, ***CUPRAC*:** Modified cupric reducing antioxidant capacity, ***Df*:** Degrees of freedom, ***dL*:** Decilitre, ***DLS*:** Druglikeness score, ***DM*:** Diabetes mellitus, ***DNA*:** Deoxyribonucleic acid, ***DPP4*:** Dipeptidyl peptidase-4, ***DPPH*:** 2,2-diphenyl-1-picrylhydrazyl, ***DRE*:** Hydroalcoholic extract of *D. repens*, ***EC50*:** Effective concentration 50, ***EDTA*:** Ethylenediaminetetraacetic acid, ***FBE*:** Hydroalcoholic extract of *F. benghalensis*, ***FBPase*:** Fructose 1,6-bisphosphatase, ***FFA*:** Free fatty acid, ***G6Pase*:** Glucose 6-phosphatase, ***GAD*:** Glutamate decarboxylase, ***GLP*:** Glucagon-like peptide, ***GLUT*:** Glucose transporter, ***GSH*:** Glutathione, ***GSK3B*:** Glycogen synthase kinase 3 beta, ***Hb1Ac*:** Hemoglobin A1C, ***HBR*:** Hydrogen bond residues, ***HDL*:** High-density lipoprotein, ***HLA*:** Human leukocyte antigen, ***HOMA-IR*:** Homeostasis model assessment-estimated insulin resistance, ***HPLC-UV*:** High-performance liquid chromatography-ultraviolet visible, ***IAEC*:** Institutional animal ethics committee, ***IC50*:** Inhibitory concentration 50, ***ICMR-NITM*:** Indian Council of Medical Research-National Institute of Traditional Medicine, ***IR*:** Insulin resistant, ***IRS*:** Insulin receptor substrate, ***ITT*:** Insulin tolerance test, ***KEGG*:** Kyoto encyclopedia of genes and genomes, ***LDH*:** Lactate dehydrogenase, ***LDL*:** Low-density lipoprotein, ***MAP*:** Microtubule-associated protein, ***MDA*:** Malondialdehyde, ***MF*:** Molecular formula, ***mg*:** Milligram, ***mL*:** Milliliter, ***mRNA*:** Messenger ribonucleic acid, ***MW*:** Molecular weight, ***NAD*:** Nicotinamide adenine dinucleotide, ***NAFLD*:** Nonalcoholic fatty liver disease, ***NCBI*:** National center for biotechnology information, ***NHB*:** Number of hydrogen bonds, ***NHBA*:** Number of hydrogen bond acceptor, ***NHBD*:** Number of hydrogen bond donor, ***NO*:** Nitric oxide, ***OECD*:** Organization for economic co-operation and development, ***OGTT*:** Oral glucose tolerance test, ***Pa*:** Pharmacological activity, ***PARP*:** Poly (adp-ribose) polymerase, ***PCIDB*:** Phytochemical interactions DB, ***PFK*:** Phosphofructokinase, ***pH*:** Potential of hydrogen, ***Pi*:** Pharmacological inactivity, ***PI3K*:** Phosphoinositide 3-kinase, ***PPAR*:** Peroxisome proliferator-activated receptors, ***PTEN*:** Phosphatase tensin homolog, ***PTP1B*:** Protein tyrosine phosphatase 1b, ***PTPN22*:** Protein tyrosine phosphatase non-receptor type 22, ***RCSB*:** Research collaboratory for structural bioinformatics, ***rDNA*:** Recombinant deoxyribonucleic acid, ***ROS*:** Reactive oxygen species, ***SD*:** Standard deviation, ***SEM*:** Standard error of the mean, ***SGLT*:** Sodium-glucose co-transporter, ***SIRT1*:** Sirtuin, ***SOD*:** Superoxide dismutase, ***STRING*:** Search tool for the retrieval of interacting genes/proteins, ***SUR1*:** Sulfonylurea receptor 1, ***T1DM*:** Type 1 diabetes mellitus, ***T2DM*:** Type 2 diabetes mellitus, ***TBARS*:** Thiobarbituric acid reactive substances, ***TC*:** Total cholesterol, ***TG*:** Triglycerides, ***TTD*:** Therapeutic target database, ***USA*:** United States of America, ***VLDL*:** Very low-density lipoprotein, ***VNTR*:** Variable number of tandem repeats

ABSTRACT

Background: Although *Ficus benghalensis* and *Duranta repens* have been reported for anti-diabetic properties, their mode of action against diabetes has not been explored yet.

Aim and objectives: The present study aimed to propose the anti-diabetic mode of action of *F. benghalensis* and *D. repens* by integrating system biology tools with experimental pharmacology (*in vitro*, *ex vivo*, and *in vivo*).

Methodology: Reported phytoconstituents of both medicinal plants were predicted for their targets, enriched in STRING; probably regulated pathways were traced concerning KEGG and molecular docking was performed using AutoDock Vina or AutoDock 4 as applicable. Later, the hydroalcoholic extract of both plants was prepared and specified groups of bioactives were fractionated from extract to obtain flavonoid, alkaloid, tannin, saponin, and steroid rich fractions as applicable. Later, each fraction was evaluated to inhibit α-amylase and α-glucosidase, promote glucose uptake, and prevent glucose diffusion including anti-oxidant potency using *in vitro* and *ex vivo* protocols. Later the extract was further evaluated for their anti-hyperglycaemic and anti-hyperinsulinaemic efficacy in streptozocin-nicotinamide-induced diabetes and fructose-induced insulin resistance respectively to assess their role over glycolysis, gluconeogenesis, pancreatic β-cell function, peripheral glucose utilization, and oxidative stress.

Results: Bioactives of *F. benghalensis* and *D. repens* primarily modulated PTP1B protein in which *F. benghalenis* primarily modulated PI3K-Akt, p53, Ca^{2+}, and galactose metabolism pathways whereas *D. repens* regulated insulin signaling pathway. Findings of *in silico*, *in vitro*, *ex vivo* pharmacology revealed that the flavonoids of *F. benghalensis* and *D. repens* were concerned against starch catabolism and glucose utilization. In addition, irrespective of the rest of the fractions, hydroalcoholic extract of *F. benghalensis* and *D. repens* had the highest efficacy to prevent glucose diffusion and also had the highest free radical scavenging and metal chelating efficacy. Also, *in vivo* pharmacology revealed the significant amelioration of the hyperglycemia and hyperinsulinemia after the treatment with extracts at the various significant levels by manipulating the glucose catabolism and anabolism, ameliorating the oxidative stress, promoting the peripheral glucose utilization, and enhancing pancreatic β-cell function.

Conclusion: The anti-diabetic action of *F. benghalensis* could be *via* PTP1B inhibition triggered *via* p53 signaling pathway, upregulated glucose utilization *via* PI3K-Akt signaling pathway, enhanced glucose secretion *via* Ca^{2+} signaling pathway, preventing the starch metabolism in the intestine and ameliorating the hepatic oxidative stress. Similarly, the anti-diabetic action of *D. repens* could be *via* the PTP1B inhibition within the insulin signaling pathway to ameliorate glucose/lipid metabolism, promote glucose utilization, improve the pancreatic β-cell function, and reverse the hepatic oxidative stress.

Keywords: Diabetes, *Duranta repens*, *Ficus benghalensis*, PTP1B, System biology

TABLE OF CONTENTS

LIST OF TABLES

LIST OF FIGURES

Chapter 1

Introduction

INTRODUCTION

Diabetes mellitus (DM) is one of the chronic metabolic disorders; an outcome of pancreatic β-cells failure to insulin release and endogenous or exogenous insulin resistance to represent type 1 (T1DM) and type 2 diabetes mellitus (T2DM) respectively.[1] T1DM is reflected in two types *i.e.* type 1a (autoimmune pathogenesis; traced *via* the presence of β-cells antibodies) and type 1b (β-cells idiopathetically deteriorate).[2] Similarly, T2DM is the progression of insulin resistance; the hyperinsulinaemic state is observed to deal with elevated hyperglycemia.[3]

The current pharmacotherapy of DM includes the supply of exogenous insulin subcutaneous (deals with T1DM)[4] or administration of synthetic oral hypoglycaemic agents; insulin secretagogues, PPAR-γ agonists, dipeptidyl-peptidase (DPP4) inhibitors, and α-glucosidase and α-amylase inhibitors (deals with T2DM).[5] However, some subjects are allergic to exogenous insulin administration[6] and the synthetic molecules are limited due to various side effects.[5] Also, it is to be understood that T2DM is a polygenic state[7] where multiple deregulated proteins interact with each other to generate a complex network that needs to be neutralized with an anti-diabetic agent composed of various bioactives by interacting with multiple proteins simultaneously. These limitations of current anti-diabetic agents suggest identifying the new therapeutic agent(s) to deal with diabetes is still called for. Additionally, in T1DM, one can think that **"*can we regenerate the pancreatic β-cells?*"[8];** may not be possible by just supplementing the exogenous insulin.

To the above limitation(s) of gold standard pharmacotherapy of the two sorts of **DM**, Traditional medicine practitioners' knowledge is utilized from the 1000 s of years as reported in the Ayurveda (आयुर्वेद)[9], Traditional Chinese Medicine (中医)[10] and other complementary medicines. Although the multiple experimental and clinical shreds of evidence are established

to demonstrate the efficacy of the traditional medicines, they are described as "***fraught with pseudoscience***" due to no logical mechanism of action[11] which is one of the chief reasons for limiting them in clinical practice. In this regard one can think ***can we add a probable mechanism of action of traditional medicine which is reported to be effective in dealing the diabetes mellitus?***

It is transcribed for the composition of medicinal plants with various bioactives under the multiple phytochemistry *i.e.* flavonoids, polyphenols, alkaloids, steroids, saponins, triterpenes, etc[12]; has mild difficulty to evaluate the compound(s)-protein(s) interaction(s). In addition, although the majority of the drugable compounds function based on the "***lock and key***" concept, it needs to be understood that a single bioactive can regulate multiple proteins as "***a single master key can unlock multiple locks***".[13] It means the majority of bioactives can regulate the multiple proteins and pathways within disease pathogenesis giving rise to complex "***bioactive-protein-pathway interaction***" which can be traced using network pharmacology.[14] Next to it, the network pharmacology also traces the lead hit molecule and majorly targeted protein and regulated pathway to specify the probable mechanism of action of traditional medicines.[15]

Ficus benghalensis L (family Moraceae), commonly recognized as Indian banyan, banyan fig, and banyan[16] is native to the Indian subcontinent and *Duranta repens* or *D. erecta* (family Verbenaceae), one of the flowering shrubs is native from Mexico to South America and the Caribbean; is one of the important traditional medicines.[17] *F. benghalensis* is also recorded in the Ayurvedic Pharmacopeia of India against "***Prameha***"; Ayurvedic terms of metabolic syndrome[18] and *D. repens* to compose multiple secondary bioactives as α-glucosidase inhibitors; inhibitors of this enzyme can be implemented to manage the postprandial hyperglycemia[19] and also possess anti-hyperglycemic activity.[20] Additionally, *F. benghalensis*[18] and *D. repens*[17] are also reported to compose multiple secondary bioactives

under the multiple phytochemistry like alkaloids, flavonoids, saponins, and sterols whose categories are demonstrated as anti-diabetes[21-24] *via* multiple *in vitro, ex vivo,* and *in vivo* protocols.

Hence, in the present study, we selected *F. benghalensis* L and *D. repens* L to evaluate their anti-diabetic activity using multiple *in silico, in vitro, ex vivo,* and *in vivo* pharmacology to propose their probable anti-diabetic mechanism.

Chapter 2

Aims and Objectives

AIM

To propose the anti-diabetic mechanism of hydroalcoholic extract of *Ficus benghalensis* L. (bark) and *Duranta repens* L. (whole plant) using *in silico*, *in vitro*, *ex vivo*, and *in vivo* pharmacology

OBJECTIVES OF THE STUDY

- To assess the effect of extract/fraction(s) of *Ficus benghalensis* and *Duranta repens* on α-amylase and α-glucosidase enzymes inhibition to hold the polysaccharide hydrolysis and glucose uptake in rat hemidiaphragm and diffusion from rat jejunum *via in vitro* and *ex vivo* approaches respectively
- To assess the effect of *Ficus benghalensis* and *Duranta repens* extract on hepatic enzymes involved in gluconeogenesis, glycolysis, and anti-oxidant biomarkers, glycogen content in liver and gastrocnemius muscle, and histopathological changes of pancreatic β-cell in streptozocin-nicotinamide-induced diabetes
- To assess the insulin-sensitizing effect of *Ficus benghalensis* and *Duranta repens* extract by evaluating the HOMA-IR index, hepatic enzymes involved in gluconeogenesis, glycolysis, and anti-oxidant biomarkers, glycogen content in liver and gastrocnemius muscle, plasma leptin level, and hepatic histological changes in fructose-induced insulin-resistant rats
- To predict the molecular mechanism of anti-diabetic action of *Ficus benghalensis* and *Duranta repens* using system biology (network pharmacology and molecular docking) approaches

Chapter 3

Review of Literature

REVIEW OF LITERATURE

1. Glucose homeostasis

Three interlinked processes *i.e.* hepatic gluconeogenesis, peripheral glucose utilization, and glucose uptake[25] majorly by skeletal muscle, and function of insulin and other counter-regulatory hormones influence the glucose uptake and metabolism.[26]

Further, insulin and glucagon function oppositely. High glucagon levels and lowered insulin levels are observed during fasting state to trigger hepatic gluconeogenesis and glycogenolysis; this decreases the glycogen synthesis in an attempt to prevent hypoglycemia. This reflects to determine the plasma glucose level primarily *via* the hepatic glucose output. After the meal, glucagon level drops responding to the huge glucose load, and insulin level increases to promote the glucose uptake and its utilization within the tissues. This glucose utilization primarily takes place within the skeletal muscle as it is the most responsive site to the postprandial glucose; plays a critical role to maintain homeostatic glucose regulation.[27]

1.1. Regulation of insulin release

Within the pancreatic β-cells, the insulin gene is expressed. From insulin mRNA in the rough endoplasmic reticulum, pre-proinsulin is synthesized and transported to the Golgi apparatus where a series of proteolytic enzymes act over it to produce the mature insulin and a cleavage peptide *i.e.* C-peptide; both are stored within secretory granules and are secreted after physiological stimulations.[28] Also, C-peptide stand-in for pancreatic β-cell function; also considered as its functional marker[29], avoids β-cells loss in **T1DM** and insulin resistance-associated hyperinsulinemia.

The synthesis and release of insulin are also triggered by the glucose itself. Insulin-dependent glucose transporters 2 (GLUT2) facilitate glucose uptake into pancreatic β-cells (Figure 1). Also, ATP-sensitive K^+ channels are expressed on the surface membrane of the

β-cells. The increased ATP/ADP ratio in the β-cell cytoplasm due to the generation of ATP *via* glycolysis inhibits the ATP-sensitive K^+ channel; membrane gets depolarized and extracellular Ca^{2+} influxes into the cell *via* voltage-gated Ca^{2+} channels. This increase in intracellular Ca^{2+} triggers insulin secretion most likely from stored hormone within β-cell granules which is also termed as the phase of immediate insulin release.[30,31] Further, if the secretory stimulus continues, a protracted and delayed response follows to synthesis active insulin synthesis.

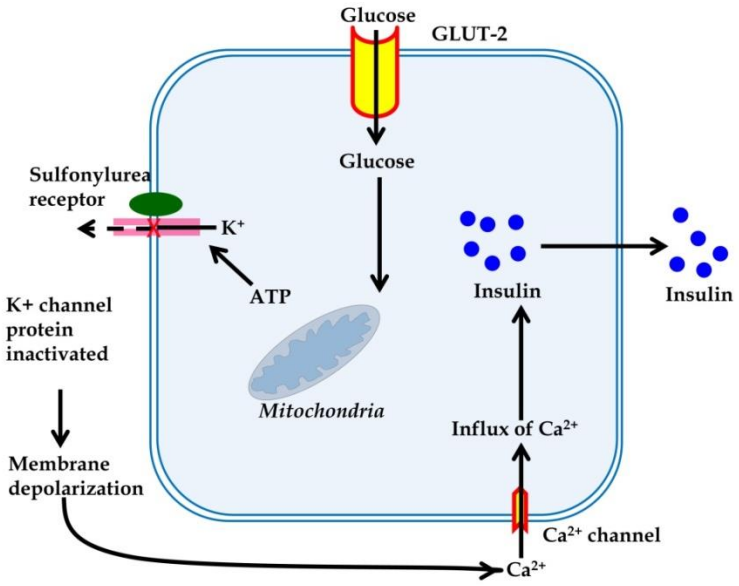

Figure 1: Insulin synthesis and secretion. An insulin-dependent glucose transporter (GLUT-2) transports the glucose into β-cells and it undergoes β-oxidation to release ATP; inhibits inward movement of K^+ leading to membrane depolarization; triggers the Ca^{2+} influx to the release of stored insulin from β-cells. The surface of the β-cell is the dimer of the K^+ channel protein (Kir6.2) and sulphonylurea receptor (SUR1); sulphonylureas bind to SUR1 receptors.

1.2.Insulin action and signaling pathways

Insulin is recognized for its potent anabolic task with its synthetic and growth-promoting effects. Primarily, it promotes the glucose transportation rate into certain cells majorly in striated muscle cells and adipocytes to a lesser amount[32]; glucose uptake to the brain is insulin-independent. In muscles, the glucose is polymerized into glycogen or oxidized to release ATP. Similarly, in the adipose tissue, glucose is stored in the form of lipid (promotes lipogenesis) and inhibits lipolysis. Additionally, it promotes the synthesis

and minimizes the degeneration of glycogen, lipid, and proteins. Further, insulin possesses multiple mitogenic tasks[32] where it triggers DNA synthesis in certain cells and stimulates their growth and differentiation (Figure 2).

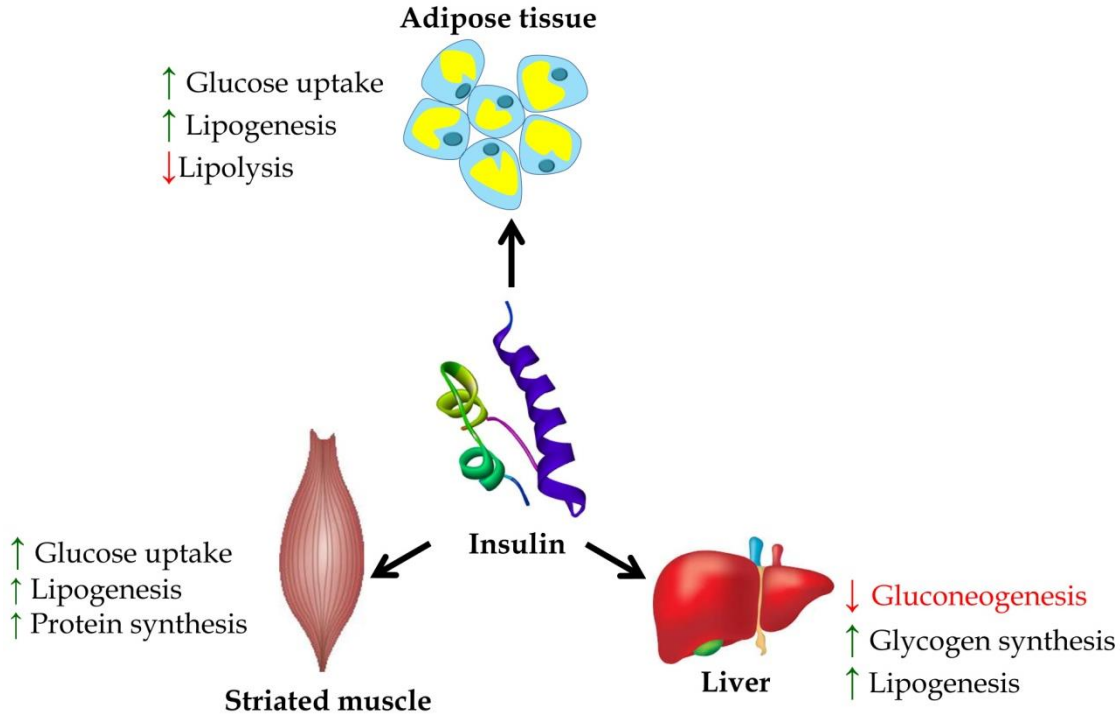

Figure 2: Metabolic actions of insulin in striated muscle, adipose tissue, and liver

Insulin receptor consists of 2 α- and β- subunits in which the cytosolic β-subunit possess the tyrosine kinase activity which is activated if insulin binds to the α-subunit of extracellular domain; autophosphorylates the receptor resulting in the phosphorylation (activation) of multiple intracellular substrates including IRS1-4 and GAB1; activates MAP and PI3K pathways to trigger the mitogenic and metabolic activities of insulin within the cells. Additionally, insulin signaling also eases traffic and dock the GLUT4 vesicle in the plasma membrane which promotes glucose uptake; the phenomenon is AKT mediated however independent of cytoplasmic CBL protein. Additionally, protein tyrosine phosphatase 1b (PTP1B) dephosphorylates the insulin receptor to downregulate insulin signaling. Also, phosphate PTEN may regulate insulin signaling *via* the blockage of AKT activation in PI3K pathways[33]; Figure 3.

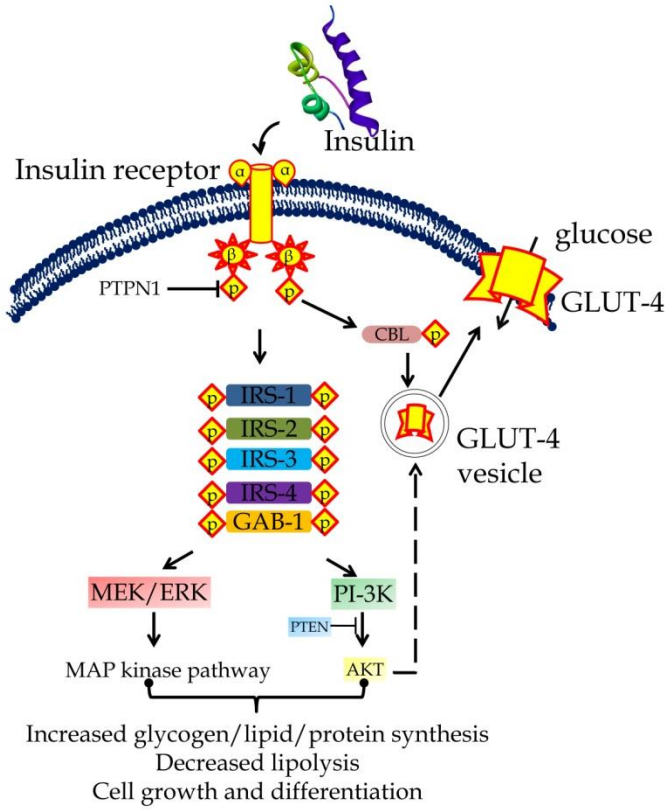

Figure 3: Action of insulin action in a cell. Insulin promotes glycogen and protein synthesis and inhibits lipolysis. Intermediate proteins of the pathways are not presented in the above figure and are presented as a dashed arrow.

2. DM and its pathogenesis

Diabetes mellitus is the hyperglycaemic state; occurs due to pancreatic β-cells failure to synthesize and release the insulin or insulin resistance or a combination of both or excessive glucagon secretion leading to the hyperinsulinaemic state; peripheral glucose is not utilized which is termed as T1DM (β-cells deterioration) and T2DM (insulin resistance or β-cells dysfunction)[34]; detailed below.

2.1.Pathogenesis of T1DM

The reaction of the immune effector cells with endogenous β-cell antigens deteriorates the islets leading to the autoimmune disease with mononuclear cells infiltration into the islets of Langerhans known as T1DM[35]; the lesion was later termed as insulitis; majorly develops in childhood, evident at puberty, and advances with age.

Since the β-cells deteriorate in this case, the survival of the subjects is dependent on the exogenous administration of the insulin to deal with the hyperglycaemic state as its absence may cause severe metabolic complications *i.e.* ketoacidosis and diabetic coma. Due to autoimmune character, its pathogenesis is closely interlinked with genetic and environmental factors.

2.1.1. Genetic susceptibility

More than 30 susceptibility loci have been reported for T1DM in which the HLA gene on chromosome 6p21 contributes around 40%-50% of the total genetic susceptibility in some estimates. The HLA polymorphism is present in or near to binding pocket with an aim that disease-linked allele codes for molecules may reflect specific antigens. However, the linkage of HLA molecules' ability with the disease to present itself as islet antigen or its role over T-cell selection and tolerance has not been established yet.[36] Further, the association of CTLA4[37] and PTPN22[38] polymorphism is also linked with the susceptibility of T1DM. Previously, the non-MHC gene was identified to be insulin[39]; had VNTRs within the promoter region being linked with disease susceptibility.[40]

2.1.2. Environmental factors

Although a report has been made to trigger T1DM with a viral infection like Enterovirus[41] *via* direct cytopathic effects; the specific reason for islet-autoimmunity has not been established yet. However, few suggestions have been made that the virus may share the common epitopes with islet antigens resulting in cross-reactivity and deteriorating the islets; termed "***molecular mimicry***" which is also linked with autoimmunity.

2.1.3. Mechanism of β-cells destruction

The immune abnormality *i.e.* self-tolerated T-cells failure towards the islet antigens can be considered as the main reason to develop **T1DM**. This failure could be the

outcome of combined regulatory T cell dysfunction, effector T cells resistance to suppress, and self-reactive T cell defective clonal deletion in the thymus. This condition may lead to the activation of T cells *e.g.* Th1 cells, traffics to the pancreas and injures the β-cells. Th1 cells also trigger the secretion of cytokines like IFN- γ, and TNF; injures the β-cells and CD8+ CTLs; directly damages the β-cells. The autoantigens may directly target β cell enzyme GAD, islet cell autoantigen 512 (ICA512), and insulin.[42,43]

2.2.Pathogenesis of T2DM

T2DM is a complex polygenic condition that is contributed by interlinking multiple genetic and environmental factors followed by proinflammatory states.[44] However, no evidence of autoimmunity has been proposed yet. This condition is characterized by the compromised response of insulin to peripheral tissues and β-cell dysfunction manifested by the deregulated insulin secretion to respond to hyperglycemia and insulin resistance[45]; Figure 4.

2.2.1. Genetic factors

Genetic susceptibility contributes to the progression of T2DM which was evidenced by a disease concordance rate of more than 90% monozygotic twins. A minimum of 30 loci has been identified to confer the risk of type 2 diabetes.[46]

2.2.2. Obesity

One of the most common risk factors for T2DM pathogenesis is visceral or central obesity.[47] Globally, more than 80 % of individuals are diagnosed with T2DM are obese leading to various metabolic defects. Free fatty acids (FFA) accumulate multiple toxic cytoplasmic intermediates *e.g.* diacylglycerol; attenuates the signal *via* the insulin receptor pathway[33]; this attenuated insulin signaling builds up the gluconeogenesis which is phosphoenolpyruvate carboxykinase mediated.[48] Also, FFA compete for substrate oxidation; inhibit glycolytic enzymes, and further progresses glucose intolerance.[49]

Further, deregulated adipokines have been reported in obesity and diabetes in which some of them contribute to hyperglycemia and few (adiponectin and leptin) increase insulin sensitivity.[50] Also, decreased insulin response is noted at skeletal muscle, liver, and adipose tissue in insulin resistance.[32] Further, inadequate insulin secretion is also reported in response to insulin resistance leading to β-cell dysfunction[45]; supports hyperglycemia[32,45]**;** pancreatic β-cell hyper-functions to develop hyperinsulinemia. Over time, β-cells fail in fulfilling insulin demand to maintain the euglycemic state; resulting in severe hyperglycemia and long-lasting complications of diabetes.[51]

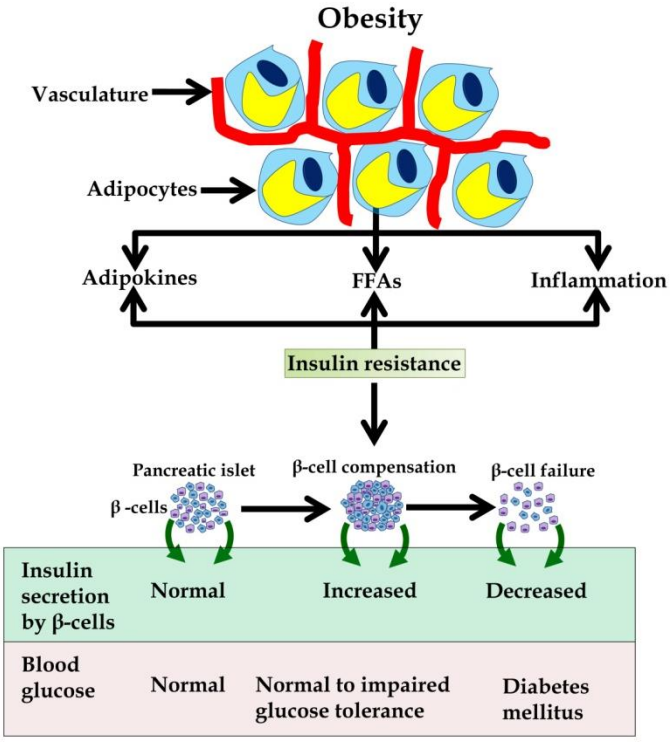

Figure 4: Development of T2DM. Obesity-associated insulin resistance is induced by adipokines, FFAs, and inflammation within adipose tissue. Over this, β-cells attempt to compensate the insulin resistance *via* insulin hypersecretion which may fall short at a particular time followed by failure of β-cells to ensue diabetes.

2.2.3. Insulin Resistance

Usually, when tissues fail to respond to the insulin; predominantly observed in the liver, skeletal muscle, and adipose tissue, it leads to abnormal glucose tolerance.[52] It fails to inhibit hepatic gluconeogenesis[53]; contributes to elevated fasting blood glucose levels.

Also, glycogenesis and glycolysis are compromised after the meal; chiefly contribute to postprandial hyperglycemia.[54] In addition, there is a failure of lipase function which elevates the FFA; amplifies the insulin resistance state.[55] Further, there is compromised insulin signaling; reduces the GLUT-4 expression on the surfaces leading to decreased glucose utilization.[56,57]

2.2.4. Inflammation

It has been reported that excessive pro-inflammatory cytokines secretion in response to surplus nutrients *e.g.* glucose and FFA results in insulin secretion and β-cell dysfunction. IL-1β secretion triggered *via* excessive FFA within β-cells and macrophages; simulates pro-inflammatory cytokines secretion from macrophages, islets, and other cells to promote insulin resistance at the major site of insulin action.[58-60]

2.2.5. β-cell dysfunction

Lipotoxicity *i.e.* excessive FFA compromises the β-cells function[60,61] and attenuates the insulin release which is also impacted by chronic hyperglycemia termed glucotoxicity.[62] Additionally, the atypical incretin effect also reduces GLP-1 (promote insulin release) secretion[63]; destructs β-cells.[64] In addition, though β-amyloid deposition has been reported within islets[65], it is still unclear whether it is a cause or a β-cell burnout effect.

3. Diagnosis of DM and its current pharmacotherapy

Blood glucose level within the range of (70-120) mg/dL is considered normal. Clinically, the subject may be considered diabetic if (a) random glucose level is greater than 200 mg/dL, (b) fasting glucose level greater than 126 mg/dL more than one occasion, and (c) glucose level is more than 200 mg/kg after 2 h of standard glucose load during oral glucose tolerance test (OGTT).

The basis of pharmacotherapy of DM is based on whether the condition is insulin-dependent or insulin-independent. For insulin-dependent diabetes (T1DM), exogenous insulin is provided. At present, human insulin produced by rDNA technology is given subcutaneously (routine use) or intravenously (emergency). Presently, insulin is available in different formulations; differs based on their duration action in which ***fast and short-acting***[66] soluble insulin has a peak action at 2-4 h after subcutaneous injection; lasts for 6-8 h. Likewise, ***intermediate-acting insulin***[66] can be mixed with soluble insulin with a peak action at 6-10 h *e.g.* isophane insulin. Similarly, ***long-acting insulin***[66] *e.g.* insulin zinc suspension peaks at 8 h; long lasts for 12 to 16 h. Sometimes, this pathogenesis is also dealt with biguanides and sodium-glucose co-transporters (SGLT-2) inhibitors[67] in combination with insulin therapy.

For the treatment of insulin-independent diabetes (T2DM), oral hypoglycaemic agents are preferred. ***Biguanides*** (metformin) possess complex peripheral action with residual insulin; promote the glucose uptake in striated muscle, inhibit hepatic gluconeogenesis and glucose absorption from the intestine. However, they are prone to weight loss and cause anorexia; contraindicated in metabolic acidosis and severe renal failure.[68] Similarly, ***sulphonylureas*** (glibenclamide, gliclazide, tolbutamide, and glipizide) stimulate insulin secretion by blocking ATP-sensitive K^+ channels in β-cells; hence, are effective only within the functional β-cells. Also, these agents are prone to cause hypoglycemia and stimulate appetite; lead to weight gain, and are contraindicated in T1DM and diabetic ketoacidosis.[68] Further, ***α-glucosidase inhibitors*** (acarbose and miglitol) inhibit α-glucosidase in the intestine and prevent long-chain polysaccharides conversion into monosaccharides (glucose and fructose). However, their utilization is limited due to diarrhea, flatulence, bloating, and abdominal pain and contraindicated in intestinal diseases including ulcers, and diabetic ketoacidosis.[68] Likewise, ***DPP4 inhibitors***

(alogliptin, linagliptin, saxagliptin, sitagliptin, vildagliptin) act over DPP4 enzyme and check over the degradation of gastric inhibitory polypeptide and glucagon-like peptide-1; inhibits the glucagon release, promotes glucose-dependent insulin release, enhances satiety, and decreases gastric emptying. However, these agents are prone to cause hypoglycemia, and acute pancreatitis, and increased creatinine and urea levels; contraindicated in renal failure and requires dose adjustment.[68] In addition, ***SGLT2 inhibitors*** (dapagliflozin and canagliflozin) inhibit SGLT-2; prevent the renal glucose absorption at proximal tubules of renal glomeruli; resulting in glycosuria in diabetic subjects to lower the plasma glucose level. However, these agents are concerned with dysuria, dyslipidemia, fungal vaginosis, bone fracture, hypovolemia, renal impairment, and urinary tract infection; these are contraindicated in the subjects undergoing the dialysis.[68] Also, *cycloset* is a D_2 receptor agonist; resets the altered hypothalamic circadian rhythm in obesity; reverses endogenous hepatic gluconeogenesis and insulin resistance; limited by rhinitis, constipation, headache, dizziness, nausea, fatigue, and weakness and contraindicated in syncopal migraine and breastfeeding.[69]

4. Natural products in managing complex diseases

Ayurveda, Kampo, Unani and traditional Chinese, and Korean medicines utilize natural products with great importance to deal with complex diseases and are being practiced for 1000 years and are a valuable repository of human knowledge though they may possess certain defects in various forms.[70,71] Till today, many developing countries are still dependent on traditional medicines; however, the concept of traditional medicine is modernized in China due to the availability of a large dataset of clinical experience and medical practice and experience; guarantee its efficacy and safety *via* the advanced techniques in pharmaceutical areas from the collection of raw material to the final dosage form processing which is under progress in India and Korea. However, with the

progression of the system biology, it has become easy in proposing the pharmacological spectra and mode of action of various traditional medicines.

In 1805 when Friedrich Sertürner isolated morphine from opium[72,73], countless pharmacologically active bioactives were isolated from natural products whether depending upon the traditional use or not. Later, the development of the technologies to synthesize the molecules led significant reduction in the importance of natural products with some concerns to completely ban the use of some natural products for medicinal purposes.[74] Even so, natural products are the important sources to identify and develop novel drugs and are in constant use with evidence of developed analgesic, anti-cancer, anti-hypertension, and anti-migraine drugs.[72, 75]

Natural products are considered as important sources of novel drug discoveries[76]; due to their affinity to target multiple proteins simultaneously, they add a beneficial effect in treating various complex polygenic pathogeneses where multiple genes are involved in the disease progression including metabolic syndrome.[77] In this regard, the bioactives of the medicinal plant can target multiple deregulated proteins involved in the disease pathogenesis and form a complex network to present "***bioactive(s)-protein(s)-pathway(s) interaction***".

4.1.Ficus benghalensis L. bark details

4.1.1. Introduction

In Ayurvedic Pharmacopeia of India, *F. benghalensis* (family: Moraceae) is recorded as "***Nyagrodha***" to utilize its matured dried stem bark in the management of metabolic disorder (***Prameha***), blood disorder (***Raktapitta***), skin diseases (***Visarpa***), wound (***Vrana***), gynecological disorders (***Yonidosa***), and Burning sensation (***Daha***).

4.1.2. Morphological character

The matured bark of *F. benghalensis* is grey adhered with ashy white with light bluish-green or grey patches; flat and slightly curved. The bark thickness varies with the age of the tree. Due to the presence of horizontal furrows and lenticels, it is extremely rough, mostly circular, and prominent with short fractures while the inner portion is astringent and fibrous fracture taste.

4.1.3. Reported bioactives and pharmacological activities of F. benghalensis

As recorded in the Ayurvedic pharmacopeia of India, *F. benghalensis* L. bark composes ***tannins, glycosides,*** and ***flavonoids***. However, the ChEBI database (*https://www.ebi.ac.uk/chebi/)* also records other secondary bioactives like sterols and other organic moieties (retrieved on 23rd December 2019); including ***triterpenes, flavonoids, sterols, ceramide, organic molecular entities,*** and ***furocoumarins*.**

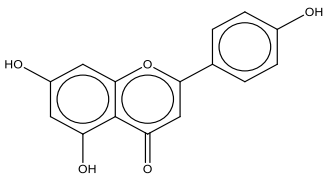

apigenin
MF:$C_{15}H_{10}O_5$
MW:270.24

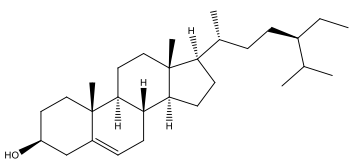

sitosterol
MF:$C_{29}H_{50}O$
MW:414.71

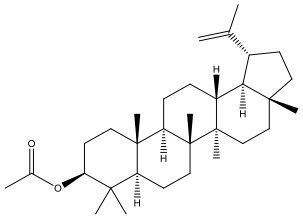

lupeol acetate
MF:$C_{32}H_{52}O_2$
MW:468.75

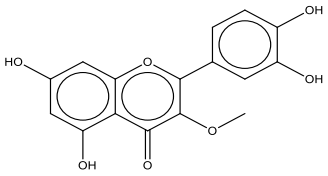

3',4',5,7-tetrahydroxy-3-methoxyflavone
MF:$C_{16}H_{12}O_7$
MW:316.26

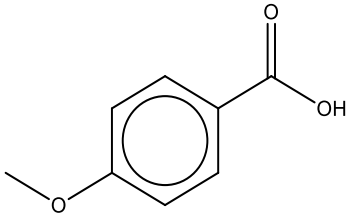

4-methoxybenzoic acid
MF:$C_8H_8O_3$
MW:152.15

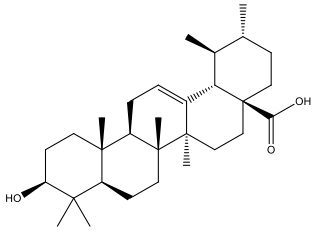

ursolic acid
MF:$C_{30}H_{48}O_3$
MW:456.71

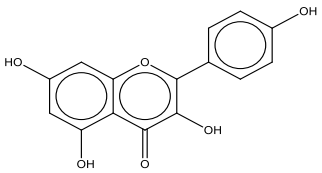

kaempferol
MF:$C_{15}H_{10}O_6$
MW:286.24

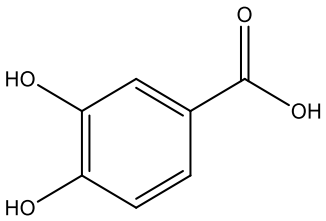

3,4-dihydroxybenzoic acid
MF:$C_7H_6O_4$
MW:154.12

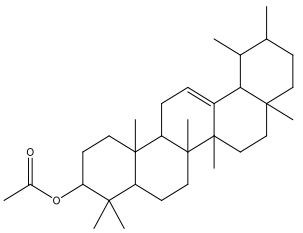

α-amyrin acetate
MF:$C_{32}H_{52}O_2$
MW: 468.80

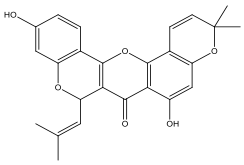

cyclomorusin A
MF:$C_{25}H_{22}O_6$
MW:418.44

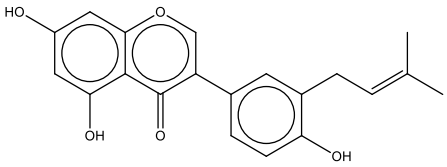

isowighteone
MF:$C_{20}H_{18}O_5$
MW:338.35

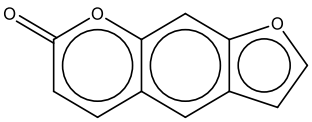

psoralen
MF:$C_{11}H_6O_3$
MW:186.16

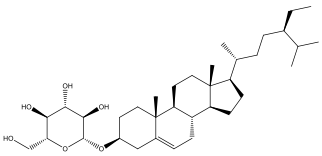

daucosterol
MF:$C_{35}H_{60}O_6$
MW:576.85

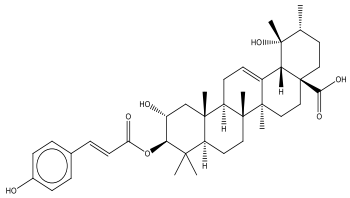

3-O-trans-p-coumaroyltormentic acid
MF:$C_{39}H_{54}O_7$
MW:634.84

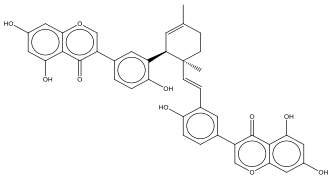

mucusisoflavone A
MF:$C_{40}H_{32}O_{10}$
MW:672.68

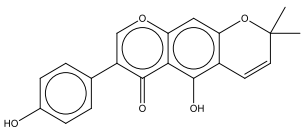

alpinumisoflavone
MF:$C_{20}H_{16}O_5$
MW:336.34

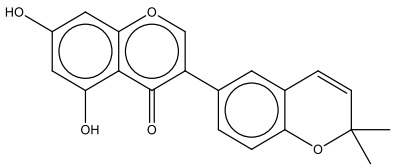

isoderrone
MF:$C_{20}H_{16}O_5$
MW:336.33

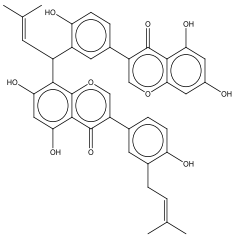

mucusisoflavone C
MF:$C_{40}H_{34}O_{10}$
MW:674.69

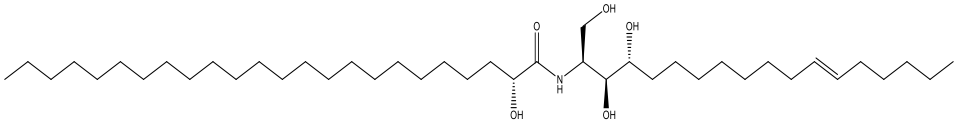

benjaminamide
MF:$C_{42}H_{83}NO_5$
MW:682.11

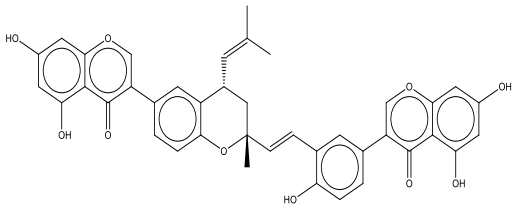

mucusisoflavone B
MF:$C_{40}H_{32}O_{10}$
MW:672.68

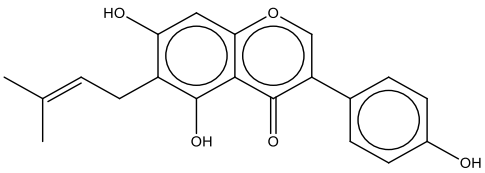

wighteone
MF:$C_{20}H_{18}O_5$
MW:338.35

Some of the extensively investigated pharmacological properties of *F. benghalensis* include ***anti-diabetic***; α-amylase and α-glucosidase inhibition[78,79], amelioration of biomarkers of the diabetes[80,81], anti-hyperglycaemic activity in alloxan-induced diabetes[82], and amelioration of glucose tolerance[82,83], ***anti-hyperlipidaemic***; α-amyrin (isolate from aerial roots) ameliorated the lipid metabolism[84], aqueous extract exhibited as anti-hyperlipidaemic agent against hypercholesterolamic rabbits[85], ***analgesic***; methanolic extract against acetic acid-induced writhing and Eddy's hot plate [86-88], ***antibacterial***; catechin and genistein isolates possessed as anti-bacterial activity against *Pseudomonas aeruginosa* and *Bacillus cereus*[89], aqueous, and methanolic extracts (stem barks) acted against multiple bacterial strains[90-92], ***anti-fungal***; aqueous extract (stem bark) as effective antifungal agent against *Candida albicans* and *Trichophyton rubrum*[90], ***anti-diarrhoeal***; ethanol extract (aerial roots) as anti-diarrhoeal agents against castor oil induced diarrhoea[93], ***antimutagenic***; aqueous extract as anti-mutagenic agent; evidenced by Ames test[94], ***anti-oxidant***; efficacy is reported due to the presence of phenolic compounds[95], effective to scavange DPPH, ABTS, and H_2O_2 free radicals including metal chelation and lipid peroxidation inhibition[96], ***hepatoprotective***; methanol extract (aerial roots), and leucopelargonin derivative (isolate of bark extract) as hepatoprotective agent against isoniazid-rifampicin and CCl_4 induced hepatotoxic respectively[97,98], ***anti-arthritic***; methanol extract (stem

bark) as anti-arithritic agent against formalin and Complete Freund's adjuvant induced arthritic rats [99], ***anti-allergic***; ethanol, ethyl acetate and aqueous extract(s) of stem bark as anti-allergic and anti-stress agents against milk-induced asthma in mice; decreased eosinophils and leukocytes count[100], and ***immunostimulator***; aqueous extract (aerial roots) as immunoregulator; demonstrated with an evidence against hypersensitivity, hemagglutination reaction and polymorphonuclear test.[101]

4.2.Duranta repens details

4.2.1. Introduction

Duranta repens (family: Verbenaceae), or *D. erecta* commonly known as golden dewdrop is a flowering shrub native to Mexico to South America and the Caribbean. It also composes α-glucosidase inhibitors[19], possesses anti-hyperglycemic efficacy[20], and is one of the traditional medicines with anti-microbial properties.

4.2.2. Morphological characters

D. repens is an upright shrub with drooping branches; carries a cluster of mature fruits, having opposite leaves (simple and paired), sometimes borne in whorls of three; has blue or light purple sometimes white. The petioles are up to 1 cm long and are elliptic to ovate. The leaf blades are 15-90 *X* 12-60 mm^2; have entire margins, sometimes slightly serrated towards acute or obtuse apices; occasionally covered with scattered appressed hairs in young turning to glabrous quickly. The plant largely blooms during summer and autumn and borne flowers (9-18 cm) are elongated clustered and are in pale purple or blue (sometimes white) colored and constitute about 1 cm long tube composed with fused petals; opens to

5 well-defined lobes. Each flower is 3-7 mm long with 5 small green sepals, fused at the base with 4 stamens. The fruits borne in large clusters are globose drupes and turn to yellow or orange from green when matured.[102]

4.2.3. Reported bioactives and pharmacological activities of D. repens

D. repens has been reported to be rich in multiple secondary bioactives under the various phytochemical categories. As retrieved on 23rd December 2019, the ChEBI and PCIDB (*https://www.genome.jp/db/pcidb*) database (s) record ***terpenes***, ***saponins***, ***fatty acid***, ***flavonoids***, ***glucosides***, ***coumarin***, ***hydroquinone***, and ***organic compounds*** as active principals for a keyword "*Duranta repens*" and "*Duranta erecta*"; sketched below.

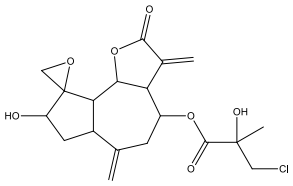

acroptilin
MF:$C_{19}H_{23}ClO_7$
MW:398.11

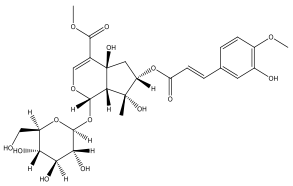

duranterectoside A
MF:$C_{27}H_{34}O_{15}$
MW:598.19

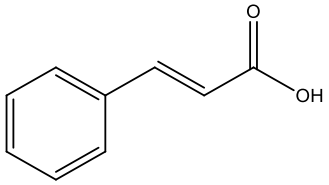

(E)-cinnamic acid
MF:$C_9H_8O_2$
MW:148.05

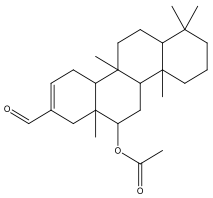

hyrtial
MF:$C_{26}H_{40}O_3$
MW:400.3

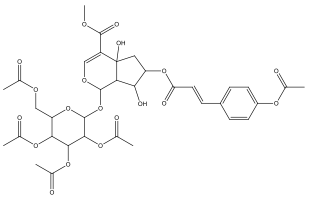

durantoside IV pentaacetate
MF:$C_{35}H_{40}O_{19}$
MW:764.22

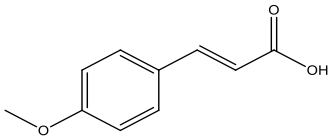

(E)-p-methoxycinnamic acid
MF:$C_{10}H_{10}O_3$
MW:178.06

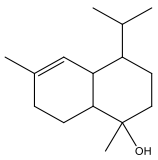

α-cadinol
MF:$C_{15}H_{26}O$
MW:222.2

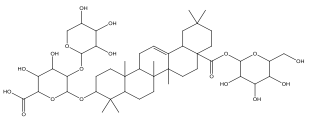

pseudo-ginsenoside-RT1
MF:$C_{47}H_{74}O_{18}$
MW:926.49

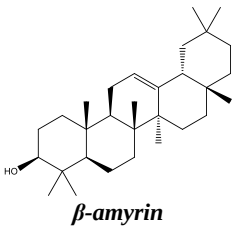

β-amyrin
MF:$C_{30}H_{50}O$
MW:426.39

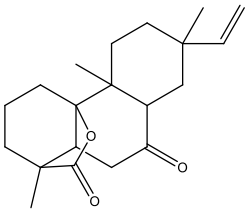

rosenonolactone
MF:$C_{20}H_{28}O_3$
MW:316.2

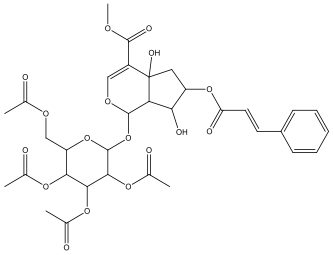

durantoside IV tetraacetate
MF:$C_{33}H_{38}O_{17}$
MW:706.21

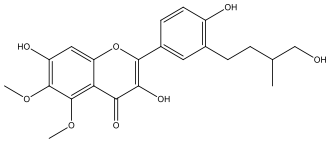

3,7-dihydroxy-2-[4-hydroxy-3-(4-hydroxy-3-methylbutyl)phenyl]-5,6-dimethoxy-4H-1-benzopyran-4-one
MF:$C_{22}H_{24}O_8$
MW:416.15

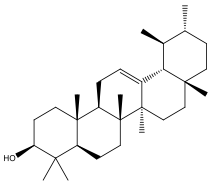

α-amyrin
MF:$C_{30}H_{50}O$
MW:426.39

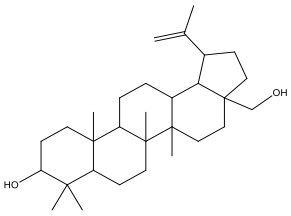

betulin
MF:$C_{30}H_{50}O_2$
MW:442.38

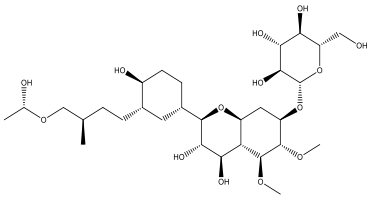

3,7,4'-trihydroxy-3'-(8''-acetoxy-7''-methyloctyl)-5,6-dimethoxyflavone
MF:$C_{28}H_{34}O_9$
MW:514.22

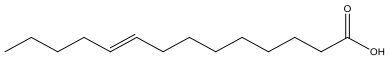

myristoleic acid
MF:$C_{14}H_{26}O_2$
MW:226.19

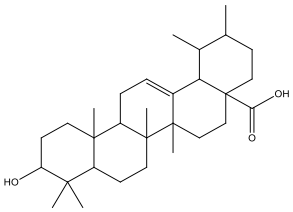

ursolic acid
MF:$C_{30}H_{48}O_3$
MW:456.36

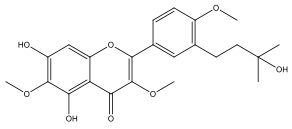

aliarin 4'-methyl ether
MF:$C_{23}H_{26}O_8$
MW:430.16

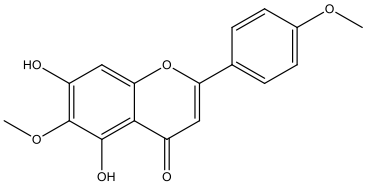

pectolinarigenin
MF:$C_{17}H_{14}O_6$
MW:314.08

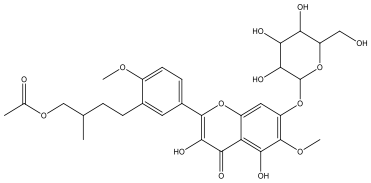

7-O-α-D-glucopyranosyl-3,5-dihydroxy-3'-(4''-acetoxyl-3''-methylbutyl)-6,4'-dimethoxyflavone
MF:$C_{30}H_{36}O_{14}$
MW:620.21

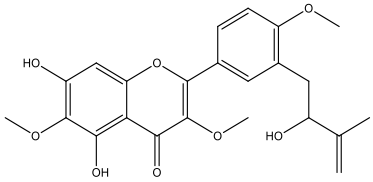

5,7-dihydroxy-3'-(2-hydroxy-3-methyl-3-butenyl)-3,6,4'-trimethoxyflavone
MF:$C_{23}H_{24}O_8$
MW:428.15

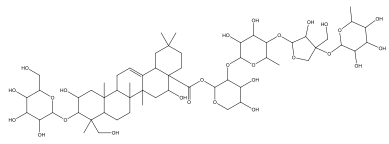

durantanin I
MF:$C_{58}H_{94}O_{27}$
MW:1222.6

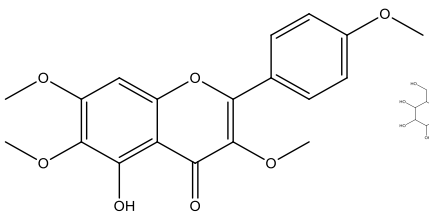

penduletin 4'-methyl ether
MF:$C_{19}H_{18}O_7$
MW:358.11

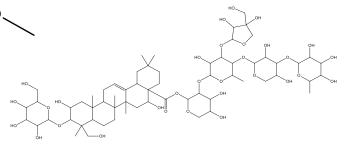

durantanin II
MF:$C_{63}H_{102}O_{31}$
MW:1354.64

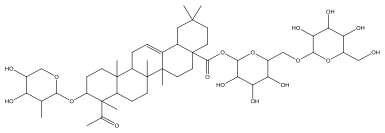

repennoside
MF:$C_{49}H_{78}O_{17}$
MW:938.52

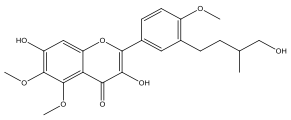

3,7-dihydroxy-2-[3-(4-hydroxy-3-methylbutyl)-4-methoxyphenyl]-5,6-dimethoxy-4H-1-benzopyran-4-one
MF:$C_{23}H_{26}O_8$
MW:430.16

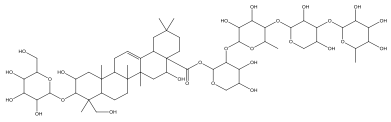

durantanin III
MF:$C_{58}H_{94}O_{27}$
MW:1222.6

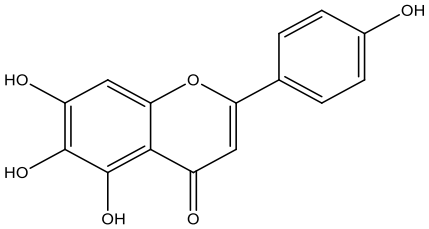

scutellarein
MF:$C_{15}H_{10}O_6$
MW:286.05

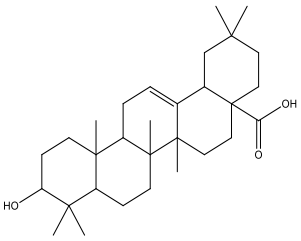

oleanolic acid
MF:$C_{30}H_{48}O_3$
MW:456.36

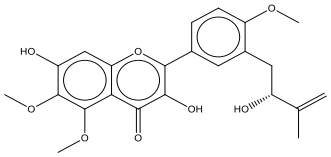

3,7-dihydroxy-3'-(2-hydroxy-3-methyl-3-butenyl)-5,6,4' trimethoxyflavone
MF:$C_{23}H_{24}O_8$
MW:428.15

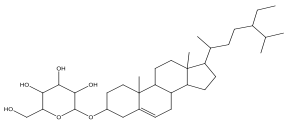

β-sitosterol glucoside
MF:$C_{35}H_{60}O_6$
MW:576.44

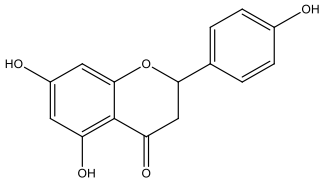

naringenin
MF:$C_{15}H_{12}O_5$
MW:272.07

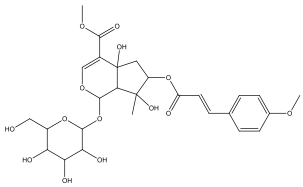

durantosideII
MF:$C_{27}H_{34}O_{14}$
MW:582.19

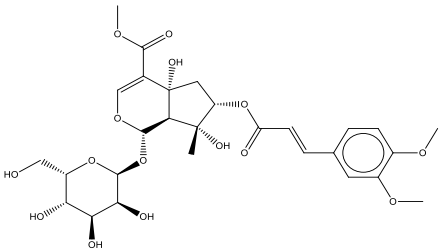

durantoside III
MF:$C_{28}H_{36}O_{15}$
MW:612.21

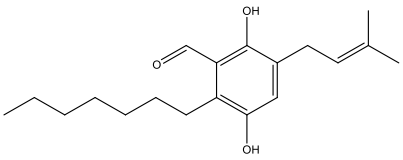

flavoglaucin
MF:$C_{19}H_{28}O_3$
MW:304.2

Secondary metabolites of *D. repens* possess multiple pharmacological spectra including ***anti-diabetic***; methanol extract (*D. repens* fruits) ameliorated the glucose tolerance in alloxan-induced hyperglycaemia and associated dyslipidaemia[20] followed by the presence of α-glucosidase inhibitors[19], ***anti-oxidant***; various extract(s), their fraction(s) and some active principles like acteoside were reported as potential free radical neutralizers using *in vitro*

methods[103-107], ***cytotoxic;*** methanol extract and durantin isolate were reported as potential cytotoxic agents HepG2 cell line[108]***, antiviral;*** ethanol and methanol extract (aerial parts) were reported against hepatitis A[109]***, thrombin inhibition***; isolates like isoprenylated acetophenone, tri-methoxyflavone, and isoprenylated flavonoids were effective[110], ***antiparasitic***; effective against *Plasmodium falciparum*[111], and ***antifungal***; methanol extract (stem and leaves) are also detailed to be effective against *Aspergillus flavus*, *Aspergillus fumigates*, *Aspergillus niger*, *Candida albicans*, and *Microsporum gypseum.*[112,113]

5. Experimental models for anti-diabetic activity

5.1.In vitro anti-diabetic models

In vitro experiments are performed outside the living system by setting an equivalent survival environment of a living system. This approach utilizes a specific target in which either the surface receptor or enzyme or cell is targeted.

In vitro, ***α-amylase and α-glucosidase inhibitory activities*** are the well-accepted approaches to investigate the anti-diabetic effect of the test agents(s) if suspected to manage postprandial hyperglycemia by inhibiting the above-mentioned enzymes.[114] The findings can be extrapolated to the *in vivo* by measuring the blood glucose level at a specified time interval(s) after administrating the polysaccharides at a particular dose.

In vitro glucose uptake assay in skeletal muscle cell lines; for this, the most popular cell line is immortalized rat skeletal (L6) myoblast in which the suspected bioactives enhance the glucose uptake either in the presence or absence of insulin.[115-117] Molecule(s)/test agent(s) suspected to ameliorate insulin resistance like biguanides can

be evaluated and the findings of this may be extrapolated *via* the estimation of hepatic and gastrocnemius muscle glycogen content.

Further, the role of the gliptins is popular to manage diabetes which can be evaluated *via* the ***in vitro DPP4 inhibitory assay.***[118,119] This assay can be extrapolated to *in vivo* findings *via* the measurement of gliptins in the plasma.

Additionally, PTP1B inhibition has been reported to upregulate the insulin signaling pathway to promote glucose utilization. Although ***in vitro PTP1B inhibitory assay***[120, 121] has been established to enhance the sensitivity of the insulin receptor and traffic the GLUT vesicles to the cell membrane[122], inhibition of this enzyme may lead to cellular apoptosis leading to cancer.

One of the popular *in vitro* anti-diabetic assays is ***glucose adsorption assay*** in which the efficacy of the test agent in adsorbing the free glucose is evaluated.[123] However, this assay is more applicable to fiber-containing agents; moreover in herbal formulations.[124] This approach is applicable to manage the postprandial hyperglycemia; which may be extrapolated with *in vivo* findings as explained for α-amylase and α-glucosidase activity with the supplementation of glucose instead of polysaccharides.

5.2.Ex-vivo anti-diabetic models

Ex vivo models utilize the tissue or organ of the living organism, particularly, rat or mice. Two famous and well-accepted *ex vivo* anti-diabetic models include ***glucose uptake assay in isolated rat hemidiaphragm*** and ***glucose diffusion assay from the isolated rat intestine***; majorly jejunum.

Glucose uptake assay in isolated rat hemidiaphragm[125] can be performed *via* the 2 approaches. Firstly, the rat hemidiaphragm of the specified size from the healthy animal is isolated and incubated in the fixed glucose concentration for a specified time in the presence of the test agent and the remaining amount of the glucose is quantified. This

assay can be performed in the presence or absence of insulin and the outcome can be extrapolated with the glucose utilization pattern within *in vivo* study. Secondly, after the treatment completion of diabetic animals, the isolated hemidiaphragm is incubated within the glucose solution for a defined time and the remaining amount of the glucose is quantified. However, the test agent may not be incorporated within the reaction mixture.

Glucose diffusion assay from the isolated rat intestine is the modified version of the glucose diffusion assay from the semi-permeable membrane[126] in which the semi-permeable membrane is replaced with either with ileum or jejunum as required.[127] The isolated ileum or jejunum from the healthy rat is filled with the test agent and defined glucose concentration; incubated at pH at 37°C and the amount of the glucose diffused to the external medium is quantified at a particular interval(s).

5.3. In vivo anti-diabetic models

To date, multiple insulin-dependent and non-insulin-dependent anti-diabetic models have been established either *via* chemical or diet/nutrient or combination of both or surgical or viral or genetic models. Some of the popular *in vivo* anti-diabetic models include ***streptozocin***[128] or in combination with ***nicotinamide***-[129], ***alloxan***-[130], ***dexamethasone***-[131], ***insulinantibodies***[131]-, ***EMC-D*** or ***Mengo-2T*** or ***CB4*** or ***Reo*** or ***Kilham rat virus***-[131], and ***pancreatectomy***-[131] induced diabetes to present insulin-dependent hyperglycemia. Additionally, NOD mice, BB rats, WBN/KOB rats, and Cohen diabetic[131] rats are also available as genetic animal models to investigate the anti-diabetic efficacy. Similarly, ***fructose supplementation*** alone[132] or in combination with ***high fat***[133] has been reported to induce diabetes in rats. Also, streptozocin injection in the neonates within the 5th day of birth causes T2DM in their adulthood[131]. Some chemicals like adrenaline and ethylenediaminetetraacetic acid (EDTA) are also reported to induce diabetes in partially depancreatized rats.[131]

Among the above-mentioned animal models, the present study utilized streptozocin-nicotinamide-induced hyperglycemia and fructose-induced insulin-resistant rat animal models which are detailed below.

5.3.1. Streptozocin- nicotinamide induced hyperglycemia rat model

Combined administration of streptozocin (deteriorates pancreatic β-cells) and nicotinamide (partially protects insulin-secreting cells against streptozocin) is a widely accepted methodology to induce diabetes in rodent models. DNA of β-cells in the pancreas is damaged by streptozocin leading to increased activity of PARP-1 to fix the damaged DNA. However, the overstated activity of PARP-1 leads to the depletion of intracellular NAD (+) and ATP; β-cells undergo necrosis. Nicotinamide inhibits PARP-1 activity and prevents the depletion of NAD (+) and ATP in cells exposed to streptozocin.[134] Multiple combinations of streptozocin and nicotinamide are available in developing diabetes to achieve various ranges of blood glucose levels.[135]

5.3.2. Fructose-induced insulin-resistant rat model

There is an enhanced glucose outflow from the livers of fructose-fed rats displaying the mutilation in whole-body insulin sensitivity followed by decreased glucose infusion rate which is demonstrated *via* hyperinsulinemic-euglycemic clamp techniques. Also, OGTT assessment reflects, the decreased insulin sensitivity index, in fructose-fed rodents which is further supported by the elevated steady-state of plasma glucose level. Further, there is decreased phosphorylation of IRS-1 and insulin receptor density in the liver and skeletal muscle; reflected by a decrease in mRNA expression.[136]

6. Theory of multi-compound and multi-protein interaction

6.1.Introduction

Principle "*similar compounds tend to bind the same proteins*" is similar to "*master key can unlock multiple locks*". In this aspect, one can observe that how a single protein can regulate multiple proteins, and these proteins interact with each other to regulate multiple pathways associated with disease pathogenesis. This concept can be explained *via* the network pharmacology; Figure 5; the term was coined by Hopkins in 2007 to understand the action and interaction of drugs with multiple targets.[137] It helps to list the drug-mediated molecular interaction within the cells and is an important tool to overview the hidden relationship of a drug(s) and the biological system.[138,139] Further, it helps in drug repurpose for multiple therapeutic conditions and identify the new lead(s) *via* unbiased investigation depending on potential target spaces.[140]

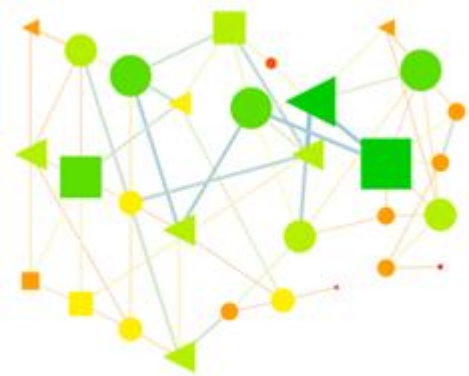

Figure 5: Basic anatomy of the network; analyzed for variable **"***Edge count***".** The nodes are represented by triangle, square, and circle and edges are presented by lines. The different shape of the node represents different association within the network *e.g.* triangle, square, and circle may represent bioactive(s), target(s), and pathway(s) respectively. Node with bright green color has a high edge count whereas red represents the node with a low edge count.

6.2.Network construction

The whole network pharmacology can be studied in 4 main steps, firstly ***identification of bioactives***[141]; multiple open-source databases like ChEBI, PCIDB, etc can be used to retrieve the compound's basic information; can be queried in PubChem (*https://pubchem.ncbi.nlm.nih.gov/*) or ChemSpider (*http://www.chemspider.com/*) database to trace their availability for 2D or 3D structure. These molecules can be investigated for their druglikeness property as explained by "***Lipinksi's rule of 5***"[142],

including pharmacokinetic, pharmacodynamic, and physiological properties. In these steps, some compounds may be eliminated if the compound(s) properties do not fall within the specified range. Secondly, ***bioactives are predicted for their potential targets***[141] using multiple chemoinformatic tools at a particular threshold and matched with previously reported disease targets; which can be retrieved from databases like Therapeutic Targets Database (TTD; *http://db.idrblab.net/ttd/*) and DisGeNET (*https://www.disgenet.org/*). Third, ***commonly regulated targets are enriched*** in STRING (*https://string-db.org/*) to identify the biological processes, molecular functions, cellular components, and probably regulated pathways. Finally, ***network is constructed*** among the bioactive(s), modulated protein(s) and regulated pathway(s) to present the "***bioactive(s)-protein(s)-pathway(s)***" interaction.

6.3.Network analysis

The constructed network can be analyzed using multiple parameters in which edge count, closeness centralities, between centralities, topological coefficient, neighborhood connectivity, node degree distribution, and stress centrality are commonly used.

In a network, a compound, target, or pathway is indicated by a node, and the connection between them is termed as edge. More the number of connections with the node; more is the ***edge count*** of that node[143] *e.g.* if the bioactives' node possesses the maximum edge count, it means it regulated the highest number of the targets; a similar concept is applied for the targets' and pathways' node. Additionally, ***closeness centralities***[144] assess the superior broadcaster within the whole network which is neighbor-dependent. Similarly, ***between centralities***[144,145] reflect the bridging of the node with another node to point the shortest path connectivity with other nodes. Likewise, the ***topological coefficient***[146] identifies the node with no or single neighbor

by assigning them as zero. Further, the average connectivity of the node with the average connectivity of all neighbors is defined by ***neighborhood connectivity***[147].

6.4.Post network analysis

After the network construction and its analysis, a highly interacting bioactive and protein can be traced. However, it becomes a bit tricky to identify which bioactive possesses the best binding affinity with the target though little idea can be made based on the similarity score during target prediction. To insight over this, *in silico* molecular docking can play an important role. Based on the binding energy of the docking score and the number of interactions, the best lead hit can be predicted. However, the possibility of the false positive or negative hit always exists that may be traced *via* the molecular dynamics simulation to some extent. Also, the findings of network pharmacology, molecular docking, and simulation are predictive meaning to validate their outcomes by sketching to functional or molecular biomarkers.[148]

Chapter 4

Materials and Methods

MATERIALS AND METHODS

The approach followed to propose the anti-diabetic mechanism of the *F. benghalensis* and *D. repens* was performed *via* the implementation of the *in silico*, *in vitro*, *ex vivo*, and *in vivo* pharmacology approaches (Figure 6).

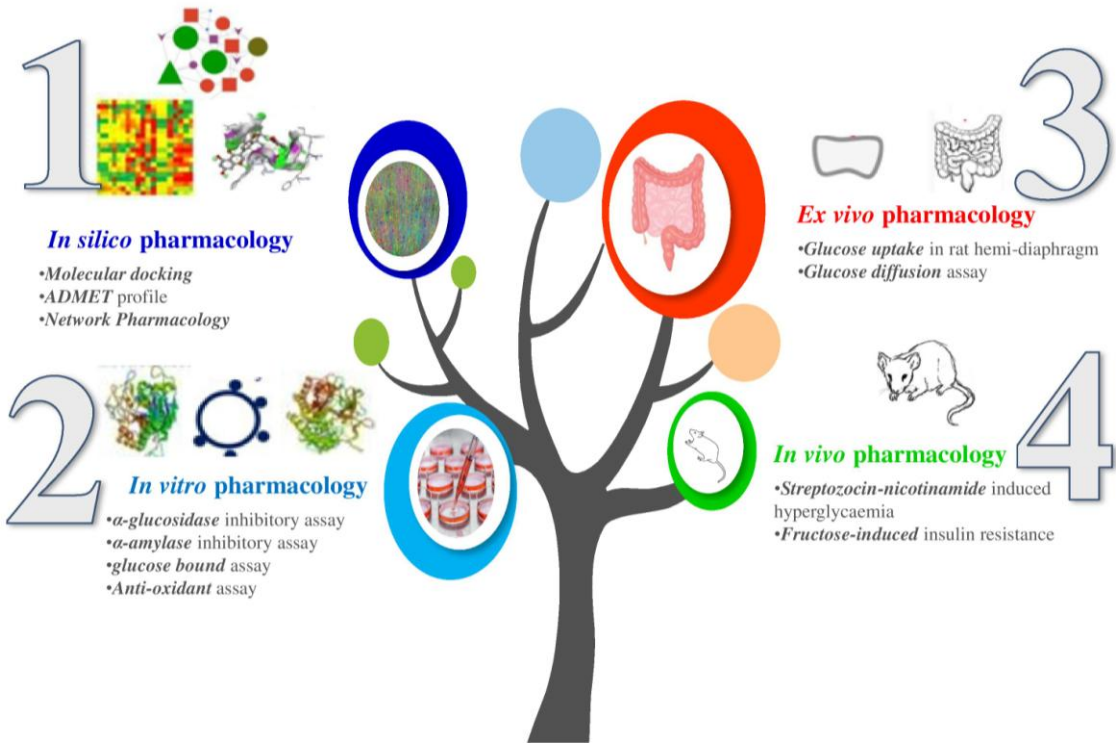

Figure 6: Brief approach followed to propose the anti-diabetic mechanism of *F. benghalensis* (bark) and *D. repens* (whole plant)

1. *In silico* pharmacology of *F. benghalensis* and *D. repens* against DM

1.1.Network pharmacology

ChEBI (*https://www.ebi.ac.uk/chebi/*) and PCIDB (*https://www.genome.jp/db/pcidb*) recorded bioactives of *F. benghalensis* and *D. repens* were retrieved and their targets were predicted in BindingDB[149]; matched with the proteins involved in the DM concerning to TTD (*http://db.idrblab.net/ttd/*) and gene code were retrieved from NCBI-gene (*https://www.ncbi.nlm.nih.gov/gene/*) or UniProt (*https://www.uniprot.org/*) as available; enriched within STRING (*https://string-db.org/*) for *Homo sapiens* and regulated pathways

in DM were identified concerning KEGG (*https://www.genome.jp/kegg/pathway.html*). Further, the bioactives *vs* proteins *vs* pathway network was constructed using Cytoscape[150] *ver* 3.5.1. The whole network was treated as directed and analyzed using an edge count score.

1.2. Prediction of druglikeness score

The druglikeness score of each bioactive was predicted using MolSoft (*https://molsoft.com/mprop/*) as explained by "Lipinski rule of 5"[142] based on molecular weight, hydrogen bond acceptor and donor count, and lipophilicity.

1.3.Molecular docking against α-amylase, α-glucosidase, and PTP1B

Before molecular docking, initially, the probable inhibitors of the α-amylase, α-glucosidase, and PTP1B were screened within BindingDB or PASS-ONLINE[151] at similarity index of 0.7 and pharmacological activity (Pa) > pharmacological inactivity (Pi) respectively as applicable.

1.3.1. Ligand preparation

The 3D (.sdf) structure of predicted bioactives of the above-mentioned targets was retrieved from PubChem (*https://pubchem.ncbi.nlm.nih.gov/*) database, converted into .pdb using Discovery Studio Visualizer 2019 (*Dassault Systèmes BIOVIA (2019) Discovery studio, 2019; Dassault Systèmes, San Diego*) and energy of each ligand was minimized using suitable forcefield (mmff94 or uff as applicable) and optimization algorithm and converted into .pdbqt.

1.3.2. Macromolecule preparation

The 3D crystallographic protein of α-amylase (PDB: 5VA9), α-glucosidase (homology modeled using query sequence; accession number: ABI53718.1 and template; PDB: 5KZW) and PTP1B (PDB: 1NNY) were designed (Modeller 9.10; *https://salilab.org/modeller/*) / retrieved (RCSB; *https://www.rcsb.org/*) as

applicable; was in complex with water and other hetero molecules; removed using Discovery studio and saved in .pdb format.

1.3.3. Ligand-macromolecule docking

After ligand and macromolecule preparation, each bioactive (ligand) was docked against the target (macromolecule) using AutoDock 4[152] or AutoDock Vina[153] as required to obtain 10 different ligand poses; pose with minimum binding energy was selected to visualize the ligand-protein interaction in Discovery studio.

1.4. Molecular docking against free radical generators

Herein, 5 free radical generators *i.e.* cytochrome P450 (PDB: 1OG5), lipoxygenase (PDB: 1N8Q), nicotinamide adenine dinucleotide phosphate (NADPH) oxidase (PDB: 2CDU), xanthine oxidase (PDB ID: 3NRZ) and myeloperoxidase (PDB: 1DNU) were retrieved from RCSB protein databank which were targeted with top 3 bioactives with maximum druglikeness *i.e. F. benghalensis*; ***3-O-trans-p-coumaroyltormentic acid*** (1), ***mucusisoflavone C*** (2), and ***wighteone*** (3) and *D. repens*; ***7-O-α-D-glucopyranosyl-3,5-dihydroxy-3'-(4''-acetoxyl- 3''-methylbutyl)-6,4'-dimethoxyflavone*** (1), ***3,7-Dihydroxy-2-[4-hydroxy-3-(4-hydroxy-3- methylbutyl)phenyl]-5,6-dimethoxy-4H-1-benzopyran-4-one*** (2), and ***naringenin*** (3). The ligands and targets were prepared as explained previously and docked using AutoDock Vina to obtain 10 different poses; pose with minimum binding energy was selected to visualize the ligand-protein interaction in Discovery Studio.

1.5.Molecular docking against the enzymes involved in the glucose catabolism and anabolism

Two crystallographic proteins *i.e.* phosphofructokinase (PFK; PDB:4OMT), and

lactate dehydrogenase (LDH; PDB:4L4S) were directly retrieved from the RCSB protein data bank and utilized as macromolecule whereas fructose 1,6-bisphosphatase (FBPase; query sequence: AAC50207.1 and template: PDB:7CVN), glucose 6-phosphatase (G6Pase; query sequence: accession: P35575.2 and GI: 206729864), hexokinase (query sequence: sp|P19367.3, and template: PDB:2NZT) were homology modeled *via* SWISS-MODEL (*https://swissmodel.expasy.org/*)[154]; all the hetero-atoms were removed and prepared as a macromolecule; all the bioactives were docked against macromolecules and results were interpreted as explained above.

2. Extraction, preliminary phytochemical evaluation, and HPLC analysis

Wild grown *F. benghalensis* L. (bark) and *D. repens* L. (whole plant) were collected from local areas of Belagavi; authenticated at ICMR-NITM, Belagavi, India, and the herbarium (accession number: RMRC-1405 and 1406) was deposited for the same for future reference. The collected plant material was washed under running water, shade dried, turned into a coarse powder, and extracted to obtain a hydroalcoholic extract of *F. benghalensis* (FBE) and *D. repens* (DRE) and fractionated as explained by Cos *et al.*[155] with minor modifications using multiple solvents *i.e.* dichloromethane, acetone, methanol, citric acid (5% w/v) and petroleum ether (Figure 7).

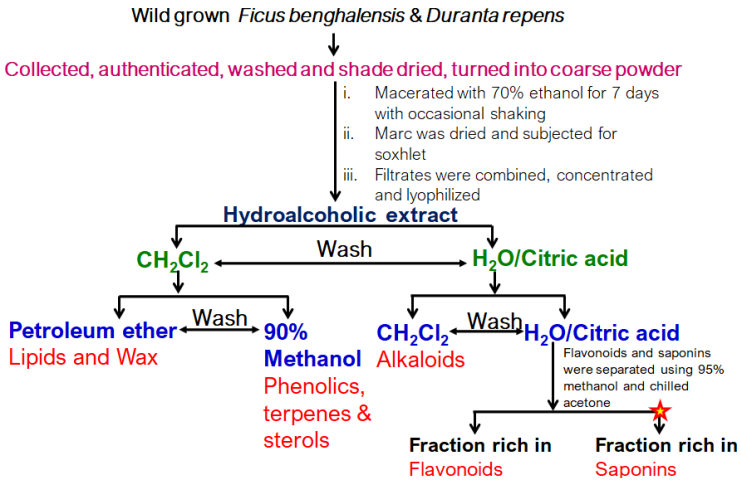

Figure 7: Scheme followed for the extraction and fraction of FBE and DRE. ★ Not applicable fraction for FBE as it was not obtained during fractionation

After extraction, each fraction was undertaken for a preliminary phytochemical investigation to confirm the presence of ***steroids***; salkowski test, ***saponins***; foam test, ***tannins***, ***phenolic compounds***; $FeCl_3$, lead acetate, bromine water, acetic acid, dilute iodine, HNO_3, and $KMnO_4$, and gelatin test, ***alkaloids***; Dragendroff's, Mayer's, Hager's, Wagner's, and tannic acid test, and ***flavonoids***; sodium hydroxide, lead acetate, and sulphuric acid test). Similarly, in both FBE and DRE, total flavonoid and polyphenol content were quantified as explained by Chandra *et al.*[156] and Ainsworth & Gillespie[157] respectively to estimate gallic acid and quercetin equivalent in triplicates.

The mobile phase composed of methanol and water (0.05% orthophosphoric acid) in the 70:30 ratio with a flow rate of 1 mL/min and detection wavelength of 352 nm for FBE and methanol and water (0.05% orthophosphoric acid) in the 70:30 ratio with a flow rate of 1 mL/min and detection wavelength of 211 nm for DRE were selected as suitable chromatographic conditions to estimate ***apigenin*** and ***quercetin*** in FBE and ***oleanolic acid*** in DRE.

The HPLC-UV analysis was performed using the Agilent 1220 Infinity II LC system (Agilent Technologies, Germany) composed of a low-pressure gradient pump, solvent delivery module, online degasser, manual sample injector, and ultraviolet-visible detector operated *via* Agilent OpenLab software (*https://www.agilent.com/en/product/software-informatics/analytical-software-suite*). The separation was carried out on a Zorbax reversed-phase C_{18} column (5 µm, 4.6 mm, 250 mm). For FBE, initially, different solvent combinations were attempted to detect ***quercetin*** and ***apigenin*** simultaneously. Samples were analyzed at a 1 mL/min flow rate at 352 nm. For each analysis, a 10 µL sample (1 mg/mL in methanol) was injected into the column. The solutions of the standard were prepared by diluting the stock solution using the mobile phase. The sample was prepared by dissolving FBE in methanol followed by dilution with the mobile phase. All the

solutions were filtered through a membrane filter (0.22 mm) before their injection into the chromatographic columns.

Further, DRE chromatographic separation was also carried using an Agilent HPLC system (1220 Infinity II LC) equipped with a low-pressure gradient pump, solvent delivery system, degasser, manual sample injector, and UV-Vis detector.

3. Evaluation of the *in-vitro* antioxidant activity of FBE and DRE

To assess the anti-oxidant potential FBE and DRE various anti-oxidant models *i.e.* DPPH scavenging assay[158], ABTS scavenging assay[159], hydrogen peroxide (H_2O_2) scavenging assay[160], total anti-oxidant capacity[161], nitric oxide (NO) scavenging capacity[162], Cu^{2+} to Cu^{+} reduction (CUPRAC) assay [163], and metal chelating assay[164] were used with minor modifications as detailed below.

3.1. Free radical scavenging assays

Herein, two assays *i.e.* DPPH and ABTS free radical scavenging assays were performed as explained by Choi *et al.*[158] and Re *et al.*[159] respectively with minor modifications.

For the DPPH scavenging assay, DPPH solution (0.1 mM, 1 mL) was incubated (dark, 25℃, 30 min) with multiple concentrations of FBE and DRE (1 mL) with suitable control (absence of test agent), and the absorbance was recorded at 518 nm. The percentage scavenging capacity of each concentration was calculated as

$$\%\ scavenging\ capacity = \left(1 - \frac{As}{Ac}\right) X100 \ldots\ldots\ldots \textbf{(1)}$$

where ***Ac*** and ***As*** refer to the absorbance of the control and test respectively and the IC_{50} values of each experiment were calculated using a linear regression plot. All the experiments were performed in triplicates.

Free radicals ($ABTS^{\bullet+}$) were produced by reacting ABTS (7 mM in H_2O) with $K_2S_2O_8$ in 1:1 ratio (stored in dark, 25℃, 12-16 h); later diluted with methanol to obtain the absorbance between 0.7-0.8 at 734 nm. For analysis, test samples of different concentrations (5 µL) were incubated (30 min) with diluted $ABTS^{\bullet+}$ solution (3.995 mL) and the absorbance was recorded at 734 nm. The percentage scavenging capacity of each concentration was calculated as per equation 1.

3.2. H_2O_2 scavenging assay

Multiple concentrations of FBE and DRE (50 µL) were incubated within the reaction mixture of $FeCl_3$ (100 mM, 100 µL), 2-deoxyribose (2.8 mM, 250 µL), EDTA (100 mM, 1:1 v/v), and H_2O_2 (200 mM, 50 µl); incubated (37℃, 60 min) followed by the addition of thiobarbituric acid (1% in NaOH (50 mM, 500 µl)) and trichloroacetic acid (2.8 %, 500 µl) and placed in boiling water bath (15 min); cooled and the absorbance was recorded at 532 nm. The percentage scavenging capacity of each concentration was calculated as per equation 1.

3.3. Total anti-oxidant capacity

Multiple concentrations of FBE and DRE samples (0.1 mL) were independently incubated in 1 mL of reagent (H_2SO_4; 0.6 M, Na_3PO_4; 28 mM, $(NH_4)_2MoO_4$; 4 mM) in a water bath (95℃, 90 min); cooled and absorbance was recorded at 765 nm against suitable control. The total antioxidant capacity of each concentration was calculated using equation 1.

3.4.NO scavenging capacity

Multiple concentrations of FBE and DRE (1 mL) was incubated (25℃) with $Na_2[Fe(CN)_5NO].2H_2O$ (10 mM, 1 mL) for 150 min followed by the addition of Griess reagent (1.0 mL, composes $C_6H_8N_2O_2S$ (1 %), $C_{12}H_{16}Cl_2N_2$ (0.1 %), H_3PO_4 (2%)) and the

absorbance was recorded at 546 nm. The NO scavenging capacity was calculated using equation 1.

3.5. CUPRAC assay

Different concentrations of FBE and DRE were independently incubated with CH_3COONH_4 buffer (1 M, 0.25 mL), neocuproine solution (0.25 mL) in ethanol, and $CuCl_2$ (0.01 M, 0.25 mL); volume was maintained up to 2 mL with distilled water; absorbance was recorded after 30 min at 450 nm; defined by the concentration-dependent change in absorbance. All the experiments were performed in triplicates. An IC_{50} of each experiment was calculated using a linear regression plot.

3.6. Metal chelating assay

Multiple concentrations of FBE and DRE (2 mL) was incubated with ferrozine (5 mM, 0.2 mL) and $FeCl_2$ (2 mM, 0.05 mL) and the volume was maintained up to 5 mL with methanol and incubated (25℃, 10 min); metal chelating capacity of each concentration was calculated using the following formula capacity was calculated using equation 1.

4. *In vitro* and *ex vivo* pharmacology of FBE and DRE against DM

4.1. Evaluation on in vitro α-glucosidase inhibitory activity

α-glucosidase inhibitory activity of FBE and DRE and associated fractions was performed as explained by Telagari & Hullatti[114] with minor modifications. Briefly, multiple concentrations of the test agents (0.5 mL) were incubated (25℃, 10 min) with α-glucosidase enzyme (1 U/mL, 0.1 mL) followed by the addition of p-NPG (3.0 mM, 0.05 mL); further incubated (37℃, 20 min). To this mixture, $NaHCO_3$ (0.1 M, 2 mL) was added; filtered to remove the residues of plant material and the absorbance was recorded at 405 nm. The percentage inhibition of α-glucosidase of an enzyme was calculated using the following formula

$$\%\ inhibitory\ activity = \left(1 - \frac{As}{Ac}\right) X100 \ldots\ldots\ldots \textbf{(2)}$$

where ***Ac*** and ***As*** refer to the absorbance of the control and test respectively. The IC_{50} values of each experiment were calculated using a linear regression plot. All the experiments were performed in triplicates.

4.2. Evaluation on in vitro α-amylase inhibitory activity

The α-amylase inhibitory activity of FBE and DRE and respective fractions was performed as explained by Telagari & Hullatti[114] with minor modifications. Briefly, multiple concentrations of test agents (0.25 mL) were incubated (25℃, 10 min) with α-amylase (500 µg/mL, 0.25 mL) followed by the addition of DNS reagent (0.5 mL); immersed in boiling water (10 min) and allowed to cool at room temperature. To this mixture, distilled water (5 mL) was added and filtered; filtrate absorbance was recorded at 540 nm. The percentage inhibition of α-amylase was calculated using equation 2.

4.3. Evaluation on in-vitro glucose adsorption capacity

Glucose adsorption assay of FBE and DRE and respective fractions was performed as explained by Ou *et al.*[123] with minor modifications in which multiple test samples (1 mL) was incubated (37℃, 6 h) with glucose solution (100 mM, 4 mL) and centrifuged to collect the supernatant; glucose concentration was measured *via* glucose peroxidation kit (ERBA glucose kits). The percentage glucose bound was calculated using the following formula

$$\%\ glucose\ bound\ = \left(1 - \frac{As}{Ac}\right) X100 \ldots\ldots\ldots \textbf{(3)}$$

where ***Ac*** and ***As*** refer to the absorbance of the control and test sample respectively and the AC_{50} values of each experiment were calculated using a linear regression plot. All the experiments were performed in triplicates.

4.4. Evaluation on ex vivo glucose uptake efficacy

A minor modification of Chattopadhyay *et al*.[165] protocol was implemented to evaluate the glucose uptake efficacy by FBE, DRE, and their fraction(s). Healthy fasted albino Wister rats were euthanized (overdosed with anesthetic ether), diaphragms were isolated; hemidiaphragm (100 *X* 100 mm^2) was incubated (37°C, 30 min) with the glucose solution (15 mL) and insulin with mild shaking. After 30 min, the glucose was estimated using the glucose peroxidation kit (ERBA glucose kits). The percentage glucose uptake was estimated using the following formula

$$\%\ glucose\ uptake = \left(1 - \frac{As}{Ac}\right) X100 \ldots\ldots\ldots \textbf{(4)}$$

where ***Ac*** and ***At*** indicate the absorbance of glucose prior and subsequent incubation of rat hemidiaphragm and the EC_{50} values of each experiment were calculated using a linear regression plot. All the experiments were performed in triplicates.

4.5. Effect on ex-vivo glucose permeation inhibitory capacity

Glucose permeation inhibitory assay of the FBE and DRE with their respective fraction(s) was performed as explained by Gallagher *et al*.[126] with minor modification of the apparatus (Figure 8); explained by Dixit *et al*.[127]. Briefly, glucose (40 mM, 0.5 mL), Tyrode's solution (1 mL), and test sample (160 mg/mL, 1 mL) were simultaneously introduced into rat jejunum (5 cm) to record the glucose appearance in the external solution which was sampled out at 0-180 min by maintaining the sink condition to quantify the glucose using glucose peroxidation kit (ERBA glucose kits). Finally, the total area under the curve (AUC) of glucose (0-180 min) was calculated using the trapezoidal rule. All the experiments were performed in triplicates.

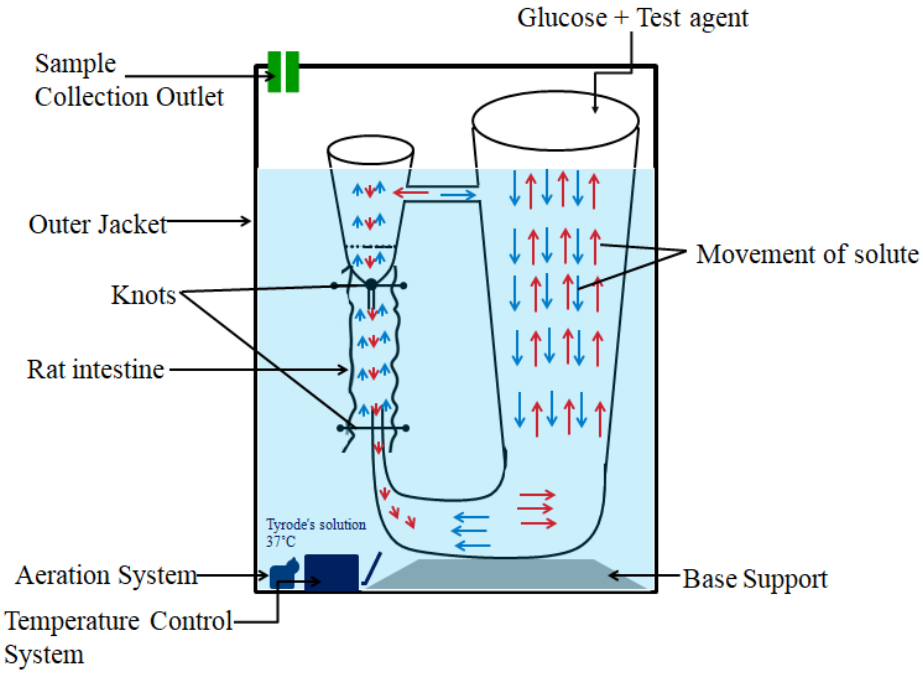

Figure 8: Instrument used to evaluate the efficacy of FBE and DRE in glucose permeability assay

5. *In vivo* pharmacology of FBE and DRE against DM

The FBE and DRE effect in deregulated glucose metabolism were evaluated in 2 different *in vivo* experimental animal models *i.e.* ***insulin-deficient*** (streptozocin & nicotinamide-induced hyperglycemia) and ***insulin-resistant*** (fructose-induced insulin resistance) after receiving ethical approval from IAEC of KLE College of Pharmacy Belagavi (resolution number: KLECOP/CPCSEA-Reg, No.221/Po/Re/S/2000/CPCSEA, Res.28-12/10/2019); animals were maintained in pathogen-free conditions throughout the study; the complete study is detailed below.

5.1. Acute oral toxicity of FBE and DRE

The therapeutic doses of FBE and DRE for *in vivo* study were selected after performing the acute oral toxicity (#OECD 423 guidelines). Since a single dose (2000 mg/kg) of FBE and DRE administration did not cause any death of animals for the next 14 days, 3 doses in geometric series *i.e.* 1/20 (100 mg/kg), 1/10 (200 mg/kg), and 1/5 (400 mg/kg) of 2000 mg/kg were considered for further study.

5.2. Induction of diabetes with streptozocin & nicotinamide and animals grouping

A minor modification of Masiello *et al.*[129] protocol was implemented to induce diabetes by the combined injection of streptozocin and nicotinamide. Briefly, streptozocin (65 mg/kg, *i.p.*) was injected after 15 min of nicotinamide (230 mg/kg, *i.p.*) injection by dissolving in citrate buffer (pH 4.5, chilled) and water for injection respectively. After 7 days of injection, fasting blood glucose level was measured; animals with >250 mg/dL were included in the study; an individual group comprised 3 cages with 2 animals in each (n=6 animals per group) for each test agent. Animals were categorized into 9 groups, including a total of 54 rats of which 48 were diabetic, and the rest of 6 served as healthy control. For treatment, FBE, DRE and glibenclamide were suspended in water for injection (vehicle) and administered *p.o.* for 28 days; detailed as (1) ***Normal***: vehicle-treated; (2) ***Diabetic***: vehicle-treated; ***(3) GLI50***: diabetic, glibenclamide (50 mg/kg)[166]-treated, *p.o.*; (4) ***FB100***: diabetic, FBE (100 mg/kg)-treated, *p.o.*; (5) ***FB200***: diabetic, FBE (200 mg/kg)-treated, *p.o.*; (6) ***FB400***: diabetic, FBE (400 mg/kg)-treated, *p.o.*; (7) ***DR100***: diabetic, DRE (100 mg/kg)-treated, *p.o.*; (8) ***DR200***: diabetic, DRE (200 mg/kg)-treated, *p.o.*; (9) ***DR400***: diabetic, DRE (400 mg/kg)-treated, *p.o.*

5.3. Induction of insulin resistance and animals grouping

Insulin resistance was induced *via* fructose supplementation in drinking water as detailed by Mamikutty *et al.*[132] with minor modifications. Briefly, fructose in drinking water was supplemented with normal chow for 54 days (10 %w/v for 42 days & 20 %w/v for next 12 days). After 54 days of fructose supplementation, OGTT was performed to confirm the insulin resistance by loading 4 g/kg of exogenous glucose and calculating the $AUC_{0\text{-}120\ min}$ of glucose. If the total AUC of glucose was significantly higher than the normal group at 95 % CI, 5% df, and $p<0.05$, animals were considered to be insulin resistant and included in the study. During the induction period, compromised food intake

and weight gain followed by enhanced fructose-supplemented water intake and mild polyurea were also noticed. Also, in this study an individual group comprised of 3 cages with 2 animals in each (n=6 animals per group) for each test agent.

Here, a total of 54 animals were grouped into 9 of which 48 were insulin resistant (IR) and 6 served as healthy control. FBE, DRE, and metformin were suspended in a vehicle (water) and 3 test doses of the FBE and DRE were administered for the next 30 days as (1) ***Normal***: vehicle-treated, *p.o.*; (2) ***IR***: vehicle-treated, p.o.; (3) MET45: IR, metformin (45 mg/kg)[167]-treated, *p.o.*; (4) ***FB100***: IR, FBE (100 mg/kg)-treated, *p.o.*; (5) ***FB200***: IR, FBE (200 mg/kg)-treated, *p.o.*; (6) ***FB400***: IR, FBE (400 mg/kg)-treated, *p.o.*; (7) ***DR100***: IR, DRE (100 mg/kg)-treated, *p.o.*; (8) ***DR200***: IR, DRE (200 mg/kg)-treated, *p.o.*; (9) ***DR400***: IR, DRE (400 mg/kg)-treated, *p.o.*

5.4. Measurements and methods

5.4.1. Measurement of body weight, food intake, and water intake

In both studies, 3 physical parameters *i.e.* body weight, food intake, and water intake were recorded. After the completion of 28 days (for insulin-deficient model) and 30 days (for insulin-resistant model) treatment, animals were fasted to perform OGTT and insulin tolerance test (ITT); ITT was performed only in the insulin-resistant model.

5.4.2. Performance of OGTT and ITT

After the treatment completion, animals fasted overnight with free access to drinking water followed by the performance of OGTT on the next day.

In both models, OGTT was performed as explained by Kumar *et al.*[168] by loading exogenous glucose (4 g/kg of fasting body weight, *p.o.*) and the blood glucose level (glucometer; Janaushadi, India) and plasma insulin level (Ray Biotech, USA) was recorded from 0-120 min at 30 min interval and the total AUC

$_{0\text{-}120\ min}$ of glucose and insulin were calculated *via* trapezoid rule. Additionally, for, insulin-resistant model HOMA-IR was calculated using the following formula

$$HOMA - IR = \frac{glucose\ level\ \left(\frac{mg}{dl}\right) X\ insulin\ level\ \left(\frac{\mu IU}{ml}\right)}{405}$$

After the performance of OGTT, in an insulin-resistant model, animals were free to access to feed for 5 h and again fasted overnight with free access to water. On the next day, ITT was performed as explained by Nair *et al*.[169] by injecting regular insulin (0.75 U/kg, *s.c.*) to record the blood glucose level 0-120 min at 30 min interval and the total AUC $_{0\text{-}120\ min}$ was calculated using the trapezoid rule.

5.4.3. Anesthesia and sample collection

After the execution of OGTT and ITT, blood samples were collected under surgical anesthesia using aesthetic ether *via* cardiac puncture; centrifuged to collect serum and plasma. Plasma was used to estimate the leptin (SPI bio, Germany) level and serum was used to assess lipid profile (TG, HDL, TC; ERBA commercial kits) in both models. The level of LDL and VLDL was calculated using the following formulae

$$VLDL = \frac{TG}{5}$$

$$LDL = TC - (HDL + VLDL)$$

5.4.4. Euthanasia and organ collection

After plasma and serum separation, animals were euthanatized with an overdose of anesthetic ether to collect pancreas (only in the insulin-deficient model), hemidiaphragm, liver, and skeletal muscle and washed with chilled phosphate buffer. The liver was sectioned into 2 halves; one part liver and whole

isolated pancreas were immersed into 10 % v/v formalin for histopathological examination. The 1 g of the second half of liver and skeletal (gastrocnemius) muscle were homogenized in chilled phosphate buffer, centrifuged and the supernatant was deep-freezed for further use.

5.4.5. Evaluation of glucose uptake in isolated rat hemidiaphragm

The freshly isolated rat hemidiaphragm was incubated in glucose solution (30 mM, 15 mL) in the presence of insulin (0.25 U); the glucose concentration was quantified by glucose peroxidation kit (ERBA glucose kits) after 15 min; percentage change in glucose in incubating medium was calculated using equation 4.

5.4.6. Estimation of hepatic and gastrocnemius muscle glycogen content

The hepatic and gastrocnemius muscle glycogen content was estimated using the anthrone method[170]. Tissue homogenate (1 mL) was treated with KOH (30 %w/v) in boiling water bath and centrifuged (15 min); volume (25 mL) was maintained with KOH (30% w/v); further, ethanol (95%, 10 mL) was added; allowed to overnight stand (25°C) overnight to precipitate glycogen; separated after centrifugation (3000 rpm, 15 min) to obtain pellet which was treated with anthrone reagent (4 mL) after dissolving in water (1 mL). Further, the content was incubated (10 min) in boiling water, and cooled; absorbance was recorded at 620 nm using a UV spectrophotometer (Shimadzu, UVProbe 2.4.3).

5.4.7. Estimation of hepatic enzymes in liver homogenate

To estimate hepatic ***hexokinase***, liver homogenate was incubated (30 min) in 0.5 mL of glucose buffer (glucose; 2.5 mM/L, K_2HPO_4; 0.01 mol/L, KCl; 77 mM/L, $MgCl_2$; 2.5 mM/L, NaF; 25 mM/L, Tris-HCl; pH 8.0, 0.03 M/L, ATP; 0.18 M/L, water; 0.45 mL) followed by glucose quantification[171] *via* glucose

peroxidation kit (ERBA glucose kits). To quantify ***G6Pase***, the liver homogenate was incubated (37℃, 1 h) in glucose-6-phosphate and citrate buffer; the reaction was terminated with trichloroethanoic acid (10%); centrifuged to quantify phosphorous in the supernatant. Later, solutions of ammonium molybdate (1 mL) and amino naphthol sulphonic acid (0.4 mL) were added over an aliquot of supernatant and incubated (20 min); produced blue color; absorbance was recorded at 680 nm[172]. To quantify ***FBPase***, liver homogenate was incubated (37℃, 5 min) in the mixture of EDTA (1 mM/L, 0.25 mL), KCl (0.1 M/L, 0.1 mL), $MgCl_2$ (0.1 m/L, 0.25 mL), substrate (0.05 M/L, 0.1 mL) and Tris-HCl buffer (0.1 M/L, pH 7.0, 1.2 mL); terminated with trichloroethanoic acid (10 %) and similar steps of G6Pase quantification was followed; produced blue color; absorbance was recorded at 680 nm[172]. Likewise, hepatic ***LDH*** activity was quantified *via* nicotinamide adenine dinucleotide coupled spectrophotometric method[173]. Also, 3 hepatic enzymes *i.e.* alanine aminotransferase (ALT; Erba Lab, India), aspartate aminotransferase (AST; Erba Lab, India) in serum, and phosphofructokinase (PFK; KinesisDx, USA) in liver homogenate, were quantified with strict manufacturer's instructions.

5.4.8. Estimation of enzymatic & non-enzymatic anti-oxidant biomarkers

The enzymatic & non-enzymatic anti-oxidant profiles of FBE and DRE in both models were quantified in liver homogenate (10% w/v, 0.5 mL) which are detailed below.

To assess the ***catalase activity***, the liver homogenate was treated with H_2O_2 (0.019 M/L, 1 mL) and change in absorbance within 0 & 60 sec was recorded at 240 nm[174]. Further, ***glutathione*** (***GSH***) ***level*** was quantified by incubating (30 min) the liver homogenate with Ellman's reagent and EDTA (20 mM/L) mixture

whose absorbance was recorded at 412 nm[175]. Likewise, the liver homogenate was incubated (10 min) with methanol and dithionitrobenzene (10 mM/L, 40 µL) and the absorbance was recorded at 412 nm to quantify the ***total thiols*** [175]. Further, to estimate ***superoxide dismutase*** (***SOD)***, the homogenate was treated with pyrogallol solution (2.5 mg/mL, 0.1 mL) and Tris-HCl buffer (0.05 M/L, 2.9 mL) mixture; change in absorbance of the whole mixture was recorded within 90 & 120 sec at 420 nm[176]. Also, ***lipid peroxidation*** was assessed by incubating (95℃, 15 min) liver homogenate within the mixture of trichloroacetic acid (15%), HCl (5 gm/L), and thiobarbituric acid (0.375% w/v); cooled and centrifuged to record the absorbance at 512 nm; presented as thiobarbituric acid reactive substances (TBARS) nmol/mg of protein[177].

5.4.9. Histopathological examination of liver and pancreas

For the histopathological examination, tissue samples were sectioned (4 µM) and were fixed with formalin (10% v/v); stained with hematoxylin and eosin to assess the effect of FBE and DRE over hepatic kupffer cell hyperplasia, venous congestion, portal triditis, ballooning degeneration, apoptosis, sinusoidal congestion, spotty necrosis, cholestasis, and inflammation and pancreatic β- cell size and count, lymphocytic infiltration, vascular degeneration and congestion at 40 X magnification.

6. Statistical analysis

For, *in silico* pharmacology, the protein-protein interaction regulated KEGG pathways were interpreted based on the gene count and the false discovery rate. The bioactives-proteins-pathways interaction was evaluated based on edge count. Lead hits of particular activity were interpreted using binding energy (kcal/mol) and *H*-bond interaction(s). All the experimental data were presented in mean±SD/SEM wherever applicable. One-way or

two-way analysis of variance (ANOVA) followed by posthoc Tukey's test or Bonferroni test were used to evaluate the quantitative data. Further, the Kruskal-Wallis tests followed by Dunn's test were used to evaluate the categorical data. Both quantitative and categorical data were evaluated using GraphPad Prism (Version 5; GraphPad Software Corporation, San Diego California, USA).

Chapter 5

Results

RESULTS

1. *In silico, in vitro, ex vivo,* and *in vivo* pharmacology of *F. benghalensis* bark against DM

1.1.In silico pharmacology of F. benghalensis

1.1.1. Network pharmacology of phytoconstituents from F. benghalensis

A total of 21 phytoconstituents from *F. benghalensis* under multiple phytochemistry *i.e.* triterpenoids, isoflavone, flavonoid, phytosterols, ceramide, furocoumarins, and the organic molecular entity were identified; targeted multiple proteins. These proteins interacted to regulate 51 pathways in which 13 were directly concerned within the pathogenesis of DM. Among them, the PI3K-Akt pathway was predicted to be majorly modulated *via* the regulation of the highest number (8) of gene set *i.e. KIT, CDK6, IKBKB, PRKCA, RXRA, GSK3B, IGF1, ITGA4* at the false discovery rate 0.00028. Additionally, though the Ca^{2+} signaling pathway was predicted to regulate 7 genes (*PRKCA, 5HTR2A, HTR2B, HTR2C, HTR4, HTR7, ADORA2A*), it was presented with the lowest false discovery rate *i.e.* 6.27E-05 (Table 1).

The phytoconstituent(s)-target(s)-pathway(s) network included the 99 nodes (65 + 21 + 13 as targets + phytoconstituents + pathways) and 228 edges (48 for targets *vs* pathways and 180 for phytoconstituents *vs* targets) in which PTP1B was majorly targeted by 9 phytoconstituents *i.e.* ***3',4',5,7- tetrahydroxy-3-methoxyflavone*** (1), ***isowighteone*** (2), ***mucusisoflavone A*** (3), ***mucusisoflavone C*** (4), ***psoralen*** (5), ***sitosterol*** (6), ***ursolic acid*** (7), ***wighteone*** (8), and ***α-amyrin*** (9); Figure 9.

Table 1: KEGG pathway analysis of proteins interaction regulated by phytoconstituents of *F. benghalensis*

Pathway ID	Pathway Description	Gene count	Genes	False Discovery Rate
4020	Calcium signaling	7	PRKCA, 5HTR2A, HTR2B, HTR2C, HTR4, HTR7, ADORA2A	6.27E-05
52	Galactose metabolism	4	AKR1B10,AKR1B1, SI, GAA	8.87E-05
4976	Bile secretion	5	SLCO, ABCB1, RXRA, SLCO1B1, HMGCR	8.87E-05
4151	PI3K-Akt signaling	8	KIT, CDK6,IKBKB, PRKCA, RXRA, GSK3B, IGF1, ITGA4	0.00028
5212	Pancreatic cancer	3	IKBKB, CDK6, CDKN2A	0.0103
4920	Adipocytokine signaling	3	RXRA, PPARA, IKBKB	0.0121
3320	PPAR signaling	3	RXRA, PPARA, PPARG	0.0123
100	Steroid biosynthesis	2	LSS, DHCR7	0.0156
51	Fructose and mannose metabolism	2	AKR1B10, AKR1B1	0.0325
4152	AMPK signaling	3	IGF1, PPARG, HMGCR	0.0402
620	Pyruvate metabolism	2	AKR1B10, AKR1B1	0.0423
4910	Insulin signaling	3	IKBKB, PTPN1, GSK3B	0.0482
4930	T2DM	2	IKBKB, PRKCD	0.0497

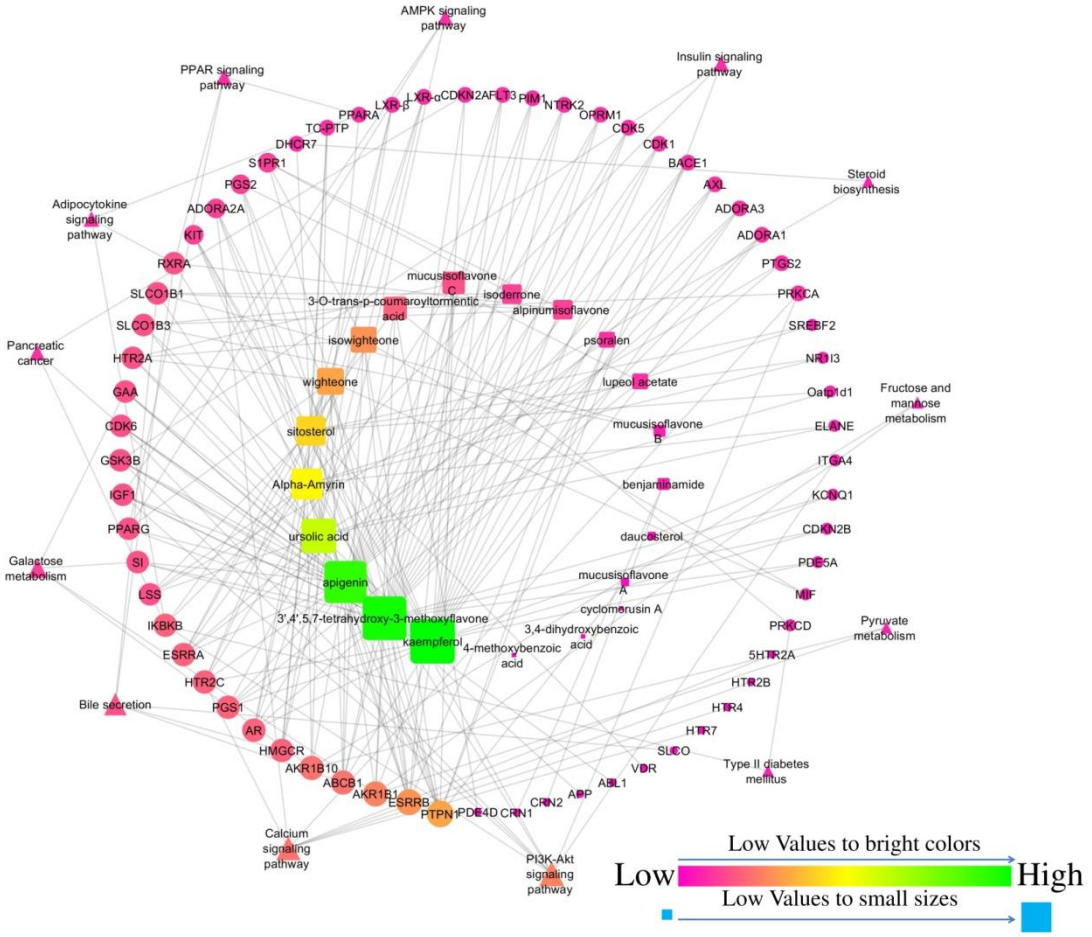

Figure 9: Interaction of phytoconstituents and proteins with respective pathways. In the network square, circle andtriangle represent phytoconstituents, targets, and pathways respectively.

1.1.2. Prediction of druglikeness score of phytoconstituents from F. benghalensis

Among the ChEBI recorded phytoconstituents of *F. benghalensis*, 85.71% had a positive druglikeness score; ***wighteone*** was predicted to possess the highest druglikeness score (1.23) as explained by "*Lipinski rule of 5*" with a 338.12 molecular weight, 5 *H*-bond acceptors, 3 *H*-bond donors, and 4.45 MolLogP. Compounds with positive druglikeness scores are summarized in Table 2.

Table 2: Druglikeness score of phytoconstituents from *F. benghalensis*

Phytoconstituents	Phytochemistry	MF	MW	NHBA	NHBD	MolLogP	DLS
3-O-trans-p-coumaroyltormentic acid	Triterpenoid	$C_{39}H_{54}O_7$	634.39	7	4	8.47	1.1
alpinumisoflavone	Isoflavanones	$C_{20}H_{16}O_5$	336.10	5	2	4.06	0.4
mucusisoflavone A	Isoflavone	$C_{40}H_{32}O_{10}$	672.20	10	6	8.06	0.94
mucusisoflavone B	Isoflavone	$C_{40}H_{32}O_{10}$	672.20	10	5	8.91	0.91
mucusisoflavone C	Isoflavone	$C_{40}H_{34}O_{10}$	674.22	10	6	8.31	1.07
isoderrone	Isoflavone	$C_{20}H_{16}O_5$	336.10	5	2	4.18	0.27
isowighteone	Isoflavone	$C_{20}H_{18}O_5$	338.12	5	3	4.57	0.97
lupeol acetate	Triterpenoid	$C_{32}H_{52}O_2$	468.40	2	0	9.45	0.32
apigenin	Flavone	$C_{15}H_{10}O_5$	270.05	5	3	3.06	0.77
3',4',5,7-tetrahydroxy-3-methoxyflavone	Flavonol	$C_{16}H_{12}O$	316.06	7	4	2.46	0.93
kaempferol	Flavonol	$C_{15}H_{10}O_6$	286.05	6	4	2.49	0.77
3,4-dihydroxybenzoic acid	Organic molecular entity	$C_7H_6O_4$	154.03	4	3	0.93	0.74
cyclomorusin A	Flavonoid	$C_{25}H_{22}O_6$	418.14	6	2	5.63	0.07
wighteone	Isoflavone	$C_{20}H_{18}O_5$	338.12	5	3	4.45	1.23
daucosterol	Steroid saponin	$C_{35}H_{60}O_6$	576.44	6	4	7.13	0.51
ursolic acid	Triterpenoid	$C_{30}H_{48}O_3$	456.36	3	2	7.84	0.65
sitosterol	Phytosterols	$C_{29}H_{50}O$	414.39	1	1	9.48	0.88
α-amyrin	Triterpene	$C_{30}H_{50}O$	426.39	1	1	9.21	0.09

MF: Molecular formula, **MW**: Molecular weight, **NHBA**: Number of hydrogen bond acceptor(s), **NHBD**: Number of hydrogen bond donor(s), **DLS**:Druglikeness score

1.1.3. Molecular docking of phytoconstituents from F. benghalensis against α-amylase, α-glucosidase, and PTP1B

PASS predicted ***3, 4-dihydroxybenzoic acid*** (1), ***4-methoxybenzoic acid*** (2), ***apigenin*** (3), ***daucosterol*** (4), ***kaempferol*** (5), and ***psoralen*** (6) as α-amylase inhibitors in which ***daucosterol*** was predicted to possess the highest binding affinity (binding energy -9.3 kcal/mol) with α- amylase; however, had no *H*-bond interactions (Figure 10); Likewise, the order of finding affinity of phytoconstituents with α-amylase was ***daucosterol*** > ***apigenin*** > ***kaempferol*** > ***psoralen*** > ***4-methoxy***

benzoic acid > ***3,4-dihydroxybenzoic acid*** (Table 3).

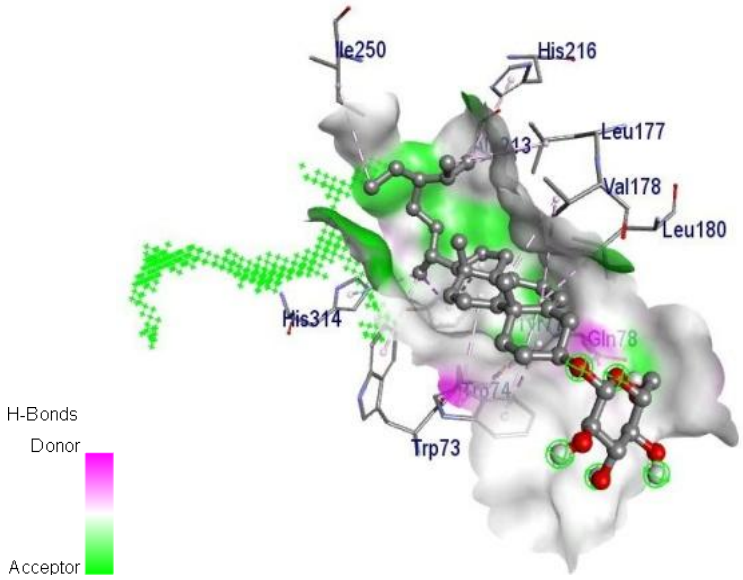

Figure 10: Interaction of *daucosterol* with α-amylase. All the bonds presented indicate hydrophobic interactions

Table 3: Binding affinity of each phytoconstituents from *F. benghalensis* with α-amylase

Ligand	Binding affinity (kcal/mol)	NHB	Hydrogen bond residues
3, 4-dihydroxybenzoic acid	-5.5	4	Arg398, Asp402, Ser289
4-methoxybenzoic acid	-5.6	2	Arg195, Asp197
Apigenin	-8.5	2	Gln63, Glu233
Daucosterol	-9.3	-	-
Kaempferol	-8.4	3	Tyr62, Gln63, Glu233
Psoralen	-6.7	1	Gln63

NHB: Number of *H*-bonds

Likewise, ***mucusisoflavone A*** (1)**,** ***mucusisoflavone B*** (2)**,** ***amyrin*** (3), ***ursolic acid*** (4), ***mucusisoflavone C*** (5), ***isoderrone*** (6), ***cyclomorusin A*** (7), ***daucosterol*** (8), ***isowighteone*** (9), ***lupeol acetate*** (10), ***wighteone*** (11), ***3', 4', 5, 7-tetrahydroxy-3-methoxyflavone*** (12), ***apigenin*** (13), ***kaempferol*** (14), ***psoralen*** (15), ***3, 4-dihydroxybenzoic acid*** (16), and ***4-methoxybenzoic acid*** (17) were predicted as α-glucosidase inhibitors; ***mucusisoflavone A*** was predicted as a potential molecule with a highest binding affinity (binding energy -10.8 kcal/mol) *via* 3 *H*-bond interactions with Tyr360 and Glu866 (Figure 11). Further, the binding affinity order of phytoconstituents with α-glucosidase was ***mucusisoflavone A*** > ***mucusisoflavone B*** >

amyrin > ***ursolic acid*** > ***mucusisoflavone C*** > ***isoderrone*** > ***cyclomorusin A*** > ***daucosterol*** > ***isowighteone*** = ***lupeol acetate*** > ***wighteone*** > ***3', 4', 5, 7-tetrahydroxy-3-methoxyflavone*** > ***apigenin*** > ***kaempferol*** > ***psoralen*** > ***3, 4-dihydroxybenzoic acid*** > ***4-methoxybenzoic acid*** (Table 4).

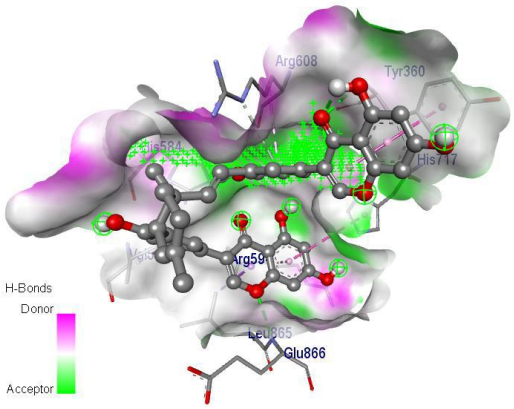

Figure 11: Interaction of *mucusisoflavone A* with α-glucosidase. Green bond indicates *H*-bonds whereas the rest of the other bonds indicate hydrophobic interactions

Table 4: Binding affinity of each phytoconstituents from *F. benghalensis* with α-glucosidase

Ligand	Binding affinity (kcal/mol)	NHB	Hydrogen bond residues
3', 4', 5, 7-tetrahydroxy-3-methoxyflavone	-7.7	3	Gln118, Gln121
3, 4-dihydroxybenzoic acid	-6.2	7	Gln118, Ala93, Asp91, Cys127, Trp126, Ile98
4-methoxybenzoic acid	-5.7	1	Gln118
Apigenin	-7.4	3	Trp126, Ile98, Gln118
Daucosterol	-8.6	2	Pro541, Gly550
Isoderrone	-8.9	1	Tyr543
Isowighteone	-8.2	2	Arg585, Val358
Kaempferol	-7.3	3	Trp126, Gln118
Psoralen	-7.2	2	Gly123, Gln118
Wighteone	-8.1	2	Val544, Asp91
Amyrin	-9.6	-	-
Cyclomorusin A	-8.8	3	Tyr543, Pro94, Gln118
Lupeol acetate	-8.2	2	Glu866, Val867
Mucusisoflavone A	-10.8	3	Tyr360, Glu866
Mucusisoflavone B	-9.8	2	Pro94, Ala93
Mucusisoflavone C	-9.3	1	Tyr360
Ursolic acid	-9.5	1	Gly123

NHB: Number of *H*-bonds

Further, all the predicted α-glucosidase inhibitors were also identified as PTP1B inhibitors by PASS in which docking study predicted ***3-O-trans-p-***

coumaroyltormentic acid (1) and ***ursolic acid*** (2) were predicted as potential PTP1B inhibitors as possessed highest binding affinity *i.e.* binding energy -8.7 kcal/mol *via* 2 *H*-bonds with Ala217 and Gly183 and 3 *H*-bonds with Arg221, Gln266 and Asp48 respectively (Figure 12). Further the order of the binding affinity with PTP1B was ***3-O-trans-p-coumaroyltormentic acid*** = ***ursolic acid*** > ***mucusisoflavone C*** > ***amyrin*** > ***lupeol acetate*** > ***mucusisoflavone A*** > ***cyclomorusin A*** > ***isoderrone*** > ***apigenin*** > ***alpinumisoflavone*** > ***kaempferol*** > ***wighteone*** > ***isowighteone*** > ***3', 4', 5, 7-tetrahydroxy-3-methoxyflavone*** > ***psoralen*** > ***3, 4-dihydroxybenzoic acid*** > ***4-methoxybenzoic acid*** (Table 5).

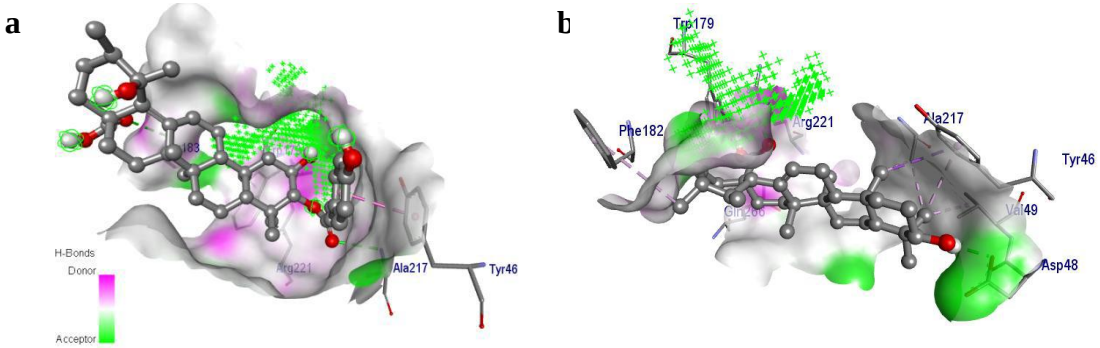

Figure 12: Interaction of (a) *3-O-trans-p-coumaroyltormentic acid* and (b) *ursolic acid* with PTP1B. Green bond indicates *H*-bond interaction(s) whereas the rest of the other bonds indicate hydrophobic interactions

Table 5: Binding energy of each phytoconstituents from *F. benghalensis* with PTP1B

Ligand	Binding affinity (kcal/mol)	NHB	Hydrogen bond residues
3', 4', 5, 7-tetrahydroxy-3-methoxyflavone	-7	5	Arg221, Gln266, Asp48
3, 4-dihydroxybenzoic acid	-5.2	2	Ser50, Lys36
3-O-trans-p-coumaroyltormentic acid	-8.7	2	Ala217, Gly183
4-methoxybenzoic acid	-5.1	2	Ser205, Val211
Alpinumisoflavone	-7.7	1	Ser80
Apigenin	-7.8	2	Arg221, Asp48
Isoderrone	-7.9	2	Arg221, Ser216
Isowighteone	-7.6	2	Ser80, Ser205
Kaempferol	-7.7	2	Glu115, Asp48
Psoralen	-6.1	-	-
Wighteone	-7.7	1	Arg221
Amyrin	-8.3	1	Cys215
Cyclomorusin A	-8.1	3	Trp179, Gln266, Arg221
Lupeol acetate	-8.3	1	Asn162
Mucusisoflavone A	-8.3	5	Arg221, Gly183, Lys116, Gly220, Gln266
Mucusisoflavone C	-8.6	3	Asp181, Pro180, Gln266
Ursolic acid	-8.7	3	Arg221, Gln266, Asp48

NHB: Number of *H*-bonds

1.1.4. Molecular docking of phytoconstituents from F. benghalensis against free radical generators

Among the top 3 hits of PASS-predicted anti-oxidant phytoconstituents from *F. benghalensis*; ***3-O- trans-p-coumaroyltormentic acid*** had the highest binding affinity with myeloperoxidase (binding energy -10.9 kcal/mol) *via* 1 *H*-bond with Ala389. Further, ***mucusisoflavone C*** was predicted to possess the highest binding affinity (-11.1 kcal/mol) with NAD(P)H oxidase *via* 4 *H*-bonds with Asn343, Ser328, and Ser326. Also, ***wighteone*** possessed the highest binding affinity (binding energy -9.3 kcal/mol) with NAD(P)H oxidase *via* 1 *H*-bond with Lys134 (Figure 13). The binding affinity and mode of interaction of each anti-oxidant with an individual target are presented in Table 6.

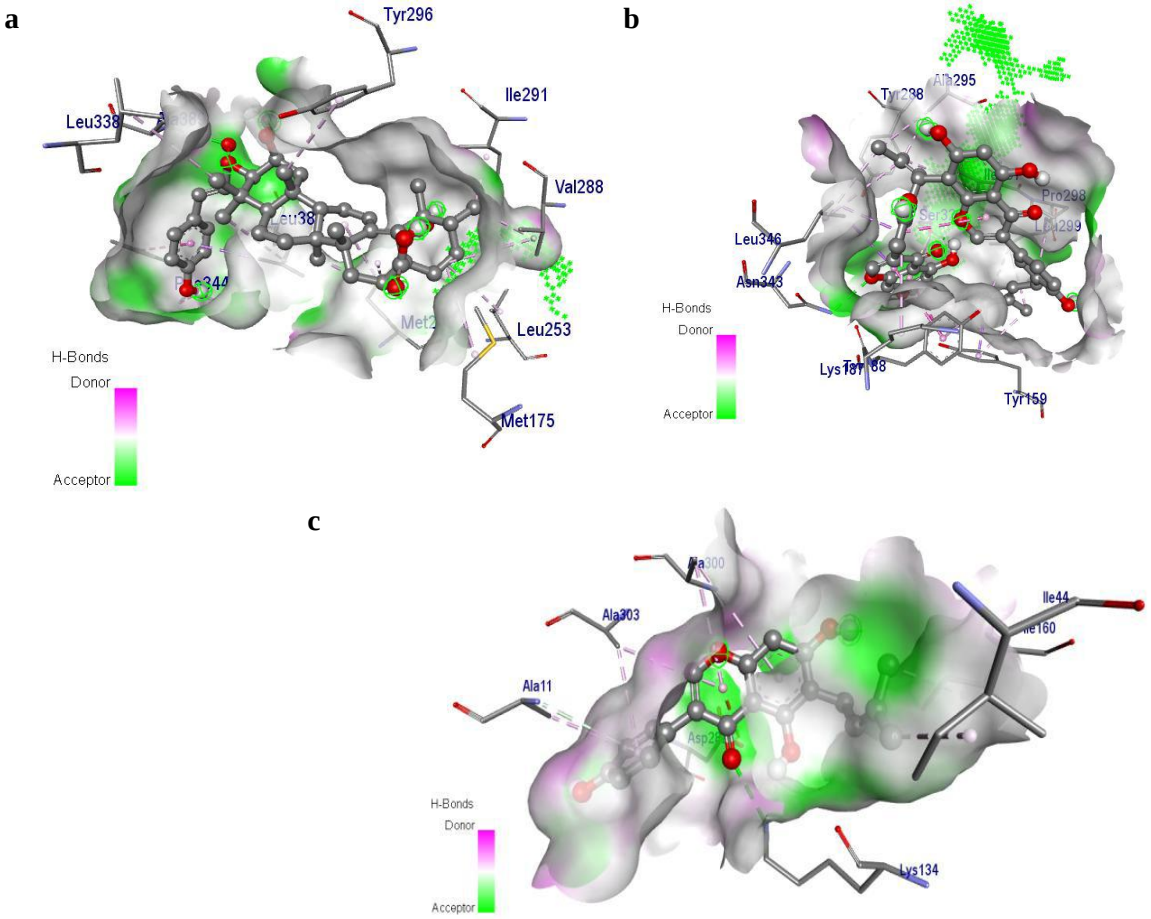

Figure 13: Interaction of (a) *3-O-trans-p-coumaroyltormentic acid* with myeloperoxidase, (b) *mucusisoflavone C* and (c) *wighteone* with NAD(P)H oxidase. Green bond indicates *H*-bond interaction(s) whereas the rest of the other bonds indicate hydrophobic interactions

Table 6: Binding affinity of each phytoconstituents from *F. benghalensis* with targets related to ROS system

Targets		Phytoconstituents		
		C1	C2	C3
Lipoxygenase (PDB: 1N8Q)	BA	-9	-10.6	-2.6
	NHB	3	2	2
	HBR	Arg786, Gly265, Asn146	Thr274, Asm556	Thr274
Myeloperoxidase (PDB: 1DNU)	BA	-10.9	-10.4	-8.1
	NHB	1	3	1
	HBR	Ala389	Thr292,Thr296, Thr168	Glu245
Xanthine oxidase (PDB: 3NRZ)	BA	-8.4	-7.7	-6.5
	NHB	2	3	1
	HBR	Gln102, Lys95	Asn71, Thr52, Asn146	Glu89
Cytochrome P450 (PDB:1OG5)	BA	-8.4	-10.6	-8.9
	NHB	2	2	3
	HBR	Tyr42, Arg377	Thr30, Gly296	Phe47, Leu20, Gln214
NAD(P)H oxidase (PDB:2CDU)	BA	-9.8	-11.1	-9.3
	NHB	1	4	1
	HBR	Glu163	Asn343, Ser328, Ser326	Lys134

C1: ***3-O-trans-p- coumaroyltormentic acid***, **C2:** ***mucusisoflavone C***, **C3:** ***wighteone***, **BA**: Binding affinity (binding energy in kcal/mol), **NHB**: Number of Hydrogen Bonds, **HBR**: Hydrogen Bond residues

1.1.5. Molecular docking of phytoconstituents from F. benghalensis against the enzymes involved in the glucose catabolism and anabolism

Based on docking score and *H*-bond interactions, majorly ***mucusisoflavone A*** (1) and ***mucusisoflavone B*** (2) were predicted to possess the highest binding affinity with FBPase, PFK, G6Pase, LDH, and hexokinase. Similarly, ***Mucusisoflavone B*** possessed the highest binding affinity (binding energy -10.0 kcal/mol) with FBPase *via* 2 *H*-bonds with Val49, Tyr168. Also, it showed the highest binding affinity (binding energy -9.7 kcal/mol) with G6Pase *via* 1 *H*-bond with Pro84. In addition, among all the phytoconstituents, ***Mucusisoflavone B*** scored the highest binding affinity (-10.4 kcal/mol) with hexokinase *via* 2 *H*-bonds with His467 and Phe766. Likewise, ***Mucusisoflavone A*** showed the highest binding affinity (binding energy -10.7 kcal/mol) with LDH *via* 5 *H*-bonds with Glu191, Asp194, Val234, Arg168, Thr247. Also, it had the highest binding affinity (binding energy -11.8 kcal/mol) with PFK *via* 4 *H*-bonds with Asp236, Tyr385, Asp226, Arg246 (Figure 14).

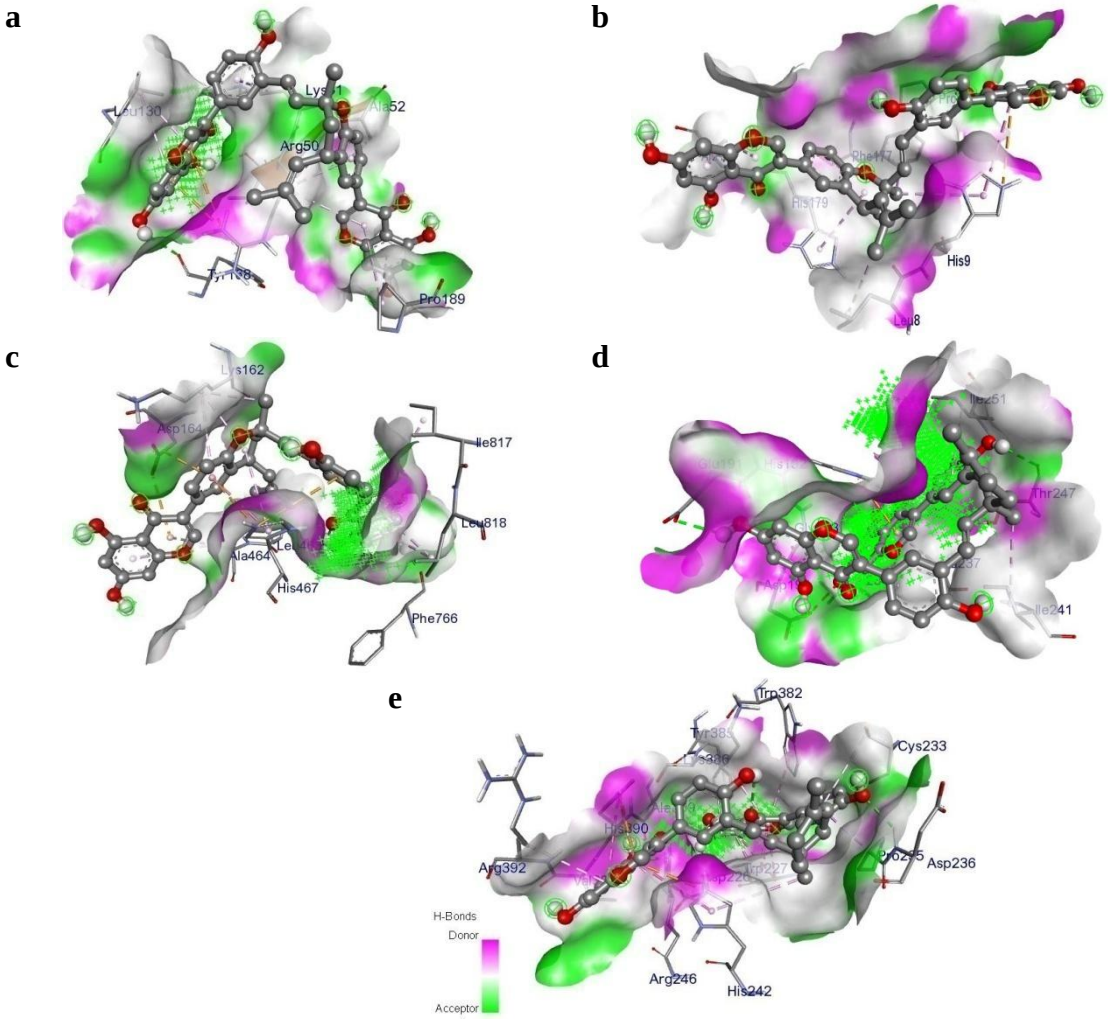

Figure 14: Interaction of *mucusisoflavone B* with (a) FBPase, (b) G6Pase, and (c) hexokinase and *mucusisoflavone A* with (d) LDH and (e) PFK. Green bond indicates *H*-bond interaction(s) whereas the rest of the other bonds indicate hydrophobic interactions

1.2. Preliminary phytochemical evaluation of FBE

FBE composed the multiple secondary phytoconstituents under various phytochemistry *i.e.* flavonoids, polyphenols, saponins, alkaloids, and triterpenes. The total polyphenols and flavonoids content were found to be (23.2±0.6) µg/mL and (100.24±4.21) µg/mL equivalent to gallic acid and rutin respectively.

1.3. HPLC analysis of FBE

The amount of quercetin and apigenin in FBE was found to be 0.41% and 0.39% respectively. HPLC chromatograms of apigenin, quercetin, and FBE are presented in Figure 15.

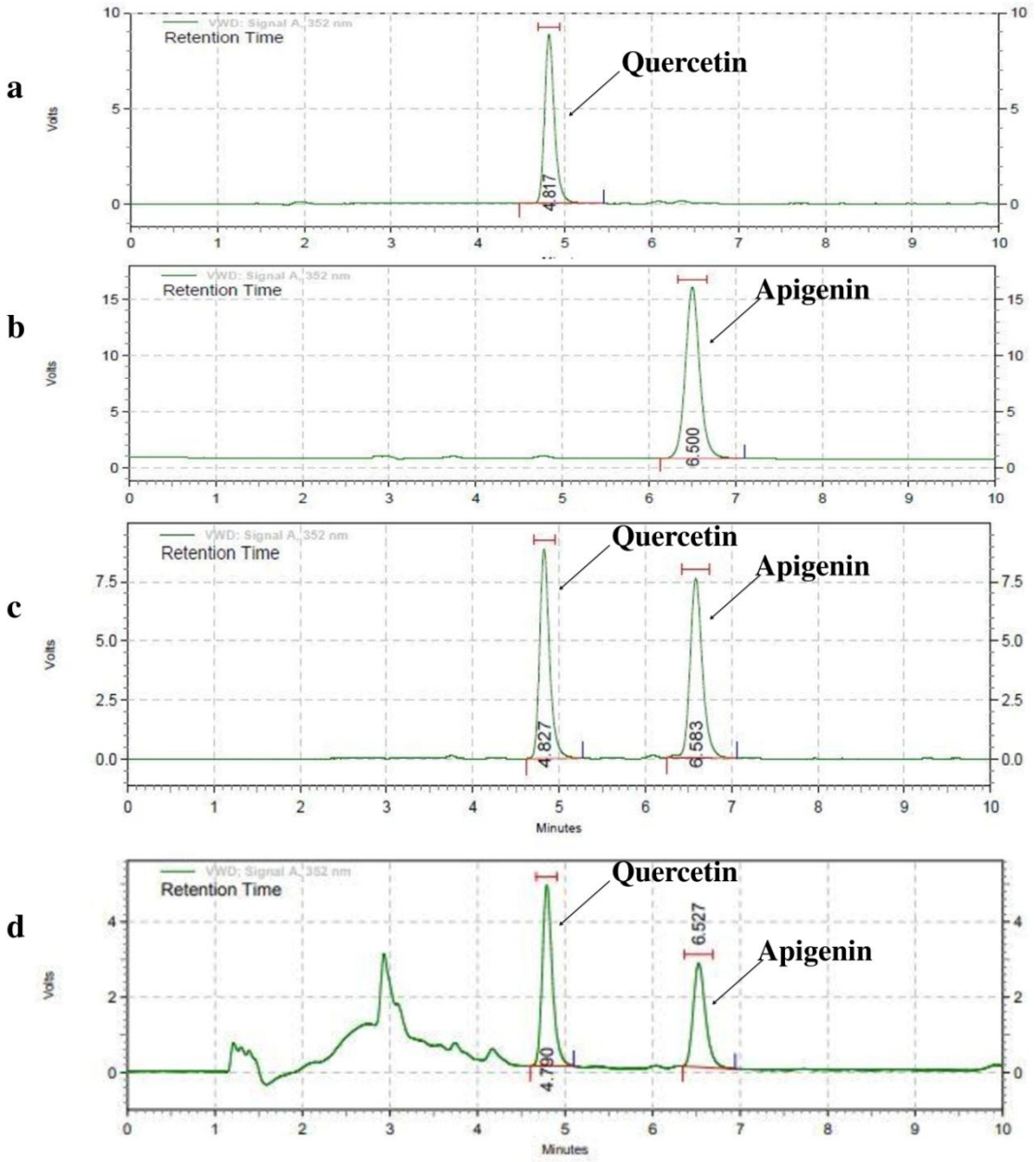

Figure 15: HPLC chromatograms for (a) *quercetin*, (b) *apigenin*, (c) simultaneous run for quercetin and apigenin, and (d) FBE

1.4. In-vitro antioxidant potential of FBE

Among 7 different anti-oxidant activities, FBE was identified to possess the highest ABTS scavenging capacity *i.e.* IC_{50} (45.73±1.17) µg/mL comparable with gallic acid *i.e.* IC_{50} (30.75±1.6) µg/mL. The order of anti-oxidant potential of FBE on various models was as ABTS free radical scavenging capacity > H_2O_2 scavenging capacity > total anti-oxidant capacity > CUPRAC > metal chelating capacity > NO scavenging capacity >

DPPH scavenging capacity (Table 7).

Table 7: *In vitro* anti-oxidant activity of FBE

***In-vitro* anti-oxidant models**	**IC_{50} (µg/mL)**			
	FBE	**Reference compounds**		
		gallic acid	**EDTA**	**ascorbic acid**
DPPH scavenging assay	73.99±2.22	-	-	25.88±4.847
H_2O_2 scavenging assay	50.67±1.77	-	-	47.71±0.71
NO scavenging assay	69.02±2.57	55.66±0.64	-	-
Total anti-oxidant capacity	51.45±1.23	-	-	-
CUPRAC assay	55.51±0.54	-	-	38.02±2.25
Metal chelating Assay	55.95±0.92	-	23.12±2.16	-
ABTS scavenging assay	45.73±1.17	30.75±1.64	-	-

All data are expressed in Mean ±SD, **IC_{50}**: Inhibitory concentration 50, **EDTA**: Ethylenediamine tetraacetic acid

1.5.In vitro and ex-vivo anti-diabetic pharmacology of FBE and its fractions

1.5.1. In vitro α-glucosidase inhibitory activity of FBE and its fractions

Among the FBE and its fractions *i.e.* FBE_flavonoid, FBE_polyphenol, FBE_alkaloid, and FBE_steroid of *F. benghalensis*, FBE_flavonoids had the highest α-glucosidase inhibitory activity; IC_{50} (316.97±5.03) µg/mL. The order of the inhibition of the α-glucosidase was FBE_flavonoid > FBE_polyphenol > FBE_alkaloid > FBE_steroid > FBE (Table 8); α-glucosidase inhibition by each concentration of individual test agent is presented in Figure 16.

1.5.2. In vitro α-amylase inhibitory activity of FBE and its fractions

Among the test agents of FBE and associated fractions *i.e.* FBE_flavonoid, FBE_polyphenol, FBE_alkaloid, and FBE_steroid of *F. benghalensis*, FBE_flavonoid possessed the highest α-amylase inhibitory activity; IC_{50} (388.39±1.94) µg/mL. Further, the order of α-amylase inhibition was FBE_flavonoid > FBE_alkaloid > FBE_polyphenol > FBE_sterol > FBE (Table 8); α-amylase inhibition by each concentration is presented in Figure 16.

Table 8: α-glucosidase and α-amylase inhibitory activity of FBE and its fractions

Test samples	IC_{50} (µg/mL)	
	α-glucosidase	α-amylase
FBE	552.33±2.96	745.44±8.08
FBE_flavonoid	316.97±5.03	388.39±1.94
FBE_polyphenol	443.24±5.99	657.23±8.29
FBE_alkaloid	511.0±5.85	621.97±9.55
FBE_steroid	519.76±8.97	855.68±4.70
Acarbose*	78.43±0.86	71.28±0.45

All data are expressed in Mean ±SD, **IC_{50}**: Inhibitory concentration 50, *Gold standard as α-glucosidase and α-amylase inhibitor,

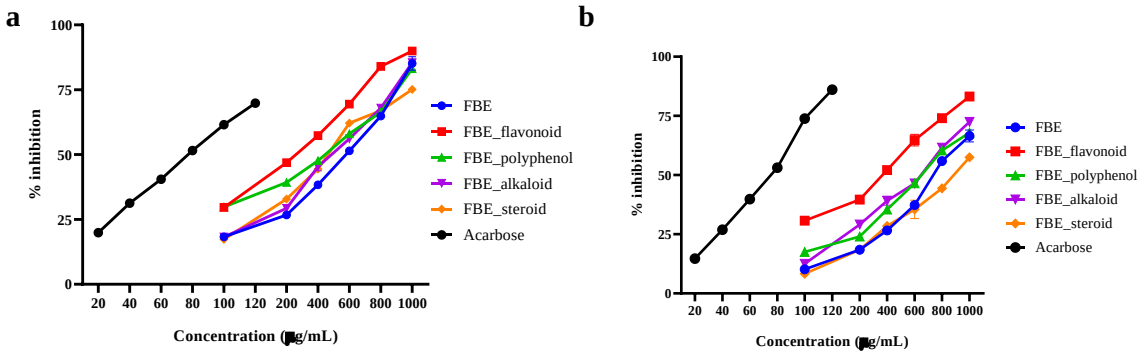

Figure 16: (a) α-glucosidase and (b) α- amylase inhibitory activity of FBE and its fractions

1.5.3. In vitro glucose adsorption assay of FBE and its fractions

FBE possessed the highest glucose absorptivity at an AC_{50} of 84.44±1.65 µg/mL compared to other fractions. The order of the test agents for the glucose adsorption was FBE > FBE_steroid > FBE_polyphenol > FBE_flavonoid > FBE_alkaloid (Table 9).

Table 9: Glucose adsorptivity of FBE its fractions

Test agents	AC_{50}
FBE	84.44±1.65
FBE_steroid	142.35±4.53
FBE_polyphenol	165.47±13.59
FBE_flavonoid	283.77±3.81
FBE_alkaloid	248.45±12.31
Cellulose*	76.25±0.67

All data are expressed in Mean ±SD, **AC_{50}**: Adsorption coefficient 50, *Gold standard for the glucose adsorption assay

1.5.4. Ex vivo glucose uptake assay of FBE and its fractions in isolated rat hemidiaphragm

Among all the fractions and FBE, FBE_flavonoid had the highest efficacy to

enhance the glucose uptake in isolated rat hemidiaphragm with an EC_{50} (335.71±10.15) µg/mL. Further, the order of test agents with their EC_{50} was FBE_flavonoid > FBE_polyphenol > FBE_steroid > FBE_alkaloid > FBE (Table 10).

Table 10: Glucose uptake efficacy of FBE fractions in isolated rat hemidiaphragm

Test Agents	EC_{50}
FBE_flavonoid	335.71±10.15
FBE_polyphenol	499.20±2.75
FBE	692.87±3.33
FBE_alkaloid	682.16±3.71
FBE_steroid	641.76±2.63
Metformin*	169.38±2.44

All data are expressed in Mean ±SD, **EC_{50}**: Effective concentration 50, *Gold standard used for glucose uptake assay in isolated rat hemidiaphragm

1.5.5. Ex vivo glucose permeability assay of FBE and its fractions in rat jejunum

FBE was identified to possess the highest efficacy to inhibit glucose diffusion compared to the rest of the fractions. The order of inhibiting glucose diffusion was FBE > FBE_polyphenol > FBE_flavonoid > FBE_flavonoid > FBE_alkaloid > FBE_steroid (Figure 17).

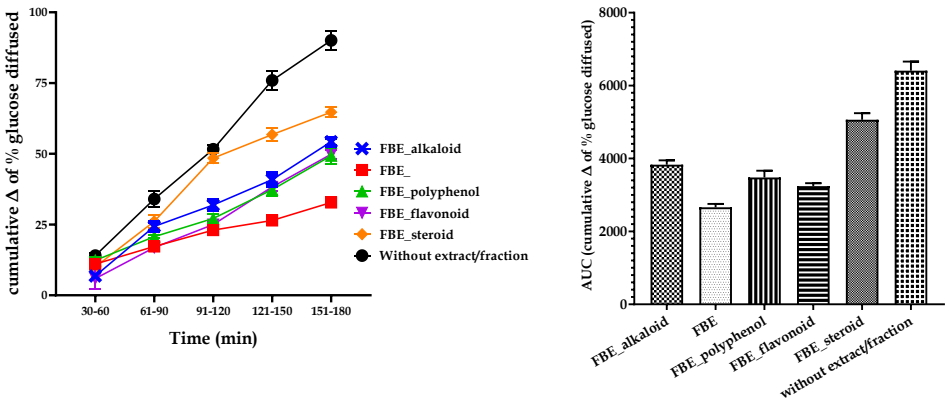

Figure 17: Effect of FBE and its fractions over the total AUC $_{0\text{-}180\ min}$ of glucose

1.6.In vivo anti-diabetic pharmacology of FBE

1.6.1. Effect of FBE in streptozocin-nicotinamide induced DM

- ***Effect of FBE on body weight, food intake, and water intake in streptozocin-nicotinamide induced DM***: Significant decrease ($p<0.001$) in body weight (Figure 18)

and food intake (Figure 19) was observed after diabetes induction compared to normal which was significantly reversed ($p<0.001$) with glibenclamide (50 mg/kg) and FBE (100, 200, and 400 mg/kg) treatment. In contrast, a significant increase ($p<0.01$) in water intake (Figure 20) was observed within the diabetic group which was significantly reversed ($p<0.05$, 0.001) with glibenclamide and FBE treatment.

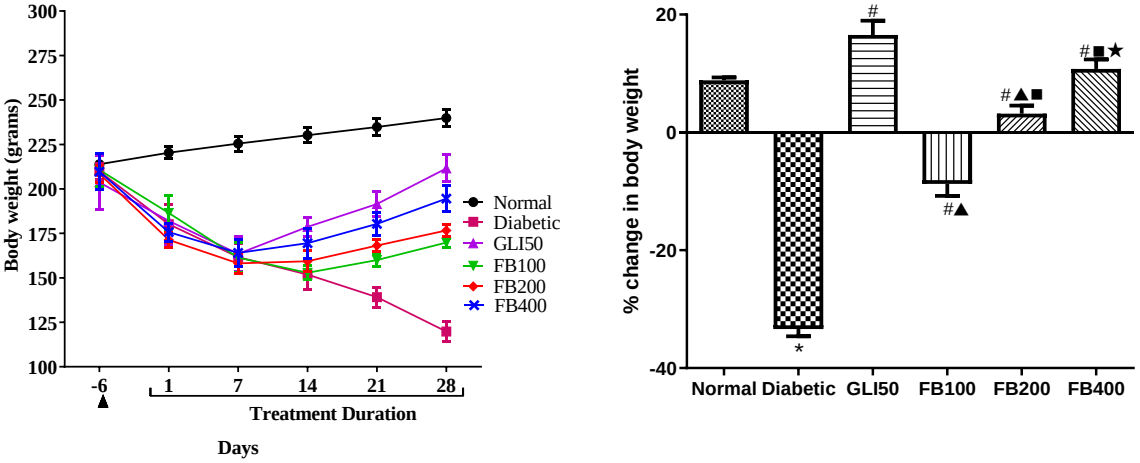

Figure 18: Effect of FBE on body weight in streptozocin-nicotinamide-induced DM. All the data are presented in Mean±SEM (n=6). *$p<0.001$ compared to normal, #$p<0.001$ compared to diabetic, ▲$p<0.001$ compared to GLI50, ▪$p<0.001$ compared to FB100, ★$p<0.05$ compared to FB200

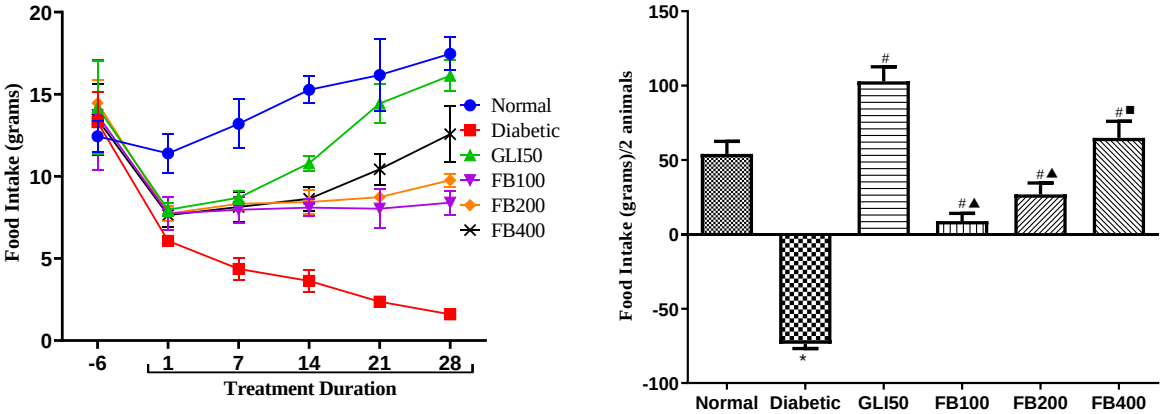

Figure 19: Effect of FBE on food intake in streptozocin-nicotinamide-induced DM. All the data are presented in Mean±SEM (n=6). *$p<0.001$ compared to normal, #$p<0.001$ compared to diabetic, ▲$p<0.001$ compared to GLI50, ▪$p<0.01$ compared to FB100

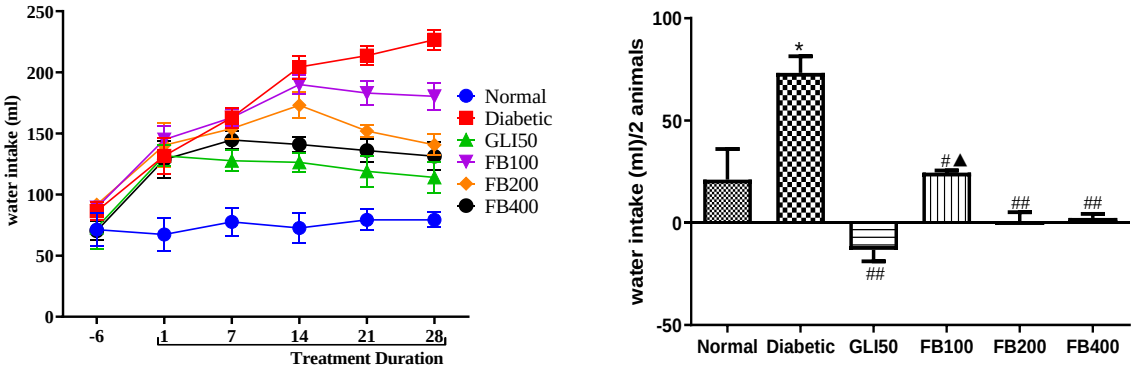

Figure 20: Effect of FBE on water intake in streptozocin-nicotinamide-induced DM. All the data are presented in Mean±SEM (n=6). *p<0.01 compared to normal, #p<0.05, ##p<0.001 compared to disease, ▲p<0.05 compared to GLI50

- ***Effect of FBE on fasting blood glucose and plasma insulin level and OGTT in streptozocin-nicotinamide induced DM***: There was a significant increase (p<0.001) in fasting blood glucose level in the diabetic group compared to normal which was significantly decreased (p<0.001) with glibenclamide and FBE (dose-dependent response was observed with FB100 *vs* FB200 *vs* FB400) treatment. Also, the total AUC $_{0\text{-}120\ min}$ of glucose during OGTT was significantly higher (p<0.001) in the diabetic group compared to normal which was reversed (p<0.001) with FBE and glibenclamide treatment; the dose-dependent effect was observed within FB100 *vs* FB200 *vs* FB400 (Figure 21). In contrast, fasting plasma insulin level was significantly lower (p<0.001) in the diabetic group compared to normal; significantly increased with glibenclamide (p<0.001) and FBE (p<0.05, 0.01) treatment; the dose-dependent effect was observed within FB100 *vs* FB200 *vs* FB400. Likewise, there was a significant decrease (p<0.001) in the total AUC $_{0\text{-}120\ min}$ of insulin in the diabetic group compared to normal; significantly reversed with glibenclamide (p<0.001) and FBE treatment (p<0.01); the dose-dependent effect was observed within FB100 *vs* FB200 *vs* FB400 (Figure 22).

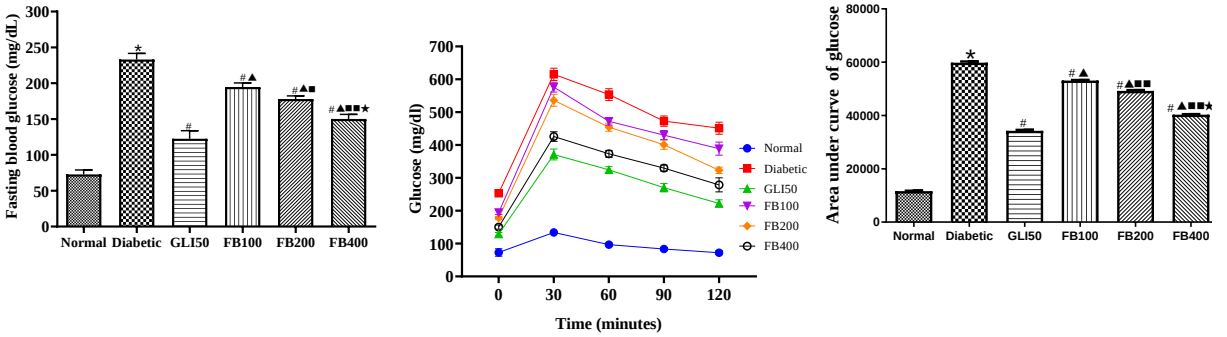

Figure 21: Effect of FBE on fasting blood glucose level in OGTT in streptozocin-nicotinamide-induced DM. All the data are presented in Mean±SEM (n=6). *p<0.001 compared to normal, #p<0.001 compared to diabetic, ▲p<0.001 compared to GLI50, ▪p<0.01, ▪▪p<0.001 compared to FB100, ★p<0.001 compared to FB200

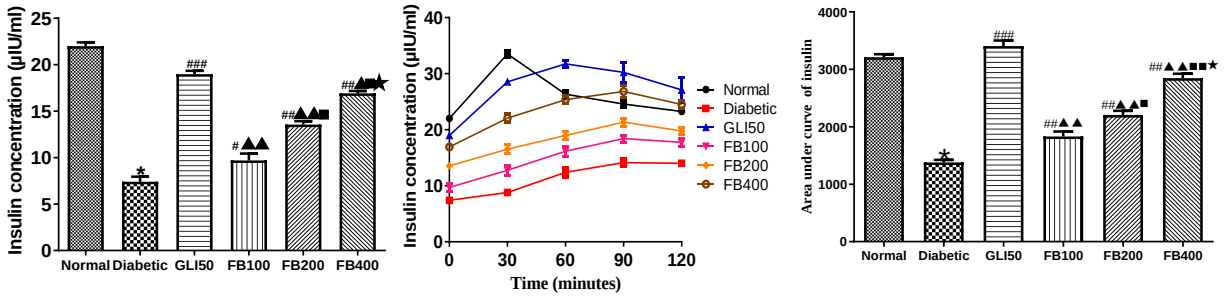

Figure 22: Effect of FBE on plasma insulin level during OGTT in streptozocin-nicotinamide-induced DM. All the data are presented in Mean±SEM (n=6). *p<0.001 compared to normal, #p<0.05, ##p<0.01, ###p<0.001 compared to diabetic, ▲p<0.05, ▲▲p<0.001 compared to GLI50, ▪p<0.05, ▪▪p<0.001 compared to FB100, ★p<0.001 compared to FB200

- ***Effect of FBE on glycated hemoglobin in streptozocin-nicotinamide induced DM***:

  There was a significant increase (p<0.001) in glycated hemoglobin level in the diabetic group compared to normal which was significantly decreased (p<0.001) with glibenclamide and FBE treatment; the dose-dependent effect was observed within FB100 *vs* FB200 *vs* FB400 (Figure 23).

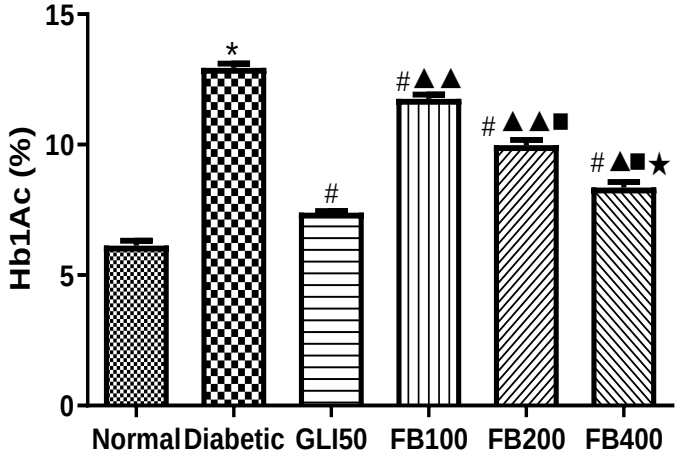

Figure 23: Effect of FBE on glycosylated hemoglobin in streptozocin-nicotinamide-induced DM. All the data are presented in Mean±SEM (n=6). *p<0.001 compared to normal, #p<0.001 compared to diabetic, ▲p<0.01, ▲▲p<0.001 compared to GLI50, ■p<0.001 compared to FB100, ★P<0.001 compared to FB200.

- ***Effect of FBE on hepatic enzymes in streptozocin-nicotinamide induced DM***: After 28 days, there was a significant increase (p<0.001) in LDH, FBPase, G6Pase, PFK, and AST: ALT ratio in the diabetic group compared to normal which was significantly decreased (p<0.05-0.001) with glibenclamide and FBE treatment. In contrast, hexokinase level was significantly decreased (p<0.001) in the diabetic group compared to normal; increased with glibenclamide (p<0.001) and FBE (p<0.01) treatment; the dose-dependent effect was observed within FB100 *vs* FB200 *vs* FB400 (Table 11).

Table 11: Effect of FBE on hepatic enzymes in streptozocin-nicotinamide-induced DM

Groups	Hexokinase (U/mg)	G6Pase (U/mg)	FBPase (U/mg)	LDH (mM/hr/mg)	PFK (units/mg of protein)	AST: ALT ratio
Normal	2.92±0.01	10.95±0.20	3.99±0.05	166.40±3.41	4.10±0.16	1.34±0.05
Diabetic	1.61±0.02*	27.67±0.79*	11.28±0.27*	377.10±8.23*	11.24±0.24*	2.75±0.10*
GLI50	2.59±0.01##	15.71±0.56##	5.49±0.23##	209.60±5.15##	4.99±0.12##	1.52±0.05##
FB100	1.80±0.02#▲▲	23.07±0.36##▲▲	12.29±0.37▲▲	328.70±4.61##▲▲	9.98±0.22##▲▲	1.58±0.04##
FB200	1.99±0.02#▲▲■	21.29±0.24##▲▲	9.86±0.25#▲▲■	293.10±3.73##▲▲■	8.23±0.13##▲▲■	1.59±0.06##
FB400	2.14±0.01#▲▲■★	18.52±0.09##■★	6.21±0.12##■★	223.50±1.62##▲▲■★	5.78±0.19##▲▲■★	1.49±0.05##

All the data are presented in Mean±SEM (n=6). *p<0.001 compared to normal, #p<0.01, ##p<0.001 compared to diabetic, ▲p<0.01, ▲▲p<0.001 compared to GLI50, ■p<0.001 compared to FB100, ★p<0.001 compared to FB200

- ***Effect of FBE on urea, uric acid, and creatinine level in streptozocin-nicotinamide induced DM***: Serum urea, uric acid, and creatinine level were significantly higher ($p<0.001$) in the diabetic group compared to normal which was significantly decreased with glibenclamide ($p<0.001$) and FBE ($p<0.05$-0.001) treatment; effect on urea level was dose-dependent with FBE treatment within FB100 *vs* FB200 *vs* FB400 (Table 12).

Table 12: Effect of FBE on urea, uric acid and creatinine level in streptozocin-nicotinamide-induced DM

Groups	Urea (mg/dL)	Uric acid (mg/dL)	Creatinine (mg/dL)
Normal	30.95±0.80	1.66±0.12	2.71±0.15
Diabetic	55.27±0.97*	2.89±0.16*	3.26±0.04*
GLI50	37.30±0.71$^{\#}$	1.58±0.03$^{\#}$	2.53±0.05$^{\#\#\#}$
FB100	50.53±0.34$^{\#▲▲}$	1.99±0.05$^{\#▲}$	2.88±0.04$^{\#▲}$
FB200	46.92±0.37$^{\#▲▲▪}$	1.88±0.05$^{\#}$	2.79±0.02$^{\#\#}$
FB400	42.90±0.44$^{\#▲▲▪▪★}$	1.80±0.04$^{\#}$	2.68±0.06$^{\#\#\#}$

All the data are presented in Mean±SEM (n=6). *$p<0.001$ compared to normal, $^{\#}p<0.05$, $^{\#\#}p<0.01$, $^{\#\#\#}p<0.001$ compared to diabetic, $^{▲}p<0.05$, $^{▲▲}p<0.001$ compared to GLI50, $^{▪}p<0.01$, $^{▪▪}p<0.001$ compared to FB100, $^{★}p<0.001$ compared to FB200

- ***Effect of FBE on lipid profile in streptozocin-nicotinamide induced DM***: TG, TC, VLDL, and LDL level was significantly increased ($p<0.001$) in the diabetic group compared to normal which was significantly decreased ($p<0.001$) with glibenclamide and FBE treatment. In contrast, the HDL level was significantly decreased ($p<0.001$) in the diabetic group which was reversed ($p<0.001$) with glibenclamide and FBE treatment; the dose-dependent effect was observed over TC, HDL, and LDL within FB100 *vs* FB200 *vs* FB400 (Table 13).

Table 13: Effect of FBE on lipid profile in streptozocin-nicotinamide-induced DM

Groups	TG (mg/dL)	TC (mg/dL)	HDL (mg/dL)	VLDL (mg/dL)	LDL (mg/dL)
Normal	45.92±0.45	90.99±0.94	59.49±0.67	9.18±0.09	22.32±0.55
Diabetic	93.11±3.53*	144.40±0.66*	36.41±0.63*	18.62±0.71*	89.39±1.59*
GLI50	51.07±0.67$^{\#}$	103.40±0.96$^{\#}$	57.93±0.39$^{\#}$	10.21±0.13$^{\#}$	35.29±0.93$^{\#}$
FB100	74.26±0.47$^{\#▲▲▲}$	131.00±1.39$^{\#▲▲}$	44.52±0.48$^{\#▲▲▲}$	14.85±0.09$^{\#▲▲▲}$	71.61±1.65$^{\#▲▲▲}$
FB200	66.04±0.55$^{\#▲▲▲▪}$	122.90±1.69$^{\#▲▲▪}$	49.39±0.45$^{\#▲▲▲▪▪}$	13.21±0.11$^{\#▲▲▲▪}$	60.26±1.67$^{\#▲▲▲▪}$
FB400	61.12±0.83$^{\#▲▲▲▪▪}$	108.60±1.05$^{\#▲▪★}$	53.12±0.25$^{\#▲▲▲▪▪★}$	12.22±0.17$^{\#▲▲▲▪▪}$	43.21±0.89$^{\#▲▲▪▪★}$

All the data are presented in Mean±SEM (n=6).*$p<0.001$ compared to normal, $^{\#}p<0.001$ compared to diabetic, $^{▲}p<0.05$, $^{▲▲}p<0.01$, $^{▲▲▲}p<0.001$ compared to GLI50, $^{▪}p<0.01$, $^{▪▪}p<0.001$ compared to FB100; $^{★}p<0.001$ compared to FB200

- ***Effect of FBE on glycogen content in gastrocnemius muscle and liver in streptozocin-nicotinamide induced DM***: Glycogen content in liver and gastrocnemius muscle was significantly decreased ($p<0.001$) in the diabetic group compared to normal which was significantly increased ($p<0.001$) after glibenclamide and FBE treatment; the effect was observed to be dose-dependent with FBE treatment within FB100 *vs* FB200 *vs* FB400 (Figure 24).

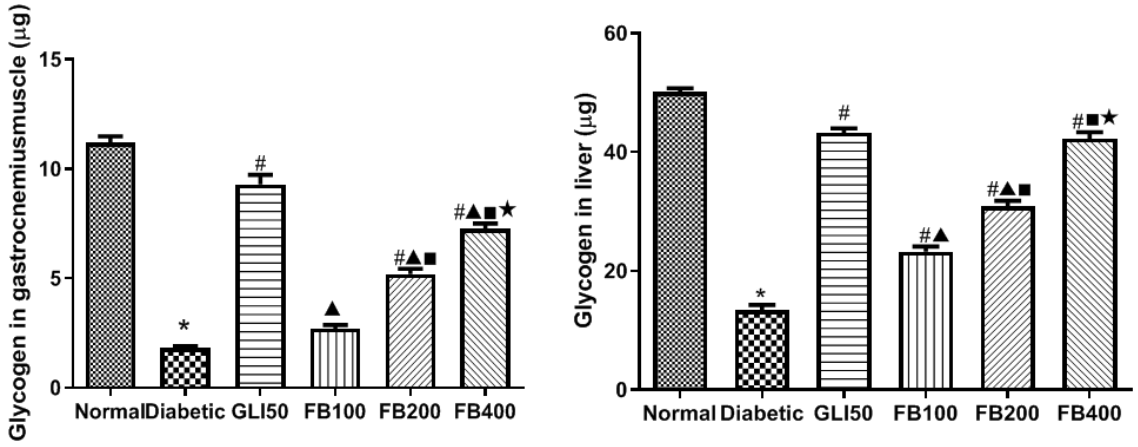

Figure 24: Effect of FBE on glycogen content in gastrocnemius muscle and liver in streptozocin-nicotinamide-induced DM. All the data are presented in Mean±SEM (n=6). *$p<0.001$ compared to normal, $^{\#}p<0.001$ compared to diabetic, $^{▲}p<0.001$ compared to GLI50, $^{▪}p<0.001$ compared to FB100, $^{★}p<0.001$ compared to FB200.

- ***Effect of FBE on glucose uptake in the isolated rat-hemidiaphragm in streptozocin-nicotinamide induced DM***: The percentage glucose uptake by rat hemidiaphragm was significantly lower ($p<0.001$) in the diabetic group compared to normal which was significantly increased ($p<0.001$) with glibenclamide and FBE treatment; however, no dose-dependent effect was observed within FB100 *vs* FB200 *vs* FB400 (Figure 25).

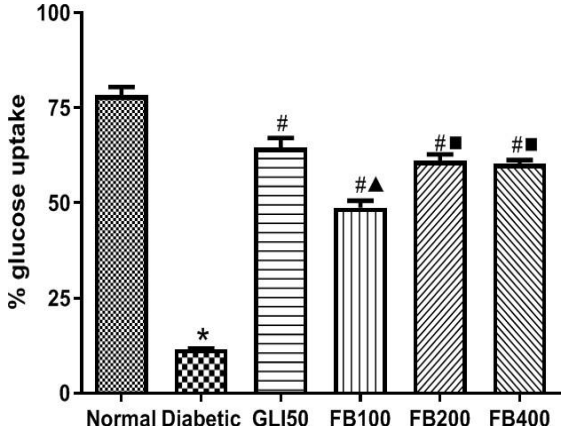

Figure 25: Effect of FBE on percentage glucose uptake in rat hemidiaphragm in streptozocin-nicotinamide-induced DM. All the data are presented in Mean±SEM (n=6). *p<0.001 compared to normal, #p<0.001 compared to diabetic, ▲p<0.001 compared to GLI50, ▪p<0.001 compared to FB100.

- ***Effect of FBE on enzymatic and non-enzymatic anti-oxidant biomarkers in streptozocin-nicotinamide induced DM***: The SOD and GSH level and catalase activity in liver homogenate was significantly decreased (p<0.001) in the diabetic group compared to normal which was significantlyincreased (p<0.05, 0.01, 0.001) with glibenclamide and FBE treatment compared to diabetic; the dose-dependent effect was observed with FBE treatment for SOD level within FB100 *vs* FB200 & FB400. Further, there was an observable (insignificant) increase in total thiols and MDA level in the diabetic group compared to normal which was observed to be ameliorated with glibenclamide and FBE treatments (Table 14).

Table 14: Effect of FBE on enzymatic and non-enzymatic anti-oxidant biomarkers in streptozocin-nicotinamide-induced DM

Groups	SOD (units/mL)	Total Thiols (µMoles/ mg of protein)	GSH (µM/mg of protein)	Catalase (units/min/mg of protein)	MDA (nMol/ unit of protein)
Normal	27.81±0.80	260.20±4.867	135.90±4.204	77.34±2.289	203.00±6.924
Diabetic	16.52±1.16*	353.80±64.72	33.76±6.279*	30.86±5.784 *	276.70±49.39
GLI50	25.72±0.34###	262.70±46.98	111.40±19.83 ###	47.89±8.522	194.70±34.52
FB100	19.10±0.53▲▲	350.20±2.418	58.19±2.752 ▲	53.51±2.227 #	292.60±2.148
FB200	24.63±0.91 ###▪	331.10±3.083	79.51±2.396 #	58.84±1.185 ##	283.90±4.618
FB400	27.73±0.37 ###▪	274.70±26.7	86.70±7.858 ##	59.71±5.847 ##	217.00±20.56

All the data are presented in Mean±SEM (n=6). *p<0.001 compared to normal, #p<0.05, ##p<0.01, ###p<0.001 compared to diabetic, ▲p<0.01, ▲▲p<0.001 compared to GLI50, ▪p<0.001 compared to FB100

- ***Effect of FBE on the pancreatic and hepatic histology in streptozocin-nicotinamide induced DM***: The average count of pancreatic islets and size was significantly decreased ($p<0.001$) in the diabetic group compared to normal which was significantly increased ($p<0.05$ & 0.01) with glibenclamide and FBE treatment. Also, congestion and vascular degeneration score were significantly increased ($p<0.001$) in the diabetic group which was significantly reversed ($p<0.05$, 0.01, 0.001) with glibenclamide and FBE treatment. Further, the lymphocytic infiltration score was observed to be significantly increased ($p<0.001$) in the diabetic group which was significantly reversed with glibenclamide treatment; however, FBE treatment did not affect it (Figure 26). Likewise, a significant increase ($p<0.001$) in sinusoidal congestion, venous congestion, and ballooning degeneration in hepatocytes was observed in the diabetic group compared to normal which was significantly reversed ($p<0.05$ & 0.01) with FBE treatment (Figure 27).

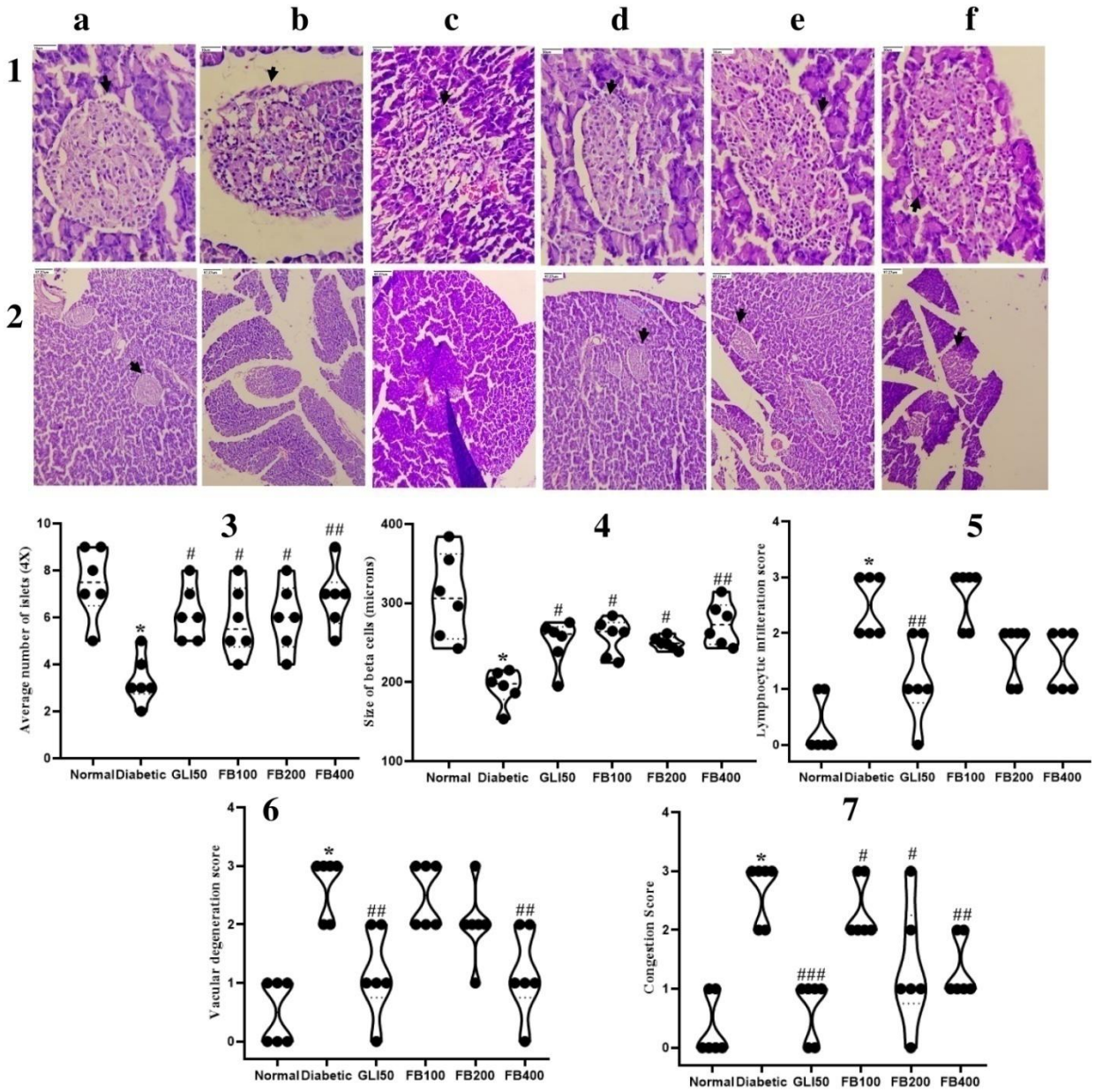

Figure 26: Effect of FBE on pancreatic histology (1; 40 & 2; 10 I) in streptozocin-nicotinamide-induced DM. ➘ pancreatic β-cell a: normal; b: diabetic; c: GLI50; d: DR100; e: DR200;f: DR400.*p<0.001 compared to normal, #p<0.05, ##p<0.01, ###p<0.001 compared to diabetic

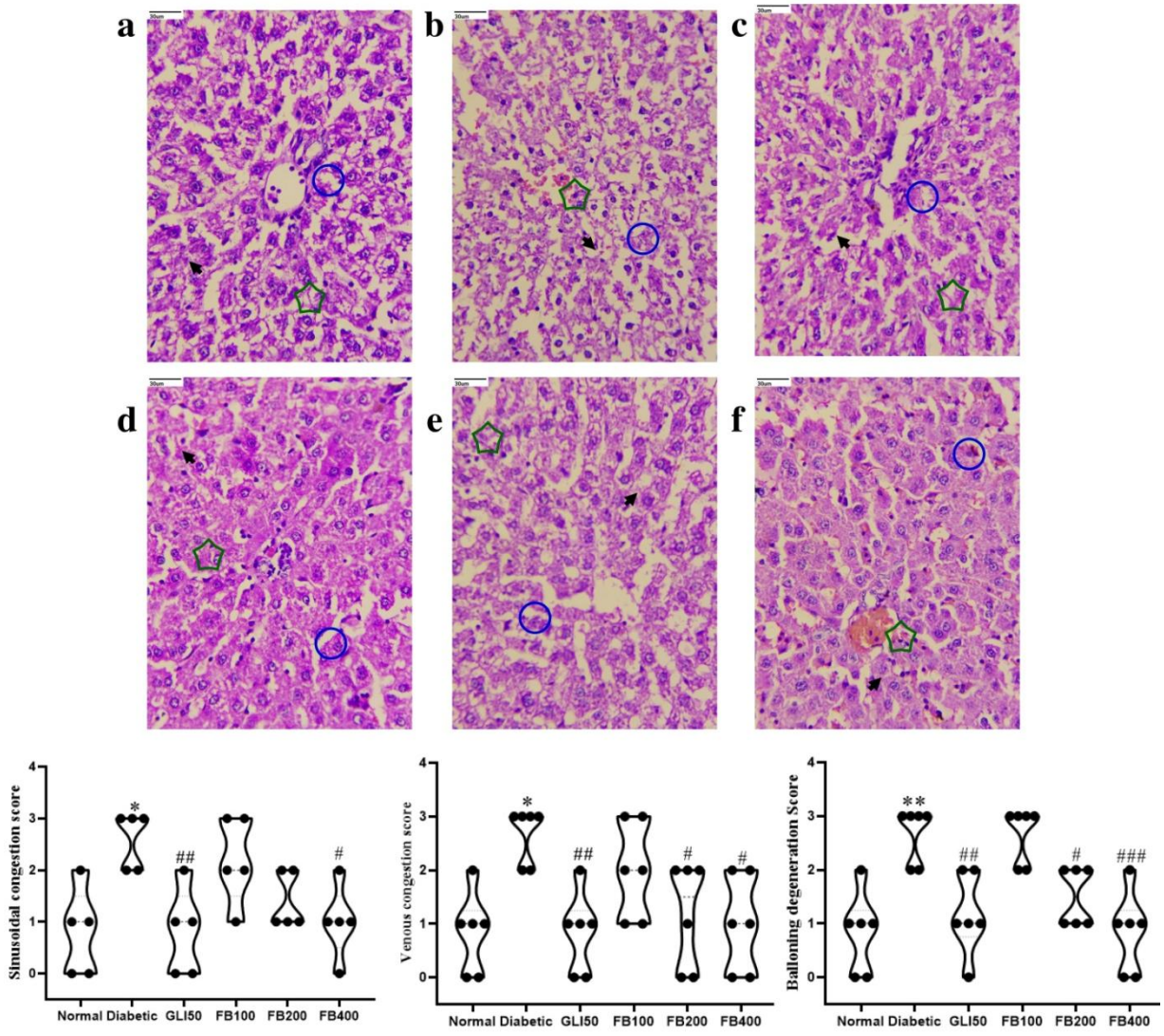

Figure 27: Effect of FBE in hepatic histology (40 X) in streptozocin-nicotinamide-induced DM. a: normal; b: diabetic; c: GLI50; d: DR100; e: DR200;f: DR400. *p<0.01, **p<0.001 compared to normal, $^{\#}$p<0.05, $^{\#\#}$p<0.01, $^{\#\#\#}$p<0.001 compared to diabetic

1.6.2. Effect of FBE in fructose-induced insulin-resistant rats

- ***Effect of FBE on body weight, food intake, and water intake in fructose-induced insulin resistance***: Supplementation of fructose significantly decreased the body weight (p<0.001); Figure 28 and food intake (p<0.001); Figure 29 in the IR group compared to normal which was significantly reversed (p<0.05, 0.01, 0.001) within 30 days of metformin and FBE treatment. Also, a significant increase (p<0.001) in fructose supplemented water intake was observed in the IR group which was

significantly reversed ($p<0.05$, 0.01, 0.001) with metformin and FBE treatment compared to IR; Figure 30.

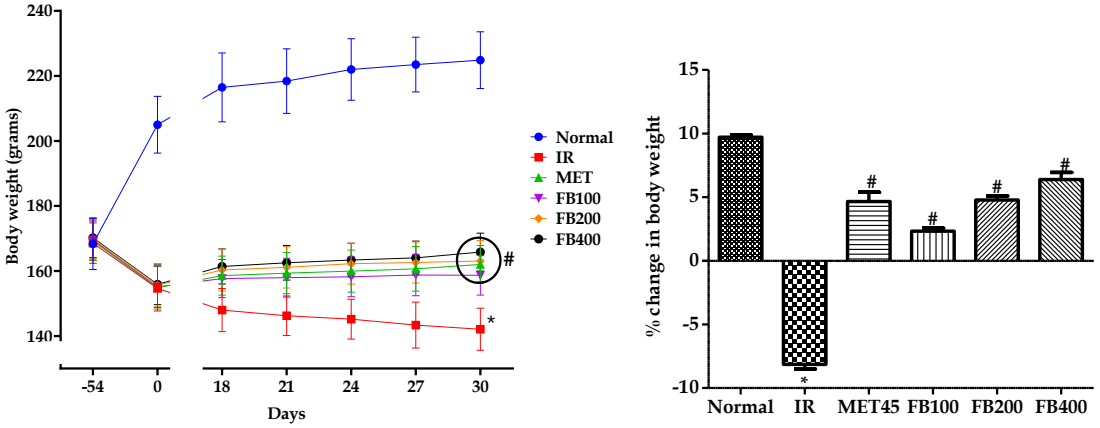

Figure 28: Effect of FBE on body weight in fructose-induced insulin resistance. All the data are presented in Mean±SEM (n=6). *p<0.001 compared to normal, #p<0.05, ##p<0.01, ###p<0.001 compared to IR

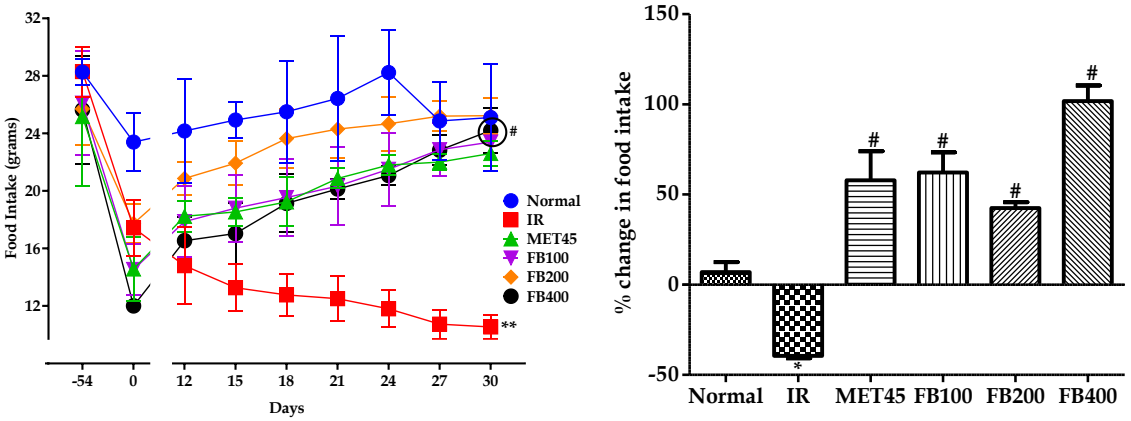

Figure 29: Effect of FBE on food intake in fructose-induced insulin resistance. All the data are presented in Mean±SEM (n=6). *p<0.05, **p<0.001 compared to normal, #p<0.001 compared to IR

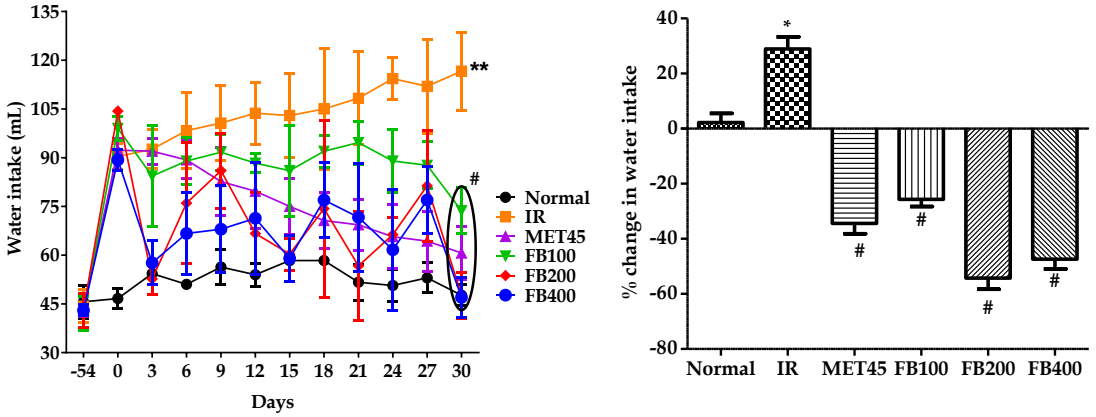

Figure 30: Effect of FBE on water intake in fructose-induced insulin resistance. All the data are presented in Mean±SEM (n=6). *p<0.01, **p<0.001 compared to Normal, #p<0.05, ##p<0.01, ###p<0.001 compared to IR

- ***Effect of FBE on fasting blood glucose and plasma insulin level in OGTT in fructose-induced insulin resistance*:** Supplementation of fructose in drinking water significantly increased (p<0.001) the fasting blood glucose (Figure 31) and plasma insulin level (Figure 32) in the IR group. However, FBE treatment had an insignificant decrease in fasting glucose level but showed a significant decrease (p<0.01) in fasting plasma insulin level with FBE (200 & 400 mg/kg) treatment. Further, there was a significant increase (p<0.001) in the total AUC $_{0\text{-}120\ min}$ of glucose and insulin in IR compared to normal which was significantly reversed (p<0.01, 0.001) with metformin and FBE treatment compared to IR; effect over the total AUC $_{0\text{-}120\ min}$ of glucose & insulin was dose-dependent within the doses of FBE treatment.

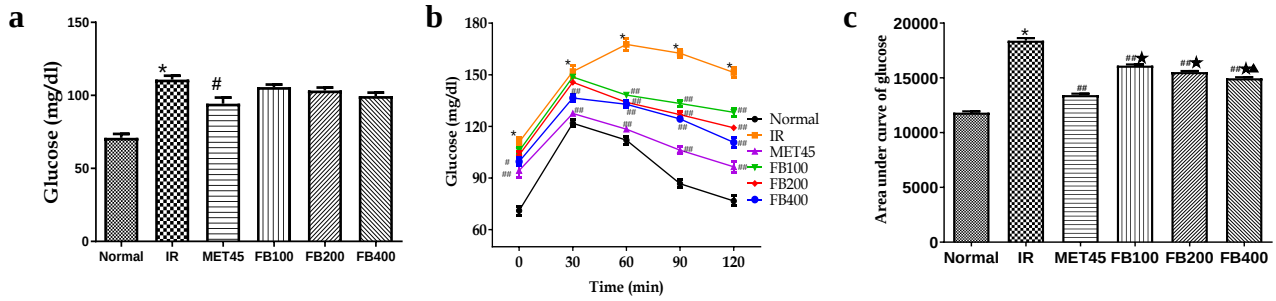

Figure 31: Effect of FBE on glucose level in the OGTT in fructose-induced insulin resistance. All the data are presented in Mean±SEM (n=6). *p<0.001 compared to normal, #p<0.01, ##p<0.001 compared to IR, ⋆p<0.001 compared to MET45, ▲P<0.001 compared to FB100

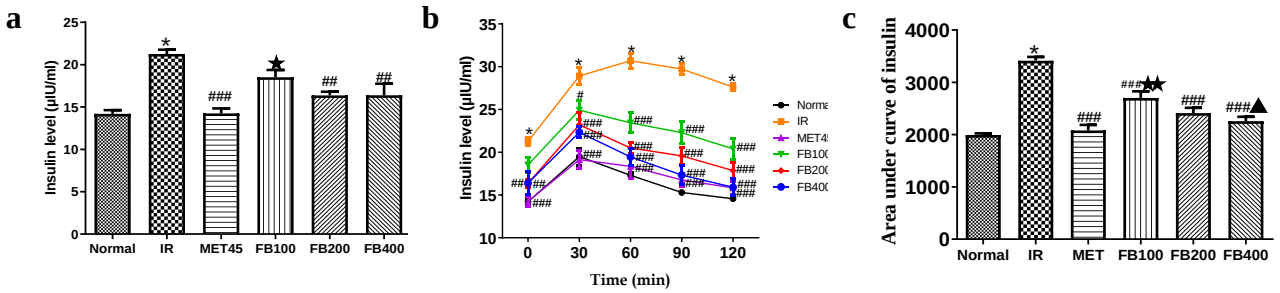

Figure 32: Effect of FBE on insulin level in the OGTT in fructose-induced insulin resistance. All the data are presented in Mean±SEM (n=6). *p<0.001 compared to normal, #p<0.05, ##p<0.01, ###p<0.001 compared to IR, ⋆p<0.01, ⋆⋆p<0.001 compared to MET45, ▲p<0.05 compared to FB100

- ***Effect of FBE on ITT in fructose-induced insulin resistance***: Significant decrease (p<0.05, 0.001) in the basal glucose level was observed after the administration of exogenous regular insulin in metformin and FBE treated groups compared to IR. Also, there was a significant decrease (p<0.001) in total AUC $_{0\text{-}120\ min}$ of glucose in metformin and FBE treated groups except at the dose of 100 mg/kg of FBE compared to IR; the dose-dependent effect was observed within the FBE treated groups for the total AUC $_{0\text{-}120\ min}$ of glucose (Figure 33).

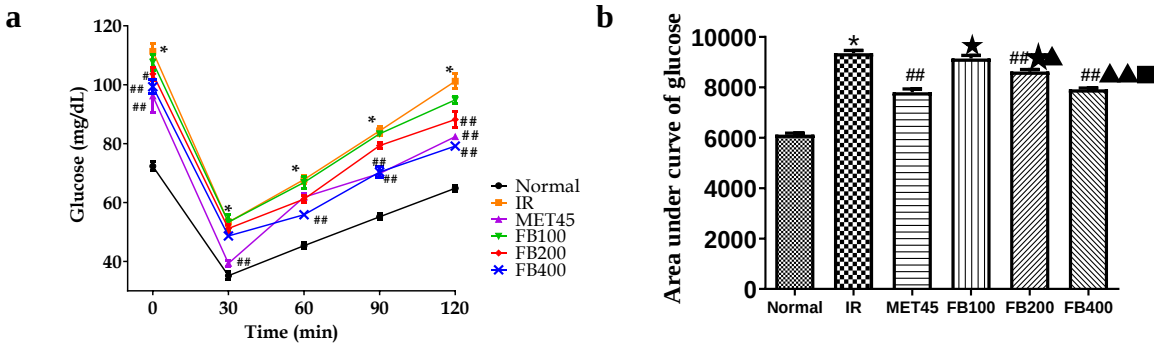

Figure 33: Effect of FBE on ITT in fructose-induced insulin resistance. All the data are presented in Mean±SEM (n=6). *p<0.001 compared to normal, #p<0.05, ##p<0.001 compared to IR, ★★p<0.001 compared to MET45, ▲p<0.05, ▲▲p<0.001 compared to FB100 ▪p<0.001 compared to FB200

- ***Effect of FBE on HOMA-IR in fructose-induced insulin resistance***: HOMA-IR was significantly increased (p<0.001) in the IR group compared to normal which was significantly reversed (p<0.001) with metformin and FBE treatment and no dose-dependent effect was observed within the multiple doses of FBE treatment (Figure 34).

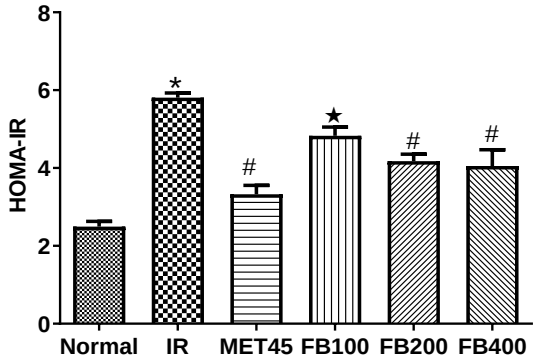

Figure 34: Effect of FBE on HOMA-IR in fructose-induced insulin resistance. All the data are presented in Mean±SEM (n=6). *p<0.001 compared to Normal, #p<0.001 compared to IR, ★p<0.01 compared to MET45.

- ***Effect of FBE on lipid profile in fructose-induced insulin resistance***: In the IR group, there was a significant increase (p<0.001) in TG level compared to normal which was significantly decreased (p<0.001) with metformin and FBE treatment. In contrast, a significant decrease (p<0.001) in TC, HDL, LDL, and VLDL was observed in IR treated groups compared to normal; significantly reversed (p<0.01, 0.001) with

metformin and FBE treatment compared to IR. Further, the effect was observed to be dose-dependent within FBE treatment *i.e.* FB100 *vs* FB200 *vs* FB 400 (Table 15).

Table 15: Effect of FBE on lipid profile in fructose-induced insulin resistance

Groups	TG (mg/dL)	TC (mg/dL)	HDL (mg/dL)	VLDL (mg/dL)	LDL (mg/dL)
Normal	45.17±1.78	119.50±2.17	55.67±0.88	9.033±0.36	54.80±2.44
IR	120.30±2.68*	90.67±1.36*	39.67±1.20*	24.07±0.54*	26.93±1.79*
MET45	58.17±2.70$^{\#\#}$	123.80±1.89$^{\#\#}$	51.17±2.27$^{\#\#}$	11.63±0.54$^{\#\#}$	61.03±2.33$^{\#\#}$
FB100	90.67±1.28$^{\#\#}$★★	92.67±1.96★★	41.17±1.25★★	18.13±0.26$^{\#\#}$★★	33.37±2.62★★
FB200	81.33±1.23$^{\#\#}$★★▲	103.30±2.47$^{\#\#}$★★▲▲	45.33±1.80	16.27±0.25$^{\#\#}$★★▲	41.73±2.60$^{\#}$★★
FB400	71.67±1.41$^{\#\#}$★★▲▲▲▪	115.20±1.60$^{\#\#}$★▲▲▲▪▪	48.67±1.45$^{\#}$▲	14.33±0.28$^{\#\#}$★★▲▲▲▪	52.17±2.18$^{\#\#}$▲▲▲▪

All the data are presented in Mean±SEM (n=6). *p<0.001 compared to normal, $^{\#}$p<0.01, $^{\#\#}$p<0.001 compared to IR, ★p<0.05, ★★p<0.001 compared to MET45, ▲p<0.05 compared to FB100, ▲▲p<0.01, ▲▲▲p<0.001 compared to FB100, ▪P<0.05, ▪▪P<0.01 compared to FB200

- ***Effect of FBE on glucose uptake in the isolated rat hemidiaphragm in fructose-induced insulin resistance***: In the IR group, a significant decrease (p<0.001) in exogenous glucose uptake was observed compared to normal which was significantly reversed (p<0.001) with metformin and FBE treatment compared to IR; the dose-dependent effect was observed with FBE treatment within FB100 *vs* FB200 & FB400 (Figure 35).

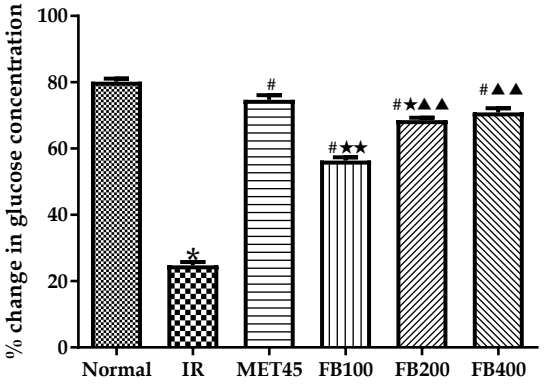

Figure 35: Effect of FBE on percentage glucose uptake in rat hemidiaphragm in fructose-induced insulin resistance. All the data are presented in Mean±SEM (n=6). *p<0.001 compared to Normal, $^{\#}$p<0.001 compared to IR, ★p<0.01, ★★p<0.001 compared to MET45, ▲▲p<0.001 compared to FB100

- ***Effect of FBE on urea, uric acid, and creatinine level in fructose-induced insulin resistance***: A significant increase (p<0.001) in urea, uric acid, and creatinine level was observed in the IR group compared to normal which was significantly reversed

(p<0.01, 0.001) with metformin and FBE treatment compared to IR. Further dose-dependent effect was observed for urea and uric acid level within FB100 & FB200 *vs* FB400 and creatinine level within FB100 *vs* FB200 (Table 16).

Table 16: Effect of FBE on urea, uric acid and creatinine level in fructose-induced insulin resistance

Groups	Urea (mg/dL)	Uric acid (mg/dL)	Creatinine (mg/dL)
Normal	17.83±1.99	2.35±0.20	1.217±0.11
IR	54.67±1.26*	8.217±0.35*	3.383±0.12*
MET45	24.17±1.62$^{\#\#}$	3.467±0.06$^{\#\#}$	1.767±0.09$^{\#\#}$
FB100	45.33±1.56$^{\#}$★★★	6.367±0.19$^{\#\#}$★★★	2.35±0.10$^{\#\#}$★
FB200	40.67±1.28$^{\#\#}$★★★	5.233±0.18$^{\#\#}$★★★▲▲	1.967±0.12$^{\#\#}$
FB400	31.33±1.52$^{\#\#}$★▲▲▲▪▪	4.183±0.19$^{\#\#}$★★★▲▲▲▪	1.783±0.15$^{\#\#}$▲

All the data are presented in Mean±SEM (n=6). *p<0.001 compared to Normal, $^{\#}$p<0.01, $^{\#\#}$p<0.001 compared to IR, ★p<0.05, ★★p<0.001, ★★★p<0.001 compared to MET45, ▲p<0.05, ▲▲p<0.01, ▲▲▲p<0.001 compared to FB100, ▪p<0.05, ▪▪p<0.01 compared to FB200

- ***Effect of FBE on glycogen content in gastrocnemius muscle and liver in fructose-induced insulin resistance***: In liver and gastrocnemius muscle of IR, a significant decrease (p<0.001) in glycogen content was observed compared to normal which was significantly reversed (p<0.001) with metformin and FBE treatment; the dose-dependent effect was observed with FBE treatment within FB100 *vs* FB200 & FB400 (Figure 36).

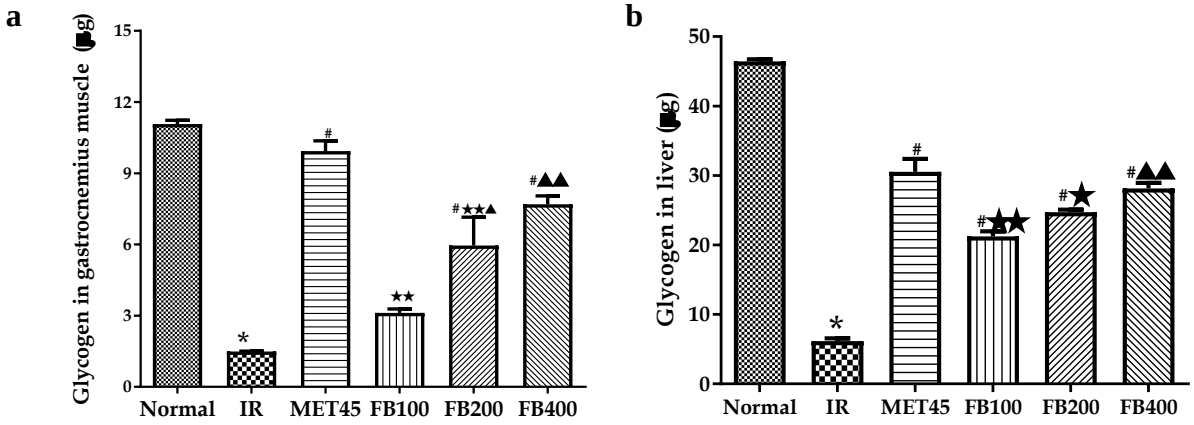

Figure 36: Effect of FBE on glycogen content in gastrocnemius muscle and liver in fructose-induced insulin resistance. All the data are presented in Mean±SEM (n=6). *p<0.001 compared to normal, $^{\#}$p<0.001 compared to IR, ★p<0.01, ★★p<0.001 compared to MET45, ▲p<0.05, ▲▲p<0.001 compared to FB100

- ***Effect of FBE on hepatic enzymes in fructose-induced insulin resistance*:** Hepatic hexokinase level was observed to be significantly decreased ($p<0.001$) in the IR group compared to normal which was significantly reversed ($p<0.05$ & 0.001) with metformin and FBE treatment; the dose-dependent effect was observed with FBE treatment within FB100 *vs* FB400. In contrast, the level of G6Pase, FBPase, PFK, and LDH, and AST: ALT ratio was significantly increased ($p<0.001$) in the IR group compared to normal which was significantly decreased ($p<0.05$, 0.001) with metformin and FBE treatment; further dose-dependent effect was observed with FBE treatment within FB100 *vs* FB200 *vs* FB400 (Table 17).

Table 17: Effect of FBE on hepatic enzymes in fructose-induced insulin resistance

Groups	Hexokinase (U/mg)	G6Pase (U/mg)	FBPase (U/mg)	PFK (U/mg)	LDH (mM/L/h/mg)	AST:ALT ratio
Normal	2.62±0.12	10.48±0.24	3.46±0.14	4.25±0.29	170.70±3.18	0.93±0.13
IR	1.50±0.12*	41.18±1.62*	18.57±0.35*	12.58±0.39*	331.30±7.60*	3.17±0.14*
MET45	2.60±0.10$^{\#\#}$	16.33±0.55$^{\#\#}$	5.88±0.40$^{\#\#}$	7.03±0.28$^{\#\#}$	203.90±4.46$^{\#\#}$	1.44±0.09$^{\#\#}$
FB100	2.01±0.16$^{\#}$★★	27.74±0.56$^{\#\#}$★★★	14.37±0.50$^{\#\#}$★★★	10.31±0.17$^{\#\#}$★★★	278.70±2.09$^{\#\#}$★★★	1.98±0.09$^{\#\#}$★
FB200	2.40±0.04$^{\#\#}$	25.22±0.64$^{\#\#}$★★★	10.83±0.28$^{\#\#}$★★★▲▲	9.89±0.30$^{\#\#}$★★★	241.50±2.74$^{\#\#}$★★★▲	1.93±0.08$^{\#\#}$★
FB400	2.77±0.07$^{\#\#}$▲	19.67±0.34$^{\#\#}$▲▪▪	6.92±0.30$^{\#\#}$▲▪▪	7.79±0.37$^{\#\#}$▲▪▪	229.40±2.34$^{\#\#}$★★▲	1.52±0.10$^{\#\#}$▪

All the data are presented in Mean±SEM (n=6). *$p<0.001$ compared to normal, $^{\#}p<0.05$, $^{\#\#}p<0.001$ compared to IR, ★$p<0.05$, ★★$p<0.01$, ★★★$p<0.001$ compared to MET45, ▲$p<0.001$ compared to FB100, ▪$p<0.05$, ▪▪$P<0.001$ compared to FB200

- ***Effect of FBE on plasma leptin level in fructose-induced insulin resistance***: Supplementation of fructose in drinking water significantly decreased ($p<0.001$) the plasma leptin level in the IR group compared to normal which was significantly reversed ($p<0.001$) with metformin and FBE treatment; the dose-dependent effect was observed with FBE treatment within FB100 *vs* FB200 *vs* FB400 (Figure 37).

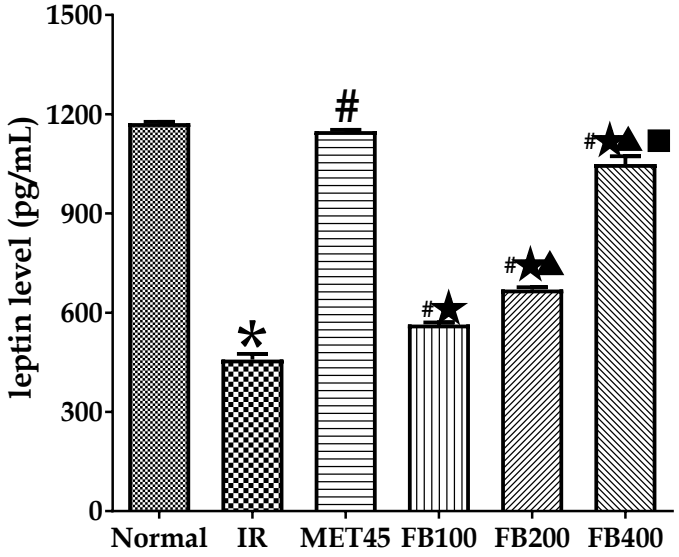

Figure 37: Effect of FBE on leptin level in fructose-induced insulin resistance. All the data are presented in Mean±SEM (n=6). *p<0.001 compared to normal, #p<0.001 compared to IR, ★ p<0.001 compared to MET45, ▲p<0.001 compared to FB100, ■P<0.001 compared to FB200

- ***Effect of FBE on enzymatic and non-enzymatic anti-oxidant biomarkers in fructose-induced insulin resistance***: In the IR group, GSH, catalase, and SOD level were significantly decreased compared to normal which was significantly increased (p<0.01 & 0.001) with metformin and FBE treatment except FB100; the dose-dependent effect was observed within FB100 *vs* FB400 (for GSH), FB100 & FB200 *vs* FB400 (for catalase), and FB100 *vs* FB200 *vs* FB400 (for SOD). In contrast, MDA and THABS levels were significantly increased (p<0.001) in the IR group compared to normal which was significantly decreased (p<0.01 & 0.001) with metformin and FBE treatment compared to normal; the dose-dependent effect was observed with FBE treatment for MDA level within FB100 *vs* FB200 *vs* FB400 (Table 18).

Table 18: Effect of FBE on enzymatic and non-enzymatic anti-oxidant biomarkers in fructose-induced insulin resistance

Groups	MDA (nM/mg of protein)	GSH (µM/mg of protein)	THABS (µM/mg of protein)	Catalase (U/[min_mg] of protein)	SOD (U/mL)
Normal	154.60±11.94	119.50±4.66	218.60±2.69	84.94±4.81	35.02±0.83
IR	290.70±19.59*	24.08±1.32*	313.20±4.88*	35.04±2.16*	22.01±1.33*
MET45	169.20±16.71$^{\#\#}$	101.60±3.65$^{\#\#}$	239.60±4.60$^{\#\#}$	82.04±3.77$^{\#\#}$	32.89±0.48$^{\#\#}$
FB100	254.60±12.94*	29.87±1.57**	292.90±3.75**	42.44±1.51**	24.91±1.41**
FB200	199.80±9.31$^{\#}$	49.84±1.86$^{\#\#\star\star\blacktriangle\blacktriangle}$	272.90±4.75$^{\#\#\star\star}$	56.63±3.26$^{\#\star\star}$	29.58±0.60$^{\#\#\blacktriangle}$
FB400	184.70±11.93$^{\#\#\blacktriangle}$	79.24±5.53$^{\#\#\star\blacktriangle\blacktriangle\blacktriangle\blacksquare\blacksquare\blacksquare}$	229.30±11.25$^{\#\#\star\blacktriangle\blacktriangle\blacktriangle\blacksquare\blacksquare\blacksquare}$	76.34±4.15$^{\#\#\blacktriangle\blacktriangle\blacktriangle\blacksquare\blacksquare}$	33.90±0.66$^{\#\#\blacktriangle\blacktriangle\blacktriangle\blacksquare}$

All the data are presented in Mean±SEM (n=6). *p<0.001 compared to normal, $^{\#}$p<0.01, $^{\#\#}$p<0.001 compared to IR, *p<0.01, **p<0.001 compared to MET45, $^{\blacktriangle}$p<0.05, $^{\blacktriangle\blacktriangle}$P<0.01, $^{\blacktriangle\blacktriangle\blacktriangle}$p<0.001 compared to FB100, $^{\blacksquare}$p<0.05, $^{\blacksquare\blacksquare}$p<0.01, $^{\blacksquare\blacksquare}$p<0.001 compared to FB200

- ***Effect of FBE on hepatic histology in fructose-induced insulin resistance***: In the IR group, there was a significant increase in sinusoidal congestion (p<0.05), inflammation (p<0.05), venous congestion (p<0.05), portal triaditis (p<0.05), cholestasis (p<0.05), spotty necrosis (p<0.05), apoptosis (p<0.01), sinusoidal congestion (p<0.05) and kupffer cell hyperplasia (p<0.05) in IR group compared to normal which was significantly reversed with metformin and FBE 400 mg/kg treatment; no dose-dependent effect was observed within FB100 *vs* FB200 *vs* FB400 (Figure 38).

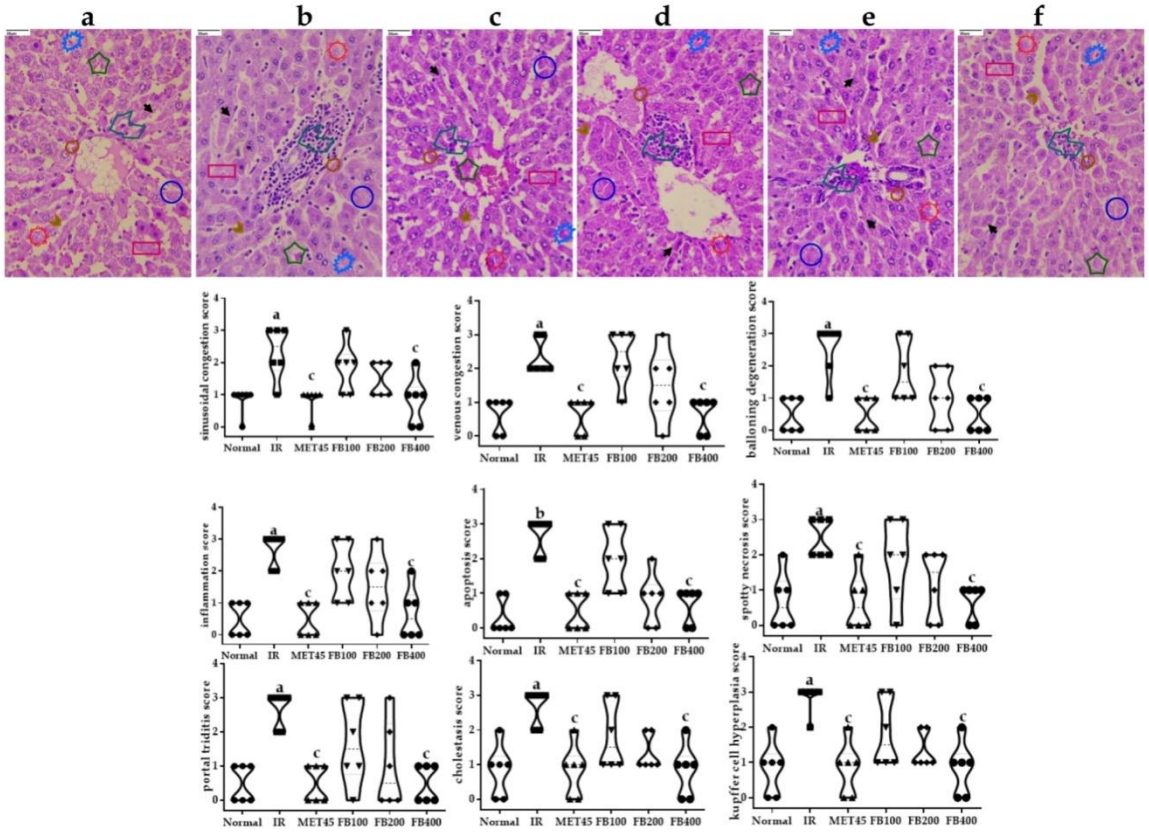

Figure 38: Effect of FBE on hepatocytes (40X) in fructose-induced insulin resistance. a: normal; b: diabetic; c: MET45; d: DR100; e: DR200;f: DR400. ➘ sinusoidal congestion, ◯ venous congestion, ⬠ ballooning degeneration, ⬡ inflammation, ▭ apoptosis, ⬠ spotty necrosis, ◯ portal triditis, ⬡ cholestasis, ◥ kuffer cell hyperplasia. *$p<0.05$ compared to normal, $^{\#}p<0.05$, $^{\#\#}p<0.01$ compared to IR.

2. *In silico, in vitro, ex vivo,* and *in vivo* pharmacology of *D. repens* whole plant against DM

2.1.In silico pharmacology of D. repens

2.1.1. Network pharmacology of phytoconstituents from D. repens

A total of 51 phytoconstituents were retrieved from the PCIDB and ChEBI database in which 36 phytoconstituents regulated 31 proteins involved in DM. Concerning the KEGG pathways record, 61 pathways were traced *via* the regulation of 31 proteins of which 11 pathways were directly concerned with DM (Figure 39). Also, the galactose metabolism pathway was traced which recorded α-glucosidase enzyme; is directly concerned with postprandial hyperglycemia. In addition, among 11 pathways, the PI3K-Akt signaling was majorly predicted to be regulated *via* the manipulation of 7 genes *i.e. FASLG*, *GSK3B*, *HSP90AB1*, *IL2*, *ITGA4*, *NFKB1*, and *TLR4* (Table 19). Also, phytoconstituents-targets-proteins network interaction reflected the presence of a total of 77 nodes composed of 36 phytoconstituents, 31 targets, and 10 pathways. Further, a total of 173 edges were present in the network in which 138 and 35 nodes reflected the phytoconstituents-proteins and proteins-pathways interactions respectively. Additionally, in the combined synergic network, ***pectolinarigenin*** was predicted to target the highest number of proteins in DM pathogenesis.

Table 19: KEGG pathway analysis of proteins interaction regulated by phytoconstituents of *D. repens*

Pathway	Description	Gene count	Genes	False discovery rate
hsa04931	Insulin resistance	5	GSK3B, PPARGC1B, NFKB1, TNFRSF1B, PTP1B	3.24×10^{-5}
hsa04151	PI3K-Akt signalling	7	GSK3B, HSP90AB1, NFKB1, ITGA4, FASLG, TLR4, IL2	3.27×10^{-5}
hsa04660	T cell receptor signalling	4	GSK3B, LCK, IL2, NFKB1	0.00028
hsa04060	Cytokine-cytokine receptor interaction	4	IL2, FASLG, TNFRSF1A, TNFRSF1B	0.0044
hsa04722	Neurotrophin signalling	3	GSK3B, NFKB1, FASLG	0.0046

Table 19 Cont…

Pathway	Description	Gene count	Genes	False discovery rate
hsa00052*	Galactose metabolism	2	AKR1B1, GAA	0.0061
hsa04960	Aldosterone-regulated sodium reabsorption	2	HSD11B2, NR3C2	0.0070
hsa04940	T1DM	2	IL2, FASLG	0.0079
hsa03320	PPAR signaling	2	PPARD, PPARG	0.0183
hsa04211	Longevity regulating	2	NFKB1, PPARG	0.0252
hsa04066	HIF-1 signaling	2	NFKB1, TLR4	0.0292
hsa04910	Insulin signaling	2	PTP1B, GSK3B	0.0465

* Pathway includes the protein involved in the diabetes mellitus; however, the pathway was not recorded by KEGG for diabetes mellitus

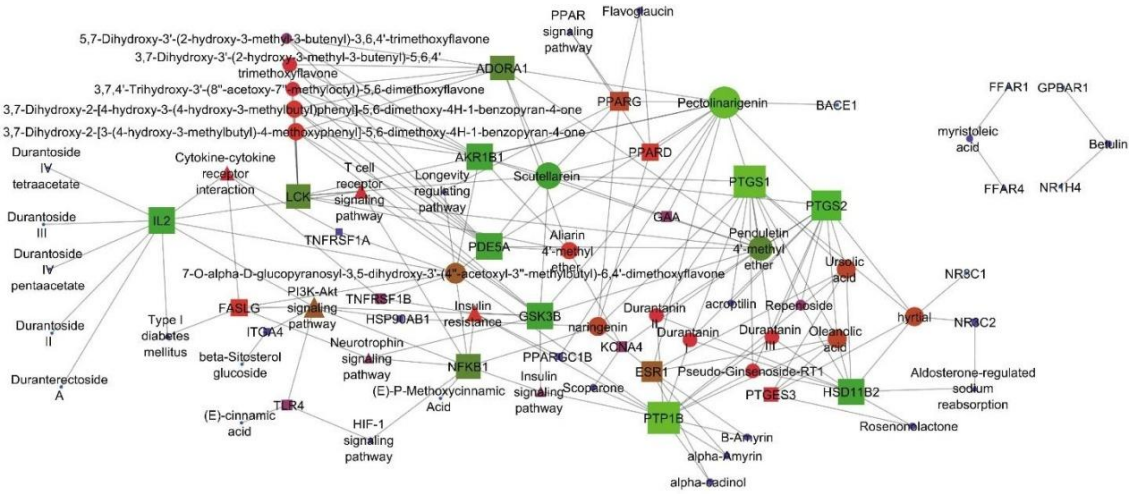

Figure 39: Interaction of phytoconstituents and proteins with respective pathways. In the network interaction, a circle represents the phytoconstituent, a rectangle represents the protein and a triangle represents the pathway.

2.1.2. Prediction of druglikeness score of phytoconstituents from D. repens

Among 36 phytoconstituents of *D. repens* ***3,7-Dihydroxy-2-[4-hydroxy-3-(4-hydroxy-3- methylbutyl)phenyl]-5,6-dimethoxy-4H-1-benzopyran-4-one*** was predicted for highest druglikeness score *i.e.* 1.29 with a molecular weight of 416.15, 8 *H*-bond acceptors, 4 *H*-bond donors, and 3.69 MolLogP; compounds with positive druglikeness score are summarized (Table 20).

Table 20: Druglikeness score of phytoconstituents from *D. repens*

Compound	MF	MW	NHBA	NHBD	MolLogP	DLS
Pectolinarigenin	$C_{17}H_{14}O_6$	314.08	6	2	3.26	0.52
Durantanin II	$C_{63}H_{102}O_{31}$	1354.64	31	18	–5.77	0.83
Durantanin III	$C_{58}H_{94}O_{27}$	1222.6	27	16	–4.12	0.71
Durantanin I	$C_{58}H_{94}O_{27}$	1222.6	27	16	–4.02	0.84

Table 20 Cont…

Compound	MF	MW	NHBA	NHBD	MolLogP	DLS
Penduletin 4'-methyl ether	$C_{19}H_{18}O_7$	358.11	7	1	3.39	0.45
5,7-Dihydroxy-3'-(2-hydroxy-3-methyl-3-butenyl)-3,6,4'-trimethoxyflavone	$C_{23}H_{24}O_8$	428.15	8	3	3.92	0.76
3,7-Dihydroxy-3'-(2-hydroxy-3-methyl-3-butenyl)-5,6,4' trimethoxyflavone	$C_{23}H_{24}O_8$	428.15	8	3	3.92	0.92
Scutellarein	$C_{15}H_{10}O_6$	286.05	6	4	2.56	0.72
Durantoside III	$C_{28}H_{36}O_{15}$	612.21	15	6	–0.99	0.23
3,7-Dihydroxy-2-[4-hydroxy-3-(4-hydroxy-3-methylbutyl)phenyl]-5,6-dimethoxy-4H-1-benzopyran-4-one	$C_{22}H_{24}O_8$	416.15	8	4	3.69	1.29
3,7-Dihydroxy-2-[3-(4-hydroxy-3-methylbutyl)-4-methoxyphenyl]-5,6-dimethoxy-4H-1-benzopyran-4-one	$C_{23}H_{26}O_8$	430.16	8	3	4.04	1.04
3,7,4'-Trihydroxy-3'-(8''-acetoxy-7''-methyloctyl)-5,6-dimethoxyflavone	$C_{28}H_{34}O_9$	514.22	9	3	6.19	1.27
Aliarin 4'-methyl ether	$C_{23}H_{26}O_8$	430.16	8	3	4.09	0.61
7-O-α-D-glucopyranosyl-3,5-dihydroxy-3'-(4''-acetoxyl-3''-methylbutyl)-6,4'-dimethoxyflavone	$C_{30}H_{36}O_{14}$	620.21	14	6	1.51	1.11
Rosenonolactone	$C_{20}H_{28}O_3$	316.2	3	0	3.17	0.1
Oleanolic acid	$C_{30}H_{48}O_3$	456.36	3	2	7.8	0.37
α-Amyrin	$C_{30}H_{50}O$	426.39	1	1	9.21	0.09
Naringenin	$C_{15}H_{12}O_5$	272.07	5	3	2.3	1.13
Duranterectoside A	$C_{27}H_{34}O_{15}$	598.19	15	7	–1.34	0.32
Durantoside IV pentaacetate	$C_{35}H_{40}O_{19}$	764.22	19	2	0.04	0.01
Repenoside	$C_{49}H_{78}O_{17}$	938.52	17	9	1.53	0.65
β -Sitosterol glucoside	$C_{35}H_{60}O_6$	576.44	6	4	7.13	0.51
Ursolic acid	$C_{30}H_{48}O_3$	456.36	3	2	7.84	0.65
Pseudo-ginsenoside-RT1	$C_{47}H_{74}O_{18}$	926.49	18	10	1.06	0.9

MF: Molecular formula, **MW**: Molecular weight, **NHBA**: number of hydrogen bond acceptors, **NHBD**: number of hydrogen bond donors, **DLS**: Druglikeness score

2.1.3. Molecular docking of phytoconstituents from D. repens against α-amylase, α-glucosidase, and PTP1B

PASS identified 13 phytoconstituents from *D. repens* in which docking study revealed ***β-sitosterol glucoside*** (-9.4 kcal/mol), ***kusaginin*** (-8.7 kcal/mol), ***naringenin***

(-8.8 kcal/mol), ***scutellarein*** (-8.7 kcal/mol), and ***7-O-α-D-glucopyranosyl-3,5-dihydroxy-3'-(4''-acetoxyl-3''-methylbutyl)-6,4'-dimethoxyflavone*** (-8.9 kcal/mol) as top 5 hits as α-amylase inhibitors. On these, kusaginin had the highest *H*-bond interactions *i.e.* 6 *via* Asn298, Glu233, Asp300, Trp59, Asp356, and Glu63 (Figure 40). The binding energy and mode of interaction of each phytoconstituent against α-amylase are summarized in Table 21.

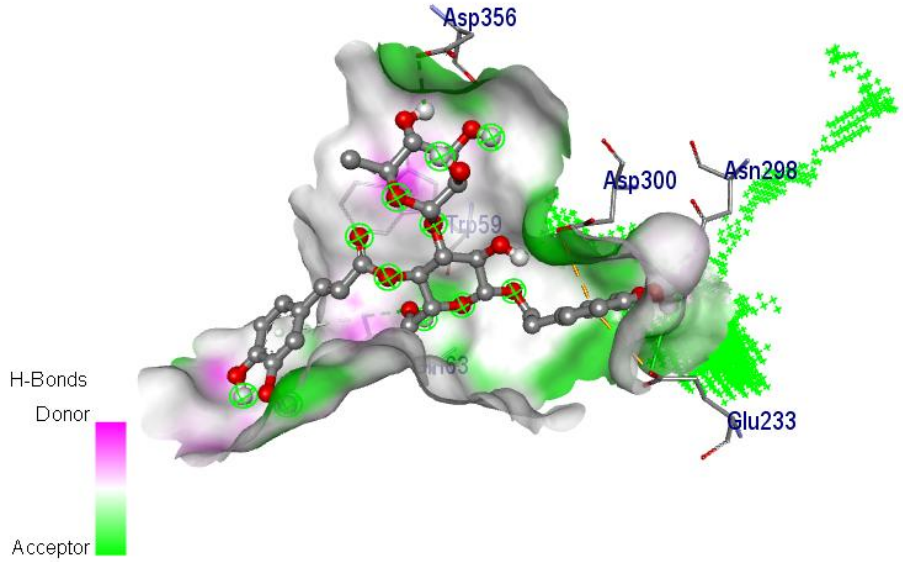

Figure 40: Interaction of *kusaginin* with α-amylase. Green bond indicates *H*-bond interaction(s) whereas the rest of the other bonds indicate hydrophobic interactions

Table 21: Binding affinity of each phytoconstituent from *D. repens* with α-amylase

Ligand	Binding affinity (kcal/mol)	NHB	Hydrogen bond residues
(E)-cinnamic acid	-6.3	2	Trp59, Gln63
(E)-p-methoxycinnamic acid	-6.6	1	Gln63
3, 7, 4'-Trihydroxy-3'-(8"-acetoxy-7"-methyloctyl)-5, 6 dimethoxyflavone	-8.3	4	Arg10, Asp402, Arg421, Ser289
7-O-α-D-glucopyranosyl-3, 5-dihydroxy-3'-(4"-acetoxyl-3"-methylbutyl)-6, 4'-dimethoxyflavone	-8.9	2	His305, Asp300
Durantoside III	-8.3	6	Asp356, His305, Asp300, Thr163
Durantoside II	-8.3	5	Gly403, Ser289, Gly334, Arg252
Durantoside I	-8.5	4	Arg195, Asp300, Glu233, Tyr151
Myristoleic acid	-5.3	2	Gln63
Naringenin	-8.8	2	Gln63, His299
Scoparone	-6.3	-	-
Scutellarein	-8.7	2	His299, Gln63

Table 21 Cont…

Ligand	Binding affinity (kcal/mol)	NHB	Hydrogen bond residues
beta-sitosterol glucoside	-9.4	2	Asp356, Asp353
Kusaginin	-8.7	6	Asn298, Glu233, Asp300, Trp59, Asp356, Glu63

NHB: Number of *H*-bonds

Based on the 70 % similarity score, BindingDB predicted ***pectolinarigenin*** (1), ***scutellarein*** (2), and ***penduletin 4'-methyl ether*** (3) as α-glucosidase inhibitors in which ***scutellarein*** possessed the highest binding affinity (binding energy -8.0 kcal/mol) *via* 2 *H*-bond interactions with Gln121 and Gly123 (Figure 41). The binding affinity and mode of interaction of each predicted α-glucosidase inhibitor are summarized in Table 22.

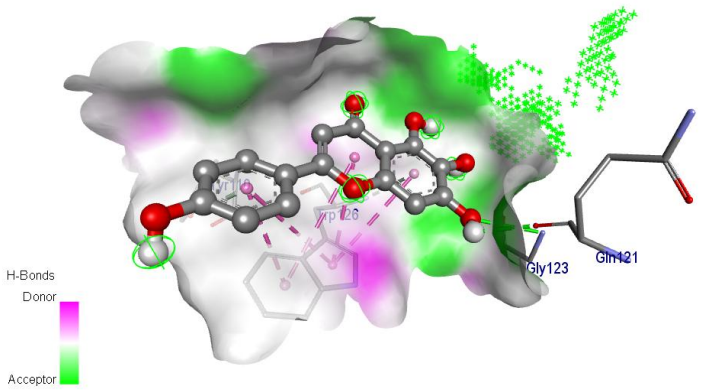

Figure 41: Interaction of *scutellarein* with α-glucosidase. Green bond indicates *H*-bond interaction(s) whereas the rest of the other bonds indicate hydrophobic interactions

Table 22: Binding affinity of each phytoconstituent from *D. repens* with α-glucosidase

Ligands	Binding affinity (kcal/mol)	NHB	Hydrogen bond residues
Pectolinarigenin	-7.1	2	Arg275, Asp95
Scutellarein	-8	2	Gly123,Gln121
Penduletin 4'-methyl ether	-7.1	2	Trp126, Tyr110
Acarbose*	-8.17	6	Ala93, Trp126, Gly116, Glp119, Gln121

NHB: Number of Hydrogen Bonds, **HBR**: Hydrogen Bond Residues, *clinically used α-glucosidase inhibitor

Among 11 PTP1B inhibitors; BindingDB predicted, docking study revealed ***durantanin I*** to possess the highest binding affinity (-8.9 kcal/mol) *via* 6 *H* - bond

interactions with Arg221, Glu115, Gly259, and Arg254 (Figure 42). The binding affinity and mode of interaction of each phytoconstituent against PTP1B are summarized in Table 23.

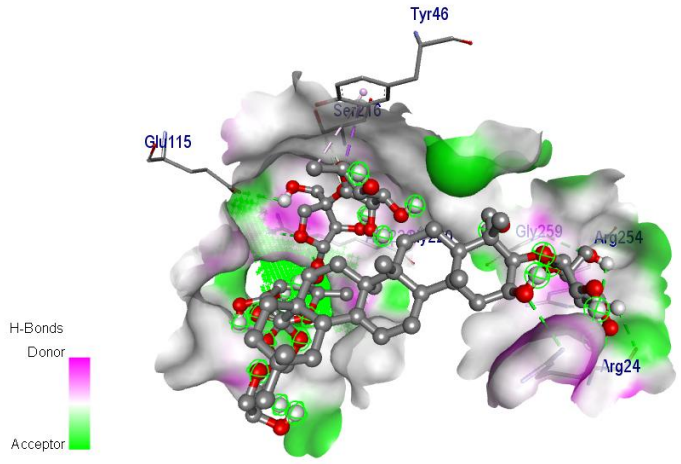

Figure 42: Interaction of *durantanin I* with PTP1B. Green bond indicates *H*-bond interaction(s) whereas the rest of the other bonds indicate hydrophobic interactions

Table 23: Binding affinity of each phytoconstituent from *D. repens* with PTP1B

Ligand	Binding affinity (kcal/mol)	NHB	Hydrogen bond residues
7-O-α-D-glucopyranosyl-3,5-dihydroxy-3'-(4"-acetoxyl-3"-methylbutyl)-6,4'-dimethoxyflavone	–7.6	3	Ala264, Asp48, Gly183
β-Amyrin	–8.4	1	Cys215
Durantanin III	–8.1	5	Ala217, Glu115, Gln266, Lys116, Val184
Durantanin II	–8.6	10	Glu97, Trp100, Leu59, Asn162, His60, Gly209, Ser205, Leu204, Ser80
Durantanin I	–8.9	6	Arg221, Glu115, Gly256, Arg254
Oleanolic acid	–8.3	1	Trp100
Pseudo-ginsenoside-RT1	–8.6	3	Arg254, Arg47, Lys36
Scoparone	–5.6	3	Gln266,Trp179
Ursolic_acid	–8.5	3	Gln266, Arg221
α-Amyrin	–8.2	1	Gly220
α-Cadinol	–6	–	–

NHB: Number of hydrogen bonds

2.1.4. Molecular docking of phytoconstituents from D. repens against free radical generators

Among the PASS predicted top 3 anti-oxidant hits, ***naringenin*** from *D. repens* was

predicted for the highest binding affinity with cytochrome P450 (binding energy -8.4 kcal/mol) and NAD(P)H oxidase (binding energy -8.4 kcal/mol) *via* 2 *H*-bonds with Val113 and Ser365 and 3 *H* - bonds with Pro298, Lys134, and Ser41 respectively. Also, ***3,7-Dihydroxy-2-[4-hydroxy-3-(4-hydroxy-3-methylbutyl)phenyl]-5,6-dimethoxy- 4H-1-benzopyran-4-one*** possessed maximum binding affinity (-9 kcal/mol) with NAD(P)H oxidase and interacted *via* 3 *H*-bonds *i.e.* Lys134, Asp282 and Ala300. Likewise, ***7-O-α-D-glucopyranosyl-3,5-dihydroxy-3'-(4''-acetoxyl-3''-methylbutyl)-6,4'- dimethoxyflavone*** scored the maximum binding affinity (-9.4 kcal/mol) with CYP450 *via* 5 *H*-bonds *via* Trp120, Arg43, Thr301 and Gly296. Interaction of lead hits with corresponding protein is presented in Figure 43. The binding energy and mode of interaction of each predicted anti-oxidant with the individual free radical generator are summarized in Table 24.

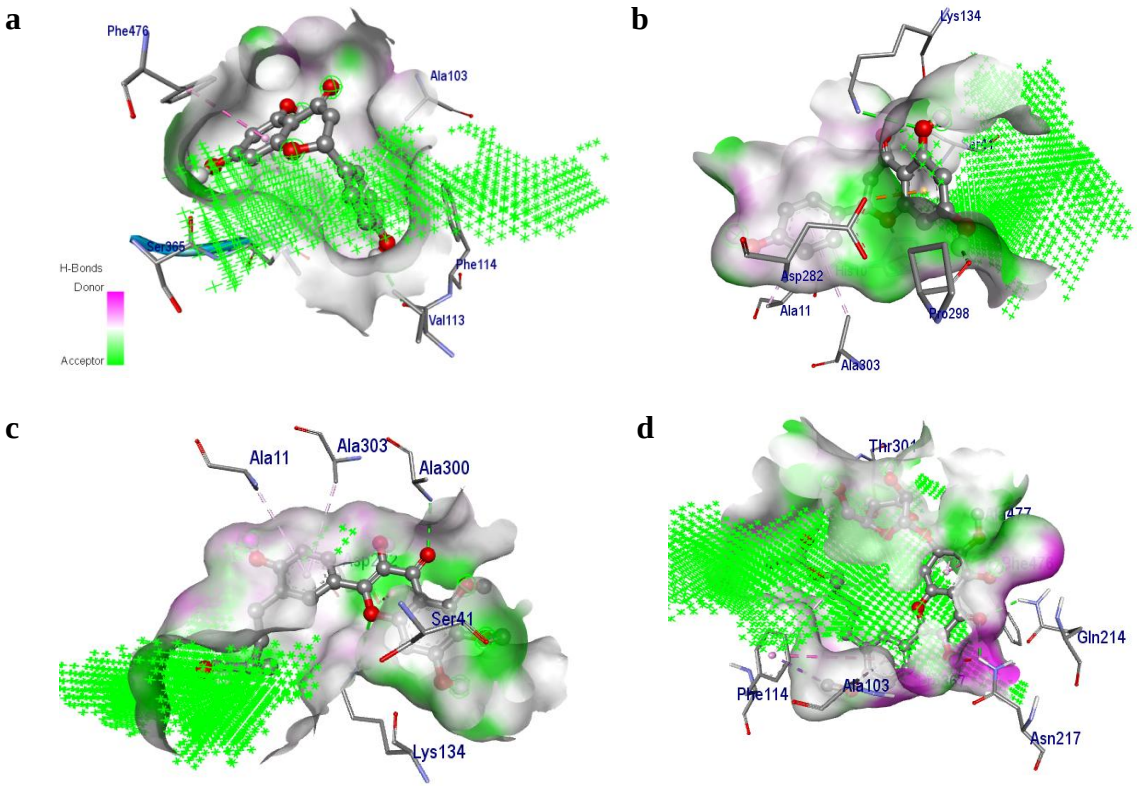

Figure 43: Interaction of *naringenin* with (a) cytochrome P450 and (b) NAD(P)H oxidase and (c) *3,7-Dihydroxy-2-[4-hydroxy-3-(4-hydroxy-3-methylbutyl)phenyl]-5,6-dimethoxy-4H-1-benzopyran-4-one* with NAD(P)H oxidase, and (d) *7-O-α-D-glucopyranosyl-3,5-dihydroxy-3'-(4''-acetoxyl-3''-methylbutyl)-6,4'-dimethoxyflavone* with CYP450. Green bond indicates *H*-bond interaction(s) whereas rest of the other bonds indicate hydrophobic interactions

Table 24: Binding affinity of phytoconstituents from *D. repens* with targets related to ROS system

Targets		Ligands		
		C1	**C2**	**C3**
Lipoxygenase (PDB: 1N8Q)	BA	-8.2	-8.1	-7.9
	NHB	6	3	2
	HBR	Thr274, Tyr275, Asn556, Arg260, Ala263	Val588, Tyr512, Asp428	Lys156, Asp190
Myeloperoxidase (PDB: 1DNU)	BA	-8.3	-7.7	-8.2
	NHB	0	3	7
	HBR	-	Ser174, Asp172	Arg23, Ser174, Thr16, Phe170, Ser169, Thr329
Xanthine oxidase (PDB: 3NRZ)	BA	-7.1	-7	-7.2
	NHB	1	5	7
	HBR	Gln144	Tyr58, Gly12, Thr86, Tyr125	Ser69, Ser123, Ala142, Gly145, Glm144
Cytochrome P450 (PDB: 1OG5)	BA	-8.4	-8.2	-9.4
	NHB	2	2	5
	HBR	Val113, Ser365	Ala103, Asn217	Trp120, Arg43, Thr301, Gly296
NAD(P)H oxidase (PDB: 2CDU)	BA	-8.4	-9	-9.1
	NHB	3	3	2
	HBR	Pro 298, Lys 134, Ser 41	Lys 134, Asp 282, Ala 300	Thr9, Ala300

C1: ***Naringenin***, C2: ***3, 7-Dihydroxy-2-[4-hydroxy-3-(4-hydroxy-3-methylbutyl)phenyl]-5, 6-dimethoxy-4H-1-benzopyran-4-one***, C3: ***7-O-α-D-glucopyranosyl-3,5-dihydroxy-3'-(4''-acetoxyl-3''-methylbutyl)-6,4'-dimethoxyflavone***, **BA**: Binding affinity(binding energy in kcal/mol), **NHB**: Number of *H*-bonds, **HBR**: *H*-bond residues

2.1.5. Molecular docking of phytoconstituents from D. repens against the enzymes involved in the glucose catabolism and anabolism

Among 36 phytoconstituents, ***scutellarein*** (1), ***Pseudo-ginsenoside-RT1*** (2), ***repennoside*** (3), and ***durantanin I*** (4) were predicted as lead hits to manipulate the enzymes involved in the glucose catabolism/anabolism. It was predicted that ***scutellarein*** possessed the highest binding affinity (binding energy -8.5 kcal/mol) with FBPase *via* 5 *H*-bonds with Thr28 and Thr32. Further, ***pseudo-ginsenoside –RT1*** possessed the highest binding affinity (binding energy -8.3 kcal/mol) with G6Pase *via* 9 *H*-bonds with Cys109, Ser34, Arg40, Glu110, Lys76, Asn72, and Val107. Likewise, ***repennoside*** had the highest binding affinity (-10.5 kcal/mol) with hexokinase *via* 8 *H*-

bonds with Glu249, His467, Asp814, Thr812, Gln466, Phe766, Asp815. Additionally, ***durantanin I*** was predicted for the highest binding affinity (binding energy-10.0 kcal/mol) with PFK *via* 10 *H*-bonds with Thr469, Ala389, His390, Arg253, Arg256, Asp190, and Arg673. Further, ***repennoside*** was predicted for the highest binding affinity (binding energy -10.7 kcal/mol) with LDH *via* 2 *H*-bonds with Tyr238, Glu103 (Figure 44).

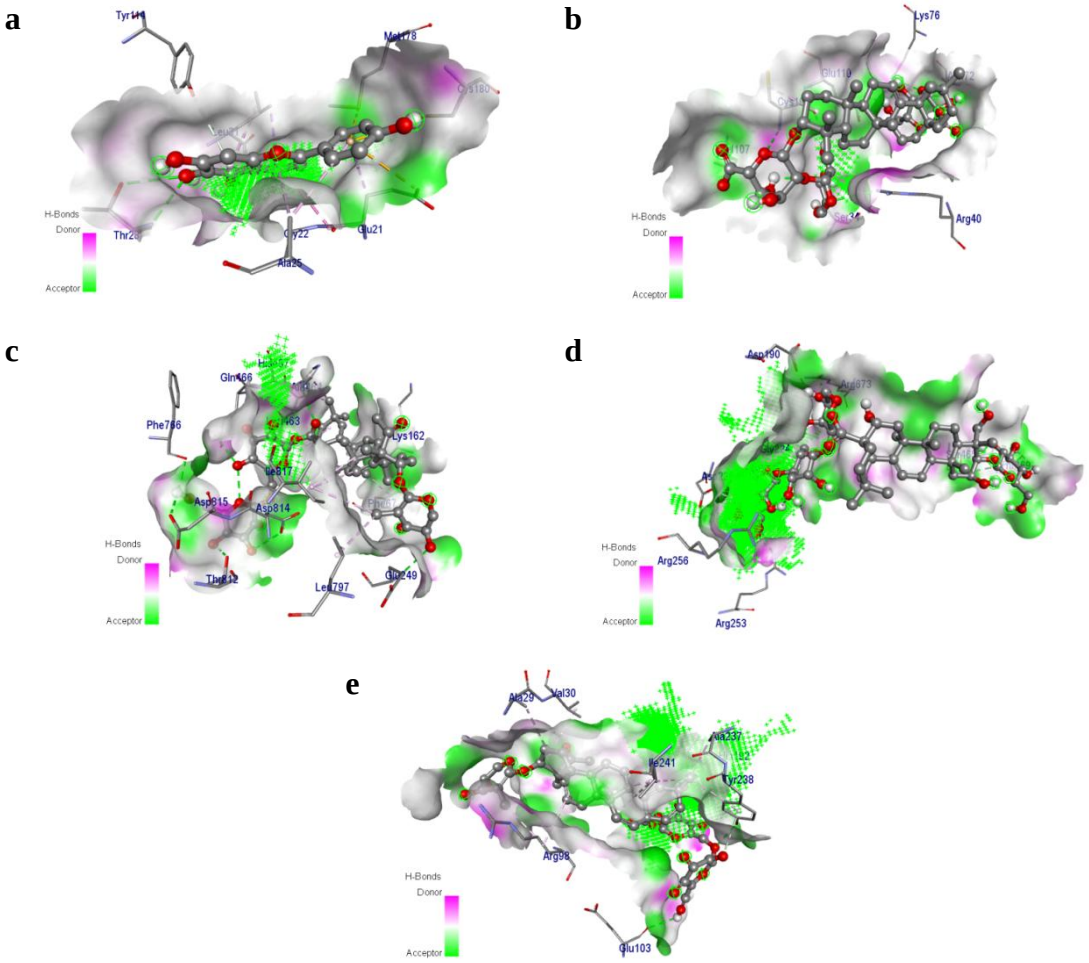

Figure 44: Interaction of (a) *scutellarein* with FBPase, (b) *pseudo-ginsenoside –RT1* with G6Pase, (c) *repennoside* with hexokinase, (d) *durantanin I* with PFK, and (e) *repennoside* with LDH. Green bond indicates *H*-bond interaction(s) whereas the rest of the other bonds indicate hydrophobic interactions

2.2.Preliminary phytochemical evaluation of DRE

A preliminary phytochemical investigation of DRE reflected the presence of alkaloids, flavonoids, polyphenols, saponins, steroids, and triterpenes, with a total polyphenols and

flavonoids contents as (52.06±2.19) µg/mL (gallic acid equivalent) and (122.36±1.94) µg/mL (rutin equivalent) respectively.

2.3.HPLC analysis of DRE

The quantitative estimation revealed the presence of 0.595 % w/w of oleanolic acid in DRE; Figure 45 presents the HPLC chromatograms for standard oleanolic acid and DRE.

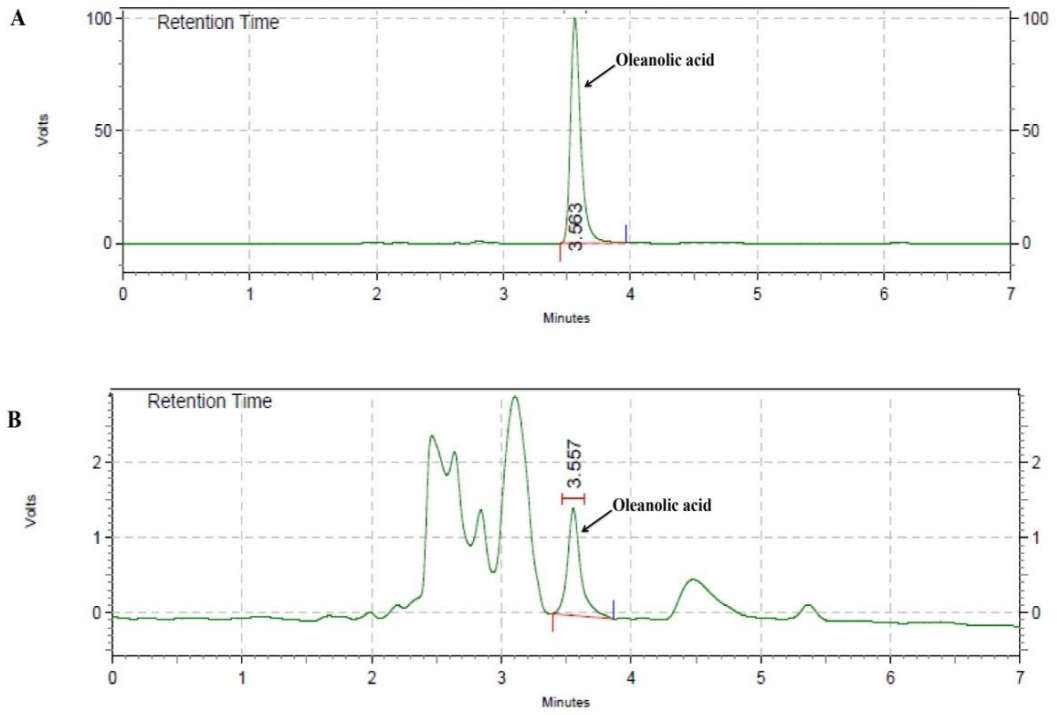

Figure 45: HPLC chromatograms for (a) standard oleanolic acid, (b) oleanolic acid in DRE.

2.4.In-vitro antioxidant activity of DRE

Over the 7 different anti-oxidant protocols, DRE showed the highest metal chelating capacity (IC_{50}: 41.21±0.69 µg/ml). Further, the order of anti-oxidant potential was metal chelating capacity > H_2O_2 scavenging capacity > ABTS scavenging capacity > total anti-oxidant capacity > CUPRAC > NO scavenging capacity > DPPH scavenging capacity (Table 25).

Table 25: *In-vitro* anti-oxidant activity DRE

***In-vitro* anti-oxidant models**	**IC_{50}**			
	DRE	**Reference compounds**		
		gallic acid	**EDTA**	**ascorbic acid**
DPPH scavenging assay	70.90±2.13	-	-	25.88±4.85
H_2O_2 scavenging assay	47.71±0.71	-	-	47.71±0.71
NO scavenging assay	67.85 ±4.25	55.66±0.64	-	-
Total anti-oxidant capacity	53.86±2.42	-	-	-
CUPRAC assay	54.52±2.93	-	-	38.02±2.25
Metal chelating assay	41.21±0.69	-	23.12±2.16	-
ABTS scavenging assay	53.72±2.13	30.75±1.64	-	-

All data are represented in Mean±SD, **IC_{50}**: Inhibitory concentration 50, **EDTA**: Ethylenediamine tetraacetic acid

2.5.In vitro and ex vivo anti-diabetic pharmacology of DRE

2.5.1. In vitro α-glucosidase inhibitory activity of DRE and its fractions

Among DRE and its fractions, DRE_ flavonoid possessed maximum α-glucosidase inhibitory activity IC_{50} (319.21±7.66) µg/mL. The order of α-glucosidase inhibition was DRE_flavonoid > DRE_polyphenol > DRE_alkaloid > DRE_saponin > DRE_steroid > DRE (Table 26). The percentage of enzyme inhibition by each test concentration is presented in Figure 46.

2.5.2. In vitro α-amylase inhibitory activity of DRE and its fractions

Among all test agents, DRE_flavonoid possessed the highest α-amylase inhibitory activity IC_{50} (644.29±4.36) µg/mL. The order α-amylase inhibition was DRE_flavonoid > DRE_polyphenol > DRE_alkaloid > DRE_saponin > DRE > DRE_steroid (Table 26). The percentage of enzyme inhibition by each test concentration is presented in Figure 46.

Table 26: α-glucosidase and α-amylase inhibitory activity of DRE and its fractions

Test agents	IC_{50} (µg/mL)	
	α-glucosidase	α-amylase
DRE	627.20±2.32	704.99±8.96
DRE_flavonoid	319.21±7.66	644.29±4.36
DRE_saponin	521.45 ±6.64	709.61±5.93
DRE_alkaloid	425.05±6.99	703.85±8.92
DRE_polyphenol	418.29±6.54	658.77±3.13
DRE_steroid	609.65±1.69	726.55±6.70
Acarbose*	71.28±0.45	71.28±0.45

*Gold standard as α-glucosidase and α-amylase inhibitor, All data are represented in Mean±SD, **IC_{50}**: Inhibitory concentration 50

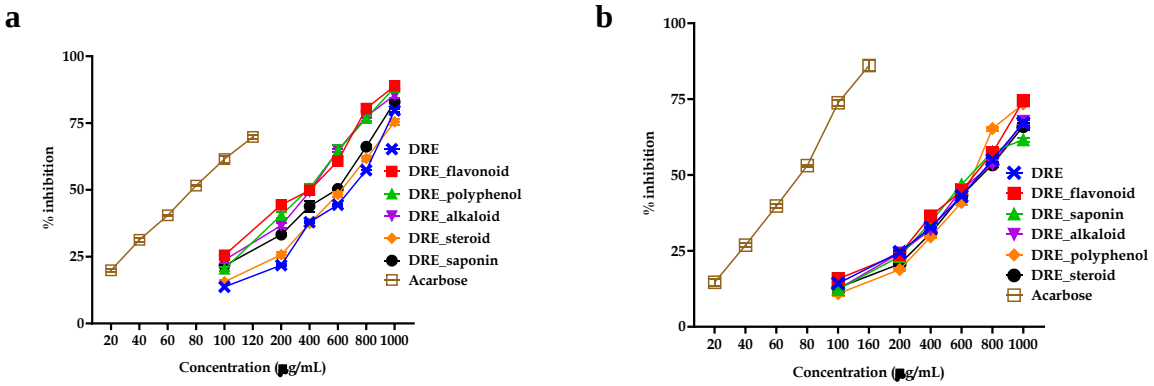

Figure 46: (a) α-glucosidase and (b) α-amylase inhibitory activity of DRE and its fractions

2.5.3. In vitro glucose adsorption assay of DRE and its fractions

DRE_steroid showed the highest efficacy in glucose adsorption AC_{50} (146.9±9.226) µg/mL. The order of the glucose adsorption efficacy was as DRE_flavonoids > DRE_steroids > DRE_saponins > DRE > DRE_alkaloids > DRE_polyphenols (Table 27).

Table 27: Glucose adsorptivity of DRE and its fractions

Test agent	AC_{50} (µg/mL)
DRE	82.93±0.29
DRE_steroid	269.85±5.34
DRE_saponin	141.30±4.86
DRE_flavonoid	358.98±5.73
DRE_polyphenol	354.35±4.85
DRE_alkaloid	230.91±5.54
Cellulose*	76.25±0.67

*Gold standard for glucose adsorptive assay, **AC_{50}**: Absorptive Concentration 50

2.5.4. Ex vivo glucose uptake assay of DRE and its fractions in isolated rat hemidiaphragm

Among all the test agents, DRE_flavonoid showed the highest glucose uptake efficacy *i.e.* EC_{50} (534.73±0.79) µg/mL in the presence of insulin in isolated rat hemidiaphragm. The order of glucose uptake efficacy was DRE_flavonoid > DRE_polyphenol > DRE_saponin > DRE_alkaloids > DRE > DRE_steroids (Table 28).

Table 28: Glucose uptake efficacy of DRE and its fractions in isolated rat hemidiaphragm

Test agent	EC_{50} (µg/mL)
DRE_polyphenol	559.16±8.13
DRE_flavonoid	534.73±0.79
DRE_saponin	604.00±2.92
DRE	723.46±6.49
DRE_alkaloid	642.75±5.15
DRE_steroid	765.38±13.45
Metformin*	169.38±2.44

*Gold standard used for enhancing the glucose uptake in the assay

2.5.5. Ex vivo glucose permeability assay of DRE and its fractions in rat jejunum

DRE_steroid showed the highest efficacy in inhibiting the glucose diffusion presenting a minimum AUC $_{0\text{-}180\ min}$. The order of inhibition of the glucose diffusion was DRE_steroid > DRE_saponin > DRE_alkaloid > DRE_flavonoid > DRE_polyphenol > DRE (Figure 47).

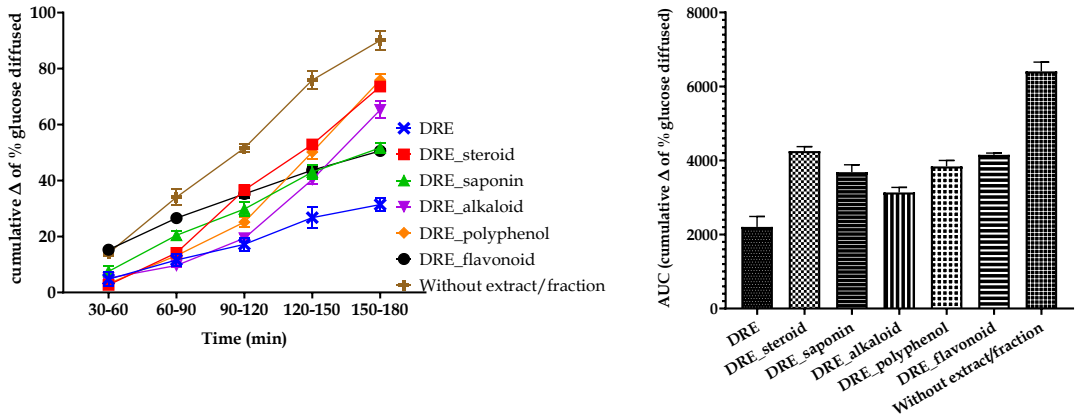

Figure 47: Effect of DRE and its fractions over the total AUC $_{0\text{-}180\ min}$ of glucose

2.6.In vivo anti-diabetic pharmacology of DRE

2.6.1. Effect of DRE in streptozocin-nicotinamide induced DM

- ***Effect of DRE on body weight, food intake, and water intake in streptozocin-nicotinamide-induced DM***: Combined injection of streptozocin and nicotinamide significantly decreased ($p<0.001$) the body weight (Figure 48) and food intake (Figure 49) compared to normal which was significantly increased ($p<0.001$) with DRE treatment compared to the diabetic. Also, water intake (Figure 50) was significantly increased ($p<0.001$) in the diabetic group compared to normal which was reversed with DRE treatment at all the test doses.

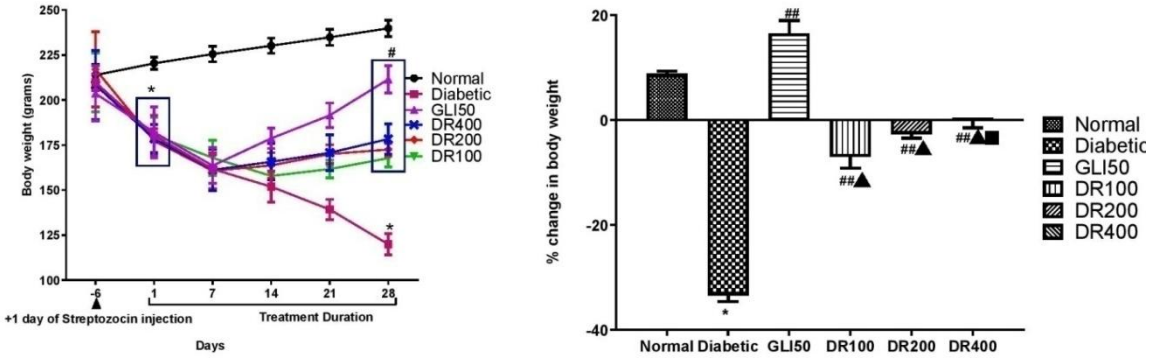

Figure 48: Effect of DRE on body weight in streptozocin-nicotinamide-induced DM. All the data are presented in Mean±SEM (n=6). *p <0.001 compared to normal; #p <0.05, ##p <0.001 compared to diabetic; ▲p <0.001 compared to GLI50; ■p <0.05, ■■p <0.01 compared to DR100.

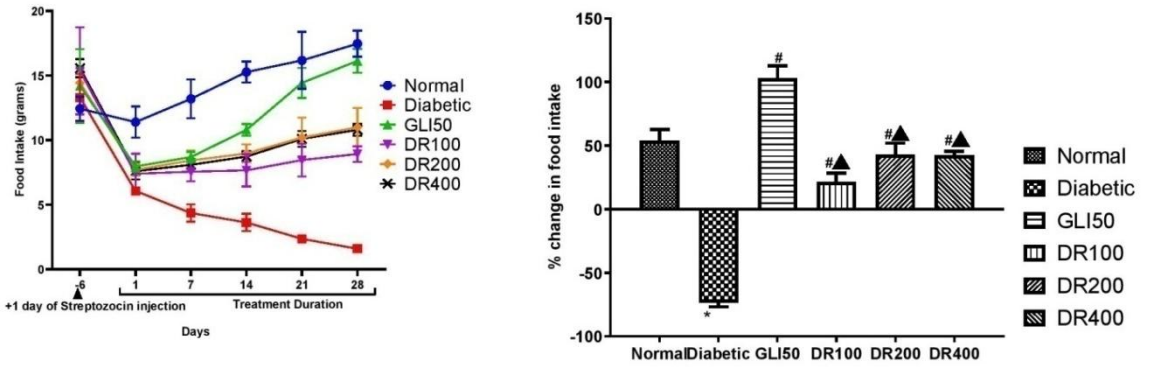

Figure 49: Effect of DRE on food intake in streptozocin-nicotinamide-induced DM. All the data are presented in Mean±SEM (n=6). *p <0.001, *vs* normal; #p <0.05, ##p <0.001 compared to diabetic; ▲p <0.001 compared to GLI50; ■p <0.05, ■■P <0.01 compared to DR100.

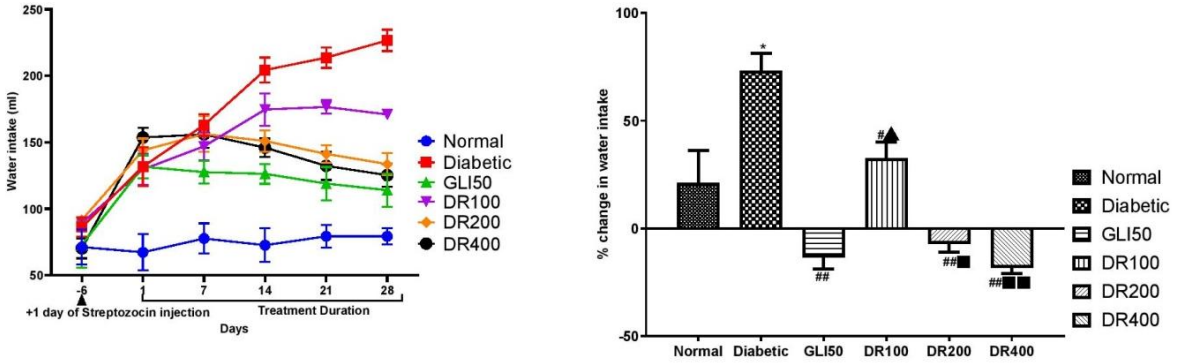

Figure 50: Effect of DRE on water intake in streptozocin-nicotinamide-induced DM. All the data are presented in Mean±SEM (n=6). *p <0.001 compared to normal; #p <0.05, ##p <0.001 compared to diabetic;▲p <0.001 compared to GLI50;▪p <0.05, ▪▪p <0.01 compared to DR100.

- ***Effect of DRE on fasting blood glucose and plasma insulin level in OGTT in streptozocin-nicotinamide-induced DM***: After 28 days of treatment, the fasting blood glucose level (Figure 51) was observed to be significantly increased (p<0.001), and insulin level (Figure 52) was significantly decreased (p<0.001) in the diabetic group compared to normal which was significantly increased with DRE and glibenclamide treatment. Further, OGTT revealed a significant increase (p<0.001) in the total AUC $_{0\text{-}120\ min}$ of glucose and a significant decrease (p<0.001) in the total AUC $_{0\text{-}120\ min}$ of insulin in the diabetic group compared to normal which was significantly reversed (p<0.01 & 0.001) with glibenclamide and DRE treatment compared to the diabetic; also, a dose-dependent effect was observed within DRE doses**.**

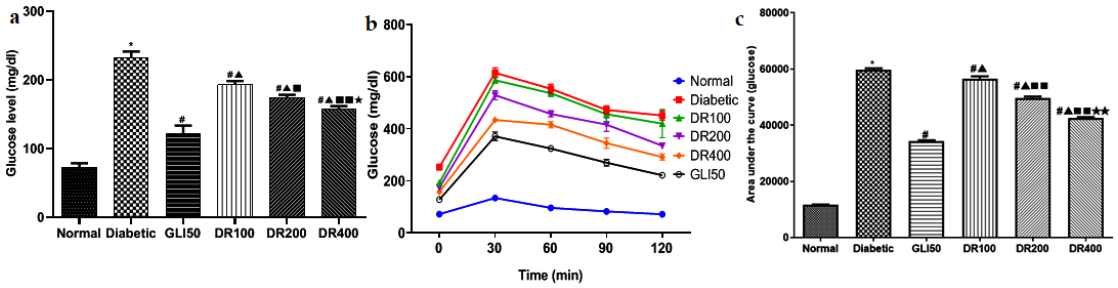

Figure 51: Effect of DRE on fasting blood glucose level in OGTT in streptozocin-nicotinamide-induced DM. All the data are presented in Mean±SEM (n=6). *p< 0.001compared to normal group, # p< 0.001compared to diabetic group,▲p< 0.001compared to GLI50 group;▪p<0.01,▪▪p< 0.001 compared to DR100 group;★ p< 0.01,★★ p< 0.001compared to DR200 group.

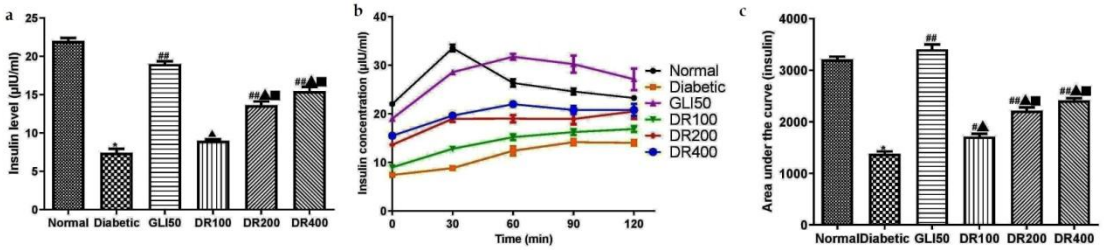

Figure 52: Effect of DRE on plasma insulin level in OGTT in streptozocin-nicotinamide-induced DM. All the data are presented in Mean±SEM (n=6). *p< 0.001 compared to normal, #p< 0.01, ##p< 0.001 compared to diabetic, ▲p< 0.001 compared to GLI50, ■p<0.001compared to DR100.

- ***Effect of DRE on glycated hemoglobin in streptozocin-nicotinamide-induced DM***: Glycated hemoglobin was significantly increased (p<0.001) in diabetic group compared to normal which was significantly decreased (p<0.01 & 0.001) within GLI50 and DRE treated groups compared to diabetic; the effect was dose-dependent within DRE treatment (Figure 53).

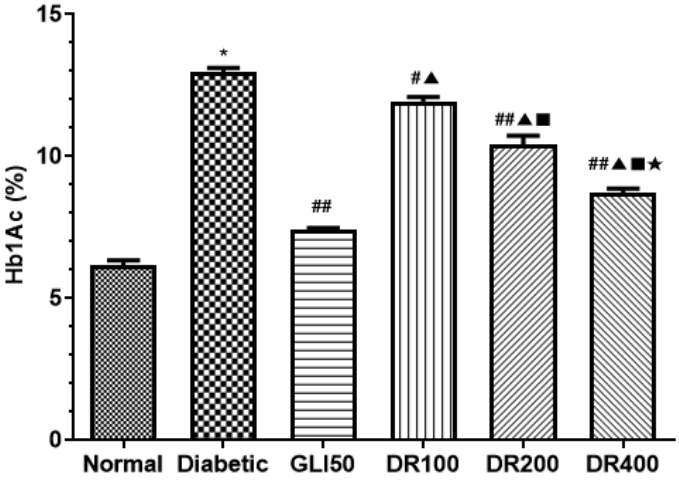

Figure 53: Effect of DRE on glycated hemoglobin in streptozocin-nicotinamide-induced DM. All the data are presented in Mean±SEM (n=6). *p< 0.001compared to normal;#p< 0.001, ##p< 0.001compared to diabetic;▲p< 0.001compared to GLI50;■p< 0.001compared to DR100;★p< 0.001compared to DR200.

- ***Effect of DRE on hepatic enzymes in streptozocin-nicotinamide-induced DM:*** There was a significant increase (p<0.001) in hepatic LDH, FBPase, G6Pase, PFK, and AST: ALT ratio and a significant decrease (p<0.001) in hepatic hexokinase level in the diabetic group compared to normal which was significantly ameliorated (p<0.01, 0.001) with glibenclamide and DRE treatment compared to the diabetic group; the

dose-dependent effect was observed within DRE treatment except AST: ALT ratio (Table 29).

Table 29: Effect of DRE on hepatic enzymes in streptozocin-nicotinamide-induced DM

Group	Hexokinase (U/mg)	G6Pase (U/mg)	FBPase (U/mg)	LDH (µmol/L/h/mg)	PFK (U/mg)	AST:ALT ratio
Normal	2.92 ± 0.01	10.95 ± 0.20	3.99 ± 0.05	166.40 ± 3.41	4.10 ± 0.16	1.34 ± 0.06
Diabetic	1.61 ± 0.02*	27.67 ± 0.79*	11.28 ± 0.27*	377.10 ± 8.23*	11.24 ± 0.25*	2.75 ± 0.10*
GLI50	2.59 ± 0.01$^{\#\#}$	15.71 ± 0.56$^{\#\#}$	5.50 ± 0.24$^{\#\#}$	209.60 ± 5.15$^{\#\#}$	4.99 ± 0.13$^{\#\#}$	1.52 ± 0.05$^{\#\#}$
DR100	1.74 ± 0.01$^{\#\#,▲▲}$	24.88 ± 0.41$^{\#,▲▲}$	10.40 ± 0.37$^{▲▲}$	333.10 ± 4.40$^{\#\#,▲▲}$	9.03 ± 0.22$^{\#\#,▲▲}$	1.38 ± 0.03$^{\#\#}$
DR200	1.93 ± 0.01$^{\#\#,▲▲,■■}$	22.90 ± 0.28$^{\#\#,▲▲}$	9.63 ± 0.28$^{\#\#,▲▲}$	281.30 ± 3.86$^{\#\#,▲▲,■■}$	7.90 ± 0.24$^{\#\#,▲▲,■}$	1.45 ± 0.08$^{\#\#}$
DR400	2.08 ± 0.02$^{\#\#,▲▲,■■,★★}$	19.70 ± 0.40$^{\#\#,▲▲,■■,★★}$	5.99 ± 0.12$^{\#\#,▲,■■,★★}$	253.50 ± 4.11$^{\#\#,▲▲,■■,★}$	5.93 ± 0.31$^{\#\#,■■,★★}$	1.58 ± 0.08$^{\#\#}$

All the data are presented in Mean±SEM (n=6). *p< 0.001 compared to normal; $^{\#}$p< 0.01, $^{\#\#}$p< 0.001 compared to Diabetic; $^{▲}$p< 0.05,$^{▲▲}$ p< 0.001compared to GLI50; $^{■}$p< 0.05, $^{■■}$p< 0.001compared to DR100;$^{★}$p< 0.01, $^{★★}$p< 0.001compared to DR200.

- ***Effect of DRE on urea uric acid and creatinine level in streptozocin-nicotinamide-induced DM***: In the diabetic group, a significant increase (p<0.001) in serum urea, uric acid, and creatinine level was observed compared to normal which was significantly decreased (p<0.05, 0.01, 0.001) with glibenclamide and DRE treatment compared to diabetic; the dose-dependent effect was observed with DRE treatment for urea level (Table 30).

Table 30: Effect of DRE on urea, uric acid and creatinine level in streptozocin-nicotinamide-induced DM

Group	Urea (mg/dL)	Uric acid (mg/dL)	Creatinine (mg/dL)
Normal	30.95 ± 0.80	1.67 ± 0.12	2.71 ± 0.15
Diabetic	55.27 ± 0.97**	2.90 ± 0.16*	3.26 ± 0.04**
GLI50	37.30 ± 0.71$^{\#\#}$	1.59 ± 0.03$^{\#\#}$	2.53 ± 0.05$^{\#\#}$
DR100	50.63 ± 0.48$^{\#\#,▲}$	2.16 ± 0.03	2.85 ± 0.06$^{\#}$
DR200	47.63 ± 0.29$^{\#\#,▲}$	1.83 ± 0.02$^{\#}$	2.82 ± 0.03$^{\#}$
DR400	43.58 ± 0.81$^{\#\#,▲,■,★}$	2.12 ± 0.45	2.56 ± 0.07$^{\#\#}$

All the data are presented in Mean±SEM (n=6). *p< 0.01, **p< 0.001 compared to normal; $^{\#}$p< 0.01, $^{\#\#}$p< 0.001 compared to diabetic;$^{▲}$p< 0.001 compared to GLI50; $^{■}$p< 0.001 compared to DR100; $^{★}$p< 0.01 compared to DR200.

- ***Effect on lipid profile***: TG, TC, VLDL, and LDL level was significantly increased (p<0.001) and HDL level significantly decreased (p<0.001) in the diabetic group compared to normal which was significantly reversed (p<0.001) with DRE treatment compared to a diabetic; the dose-dependent effect was observed within DRE treatment for all variables (Table 31).

Table 31: Effect of DRE on lipid profile in streptozocin-nicotinamide-induced DM

Group	TG (mg/dL)	TC (mg/dL)	HDL (mg/dL)	VLDL (mg/dL)	LDL (mg/dL)
Normal	45.92 ± 0.49	90.99 ± 0.94	59.49 ± 0.67	9.183 ± 0.09	22.32 ± 0.55
Diabetic	93.11 ± 3.54*	144.40 ± 0.66*	36.41 ± 0.63*	18.62 ± 0.71*	89.39 ± 1.60*
GLI50	51.07 ± 0.67$^{\#}$	103.4 ± 0.96$^{\#}$	57.93 ± 0.39$^{\#}$	10.21 ± 0.13$^{\#}$	35.29 ± 0.93$^{\#}$
DR100	77.07 ± 0.62$^{\#,▲}$	136.10 ± 1.71$^{\#,▲}$	42.04 ± 0.64$^{\#,▲}$	15.41 ± 0.12$^{\#,▲}$	78.66 ± 1.86$^{\#,▲}$
DR200	67.35 ± 1.00$^{\#,▲,■}$	121.00 ± 1.24$^{\#,▲,■■}$	48.4 ± 0.38$^{\#,▲,■■}$	13.47 ± 0.20$^{\#,▲,■}$	59.13 ± 1.18$^{\#,▲,■■}$
DR400	57.09 ± 3.18$^{\#,■■,★}$	114.60 ± 1.23$^{\#,▲,■■,★★}$	52.08 ± 0.34$^{\#,▲,■■,★★★}$	11.42 ± 0.64$^{\#,▲,■■,★}$	51.06 1.53$^{\#,▲,■■,★★}$

All the data are presented in Mean±SEM (n=6). *p< 0.001 compared to normal; #p< 0.001 compared to diabetic;▲p< 0.001 compared to GLI50; ■p< 0.05; ■■p< 0.001 compared to DR100; ★p< 0.05, ★★p< 0.01, ★★★p< 0.001 compared to DR200.

- ***Effect of DRE on glycogen content in gastrocnemius muscle and liver in streptozocin-nicotinamide-induced DM***: The hepatic and gastrocnemius muscle glycogen content was significantly decreased (p<0.001) in the diabetic group compared to normal which was significantly increased (p<0.05, 0.001) with glibenclamide and DRE (except 100 mg/kg) treatment in gastrocnemius muscle; the effect was dose-dependent with DRE treatment in both tissues (Figure 54).

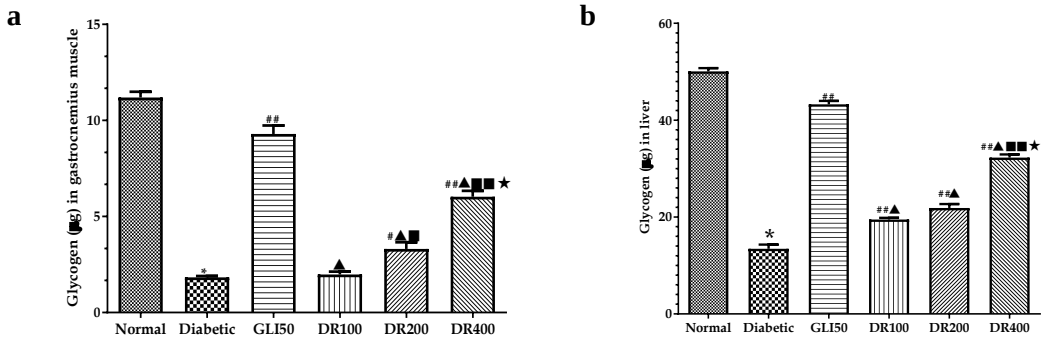

Figure 54: Effect of DRE on glycogen content in gastrocnemius muscle (a) and liver (b) in streptozocin-nicotinamide-induced DM. All the data are presented in Mean±SEM (n=6). *p< 0.001 compared to normal, #p< 0.05, ##p< 0.001 compared to diabetic, ▲p< 0.001 compared to GLI50, ■p< 0.05, ■■p< 0.001 compared to DR100, ★p< 0.001 compared to DR200.

- ***Effect of DRE on glucose uptake in isolated rat hemidiaphragm in streptozocin-nicotinamide-induced DM***: The percentage glucose uptake in isolated rat hemidiaphragm was significantly decreased (p<0.001) in the diabetic group compared to normal which was significantly increased (p<0.001) with glibenclamide and DRE

treatment (Figure 55).

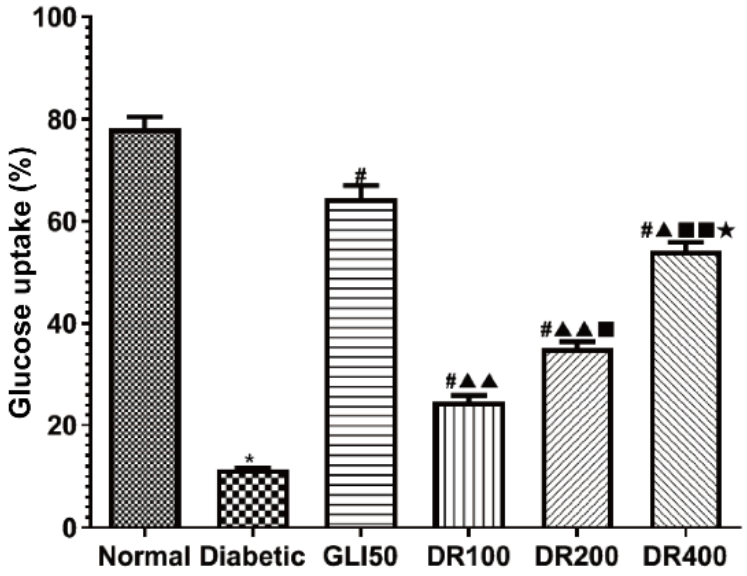

Figure 55: Effect of DRE on glucose uptake in isolated rat-hemidiaphragm in streptozocin-nicotinamide-induced DM. *p< 0.001 compared to normal, #p< 0.001 compared to diabetic, ▲p< 0.01, ▲▲p< 0.001 compared to GLI50, ▪p< 0.01, ▪▪p< 0.001 compared to DR100, ★p< 0.001 compared to DR200.

- ***Effect of DRE on enzymatic and non-enzymatic anti-oxidant biomarkers in streptozocin-nicotinamide-induced DM***: SOD, and GSH level and catalase activity were significantly decreased (p<0.001) in the diabetic group compared to normal; significantly increased (p<0.05, 0.01, 0.001) with glibenclamide and DRE treatment (200 & 400 mg/kg) compared to the diabetic. Nonetheless, an insignificant difference was noted within the total thiols and MDA levels among the groups (Table 32).

Table 32: Effect of DRE on enzymatic and non-enzymatic antioxidant biomarkers in streptozocin-nicotinamide-induced DM

Groups	SOD (U/mL)	Total thiols (µM/mg of protein)	GSH (µM/mg of protein)	Catalase (U/min/mg of protein)	MDA (nM/mg of protein)
Normal	27.81 ± 0.81	260.20 ± 4.87	135.90 ± 4.20	77.34 ± 2.29	203.00 ± 6.924
Diabetic	16.52 ± 1.16*	353.80 ± 64.72	33.76 ± 6.28*	30.86 ± 5.78*	276.70 ± 49.39
GLI50	25.72 ± 0.34$^{\#\#\#}$	262.70 ± 46.98	111.40 ± 19.83$^{\#\#\#}$	47.89 ± 8.52	194.70 ± 34.52
DR100	20.96 ± 0.45$^{\#\#\#▲▲▲}$	356.30 ± 2.73	51.38 ± 1.94$^{▲▲▲}$	45.88 ± 1.46	296.20 ± 2.25
DR200	25.95 ± 0.50$^{\#\#\#▪▪}$	340.00 ± 3.51	76.05 ± 3.09$^{\#}$	56.89 ± 1.87$^{\#\#}$	275.30 ± 3.97
DR400	27.02 ± 0.44$^{\#\#\#▪▪}$	303.50 ± 6.83	104.80 ± 4.22$^{\#\#▪}$	64.93 ± 1.27$^{\#\#\#}$	253.70 ± 3.93

All the data are presented in Mean±SEM (n=6). *p< 0.001 compared to normal; $^{\#\#\#}$p< 0.001 compared to diabetic, $^{▲▲▲}$p< 0.001 compared to GLI50; ▪p< 0.01, ▪▪p< 0.001 compared to DR100.

- ***Effect of DRE on the pancreatic and hepatic histology in streptozocin-nicotinamide-induced DM***: The average count of pancreatic β-cells and their size were significantly decreased ($p<0.001$) in the diabetic group compared to normal which was significantly increased ($p<0.05$, 0.001) with DRE treatment compared to the diabetic group. Although glibenclamide treatment showed a significant increase ($p<0.01$) in the average number of pancreatic β-cell, it had an insignificant role in their size. Similarly, lymphocytic infiltration, vascular degeneration, and congestion score were significantly increased ($p<0.001$) in the diabetic group; significantly reversed ($p<0.05$, 0.01, 0.001) with glibenclamide and DRE treatment (400 mg/kg) compared to the diabetic. Also, 200 mg/kg of DRE had a significant influence ($p<0.05$) in decreasing the vascular decongestion score compared to diabetic (Figure 56).

  Further, in hepatocytes, there was a significant increase ($p<0.01$, 0.001) in ballooning degeneration, sinusoidal congestion, and venous congestion score compared to normal which was significantly decreased ($p<0.01$) with glibenclamide treatment compared to normal. However, 400 mg/kg of DRE treatment only significantly decreased ($p<0.05$) the sinusoidal congestion score (Figure 57).

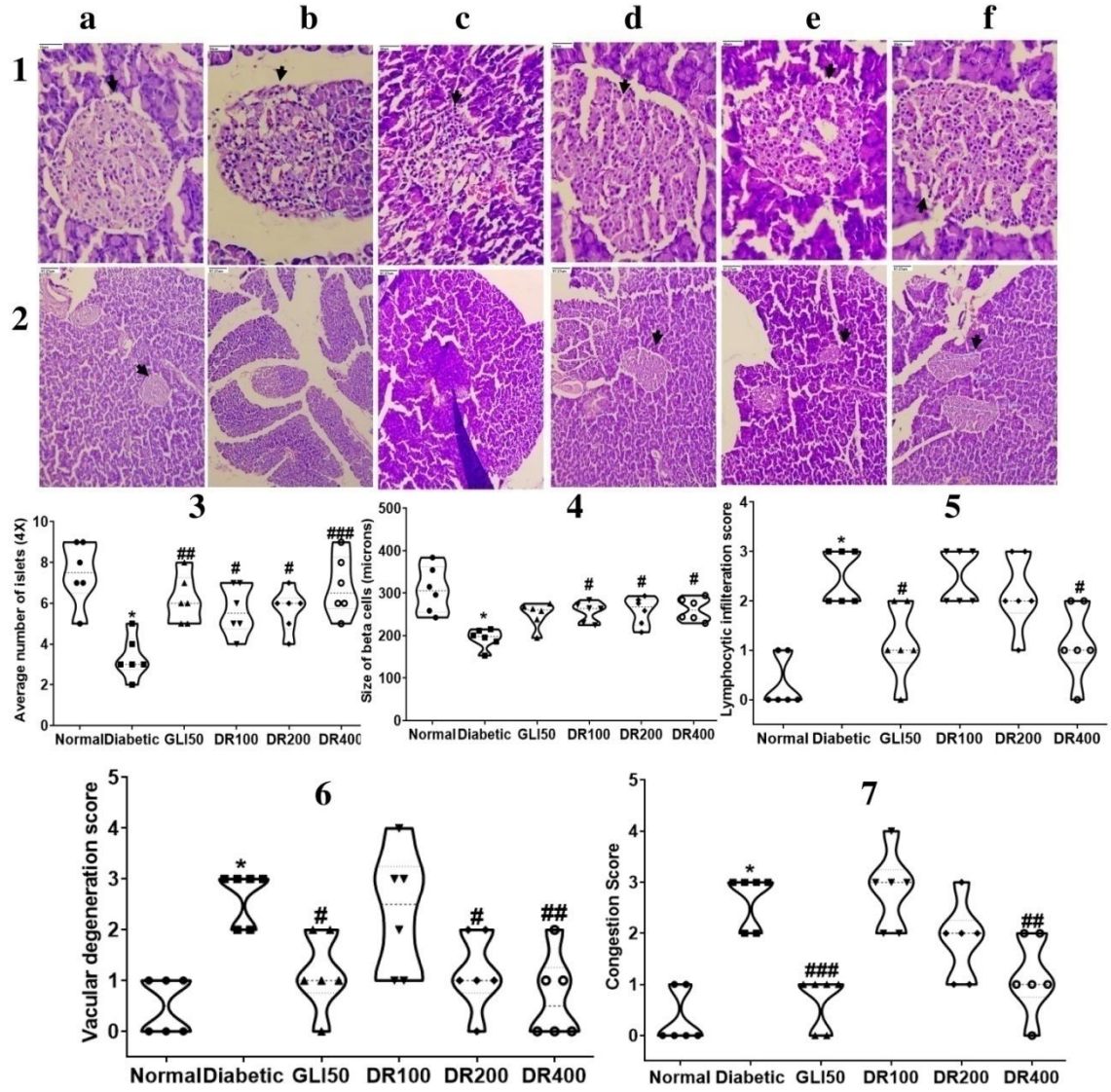

Figure 56: Effect of DRE on pancreatic histology (1; 40 & 2: 10 *X*) in streptozocin-nicotinamide-induced DM. ➘ pancreatic β-cell. a: normal; b: diabetic; c: MET45; d: DR100; e: DR200;f: DR400. *p< 0.001 compared to normal, #p< 0.05, ## p< 0.01 compared to diabetic.

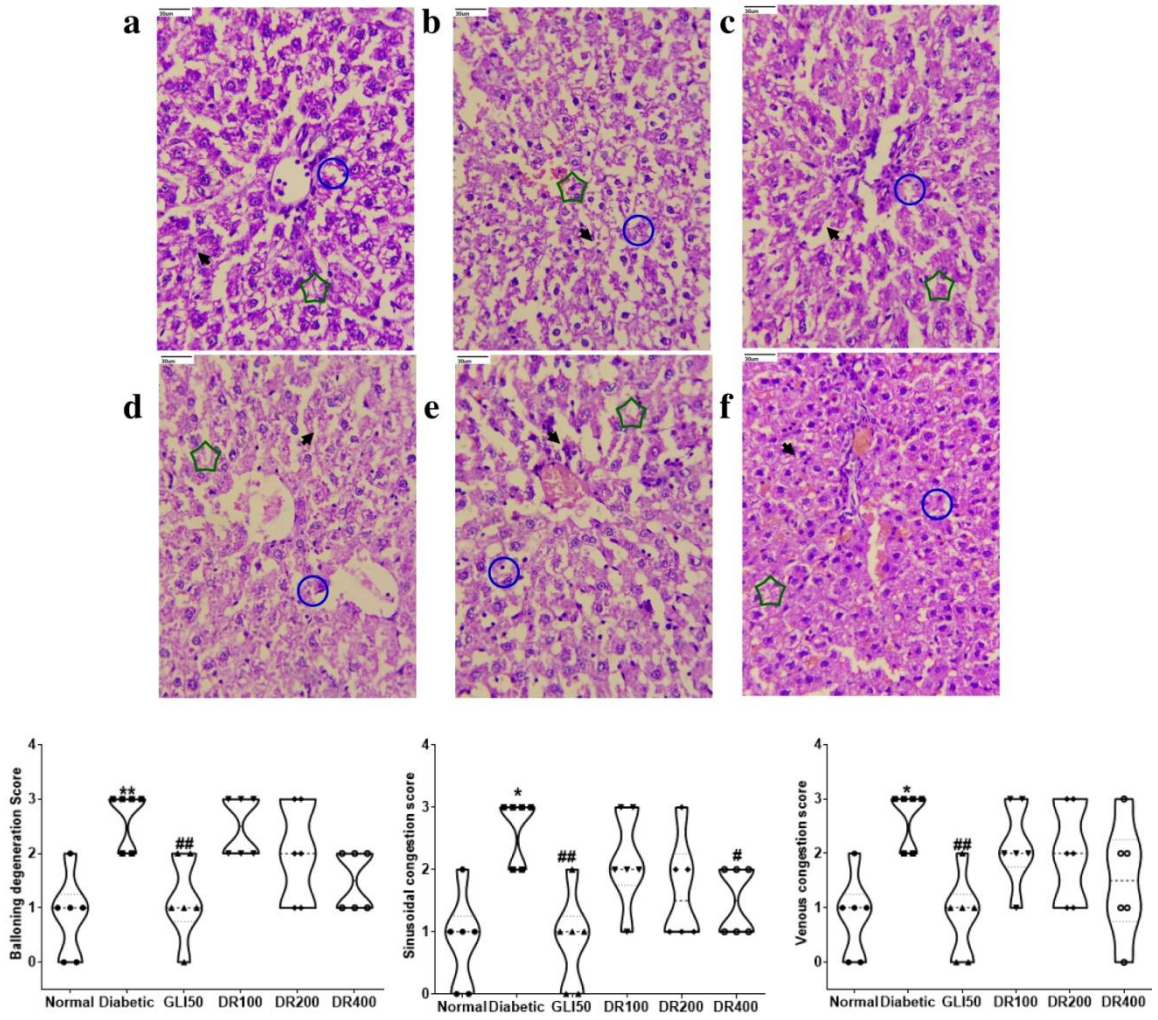

Figure 57: Effect of DRE on hepatocytes (40X) in streptozocin-nicotinamide-induced DM. a: normal; b: diabetic; c: MET45; d: DR100; e: DR200;f: DR400. ↘ sinusoidal congestion, ○ venous congestion, ⬠ ballooning degeneration. *p<0.01, **p<0.001 compared to normal group, #p<0.05, ##p<0.01 compared to diabetic group

2.6.2. Effect of DRE on fructose-induced insulin-resistant rats

- ***Effect of DRE on body weight, food intake, and water intake in fructose-induced insulin resistance***: Fructose supplementation in drinking water significantly decreased the body weight (p<0.001); Figure 58 and food intake (p<0.01); Figure 59 in the IR group compared to normal which was significantly reversed (p<0.05-0.001) with metformin and DRE treatment. Also, there was a significant increase (p<0.001) in water intake (Figure 60) in the IR group which was significantly decreased (p<0.001) with metformin and DRE treatment.

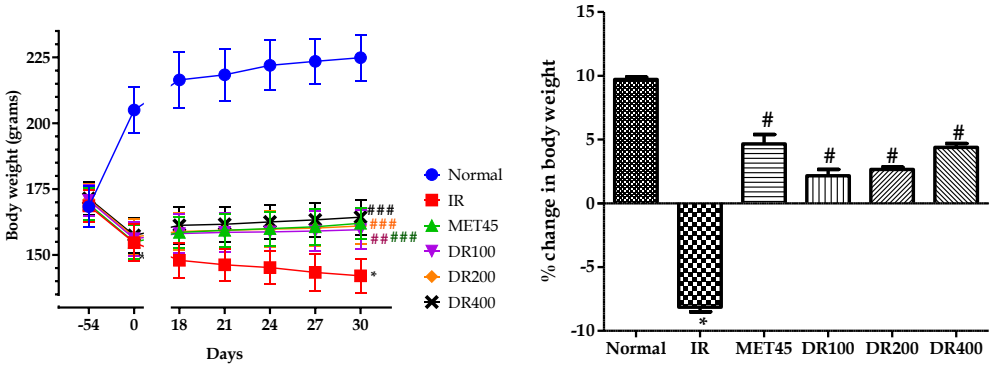

Figure 58: Effect of DRE on body weight in fructose-induced insulin resistance. All the data are presented in Mean±SEM (n=6). *p<0.001 compared to normal, #p<0.001 compared to IR

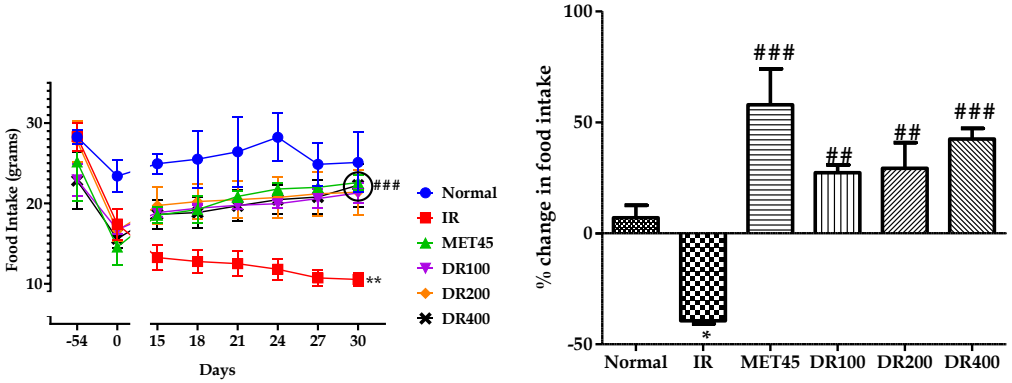

Figure 59: Effect of DRE on food intake in fructose-induced insulin resistance. All the data are presented in Mean±SEM (n=6). **p<0.001 compared to Normal, #p<0.05, ##p<0.01, ###p<0.001 compared to IR

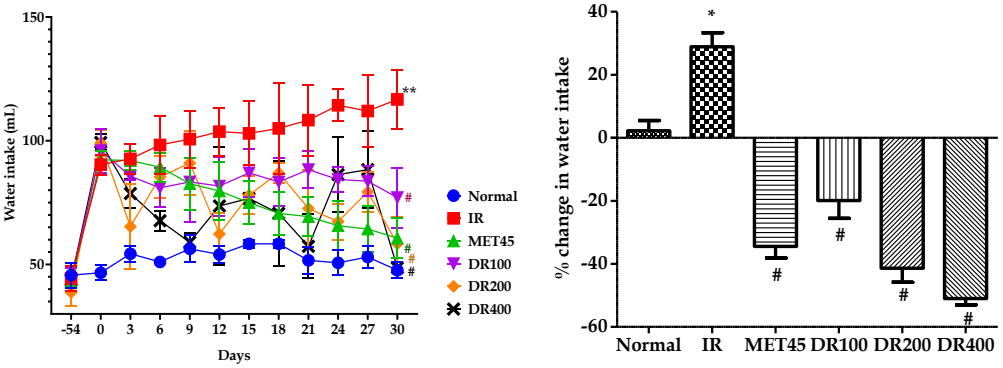

Figure 60: Effect of DRE on water intake in fructose-induced insulin resistance. All the data are presented in Mean±SEM (n=6). *p<0.01, **p<0.001 compared to normal, #p<0.05, ##p<0.01, ###p<0.001 compared to IR

- ***Effect of DRE on fasting blood glucose and plasma insulin level in OGTT in fructose-induced insulin resistance***: There was a significant increase (p<0.001) in fasting blood glucose, plasma insulin, and total AUC $_{0\text{-}120\ min}$ of glucose (Figure 61) and insulin (Figure 62) during OGTT in IR compared to normal. Treatment with DRE

significantly ameliorated (p<0.05-0.001) total AUC $_{0\text{-}120\ min}$ of glucose and insulin. However, DRE treatment did not affect reversing the fasting mild hyperglycaemic state compared to the IR group.

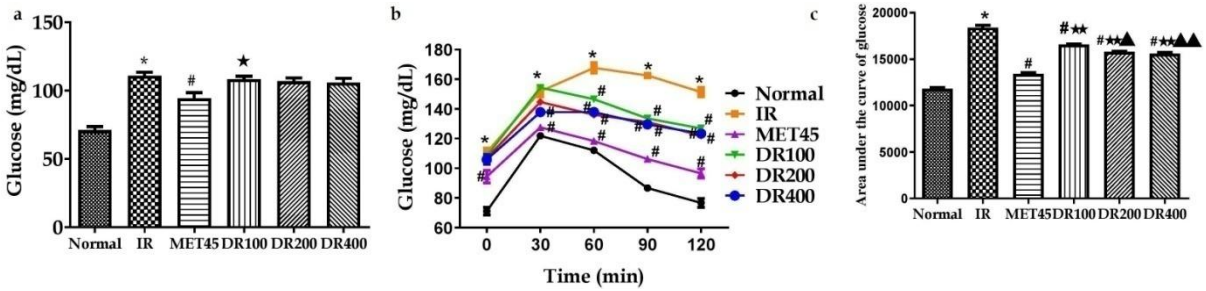

Figure 61: Effect of the DRE on blood glucose level in OGTT in fructose-induced insulin resistance. All the data are presented in Mean±SEM (n=6). *p<0.001 compared to normal, #p<0.001 compared to IR, ★p<0.05, ★★p<0.01 compared to MET45, ▲p<0.01, ▲▲p<0.001 compared to DR100.

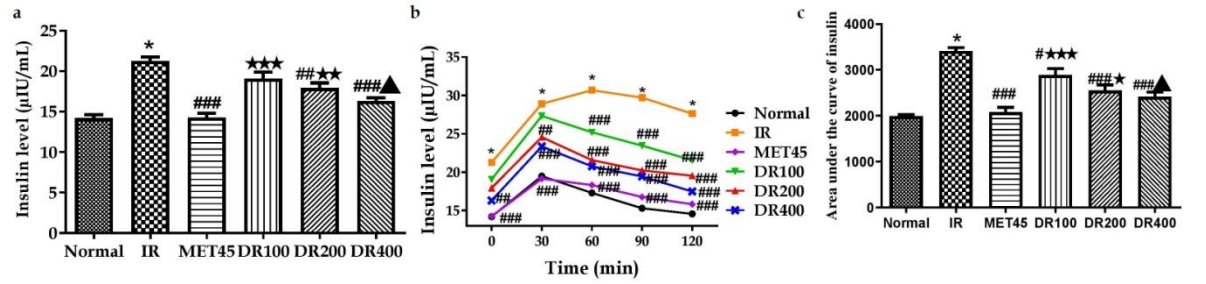

Figure 62: Effect of the DRE on plasma insulin level in OGTT in fructose-induced insulin resistance. All the data are presented in Mean±SEM (n=6). *p<0.001 compared to normal, #p<0.05, ##p<0.01, ###p<0.001 compared to IR, ★p<0.05, ★★p<0.01, ★★★p<0.001 compared to MET45, ▲p<0.05 compared to DR100

- ***Effect of DRE on ITT in fructose-induced insulin resistance***: Blood glucose level in the IR group was observed to be significantly high (p<0.001) compared to normal within 0-120 min which was significantly reversed (p<0.05-0.001) with metformin and DRE treatment compared to IR. Further, the total AUC $_{0\text{-}120\ min}$ of glucose was significantly higher (p<0.001) in the IR group compared to normal which was significantly lowered (p<0.001) with metformin and DRE treatment except 100 mg/kg of DRE; the dose-dependent effect was observed within DR100 *vs* DR200 *vs* DR400 (Figure 63).

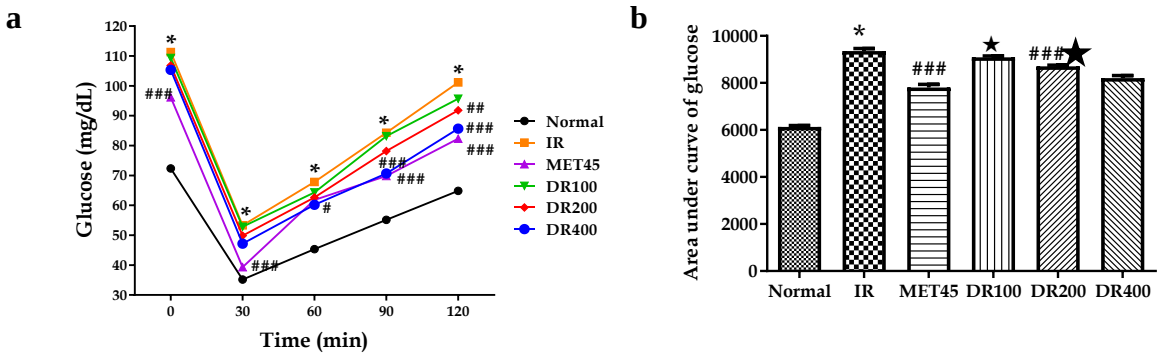

Figure 63: Effect of the DRE on glucose level in the ITT in fructose-induced insulin resistance. All the data are presented in Mean±SEM (n=6). *p<0.001 compared to normal, #p<0.05, ##p<0.01, ###p<0.001 compared to IR, ★p<0.001 compared to MET45, ▲p<0.001 compared to DR100, ▪p<0.01 compared to DR200

- ***Effect of DRE on HOMA-IR in fructose-induced insulin resistance***: In the IR group, HOMA-IR was significantly higher (p<0.001) compared to normal which was significantly decreased (p<0.01, 0.001) with metformin and DRE (except 100 mg/kg) treatment compared to IR; the dose-dependent effect was observed with DRE treatment within DR100 & DR200 *vs* DR400 (Figure 64).

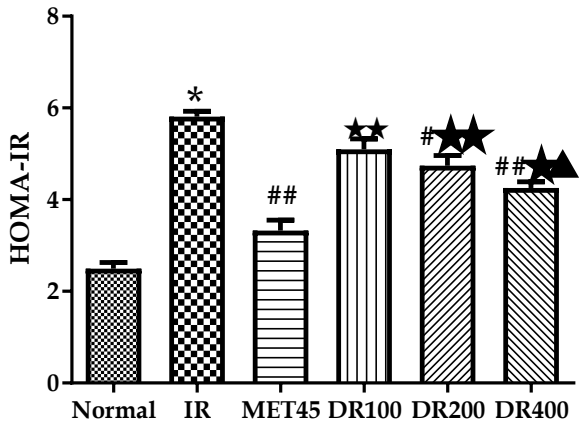

Figure 64: Effect of the DRE on HOMA-IR in fructose-induced insulin resistance. All the data are presented in Mean±SEM (n=6). *p<0.001 compared to normal, #p<0.01, ##p<0.001 compared to IR, ★p<0.05, ★★p<0.001 compared to MET45, ▲p<0.05 compared to DR100

- ***Effect of DRE on lipid profile in fructose-induced insulin resistance*:** There was a significant decrease (p<0.001) in TC, HDL, VLDL, and LDL level and a significant increase in TG level (p<0.001) in the IR group compared to normal which was significantly reversed (p<0.001) with DRE treatment except HDL; however, only 400

mg/kg of DRE was observed to be effective in ameliorating TC and LDL level; further dose-dependent effect was observed with DRE treatment within DR100 & DR200 *vs* DR400 except for HDL level (Table 33).

Table 33: Effect of the DRE on lipid profile in fructose-induced insulin resistance

	TG (mg/dL)	TC (mg/dL)	HDL (mg/dL)	VLDL (mg/dL)	LDL (mg/dL)
Normal	45.17±1.78	119.50±2.17	55.67±0.88	9.03±0.356	54.80±2.44
IR	120.30±2.68*	90.67±1.36*	39.67±1.20*	24.07±0.54*	26.93±1.79*
MET45	58.17±2.70$^{\#}$	123.8±1.89$^{\#}$	51.17±2.27$^{\#}$	11.63±0.54$^{\#}$	61.03±2.33$^{\#}$
DR100	91.17±1.38$^{\#}$★★★	92.33±1.52★★★	39.83±1.62★★★	18.23±0.28$^{\#}$★★★	34.27±1.69★★★
DR200	85.33±1.93$^{\#}$★★★	96.17±1.99★★★	43.83±1.47★	17.07±0.39$^{\#}$★★★	35.27±3.34★★★
DR400	74.33±1.54$^{\#}$★★★▲▲▪	112.50±2.14$^{\#}$★★★▲▲▪▪	46.83±2.27	14.87±0.31$^{\#}$★★★▲▲▪	50.80±4.36$^{\#\#\#}$▲▲▪

All the data are presented in Mean±SEM (n=6). *p<0.001 compared to normal, $^{\#}$p<0.001 compared to IR, ★p<0.05, ★★p<0.01, ★★★p<0.001 compared to MET45, ▲p<0.01, ▲▲p<0.001 compared to DR100, ▪p<0.01, ▪▪p<0.001 compared to DR200

- ***Effect DRE on glucose uptake in the isolated rat hemidiaphragm in fructose-induced insulin resistance***: In the IR group, there was a significant decrease (p<0.001) in % glucose uptake in isolated rat hemidiaphragm compared to normal which was significantly increased (p<0.001) with metformin and DRE treatment compared to IR; the dose-dependent effect was observed with DRE treatment within DR100 *vs* DR200 *vs* DR400 (Figure 65).

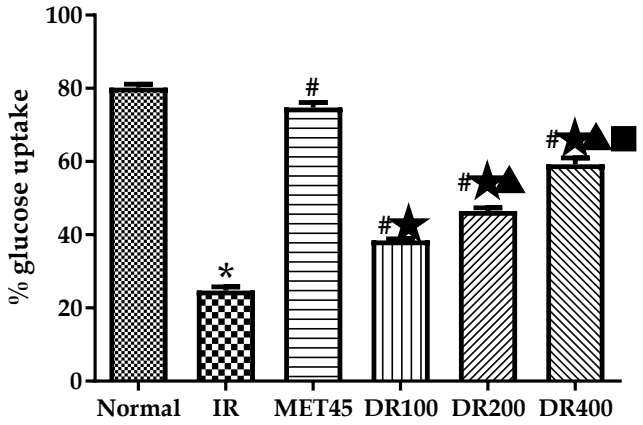

Figure 65: Effect of the DRE on percentage glucose uptake in fructose-induced insulin resistance. All the data are presented in Mean±SEM (n=6). *p<0.001 compared to normal, $^{\#}$p<0.001 compared to IR, ★p<0.001 compared to MET45, ▲p<0.001 compared to DR100, ▪p<0.001 compared to DR200

- ***Effect of DRE on glycogen content in gastrocnemius muscle and liver in fructose-induced insulin resistance***: Fructose supplementation significantly decreased ($p<0.001$) the glycogen content in liver and gastrocnemius muscle in the IR group which was significantly increased ($p<0.01$, 0.001) with metformin and DRE (except 100 mg/kg in gastrocnemius muscle) treatment compared to IR; the response was observed to be dose-dependent in the liver within DR100 *vs* DR200 *vs* DR400 and gastrocnemius muscle within DR100 & DR200 *vs* DR400 (Figure 66).

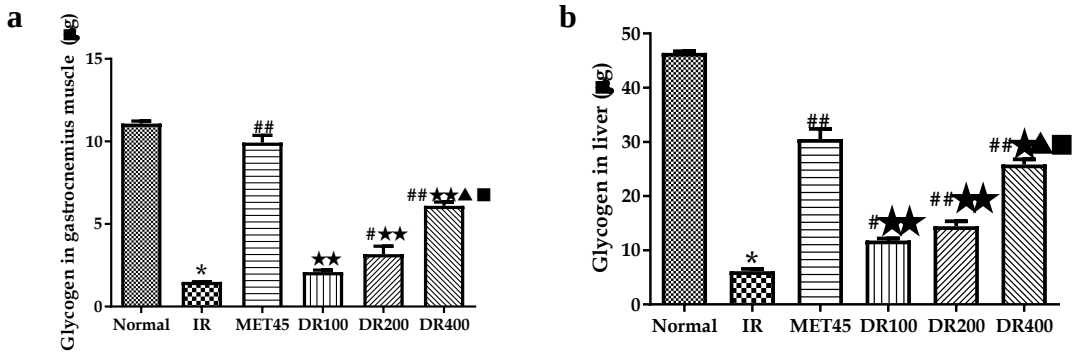

Figure 66: Effect of FBE on glycogen content in gastrocnemius muscle and liver in fructose-induced insulin resistance. All the data are presented in Mean±SEM (n=6). *$p<0.001$ compared to normal, $^{\#}p<0.01$, $^{\#\#}p<0.001$ compared to IR, $^{\star}p<0.05$, $^{\star\star}p<0.001$ compared to MET45, $^{\blacktriangle}p<0.001$ compared to DR100, $^{\blacksquare}p<0.001$ compared to DR200.

- ***Effect of DRE on hepatic enzymes in fructose-induced insulin resistance***: There was a significant decrease ($p<0.001$) in hepatic hexokinase level and a significant increase ($p<0.001$) in G6Pase, FBPase, PFK, and LDH level and AST: ALT ratio in IR group compared to normal which was significantly ameliorated ($p<0.05$ & 0.001) with metformin and DRE treatment compared to IR. Further, a dose-dependent effect was observed with DRE treatment within all hepatic enzymes except AST: ALT ratio (observed within DR100 & DR200 *vs* DR400); Table 34.

Table 34: Effect of DRE on hepatic enzymes in fructose-induced insulin resistance

Groups	Hexokinase (U/mg)	G6Pase (U/mg)	FBPase (U/mg)	PFK (U/mg)	LDH (µmol/L/h/mg)	AST: ALT ratio
Normal	2.62±0.12	10.48±0.24	3.46±0.14	4.25±0.29	170.70±3.18	0.93±0.13
IR	1.502±0.12*	41.18±1.62*	18.57±0.349*	12.58±0.386*	331.30±7.60*	3.17±0.14*
MET45	2.60±0.10$^{\#\#}$	16.33±0.55$^{\#\#}$	5.88±0.40$^{\#\#}$	7.03±0.28$^{\#\#}$	203.90±4.46$^{\#\#}$	1.436±0.09$^{\#\#}$
DR100	1.93±0.10$^{\#}$★★	27.96±0.66$^{\#\#}$★★	15.36±0.45$^{\#\#}$★★	11.01±0.49$^{\#}$★★	282.90±2.26$^{\#\#}$★★	2.20±0.05$^{\#\#}$★★
DR200	2.36±0.05$^{\#\#}$▲	24.01±0.52$^{\#\#}$★★▲	11.46±0.63$^{\#\#}$★★▲▲	9.367±0.26$^{\#\#}$★★▲	247.50±2.53$^{\#\#}$★★▲▲	1.96±0.07$^{\#\#}$★
DR400	2.74±0.047$^{\#\#}$▲▲	18.65±0.47$^{\#\#}$▲▲▪	8.36±0.17$^{\#\#}$★★▲▲▪	8.60±0.29$^{\#\#}$★★▲▲	231.90±2.40$^{\#\#}$★★▲▲	1.74±0.05$^{\#\#}$▲

All the data are presented in Mean±SEM (n=6). *p<0.001 compared to normal, $^{\#}$p<0.05, $^{\#\#}$p<0.001, ★ p<0.01, ★★p<0.001, ▲p<0.05, ▲▲p<0.001 comapred to DR100, ▪p<0.001 compared to DR200.

- ***Effect of DRE on enzymatic and non-enzymatic antioxidant biomarkers in fructose-induced insulin resistance***: There was a significant increase (p<0.001) in LPO and THABS level in liver homogenate in the IR group compared to normal which was significantly decreased (p<0.05, 0.01, 0.001) with metformin and DRE (400 mg/kg for LPO & 200 & 400 mg/kg for THABS) treatment compared to IR. In contrast, there was a significant decrease (p<0.001) in GSH, and SOD level and catalase activity in liver homogenate in the IR group compared to normal which was significantly increased (p<0.001) with DRE (400 mg/kg) treatment compared to IR. Further, dose-dependent effect was observed with DRE treatment within DR100 *vs* DR400 (LPO & SOD) and DR100 & DR200 *vs* DR400 (GSH & catalase); Table 35.

Table 35: Effect of the DRE on enzymatic and non-enzymatic anti-oxidant biomarkers in fructose-induced insulin resistance

Groups	LPO (nM/mg of protein)	GSH (µM/mg of protein)	THABS (µM/mg of protein)	Catalase (U/[min/mg] of protein)	SOD (U/mL)
Normal	154.6±11.94	119.50±4.66	218.60±2.69	84.94±4.81	35.02±0.83
IR	290.7±19.59*	24.08±1.32*	313.20±4.88*	35.04±2.16*	22.01±1.33*
MET45	169.2±16.71$^{\#\#\#}$	101.60±3.65$^{\#\#\#}$	239.60±4.60$^{\#\#\#}$	82.04±3.77$^{\#\#\#}$	32.89±0.48$^{\#\#\#}$
DR100	279.4±15.62★★★	25.69±2.18★★★	294.20±6.57★★★	34.78±2.84★★★	22.29±1.26★★★
DR200	231.7±13.23	33.56±0.63★★★	283.80±6.15$^{\#}$★★★	47.37±2.71★★★	25.34±2.15★★
DR400	201.60±7.74$^{\#\#}$▲	53.90±1.80$^{\#\#\#}$★★★▲▲▪▪	274.00±8.12$^{\#\#\#}$★★	64.53±4.63$^{\#\#\#}$★▲▲▪	30.64±0.55$^{\#\#\#}$▲▲

All the data are presented in Mean±SEM (n=6). *p<0.001 compared to normal, $^{\#}$p<0.05, $^{\#\#}$p<0.01, $^{\#\#\#}$p<0.001 compared to IR, ★p<0.05, ★★p<0.01, ★★★p<0.001 compared to MET45, ▲p<0.01, ▲▲p<0.001 compared to DR100, ▪p<0.05, ▪▪p<0.001 compared to DR200

- ***Effect of DRE on urea, uric acid, and creatinine level in fructose-induced insulin resistance***: The urea, uric acid, and creatinine level were observed to be significantly

higher ($p<0.001$) in the IR group compared to normal which was significantly reversed with metformin and DRE treatment ($p<0.01$ & 0.001) compared to IR; the dose-dependent effect was observed with DRE treatment within DR100 & DR200 *vs* DR400 for urea, DR100 *vs* DR200 *vs* DR400 for uric acid and DR100 *vs* DR200 & DR400 (Table 36).

Table 36: Effect of the DRE on urea, uric acid, and creatinine level in fructose-induced insulin resistance

Groups	Urea (mg/dL)	Uric acid (mg/dL)	Creatinine (mg/dL)
Normal	17.83±1.99	2.35±0.20	1.22±0.11
IR	54.67±1.26*	8.22±0.35*	3.38±0.12*
MET45	24.17±1.62$^{\#\#}$	3.47±0.06$^{\#\#}$	1.77±0.09$^{\#\#}$
DR100	44.17±1.72$^{\#}$★★	6.58±0.08$^{\#\#}$★★	2.43±0.15$^{\#\#}$★
DR200	39.33±1.91$^{\#\#}$★★	5.08±0.11$^{\#\#}$★★▲▲▲	1.87±0.14$^{\#\#}$▲
DR400	31.17±1.45$^{\#\#}$▲▲▲▪	3.52±0.06$^{\#\#}$▲▲▲▪▪	1.68±0.14$^{\#\#}$▲▲

All the data are presented in Mean±SEM (n=6). *$p<0.001$ compared to normal, $^{\#}p<0.01$, $^{\#\#}p<0.001$ compared to IR, ★$p<0.01$, ★★$p<0.001$ compared to MET45, ▲$p<0.05$, ▲▲$p<0.01$, ▲▲▲$p<0.001$ compared to DR100, ▪$p<0.05$, ▪▪$p<0.001$ compared to DR200

- ***Effect of DRE on plasma leptin level in fructose-induced insulin resistance***: There was a significant decrease ($p<0.001$) in plasma leptin level in the IR group compared to normal which was significantly increased ($p<0.01$ & 0.001) with metformin and DRE treatment compared to IR; the dose-dependent effect was observed with DRE treatment within DR100 *vs* DR200 *vs* DR400 (Figure 67).

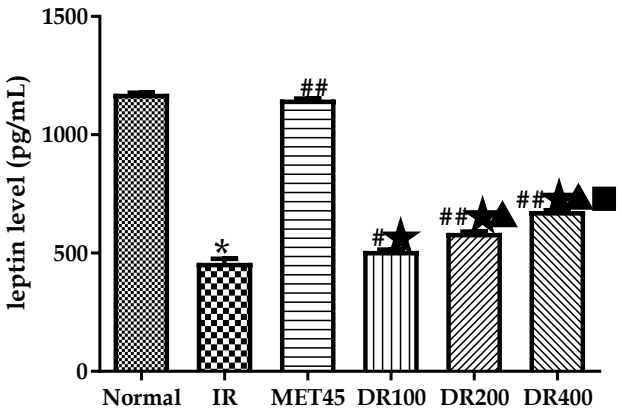

Figure 67: Effect of the DRE on leptin level in fructose-induced insulin resistance. All the data are presented in Mean±SEM (n=6). *$p<0.001$ compared to normal, $^{\#}p<0.01$, $^{\#\#}p<0.01$ compared to IR, ★$p<0.001$ compared to MET45, ▲$p<0.001$ compared to DR100, ▪$p<0.001$ compared to DR200

- ***Effect of DRE on hepatic histology in fructose-induced insulin resistance***: There was an observable increase in sinusoidal congestion score in hepatocytes in the IR group compared to normal; was significantly reversed DRE (400 mg/kg) compared to IR. Further, in IR group, there was significant increase in venous congestion ($p<0.05$), ballooning degeneration ($p<0.05$), inflammation ($p<0.05$), apoptosis ($p<0.001$), spotty necrosis ($p<0.05$), portal triditis ($p<0.01$), and cholestasis score ($p<0.01$) and kupffer cell hyperplasia ($p<0.05$) compared to normal which was significantly reversed within MET45 ($P<0.05$), DR200 ($P<0.01$) and DR400 ($p<0.05$) for sinusoidal congestion, MET45 ($p<0.05$) for ballooning degeneration, MET45, DR200 & DR400 ($p<0.05$) for inflammation, MET45 ($p<0.01$) and DR400 ($p<0.05$) for apoptosis, MET45 ($p<0.05$) for spotty necrosis, MET45 ($p<0.01$) for portal triditis, MET45, DR200 & DR400 ($p<0.05$) for cholestatis score and MET45 ($p<0.05$), DR200 ($p<0.05$) and DR400 ($p<0.01$) for kupffer cell hyperplasia (Figure 68).

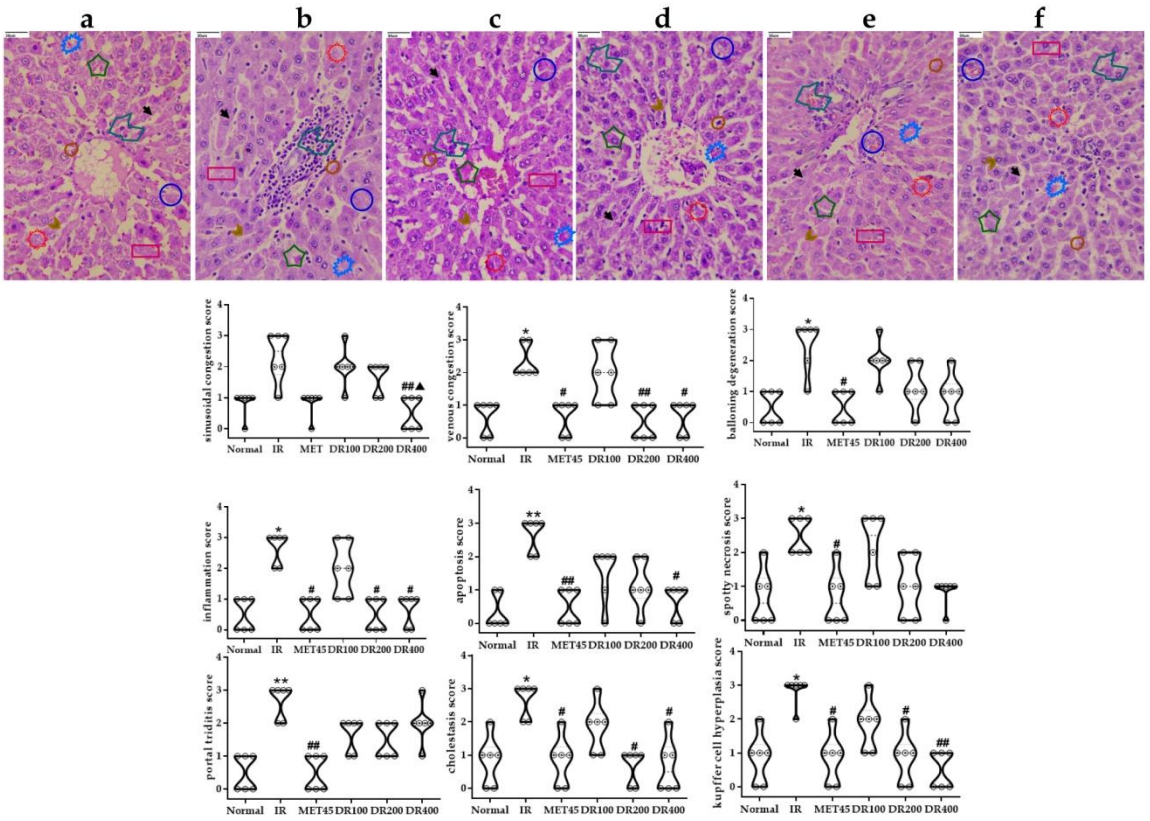

Figure 68: Effect of DRE on hepatocytes (40X) in fructose-induced insulin resistance. a: normal; b: diabetic; c: MET45; d: DR100; e: DR200;f: DR400. sinusoidal congestion, venous congestion, ballooning degeneration, inflammation, apoptosis, spotty necrosis, portal triditis, cholestasis, kuffer cell hyperplasia. *$p<0.05$ compared to normal, $^{\#}p<0.05$, $^{\#\#}p<0.01$ compared to IR, $^{\blacktriangle}p<0.05$ compared to DR100.

Chapter 6

Discussion

DISCUSSION

This work attempted to propose the probable anti-diabetic mechanism of *Ficus benghalensis* and *Duranta repens via* the computational approach followed by an experimental assessment. In this regard, initially, we performed the network pharmacology to predict the ***bioactive(s)-protein(s)-pathway(s)*** interaction *via* the concept of "*multi compound-multi protein*" interaction(s) as explained previously.[13] Since the pathogenesis of DM is further complicated with the ROS system[178], we assessed the binding affinity of bioactives from both medicinal plants with free radical generators, and the extracts were further tested in multiple *in vitro* anti-oxidant models. Based on the inputs from *in silico* studies, 5 different anti-diabetic models were chosen majorly focusing on the functional biomarkers which were demonstrated *via in vitro* and *ex vivo* protocols; further expanded to *in vivo* anti-diabetic activity in insulin-deficient (streptozocin-nicotinamide-induced hyperglycemia[129]) and insulin-resistant (fructose-induced insulin resistant[132]) models.

1. *In-silico* (network pharmacology and molecular docking) studies

Network pharmacology reveals the multiple compounds interactions with multiple proteins to trigger various pathways[13] from which majorly targeted protein and chief bioactives can be traced; this can be further evaluated using molecular docking. In this regard, we identified the potential bioactives from ChEBI and PCIDB and related literature. The compounds mined from the open-source platform were further confirmed *via* the HPLC analysis using specific biomarkers for FBE (apigenin) and DRE (ursolic acid) which were also indicated in network interactions.

1.1. FBE primarily modulates PTP1B in DM

Previously PTP1B has been indicated as a negative regulator of insulin signaling in

various organs[179] and its upregulation triggers the pancreatic β-cell apoptosis[180]. Also, we observed the chief modulation of PTP1B in which ***3-O-trans-p-coumaroyltormentic acid*** (1) and ***ursolic acid*** (2) had the highest binding affinity with it with positive druglikeness score *i.e.* 1.1 and 0.65 respectively reflecting their oral bioavailability. In addition, previously ursolic acid has been reported to inhibit the PTP1B and stimulate the phosphorylation of insulin receptors and stimulate glucose uptake[181]. Hence, the regenerated pancreatic β-cells and enhanced glucose uptake (demonstrated *via ex-vivo* and *in-vivo* protocols) could be the outcome of PTP1B inhibition in both pancreas and other tissues including liver and gastrocnemius muscle. However, we reported the action of ***3-O-trans-p-coumaroyltormentic acid*** over the PTP1B inhibition for the first time *via* the computational studies that need to be further confirmed *via* experimental protocols. In addition, we observed AMPK, PPAR, PI3K-Akt, and insulin signaling pathways regulation that are concerned with lipid, protein, and glucose homeostasis[182-184] which was further confirmed *via* the glucose, lipid, and nitrogen metabolites measurement in both diabetic and insulin-resistant states.

1.2. DRE primarily triggers insulin signaling pathway in diabetes

Through network pharmacology, we identified the PI3K-Akt, insulin, and PPAR signaling pathways *via* the combined action of bioactives of *D. repens*. Herein, also the majority of the bioactives targeted PTP1B in which ***pseudo-ginsenoside-RT1*** had the highest binding affinity with a 0.9 druglikeness score. As reported earlier, PTP1B is directly concerned with the negative regulation of insulin signaling[179] and was allocated within the insulin signaling pathway, it can be speculated that DRE is directly concerned with ameliorating the insulin function by inhibiting PTP1B to stimulate the insulin receptor phosphorylation[185] to promote glucose uptake[181] as demonstrated *via* the *ex-vivo* study leading to enhanced glycogen synthesis in liver and gastrocnemius muscle in both diabetic

and insulin-resistant states (*in vivo*).

2. An *in-vitro* and *ex-vivo* studies

2.1. α-amylase and α-glucosidase contribute to postprandial hyperglycemia

Enzymes α-amylase hydrolyze the starch into smaller oligosaccharides which are further hydrolyzed into α-oligoglucans by α-glucosidase[114]; monomers get absorbed into systemic circulation *via* GLUT transporters[186]; contributes to the postprandial hyperglycemia. Inhibition of the above enzymes or blocking the GLUTs in the gastrointestinal tract could contribute to managing postprandial hyperglycemia.

2.1.1. FBE inhibits starch hydrolyzing enzymes and inhibits the glucose diffusion

Here, FBE's flavonoid fraction had maximum α-glucosidase & α-amylase inhibition (*in vitro*); ***apigenin*** (1) & ***kaempferol*** (2) -mediated over α-amylase and ***3', 4', 5, 7-tetrahydroxy-3-methoxyflavone*** (1), ***apigenin*** (2), ***isowighteone*** (3), ***mucusisoflavone A*** (4), ***B*** (5), and ***C*** (6), ***kaempferol*** (7), ***wighteone*** (8), and ***cyclomorusin A*** (9)-mediated over α-glucosidase as demonstrated *via* molecular docking (*in silico*).

In addition, we observed the inhibition of glucose diffusion by multiple groups of bioactives including FBE to inhibit glucose transportation from the jejunum. It was further noted that the fractions of multiple phytochemistry had less glucose diffusion efficacy compared to FBE meaning that the bioactives may not be directly involved to act over the GLUT transporters in the intestine; however, inhibited glucose diffusion could be *via* the interaction of fibers present in the extract with free glucose as explained previously[123] contributing to managing the post-prandial hyperglycemia.

2.1.2. DRE inhibits starch hydrolyzing enzymes and inhibits the glucose diffusion

Herein, we observed α-amylase and α-glucosidase inhibition with multiple class of DRE's bioactives in which flavonoid fraction had the highest efficacy to act over both enzymes which could be *via* ***scutellarein*** (1), ***naringenin*** (2), ***3, 7, 4'-Trihydroxy-3'-(8''-acetoxy-7''-methyl octyl)-5,6 dimethoxyflavone*** (3), & ***7-O-α-D-glucopyranosyl-3,5-dihydroxy-3'-(4''-acetoxyl-3''-methylbutyl)-6,4'-dimethoxyflavone*** (4) over α-amylase & ***pectolinarigenin*** (1), and ***scutellarein*** (2) over α-glucosidase. These findings further support Iqbal *et al*[20] where ***7-O-α-D-glucopyranosyl-3,5-dihydroxy-3'-(4''-acetoxyl-3''-methylbutyl)-6,4'-dimethoxyflavone*** from *D. repens* was identified as an α-glucosidase inhibitor. In addition, ***pectolinarigenin*** has also been reported to inhibit α-glucosidase[187] which may have contributed to the DRE's flavonoid fraction over the enzyme action to hold polysaccharide hydrolysis.

Further, the DRE's fractions had the minimum role to inhibit the glucose diffusion compared to DRE. Thus, it can be speculated that bioactive(s) from *D. repens* may not be directly involved to act over the GLUTs in the intestine which was cross-confirmed within the *in silico* pharmacology where none of the bioactive(s) were predicted to allocate the GLUTs function. Further, DRE's action over the glucose diffusion could be an outcome of fiber interaction with free glucose[124] and limit the rate of glucose diffusion from the jejunum.[128]

2.2.Promotion of glucose utilization ameliorates the diabetes

Defective glucose transport is linked with GLUT-4 malfunction due to altered insulin signaling that has been evidenced as a prime link in insulin resistance[188]. The efficacy of bioactive(s) to regulate this protein or ameliorate insulin function could promote peripheral glucose utilization; promotes glycogenesis; cross-confirmed *via* the quantification of the

glycogen in hepatic and gastrocnemius muscle.

2.2.1. FBE upregulates the peripheral glucose utilization in isolated rat hemidiaphragm

Herein, we observed the significant increase in glucose uptake efficacy of FBE and its fractions; primarily flavonoids in the presence of insulin. Since the glucose uptake was not observed in the absence of insulin, it can be further pointed that, FBE and its fraction themselves may not promote the glucose uptake. As detailed earlier, since the majority of the bioactives from *F. benghalensis* manipulate PTP1B function, they promote insulin function as PTP1B are identified to oppose protein tyrosine kinase effects, physiologically activated by insulin receptor; dephosphorylated by PTP1B; thus its inhibition may prolog insulin action[179,185] by ***wighteone*** (1), ***3',4',5,7-tetrahydroxy-3-methoxyflavone*** (2), and ***mucusisoflavone A*** (3), ***B*** (4), and ***C*** (5) as they had the druglikeness score >0.9; reflects good oral bioavailability and could be majorly triggered *via* ***mucusisoflavone C***-inhibited PTP1B action. Since the independent action of the above-mentioned bioactives over the glucose uptake assay has not been traced yet *via* the experimental protocols, it is slightly knotty to explain whether FBE and its fraction have a direct action over glucose uptake or not. However, since the glucose uptake was observed only in the presence of insulin, it can be reflected that FBE directly doesn't contribute to the glucose uptake independently but promotes the insulin function *via* PTP1B inhibition as demonstrated *via* the molecular docking (*in silico*).

2.2.2. DRE upregulates the peripheral glucose utilization in isolated rat hemidiaphragm

DRE also promoted peripheral glucose utilization which was majorly contributed by the flavonoid in the presence of insulin. Hence, the majority of the flavonoids with positive druglikeness characters *i.e.* ***naringenin*** (1), ***scutellarein*** (2),

3,7-Dihydroxy-3'-(2-hydroxy-3-methyl-3-butenyl)-5,6,4' trimethoxyflavone (3), ***5,7-Dihydroxy-3'-(2-hydroxy-3-methyl-3-butenyl)-3,6,4'-trimethoxyflavone*** (4), and ***pectolinarigenin*** (5) may get absorbed into the systemic circulation and may have promoted the glucose uptake into the hepatic and gastrocnemius tissue in both diabetic and insulin-resistant states (*in vivo*); confirmed *via* the glycogen estimation. Since, in the absence of the insulin, DRE and its fractions failed to utilize the glucose in rat hemidiaphragm, it can be speculated that they may not directly stimulate glucose transporters; the observed effect could be due to insulin receptor activation *via* PTP1B inhibition by ***7-O- α- D- glucopyranosyl- 3, 5- dihydroxy- 3'- (4''-acetoxyl- 3''-methylbutyl)- 6, 4'-dimethoxyflavone*** (*in silico*).

3. *In vivo* study

3.1.Streptozocin-nicotinamide-induced DM in rats

Streptozocin (one of the potent alkylating agents) interferes with the glucokinase and glucose transport function, breaks the DNA strand; increases activity of PARP-1 to depict the intracellular NAD(+) and ATP[135], and also generates the free radicals leading to pancreatic β-cell necrosis; induces T1DM.[189] However, the combined injection of nicotinamide with streptozocin checks PARP-1 function to minimize the intracellular NAD (+) and ATP depletion[135].

Pancreatic β-cell apoptosis leads to insulin deficiency leading to hyperglycemia which is majorly observed in T1DM[190]. In streptozocin-nicotinamide-induced hyperglycemia, PTP1B is also upregulated in the pancreas affecting the glucose homeostasis as it deteriorates the β-cell function[180]. Since streptozocin injection develops oxidative stress in the pancreas[191], it may further activate PTP1B[180]. Hence, direct PTP1B inhibition in the pancreas or neutralization of free radicals or blocking the action of free radical generators may check

the β-cell apoptosis and help in cells regeneration.

Also, multiple investigations have been traced to report the markable rise of the hepatic enzymes involved in gluconeogenesis in streptozocin-induced hyperglycemia including PFK, G6Pase, and FBPase followed by a drastic decline in hexokinase (an enzyme involved in glucose catabolism)[192]; which could be the output of chronic glucotoxicity and declined insulin level; was also observed in the present study. In addition, in streptozocin-induced hyperglycemia, it was indicated towards compromised glycogen synthesis[193] as there is a failure to fulfill insulin demand to activate GSK3B.

Further, since insulin is involved in protein metabolism[194], its deregulation could enhance the nitrogen metabolites (urea, uric acid, and creatine) in hyperglycemia[195] as demonstrated in streptozocin-nicotinamide diabetes.

3.1.1. FBE action over streptozocin-nicotinamide-induced DM in rats

Within 28 days of FBE treatment, there was a significant increase in pancreatic β-cell number which was confirmed *via* the histopathological examination and increased fasting plasma insulin level; reflects the possibility of the PTP1B inhibition by ***3-O-trans-p-coumaroyltormentic acid*** (1) and ***ursolic acid*** (2) (*in silico* prediction) in the pancreas as predicted *via* molecular docking. In addition, three bioactives *i.e.* ***3-O-trans-p-coumaroyltormentic acid*** (1), ***mucusisoflavone C*** (2), and ***wighteone*** (3) (*in silico* prediction) could directly inhibit free radical generators and inhibit the PTP1B function; suggesting the efficacy of FBE in regenerating the pancreatic β-cells.

Since FBE treatment significantly increased insulin level, it could have enhanced the hexokinase level[196]; stimulated by ***mucusisoflavone B***. Also, GSK3B

was traced within bioactives-targets-pathways interaction (network pharmacology); its stimulation might be the reason for uplifted glycogen synthesis in streptozocin-nicotinamide induced hyperglycemia.

In addition, since FBE treatment enhanced insulin level, it may have activated GSK3B to promote glucose efflux into hepatocytes and stratified myocytes to support the glycogen synthesis as observed in the present study.

3.1.2. DRE action over streptozocin-nicotinamide-induced DM in rats

After 28 days of DRE treatment, we observed a significant increase in insulin level which further increased to respond to the exogenous glucose load during OGTT which could be the outcome of increased β-cells in the pancreas; this was confirmed *via* the histological examination of the pancreas (*in vivo*). Since PTP1B is directly concerned with the pancreatic β-cell apoptosis[180], its direct inhibition in the pancreas could help in glucose homeostasis *via* the regeneration of β-cells which could be due to ***durantanin I*** (*in silico* prediction). In addition, the regenerated β-cells could be the output of potent anti-oxidant action of DRE (*in vitro* and *in vivo*) by terminating the redox reactions and blocking the action of free radical generators by ***naringenin*** (1), ***3,7-Dihydroxy-2-[4-hydroxy-3-(4-hydroxy-3-methylbutyl)phenyl]-5,6-dimethoxy-4H-1-benzopyran-4-one*** (2), and ***7-O-α-D-glucopyranosyl-3,5-dihydroxy-3'-(4''-acetoxyl-3''-methylbutyl)-6,4'-dimethoxyflavone*** (3) (*in silico* prediction).

DRE treatment significantly increased the hepatic hexokinase level (*in vivo*); probably activated by ***repennoside*** (*in silico*). In addition, an increase in the hepatic and skeletal muscle glycogen content could be *via* GSK3B activation[197]. Since there was PI3K-Akt, and insulin signaling pathways regulation by DRE's bioactives (network pharmacology), it could improve the insulin function; leading to improved

glucose homeostasis as evidenced *via* the OGTT. As there was increased insulin level with DRE treatment, it might have activated GSK3B and effluxed glucose into hepatocytes and stratified myocytes to upregulate glycogen synthesis followed by the amelioration of nitrogen metabolites to regulate the nitrogen metabolites.

3.2.Fructose-induced insulin resistance in rats

Previously, it has been reported that chronic fructose administration in rodents may decrease the insulin receptors in the liver and skeletal muscle to contribute to insulin resistance[136]. In addition, fructose also provokes lipogenesis and gluconeogenesis *via* the SIRT1 dependent process.[198] In addition, insulin resistance can be indicated by increased HOMA-IR; reflects the association of pancreatic β-cell response with hepatic gluconeogenesis and blood glucose level[199] which is reported to be increased in fructose-induced hyperinsulinemia. In addition, hyperinsulinemia, elevated TG level, and increased HOMA-IR are the indicators of insulin resistance.[3,200,201] Supporting this literature, in the present study, we observed a significant increase in the above indicators suggesting the development of insulin resistance in fructose-supplemented rats. In addition, in insulin resistance and diabetic state, there is increased hepatic oxidative stress which manipulates the insulin function which was also observed[202] in the present study.

Leptin regulates the appetite[203] which is directly corresponded with bodyweight gain. Also, it contributes to glucose metabolism; decreased leptin levels develop insulin resistance[204]. In addition, it possesses various glucoregulatory actions like declining glucagon production and regulating hepatic glucose efflux followed by the promotion of glucose utilization[205]. In the previous study, fructose supplementation and deregulated plasma leptin level has been reported[169] which was also demonstrated in our study in fructose-induced insulin-resistant animals.

Hepatic gluconeogenesis is one of the major contributors in the development of T2DM[53] moreover contributed by G6Pase, PFK, and FBPase[206,207]; reflected to be increased in fructose-induced hyperinsulinaemic rats[169]. In addition, the activation of ROS also leads to peripheral insulin resistance as it affects the insulin receptor signal transduction. This further compromises the GLUT4 expression in the cell membrane leading to limited glucose uptake.[208]

In fructose-induced insulin resistance, due to PTP1B upregulation in peripheral tissue, there is insulin receptor desensitization ultimately compromises the glucose uptake[185], and deactivation of GSK3B could be one of the reasons for decreased glycogen content in liver and skeletal muscle as observed in our findings.

Nitrogen metabolites *i.e.* urea, uric acid, or creatinine levels are altered in fructose-induced hyperinsulinemia[169]; also observed in our present study. Similarly, the previous report reflected no association of the insulin and hepatic urea cycle; insulin may not have a direct influence over the urea level as glucose gets itself reduced into hepatic amino group conversion, and is independent of hormonal response to glucose,[209] which could be the reason why these by-products were elevated; could be due glucose- alanine cycle regulation.[210]

Hepatic fat accumulation enhanced FFAs delivery to the liver and oxidation, and raised de novo lipogenesis *via* hyperinsulinaemic state could stimulate anabolic processes to develop the nonalcoholic fatty liver disease (NAFLD)[211] contributed by chronic fructose administration[212]; promotes T2DM development[213].

3.2.1. FBE action over fructose-induced insulin-resistant rats

Within 30 days of FBE treatment, we observed a significant decrease in the HOMA-IR index which reflects the insulin sensitivity effect; further supported by the

ITT where the treated animals had an effective response towards the exogenous insulin compared to insulin-resistant animals. In addition, we observed ameliorated lipid profile which suggests the improved function or response towards the lipid metabolism. Another, indicator for the FBE's insulin sensitivity effect is also reflected *via* the promoted glucose uptake after the chronic treatment or exposure with FBE in isolated rat hemidiaphragm. Previously, it was demonstrated that exogenous insulin administration with previously treated insulin sensitizer lowers the glucose level in its peak time.[169] This is further supported by PI3K-Akt, PPAR, and insulin signaling pathways regulation; reflected from network pharmacology. In addition, FBE treatment (30 days, fructose-induced insulin resistant animal model) revealed its efficacy to ameliorate the deregulated appetite (confirmed *via* the food intake) and insulin sensitivity could have been influenced by upregulated plasma leptin with FBE treatment.

Also, hepatic G6Pase, PFK, and FBPase levels were significantly decreased; indicating the reversal of the hepatic gluconeogenesis. This could be the inhibitory action of the bioactives over the above-mentioned enzymes majorly by ***mucusisoflavone B*** (1) as revealed *via* molecular docking. In addition, FBE was demonstrated for its potential anti-oxidant activity majorly by scavenging the free radicals and terminating the redox or Fenton reactions within ROS to some extent (*in vitro*) followed by checking the function of free radicals by ***3-O-trans-p-coumaroyltormentic acid*** (1), ***mucusisoflavone C*** (2), and ***wighteone*** (3) as predicted *via* docking study.

Since FBE was presented as an insulin sensitizer (*via* OGTT and ITT) and composes PTP1B inhibitors; including ***3-O-trans-p-coumaroyltormentic acid*** (1) and

ursolic acid (2), it can be theorized that insulin receptor could have been activated with PTP1B inhibition to enhance the glucose efflux into hepatocytes and skeletal myocytes ultimately promoting glycogen synthesis.

FBE treatment markedly ameliorated the hyperinsulinemia which could have amended the lipid oxidation and may have declined excessive transport of FFAs in the liver which might have resulted in checking the NAFLD progression. In addition, FBE might have acted over glucose- alanine cycle independent of insulin action; ameliorated nitrogen metabolites could be the output of the ameliorated glucose, lipid, and proteins homeostasis.

3.2.2. DRE action over fructose-induced DM in rats

Herein, we observed the significant amelioration of lipid profile including TG level which could be the output of improved insulin sensitivity[201] after DRE treatment. This could be the outcome of improved insulin sensitivity; further confirmed by the decreased HOMA-IR, and AUC of glucose and insulin in OGTT and ITT. Also, DRE's efficacy to enhance the glycogenesis could be the outcome of glucose efflux into the peripheral tissue to promote glycogen synthesis; supported by enhanced glucose uptake (*ex-vivo*); could be through PTP1B inhibition by ***durantanin I*** (*in silico*). Also, DRE treatment significantly increased plasma leptin levels within 30 days. Hence, it may have influenced the insulin function by promoting glucose uptake which consequently triggers glycogenesis; confirmed *via* the glycogen quantification in the liver and gastrocnemius muscle which evidences DRE as an insulin sensitizer.

In molecular docking we observed the higher affinity of ***scutellarein*** with FBPase, ***pseudo-ginsenoside–RT1*** with G6Pase, and ***durantanin I*** with PFK (*in*

silico) which could have inhibited their action; also confirmed *via* enzymes quantification (*in vivo*). In addition, DRE was involved in terminating redox and Fenton reactions within the ROS (*in vitro*), followed by the inactivation of free radical generators by ***3,7-Dihydroxy-2-[4-hydroxy-3-(4-hydroxy-3-methylbutyl)phenyl]-5,6-dimethoxy-4H-1-benzopyran-4-one*** (1)**,** and ***7-O-α-D-glucopyranosyl-3,5-dihydroxy-3'-(4''-acetoxyl-3''-methylbutyl)-6,4'-dimethoxyflavone*** (2), and ***naringenin*** (3); evidenced with molecular docking.

DRE ameliorated hyperinsulinemia; may amend β-oxidation and have declined excessive FFAs transport in the liver in minimizing the NAFLD progression. Further, DRE might have regulated the multiple pathways of nitrogen metabolism; could be the indirect effect of ameliorated glucose, lipid, and proteins homeostasis with enhanced insulin sensitivity.

Summary of the mechanism of action of FBE against DM

- **FBE** could act over the multiple proteins and pathways to deal with hyperglycemia which was demonstrated using predictive and experimental data.
- It was observed that **FBE** has a potency to promote glucose utilization by flushing it into gastrocnemius muscle and liver; promoting glycogenesis.
- **FBE** promotes insulin sensitivity; confirmed *via* the OGTT, ITT, HOMA-IR.
- Additionally, **FBE** may inhibit glucose diffusion from the intestine.
- Further, **FBE** may act on multiple hepatic enzymes involved in gluconeogenesis to deal with high hepatic glucose outflow.
- Since the elevated level of insulin was observed with **FBE** treatment in insulin deficiency, it can be confirmed that FBE had the potency to regenerate the pancreatic β-cells and also facilitate insulin synthesis and release which was confirmed *via* histopathological examination by assessing pancreatic β-cell(s) size and count.
- Further, **FBE** ameliorated the lipid profile; reduced the FFAs as competitors with glucose as a substrate for glycolytic enzymes; could have supported in improving glucose homeostasis.
- In addition, **FBE** reduced hepatic oxidative stress by ameliorating enzymatic and non-enzymatic antioxidant biomarkers.
- Ca^{2+}, PI3K-Akt, PPAR, and insulin signaling pathways were identified to be directly concerned against DM which was triggered with bioactives of *F. benghalensis*.

The probably regulated sites in T2DM pathogenesis (KEGG: hsa04930) by the bioactives of F. benghalensis are summarized in Figure 69.

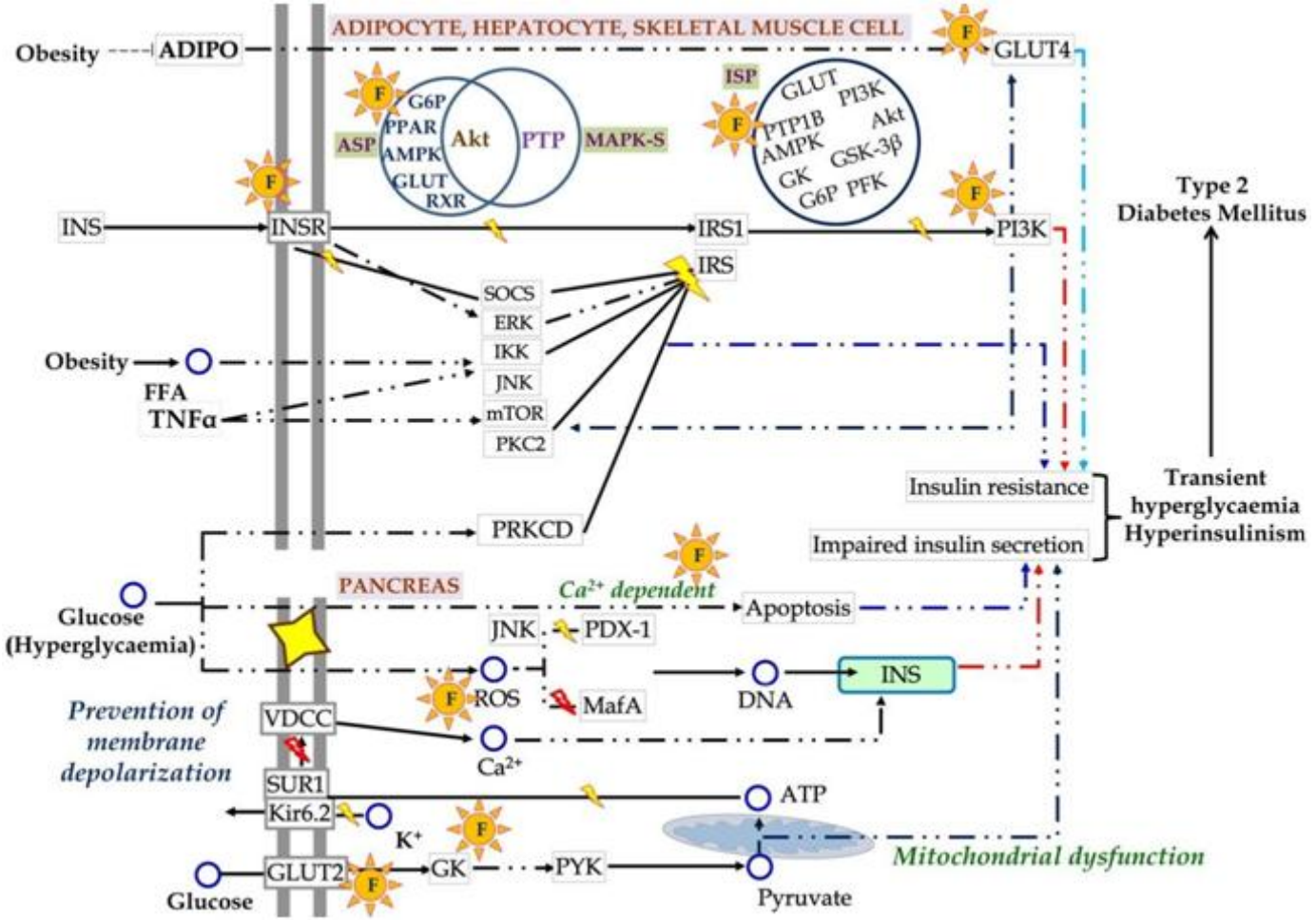

Figure 69: Probable anti-diabetic mechanism of *F. benghalensis*L. bark. glycation, hexosamine pathway, respiratory chain, inhibited points, checkpoints affected by *F. benghalensis*. **ASP**: Adipocytokine signaling pathway (KEGG: hsa04920), **MAPK-S**: MAPK signaling pathway (KEGG: hsa04010), **INS**: Insulin signaling pathway (KEGG:hsa04910)

Summary of the mechanism of action of DRE against DM

- **DRE** ameliorated the hepatic oxidative stress by neutralizing the free radicals either by donating the *H-* or terminating the redox and Fenton's reaction which; confirmed *via* the *in vitro* studies; also supported by the enhanced activity of the catalase and SOD (*in vivo*).

- **DRE** may downregulate the hepatic gluconeogenesis and upregulate the glycolysis which was confirmed *via* the quantification of hepatic enzymes involved in glucose and fructose catabolism and anabolism.

- **DRE** promotes glucose utilization within the hepatic and gastrocnemius muscle which was confirmed *via* the glycogen quantification; supported by the glucose uptake efficacy in isolated rat hemidiaphragm; supports its insulin sensitivity effect.

- **DRE** enhances insulin synthesis and release; demonstrated *via* pancreatic β-cells size and number quantification.

- *In silico* findings identified the prime inhibition of the PTP1B *via* a majority of the bioactives from *D. repens*; this could be one of the reasons why the insulin-sensitizing effect of **DRE** was observed.

- **DRE** increased plasma leptin level; could have contributed to ameliorating the insulin resistance.

The probably regulated sites in T2DM pathogenesis (KEGG: hsa04930) by the bioactives of D. repens are summarized in Figure 70.

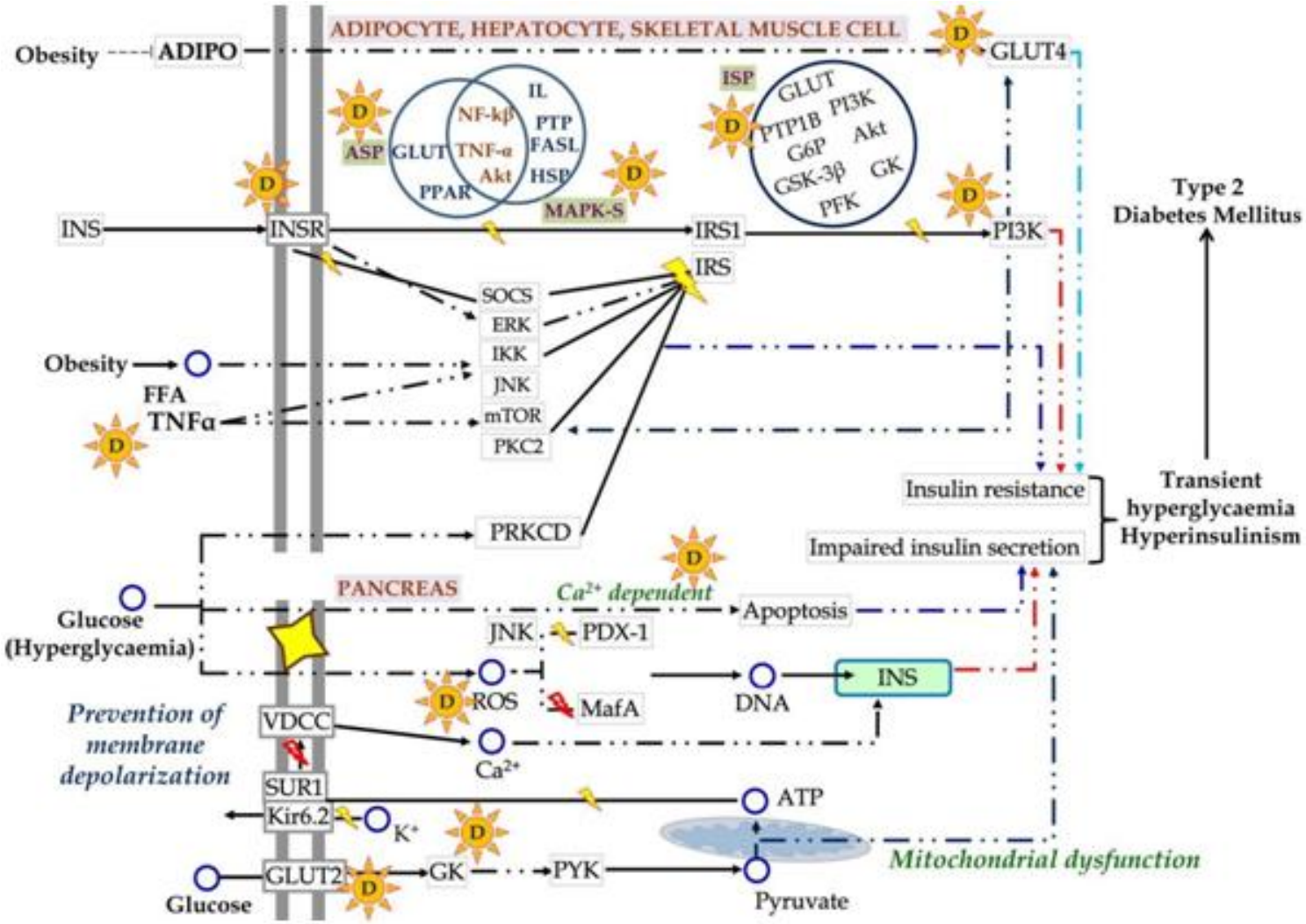

Figure 70: Probable anti-diabetic mechanism of *D. repens*. glycation, hexosamine pathway, respiratory chain, inhibited points, checkpoints affected by *D. repens*. **ASP**: Adipocytokine signaling pathway (KEGG: hsa04920), **MAPK-S**: MAPK signaling pathway (KEGG: hsa04010), **INS**: Insulin signaling pathway (KEGG: hsa04910).

Chapter 7

Conclusion

Conclusion

The present study utilized the series of system biology tools *via* the application of network pharmacology, molecular docking, and druglikeness of the reported bioactives from *F. benghalensis* and *D. repens* against the DM which was further integrated with experimental pharmacology using *in vitro*, *ex vivo*, and *in vivo* approaches.

Herein, we observed the significant amelioration of DM with the FBE and DRE treatment in both hyperglycaemic and hyperinsulinaemic states. Also, we observed the significant efficacy of bioactives (mainly flavonoids) to act over the α-glucosidase and α-amylase enzymes to deal with postprandial hyperglycemia and also enhanced glucose uptake in insulin presence. Additionally, we observed the efficacy of FBE and DRE to inhibit the glucose absorption from the jejunum meaning to the interaction of the fibers with free glucose; the effect of the extract was comparatively higher if compared with fractions rich in polyphenols, alkaloids, saponins, flavonoids, and steroids. Additionally, we observed a significant amelioration of the glucose, lipid, and nitrogen homeostasis which were deregulated in the diabetic and insulin-resistant conditions. Further, significant amelioration of multiple enzymatic and non-enzymatic anti-oxidant biomarkers within *in vivo* models was observed with FBE and DRE treatment; could be the outcome of free radicals scavenging capacity or terminate the Fenton or redox reactions respectively. One of the compromised actions in diabetic pathogenesis is linked with pancreatic β-cell function; was ameliorated with FBE and DRE treatment either by upregulating the insulin signaling pathway or regenerating the pancreatic β-cells which was crossed mapped by measuring the glucose or insulin level during OGTT or ITT followed by histological examination of pancreas.

All the above-mentioned outputs are directly concerned with the multiple pathways like PI3K-Akt, p53, $Ca^{2+,}$ and insulin signaling pathways to contribute to glucose

homeostasis. In the present study, we mapped the output of the PI3K, p53, and Ca^{2+} signaling pathways in DM with the reported bioactives of the *F. benghalensis* and insulin signaling and PI3K-Akt signaling pathway with the reported bioactives of *D. repens* respectively to propose their mode of actions.

Chapter 8

Summary

SUMMARY

The anti-diabetic action of *F. benghalensis* (bark) could be *via* the PI3K-Akt and p53 signaling mediated PTP1B downregulation; primarily modulated by flavonoids including ***apigenin*** (1) and ***3',4',5,7-tetrahydroxy-3-methoxyflavone*** (2) upregulating insulin signaling pathway to ameliorate glucose/lipid catabolism followed by reversing hepatic oxidative stress by donating H^+ from specific pharmacophore skeleton primarily by ***3-O-trans-p-coumaroyltormentic acid*** (3), ***mucusisoflavone C*** (4) and ***wighteone*** **(5)** to free radicals.

The anti-diabetic action of *D. repens* (whole plant) could be *via* the PI3K-Akt mediated PTP1B and gluconeogenesis downregulation; primarily modulated by flavonoids and terpenes *i.e.* ***pectolinarigenin*** (1) and ***durantanin I*** (2) leading to ameliorated glucose/lipid catabolism; upregulates glycogenesis with anti-oxidant efficacy by neutralizing Fenton and redox reactions primarily by ***naringenin*** (3), ***3,7-dihydroxy-2-[4-hydroxy-3-(4-hydroxy-3-methylbutyl)phenyl]-5,6-dimethoxy-4H-1-benzopyran-4-one*** (4), and ***7-O-α-D-glucopyranosyl-3,5-dihydroxy-3'-(4''-acetoxyl-3''-methylbutyl)-6,4'-dimethoxyflavone*** (5).

Chapter 9

Limitations & Prospective

LIMITATION & PROSPECTIVE

For the first time, the bioactives from *F. benghalensis* and *D. repens* were mapped with the reported targets of diabetes mellitus to correlate its outcome with experimental pharmacology and analytical chemistry to decode their anti-diabetic mode of action

However, the outcome of the system biology is mapped only with functional biomarkers which could be the output of the common homologous proteins; need to be further cross-mapped with specific molecular biomarkers related to a definite gene and is the perspective of the present findings.

Chapter 10

References

REFERENCES

1. Blair M. Diabetes Mellitus Review. Urol Nurs. 2016;36(1):27-36.
2. Skyler JS. Characterizing subgroups of type 1 diabetes. Diabetes. 2014;63(11):3578-80.
3. Shanik MH, Xu Y, Skrha J, Dankner R, Zick Y, Roth J. Insulin resistance and hyperinsulinemia: is hyperinsulinemia the cart or the horse? Diabetes Care. 2008;31(S 2):S262-8.
4. Otto-Buczkowska E, Jainta N. Pharmacological Treatment in Diabetes Mellitus Type 1 - Insulin and What Else? Int J Endocrinol Metab. 2017;16(1):e13008.
5. Marín-Peñalver JJ, Martín-Timón I, Sevillano-Collantes C, Del Cañizo-Gómez FJ. Update on the treatment of type 2 diabetes mellitus. World J Diabetes. 2016;7(17):354-95.
6. Akinci B, Yener S, Bayraktar F, Yesil S. Allergic reactions to human insulin: a review of current knowledge and treatment options. Endocrine. 2010;37(1):33-9.
7. Hansen T. Type 2 diabetes mellitus--a multifactorial disease. Ann Univ Mariae Curie Sklodowska Med. 2002;57(1):544-9.
8. Zhong F, Jiang Y. Endogenous Pancreatic β Cell Regeneration: A Potential Strategy for the Recovery of β Cell Deficiency in Diabetes. Front Endocrinol (Lausanne). 2019;10:101.
9. Hankey A. Ayurveda and the battle against chronic disease: An opportunity for Ayurveda to go mainstream? J Ayurveda Integr Med. 2010;1(1):9-12.
10. Lu AP, Jia HW, Xiao C, Lu QP. Theory of traditional Chinese medicine and therapeutic method of diseases. World J Gastroenterol. 2004;10(13):1854-6.
11. Hard to swallow. Nature 2007;448:106.
12. Fitzgerald M, Heinrich M, Booker A. Medicinal Plant Analysis: A Historical and Regional Discussion of Emergent Complex Techniques. Front Pharmacol. 2020;10:1480.

13. Patwardhan B. The new pharmacognosy. Comb Chem High Throughput Screen. 2014;17(2):97.
14. Hopkins A. Network pharmacology. Nat Biotechnol. 2007;25:1110–1111.
15. Zhang R, Zhu X, Bai H, Ning K. Network Pharmacology Databases for Traditional Chinese Medicine: Review and Assessment. Front Pharmacol. 2019;10:123.
16. "*Ficus benghalensis* L." Germplasm Resources Information Network (GRIN). Agricultural Research Service (ARS), United States Department of Agriculture (USDA). Retrieved 8 May 2016
17. Subsongsang R, Jiraungkoorskul W. An Updated Review on Phytochemical Properties of "Golden Dewdrop" *Duranta erecta*. Pharmacogn Rev. 2016;10(20):115-117.
18. Iqbal K, Malik A, Mukhtar N, Anis I, Khan SN, Choudhary MI. Alpha-glucosidase inhibitory constituents from *Duranta repens*. Chem Pharm Bull (Tokyo). 2004;52(7):785-9.
19. Eke IG, Okpara GC. Anti-hyperglycemic and anti-dyslipidemic activities of methanol ripe fruit extract of *Duranta erecta* L (Verbenaceae) in normoglycemic and hyperglycemic rats. J Tradit Complement Med. 2020;11(3):209-216.
20. Rasouli H, Yarani R, Pociot F, Popović-Djordjević J. Anti-diabetic potential of plant alkaloids: Revisiting current findings and future perspectives. Pharmacol Res. 2020;155:104723.
21. Al-Ishaq RK, Abotaleb M, Kubatka P, Kajo K, Büsselberg D. Flavonoids and Their Anti-Diabetic Effects: Cellular Mechanisms and Effects to Improve Blood Sugar Levels. Biomolecules. 2019;9(9):430.
22. Elekofehinti OO. Saponins: Anti-diabetic principles from medicinal plants - A review. Pathophysiology. 2015;22(2):95-103.

23. Gupta R, Sharma AK, Dobhal MP, Sharma MC, Gupta RS. Antidiabetic and antioxidant potential of β-sitosterol in streptozotocin-induced experimental hyperglycemia. J Diabetes. 2011;3(1):29-37.
24. Petersen MC, Vatner DF, Shulman GI. Regulation of hepatic glucose metabolism in health and disease. Nat Rev Endocrinol. 2017;13(10):572-587.
25. Qaid MM, Abdelrahman MM. Role of insulin and other related hormones in energy metabolism—A review. Cogent Food & Agriculture. 2016;2(1):1267691.
26. Ojha A, Ojha U, Mohammed R, Chandrashekar A, Ojha H. Current perspective on the role of insulin and glucagon in the pathogenesis and treatment of type 2 diabetes mellitus. Clin Pharmacol. 2019;11:57-65.
27. Fu Z, Gilbert ER, Liu D. Regulation of insulin synthesis and secretion and pancreatic Beta-cell dysfunction in diabetes. Curr Diabetes Rev. 2013;9(1):25-53.
28. Wysham C, Shubrook J. Beta-cell failure in type 2 diabetes: mechanisms, markers, and clinical implications. Postgrad Med. 2020;132(8):676-686.
29. Chang TW, Goldberg AL. The metabolic fates of amino acids and the formation of glutamine in skeletal muscle. J Biol Chem. 1978;253(10):3685–93.
30. Maechler P, Wollheim CB. Mitochondrial glutamate acts as a messenger in glucose-induced insulin exocytosis. Nature. 1999;402(6762):685–9.
31. Wilcox G. Insulin and insulin resistance. Clin Biochem Rev. 2005;26(2):19-39.
32. Boucher J, Kleinridders A, Kahn CR. Insulin receptor signaling in normal and insulin-resistant states. Cold Spring Harb Perspect Biol. 2014;6(1):a009191.
33. Blair M. Diabetes Mellitus Review. Urol Nurs. 2016;36(1):27-36.

34. Opie EL. On the Relation of chronic interstitial pancreatitis to the islands of Langerhans and to diabetes melutus. J Exp Med 1901;5:397–428.

35. Noble JA, Valdes AM. Genetics of the HLA region in the prediction of type 1 diabetes. Curr Diab Rep. 2011;11(6):533-42.

36. Nisticò L, Cascino I, Buzzetti R, et al. CTLA-4 in Type 1 Diabetes Mellitus. In: Madame Curie Bioscience Database [Internet]. Austin (TX): Landes Bioscience; 2000-2013. Available from: https://www.ncbi.nlm.nih.gov/books/NBK5997/

37. Rich SS, Concannon P, Erlich H, Julier C, Morahan G, Nerup J, Pociot F, Todd JA. The Type 1 Diabetes Genetics Consortium. Ann N Y Acad Sci. 2006;1079:1-8.

38. Morran MP, Vonberg A, Khadra A, Pietropaolo M. Immunogenetics of type 1 diabetes mellitus. Mol Aspects Med. 2015;42:42-60.

39. Khoshroo M, Khamseh ME, Amir Zargar AA, Malek M, Falak R, Shekarabi M. The Relationship between insulin variable number of tandem repeats (INS-VNTR) -23 A/T and cytotoxic Tlymphocyte associated protein-4 (CTLA-4) +49 A/G polymorphisms with islet autoantibodies in persons with diabetes. Med J Islam Repub Iran. 2017;31:83.

40. Hyöty H, Hiltunen M, Knip M, Laakkonen M, Vähäsalo P, Karjalainen J, Koskela P, Roivainen M, Leinikki P, Hovi T, et al. A prospective study of the role of coxsackie B and other enterovirus infections in the pathogenesis of IDDM. Childhood Diabetes in Finland (DiMe) Study Group. Diabetes. 1995;44(6):652-7.

41. Burrack AL, Martinov T, Fife BT. T Cell-Mediated Beta Cell Destruction: Autoimmunity and Alloimmunity in the Context of Type 1 Diabetes. Front Endocrinol (Lausanne). 2017;8:343.

42. Roep BO. The role of T-cells in the pathogenesis of Type 1 diabetes: from cause to cure. Diabetologia. 2003;46(3):305-21.

43. Galicia-Garcia U, Benito-Vicente A, Jebari S, Larrea-Sebal A, Siddiqi H, Uribe KB, Ostolaza H, Martín C. Pathophysiology of Type 2 Diabetes Mellitus. Int J Mol Sci. 2020;21(17):6275.

44. Cerf ME. Beta cell dysfunction and insulin resistance. Front Endocrinol (Lausanne). 2013;4:37.

45. Prasad RB, Groop L. Genetics of type 2 diabetes-pitfalls and possibilities. Genes (Basel). 2015;6(1):87-123.

46. Wu Y, Ding Y, Tanaka Y, Zhang W. Risk factors contributing to type 2 diabetes and recent advances in the treatment and prevention. Int J Med Sci. 2014;11(11):1185-200.

47. Koren D, Palladino A. Hypoglycaemia. Genetic Diagnosis of Endocrine Disorders .2016; 2nd edition:31.75. Available at: https://doi.org/10.1016/B978-0-12-800892-8.00003-8

48. Roden M. How free fatty acids inhibit glucose utilization in human skeletal muscle. News Physiol Sci. 2004;19:92-6.

49. Kwon H, Pessin JE. Adipokines mediate inflammation and insulin resistance. Front Endocrinol (Lausanne). 2013;4:71.

50. Chang-Chen KJ, Mullur R, Bernal-Mizrachi E. Beta-cell failure as a complication of diabetes. Rev Endocr Metab Disord. 2008;9(4):329-43.

51. Goyal R, Nguyen M, Jialal I. Glucose Intolerance. [Updated 2020 Dec 8]. In: StatPearls [Internet]. Treasure Island (FL): StatPearls Publishing; 2021 Jan-. Available at: https://www.ncbi.nlm.nih.gov/books/NBK499910/

52. Hatting M, Tavares CDJ, Sharabi K, Rines AK, Puigserver P. Insulin regulation of gluconeogenesis. Ann N Y Acad Sci. 2018;1411(1):21-35.

53. Rizza RA. Pathogenesis of fasting and postprandial hyperglycemia in type 2 diabetes: implications for therapy. Diabetes. 2010;59(11):2697-707.

54. Boden G, Lebed B, Schatz M, Homko C, Lemieux S: Effects of acute changes of plasma free fatty acids on intramyocellular fat content and insulin resistance in healthy subjects. Diabetes. 2001;50:1612-1617.

55. Vargas E, Podder V, Carrillo Sepulveda MA. Physiology, Glucose Transporter Type 4. [Updated 2021 May 9]. In: StatPearls [Internet]. Treasure Island (FL): StatPearls Publishing; 2021 Jan-. Available at: https://www.ncbi.nlm.nih.gov/books/NBK537322/

56. Shan WF, Chen BQ, Zhu SJ, Jiang L, Zhou YF. Effects of GLUT4 expression on insulin resistance in patients with advanced liver cirrhosis. J Zhejiang Univ Sci B. 2011;12(8):677-82.

57. Tripathy D, Mohanty P, Dhindsa S, Syed T, Ghanim H, Aljada A, Dandona P. Elevation of free fatty acids induces inflammation and impairs vascular reactivity in healthy subjects. Diabetes. 2003;52(12):2882-7.

58. Nordmann TM, Dror E, Schulze F, Traub S, Berishvili E, Barbieux C, Böni-Schnetzler M, Donath MY. The Role of Inflammation in β-cell Dedifferentiation. Sci Rep. 2017;7(1):6285.

59. Kharroubi I, Ladrière L, Cardozo AK, Dogusan Z, Cnop M, Eizirik DL. Free fatty acids and cytokines induce pancreatic beta-cell apoptosis by different mechanisms: role of nuclear factor-kappaB and endoplasmic reticulum stress. Endocrinology. 2004;145(11):5087-96.

60. Oh YS. Mechanistic insights into pancreatic β-cell mass regulation by glucose and free fatty acids. Anat Cell Biol. 2015;48:16–24.

61. Kaiser N, Leibowitz G, Nesher R. Glucotoxicity and beta-cell failure in type 2 diabetes mellitus. J Pediatr Endocrinol Metab. 2003;16(1):5-22.

62. Holst JJ, Orskov C. The incretin approach for diabetes treatment: modulation of islet hormone release by GLP-1 agonism. Diabetes. 2004;53(S3):S197-204.

63. Garber AJ. Incretin effects on β-cell function, replication, and mass: the human perspective. Diabetes Care. 2011;34(S2):S258-63.

64. Kulas JA, Puig KL, Combs CK. Amyloid precursor protein in pancreatic islets. J Endocrinol. 2017;235(1):49-67.

65. Donner T, Sarkar S. Insulin – Pharmacology, Therapeutic Regimens, and Principles of Intensive Insulin Therapy. [Updated 2019 Feb 23]. In: Feingold KR, Anawalt B, Boyce A, *et al.*, editors. Endotext [Internet]. South Dartmouth (MA): MDText.com, Inc.; 2000-. Available at: https://www.ncbi.nlm.nih.gov/books/NBK278938/

66. Otto-Buczkowska E, Jainta N. Pharmacological Treatment in Diabetes Mellitus Type 1 - Insulin and What Else? Int J Endocrinol Metab. 2017;16(1):e13008.

67. Marín-Peñalver JJ, Martín-Timón I, Sevillano-Collantes C, Del Cañizo-Gómez FJ. Update on the treatment of type 2 diabetes mellitus. World J Diabetes. 2016;7(17):354-95.

68. Weiland CM, Hilaire ML. Bromocriptine mesylate (Cycloset) for type 2 diabetes mellitus. Am Fam Physician. 2013;87(10):718-20.

69. Fabricant DS, Farnsworth NR. The value of plants used in traditional medicine for drug discovery. Environ Health Perspect. 2001;109(S1):69-75.

70. Alves RR, Rosa IM. Biodiversity, traditional medicine and public health: where do they meet? J Ethnobiol Ethnomed. 2007;3:14.

71. Hamilton GR, Baskett TF. In the arms of Morpheus the development of morphine for postoperative pain relief. Can J Anaesth. 2000;47(4):367-74.

72. Joo YE. Natural product-derived drugs for the treatment of inflammatory bowel diseases. Intest Res. 2014;12(2):103-9.

73. Yuan H, Ma Q, Ye L, Piao G. The Traditional Medicine and Modern Medicine from Natural Products. Molecules. 2016;21(5):559.

74. Newman DJ, Cragg GM, Snader KM. Natural products as sources of new drugs over the period 1981-2002. J Nat Prod. 2003;66(7):1022-37.

75. Atanasov AG, Zotchev SB, Dirsch VM; International Natural Product Sciences Taskforce, Supuran CT. Natural products in drug discovery: advances and opportunities. Nat Rev Drug Discov. 2021;20(3):200-216.

76. Graf BL, Raskin I, Cefalu WT, Ribnicky DM. Plant-derived therapeutics for the treatment of metabolic syndrome. Curr Opin Investig Drugs. 2010;11(10):1107-15.

77. Honda M, Hara Y. Inhibition of rat small intestinal sucrase and α-glucosidase activities by tea polyphenols. Biosci. Biotechnol. Biochem. 1993;57:123-124.

78. Ahmed F, Chavan S, Satish A, Punith KR. Inhibitory activities of *Ficus benghalensis* bark against carbohydrate hydrolyzing enzymes-An *in vitro* study. Pharmacogn. Mag. 2011; 3:33-37.

79. Gayathri M, Kannabiran K. Antidiabetic and ameliorative potential of Ficus bengalensis bark extract in streptozotocin induced diabetic rats. Indian J Clin Biochem. 2008; 23:394-400.

80. Gayathri M, Kannabiran K. The Effects of oral administration of an aqueous extract of *Ficus bengalensis* stem bark on some hematological and biochemical parameters in rats with streptozotocin-induced diabetes. Turk. J. Biol. 2009; 33:9-13.

81. Singh RK, Mehta S, Jaiswal D, Rai PK, Watal G. Antidiabetic effect of *Ficus bengalensis* aerial roots in experimental animals. J. Ethnopharmacol. 2009;123:110-114.

82. Shukla R, Anand K, Prabhu K, Murthy PS. Hypoglycaemic effect of the water extract of Ficus bengalensis in alloxan recovered, mildly diabetic and severely diabetic rabbits. Int. J. Diabetes Dev. Ctries. 1994;14:78-81.

83. Singh AB, Yadav DK, Maurya R, Srivastava AK. Antihyperglycaemic activity of alpha-amyrin acetate in rats and db/db mice. Nat Prod Res. 2009;23(9):876-82.

84. Shukla R, Anand K, Prabhu K, Murthy PS. Hypocholesterolemic effect of water extract of the bark of Banyan tree, *Ficus bengalensis*. Indian J Clin Biochem. 1995;10:14-18

85. Mahajan MS, Gulecha VS, Khandare RA, Upaganlawar AB, Gangurde HH, Upasani CD. Anti-edematogenic and analgesic activities of *Ficus benghalensis*. Int. J. Nutr. Pharmacol. Neurol. Dis. 2012;2:100-104.

86. Kothapalli PK, Sanganal SJ, Shridhar N, Narayanaswamy H, Narayanaswamy M. In-vivo anti-inflammatory and analgesic screening of *Ficus bengalensis* leaf extract in rats. Asian J. Pharm. Sci. 2014;4:174-178.

87. Thakare VN, Suralkar AA, Deshpande AD, Naik SR. Stem bark extraction of *Ficus bengalensis* Linn for anti-inflammatory and analgesic activity in animal models. Indian J. Exp. Biol. 2010; 48:39-45.

88. Almahy HA, Alhassan NI. Studies on the chemical constituents of the leaves of *Ficus bengalensis* and their antimicrobial activity. J Sci Tech 2011;12:111-116.

89. Ogunlowo O, Arimah B, Adebayo M. Phytochemical analysis and comparison of *in-vitro* antimicrobial activities of the leaf, stem bark and root bark of *Ficus benghalensis*. IOSR J. Pharm. 2013; 3:33-38.

90. Bhangale SC, Patil VV, Patil VR. Antibacterial activity of *Ficus bengalensis* Linn bark on Actinomyces viscosus. Int. j. pharm. sci. 2010; 2:39-43.

91. Uma B, Prabhakar K, Rajendran S. *In vitro* antimicrobial activity and phytochemical analysis of *Ficus religiosa* L. and *Ficus bengalensis* L. against diarrhoeal enterotoxigenic *E. coli*. Ethnobot. leafl. 2009;13:472-474.

92. Mukherjee PK, Saha K, Murugesan T, Mandal S, Pal M, Saha B. Screening of anti-diarrhoeal profile of some plant extracts of a specific region of West Bengal, India. J. Ethnopharmacol. 1998;60:85-89.

93. Satish A, Kumar RP, Rakshith D, Satish S, Ahmed F. Antimutagenic and antioxidant activity of *Ficus benghalensis* stem bark and *Moringa oleifera* root extract. International Journal of Chemical and Analytical Science 2013;4:45-48.

94. Sharma RK, Chatterji S, Rai DK, Mehta S, Rai PK, Singh RK, et al. Antioxidant activities and phenolic contents of the aqueous extracts of some Indian medicinal plantsJ. Med. Plant Res. 2009;3:944-948.

95. Manian R, Anusuya N, Siddhuraju P, Manian S. The antioxidant activity and free radical scavenging potential of two different solvent extracts of *Camellia sinensis* (L.) O. Kuntz, *Ficus bengalensis* L. and *Ficus racemosa* L. Food Chem. 2008; 107:1000-1007

96. Parameswari SA, Saleem T, Chandrasekar K, Chetty CM. Protective role of *Ficus benghalensis* against isoniazid-rifampicin induced oxidative liver injury in rat. Rev. bras. farmacogn. 2012;22:604-610.

97. Augusti K, Anuradha PS, Smitha K, Sudheesh M, George A, Joseph M. Nutraceutical effects of garlic oil, its nonpolar fraction and a Ficus flavonoid as compared to vitamin E in CCl4 induced liver damage in rats. Indian J Exp Biol. 2005;43:437-444.

98. Thite AT, Patil RR, Naik SR. Anti-arthritic activity profile of methanolic extract of Ficus bengalensis: Comparison with some clinically effective drugs. Biomed. Aging Pathol. 2014;4:207-217.

99. Taur D, Nirmal S, Patil R, Kharya M. Antistress and antiallergic effects of *Ficus bengalensis* bark in asthma. Nat. Prod. Res. 2007;21:1266-1270.

100. Khan T, Tatke P, Gabhe S. Immunological studies on the aerial roots of the Indian banyan. Indian J Pharm Sci. 2008; 70:287-291.

101. *Duranta erecta* L. Fact Sheet. Weeds of Australia. Available at: https://keyserver.lucidcentral.org/weeds/data/media/Html/duranta_erecta.htm

102. Ugwu CC, Anosike CA. Phytochemical screening and antioxidant potentials of methanol extract of Duranta erecta leaves. Asian J. Biochem. 2020 Sep 15:16-26.

103. Khan MA, Rahman MM, Tania M, Shoshee NF, Xu AH, Chen HC. Antioxidative potential of *Duranta repens* (Linn.) fruits against H_2O_2 induced cell death *in vitro*. Afr J Tradit Complement Altern Med. 2013;10(3):436-41.

104. Ijaz F, Ul Haq A, Ahmad I, Ahmad N, Hussain J, Chen S. Antioxidative iridoid glycosides from the sky flower (*Duranta repens* Linn). J Enzyme Inhib Med Chem. 2011;26(1):88-92.

105. Shahat AA, Nazif NM, Abousetta LM, Ibrahim NA, Cos P, Van Miert S, Pieters L, Vlietinck AJ. Phytochemical investigation and antioxidant activity of *Duranta repens*. Phytother Res. 2005;19(12):1071-3.

106. Donkor S, Larbie C, Komlaga G, Emikpe BO. Phytochemical, Antimicrobial, and Antioxidant Profiles of *Duranta erecta* L. Parts. Biochem Res Int. 2019;2019:8731595.

107. Ahmed WS, Mohamed MA, El-Dib RA, Hammed MM. New triterpene saponins from *D. repens* Linn. And their cytotoxic activity. Molecules. 2009;14:1952-65.

108. Abou-Setta LM, Nazif NM, Shahat AA. Phytochemical investigation and antiviral activity of *D. repens*. J Appl Sci Res. 2007;3:1426-33.

109. Anis I, Ahmed S, Malik A, Yasin A, Choudhary MI. Enzyme inhibitory constituents from *Duranta repens*. Chem Pharm Bull. 2002;50:515-18.

110. Ijaz F, Ahmad N, Ahmad I, ul Haq A, Wang F. Two new anti-plasmodial flavonoid glycosides from *D. repens*. J Enzyme Inhib Med Chem. 2010;25:773-8.

111. Sharma P, Khandelwal S, Singh T, Vijayvergia R. Phytochemical analysis and antifungal potential of *Duranta erecta* against some phytopathogenic fungi. Int J Pharm Sci Res. 2012;3:2686-9.

112. Sikarwar M, Ganie SA, Agnihotri RK, Sharma R. Evaluation of *D. repens* for its antifungal potential. Int J Med Plants. 2014;106:390-5.

113. Telagari, Madhusudhan, and Kirankumar Hullatti. In-vitro α-amylase and α-glucosidase inhibitory activity of *Adiantum caudatum* Linn. and Celosia argentea Linn. extracts and fractions. Indian J. Pharmacol. 2015;47(4):425-9.

114. Gupta RN, Pareek A, Suthar M, Rathore GS, Basniwal PK, Jain D. Study of glucose uptake activity of *Helicteres isora* Linn. fruits in L-6 cell lines. Int J Diabetes Dev Ctries. 2009;29(4):170-3.

115. Takigawa-Imamura H, Sekine T, Murata M, Takayama K, Nakazawa K, Nakagawa J, Stimulation of glucose uptake in muscle cells by prolonged treatment with scriptide, a histone deacetylase inhibitor. Biosci. Biotechnol. Biochem. 2003;67:1499-1506.

116. Yap A, Nishiumi S, Yoshida K, Ashida H, Rat L6 myotubes as an *in vitro* model system to study GLUT4-dependent glucose uptake stimulated by inositol derivatives. Cytotechnology, 2007;55(2-3):103- 108.

117. Kim BR, Kim HY, Choi I, Kim JB, Jin CH, Han AR. DPP-IV Inhibitory Potentials of Flavonol Glycosides Isolated from the Seeds of *Lens culinaris*: *In Vitro* and Molecular Docking Analyses. Molecules. 2018;23(8):1998.

118. Gao J, Gong H, Mao X. Dipeptidyl Peptidase-IV Inhibitory Activity and Related Molecular Mechanism of Bovine α-Lactalbumin-Derived Peptides. Molecules. 2020;25(13):3009.

119. Song YH, Uddin Z, Jin YM, Li Z, Curtis-Long MJ, Kim KD, Cho JK, Park KH. Inhibition of protein tyrosine phosphatase (PTP1B) and α-glucosidase by geranylated flavonoids from Paulownia tomentosa. J Enzyme Inhib Med Chem. 2017;32(1):1195-1202.

120. Ha MT, Shrestha S, Tran TH, Kim JA, Woo MH, Choi JS, Min BS. Inhibition of PTP1B by farnesylated 2-arylbenzofurans isolated from Morus alba root bark: unraveling the mechanism of inhibition based on in vitro and in silico studies. Arch Pharm Res. 2020;43(9):961-975.

121. Ukkola O, Santaniemi M. Protein tyrosine phosphatase 1B: a new target for the treatment of obesity and associated co-morbidities. J Intern Med. 2002;251(6):467-75.

122. Ou S, Kwok K, Li Y, Fu L. In vitro study of possible role of dietary fiber in lowering postprandial serum glucose. J Agric Food Chem. 2001;49(2):1026-9.

123. Das MSC, Devi G. *In vitro* glucose binding activity of *Terminalia bellirica*. Asian J Pharm Clin Res. 2015;8(2):320–323

124. Kumar M, Prasad SK, Hemalatha S. *In Vitro* Study on Glucose Utilization Capacity of Bioactive Fractions of *Houttuynia cordata* in Isolated Rat Hemidiaphragm and Its Major Phytoconstituent. Adv Pharmacol Sci. 2016;2016:2573604.

125. GallagherAM, Flatt PR, Duffy G, Abdel-Wahab YHA. The effects of traditional antidiabetic plants on *in vitro* glucose diffusion. Nutr Res. 2003;23(3):413–24.

126. Dixit P, Jain DK, Dumbwani J. Standardization of an ex vivo method for determination of intestinal permeability of drugs using everted rat intestine apparatus. J Pharmacol Toxicol Methods. 2012;65(1):13-7.

127. Graham ML, Janecek JL, Kittredge JA, Hering BJ, Schuurman HJ. The streptozotocin-induced diabetic nude mouse model: differences between animals from different sources. Comp Med. 2011;61(4):356-60.

128. Masiello P, Broca C, Gross R, Manteghetti M, Hillairs-Boys D, Novelli M, et al. Experimental NIDDM: development of a new model in adult rats administered streptozotocin and nicotinamide. Diabetes 1998;47(2):224–9.

129. Ighodaro OM, Adeosun AM, Akinloye OA. Alloxan-induced diabetes, a common model for evaluating the glycemic-control potential of therapeutic compounds and plants extracts in experimental studies. Medicina (Kaunas). 2017;53(6):365-374.

130. Gupta SK. Drug Screening Methods. Anti-diabetic agents. 3rd Edition. 2016. page. 616-619

131. Mamikutty N, Thent ZC, Sapri SR, Sahruddin NN, Mohd Yusof MR, Haji Suhaimi F, The establishment of metabolic syndrome model by induction of fructose drinking water in male Wistar rats. Biomed Res Int. 2014;2014:263897.

132. Huang BW, Chiang MT, Yao HT, Chiang W. The effect of high-fat and high-fructose diets on glucose tolerance and plasma lipid and leptin levels in rats. Diabetes Obes Metab. 2004;6(2):120-6.

133. Szkudelski T. Streptozotocin-nicotinamide-induced diabetes in the rat. Characteristics of the experimental model. Exp Biol Med. 2012;237(5):481–90.

134. Ghasemi A, Khalifi S, Jedi S. Streptozotocin-nicotinamide-induced rat model of type 2 diabetes (review). Acta Physiol Hung. 2014;101(4):408–20.

135. Catena C, Giacchetti G, Novello M, Colussi G, Cavarape A, Sechi LA. Cellular mechanisms of insulin resistance in rats with fructose-induced hypertension. Am J Hypertens. 2003;16(11 Pt 1):973-8

136. Hopkins AL. Network pharmacology. Nat. Biotechnol. 2007;25:1110-1111.

137. Zhang B, Wang X, Li S. An integrative platform of TCM network pharmacology and its application on a herbal formula, Qing-Luo-Yin. Evid. Based Complement Alternat. Med. 2013;2013:456747.

138. Berger SI, Iyengar R. Network analyses in systems pharmacology. Bioinformatics. 2009;25:2466-2472.

139. Kibble M, Saarinen N, Tang J, Wennerberg K, Makela S, Aittokallio T. Network pharmacology applications to map the unexplored target space and therapeutic potential of natural products. Nat. Prod. Rep. 2015;32:1249-1266.

140. Chandran U, Mehendale N, Tillu G, Patwardhan B. Network Pharmacology of Ayurveda Formulation Triphala with Special Reference to Anti-Cancer Property. Comb Chem High Throughput Screen. 2015;18(9):846-54.

141. Lipinski CA. Lead- and drug-like compounds: The rule-of-five revolution. Drug Discov Today Technol. 2004;1(4):337-41.

142. Morris JS, Kuchinsky A, Pico A, Institutes G. Analysis and Visualization of Biological Networks with Cytoscape. UCSF. 2012. Available at: http://www.cgl.ucsf.edu/Outreach/Workshops/NIH-Oct-2012/Cytoscape/Analysis%20and%20Visualization%20of%20Biological%20Networks%20with%20Cytoscape%20v6.pdf

143. Newman MEJ. A measure of betweenness centrality based on random walks. Social Networks. 2005;27(1):39-54.

144. Brandes U. A faster algorithm for betweenness centrality. J Math Sociol. 2001;25(2):163-177

145. Stelzl U, Worm U, Lalowski M, Haenig C, Brembeck FH, Goehler H, Stroedicke M, Zenkner M, Schoenherr A, Koeppen S, Timm J, Mintzlaff S, Abraham C, Bock N, Kietzmann S, Goedde A, Toksöz E, Droege A, Krobitsch S, Korn B, Birchmeier W, Lehrach H, Wanker EE. A human protein-protein interaction network: a resource for annotating the proteome. Cell. 2005;122(6):957-68.

146. Maslov S, Sneppen K. Specificity and stability in topology of protein networks. Science. 2002;296(5569):910-3.

147. Khanal P, Chikhale R, Dey YN, Pasha I, Chand S, Gurav N, Ayyanar M, Patil BM, Gurav S. Withanolides from *Withania somnifera* as an immunity booster and their therapeutic options against COVID-19. J Biomol Struct Dyn. 2021. doi: 10.1080/07391102.2020.1869588.

148. Liu T, Lin Y, Wen X, Jorissen RN, Gilson MK. BindingDB: a web-accessible database of experimentally determined protein-ligand binding affinities. Nucleic Acids Res. 2007;35(Database issue):D198-201.

149. Shannon P, Markiel A, Ozier O, Baliga NS, Wang JT, Ramage D, Amin N, Schwikowski B, Ideker T. Cytoscape: a software environment for integrated models of biomolecular interaction networks. Genome Res. 2003;13(11):2498-504.

150. Poroikov VV, Filimonov DA, Ihlenfeldt WD, Gloriozova TA, Lagunin AA, Borodina YV, Stepanchikova AV, Nicklaus MC. PASS biological activity spectrum predictions in the enhanced open NCI database browser. J Chem Inf Comput Sci. 2003;43(1):228-36.

151. Morris GM, Huey R, Lindstrom W, Sanner MF, Belew RK, Goodsell DS, Olson AJ.

AutoDock4 and AutoDockTools4: Automated docking with selective receptor flexibility. J Comput Chem. 2009;30(16):2785-91.

152. Trott O, Olson AJ. AutoDock Vina: improving the speed and accuracy of docking with a new scoring function, efficient optimization, and multithreading. J Comput Chem. 2010;31(2):455-61.
153. Schwede T, Kopp J, Guex N, Peitsch MC. SWISS-MODEL: An automated protein homology-modeling server. Nucleic Acids Res. 2003;31(13):3381-5.
154. Cos P, Vlietinck AJ, Berghe DV, Maes L. Anti-infective potential of natural products: how to develop a stronger in vitro 'proof-of-concept'. J Ethnopharmacol. 2006;106(3):290-302.
155. Chandra S, Khan S, Avula B, Lata H, Yang MH, ElSohly MA et al. Assessment of total phenolic and flavonoid content, antioxidant properties, and yield of aeroponically and conventionally grown leafy vegetables and fruit crops: A comparative study. Evid Based Complement Alternat Med. 2014;2014:253875
156. Ainsworth EA, Gillespie KM. Estimation of total phenolic content and other oxidation substrates in plant tissues using Folin-Ciocalteu reagent. Nature Protocols. 2007;2(4):875-877
157. Choi CW, Kim SC, Hwang SS, Choi BK, Ahn HJ, Lee MY, Park SH,Kim SK. Antioxidant activity and free radical scavenging capacity between Korean medicinal plants and flavonoids by assay-guided comparison. Plant Science. 2002;163(6):1161–1168.
158. Re R, Pellegrini N, Proteggente A, Pannala A, Yang M, Rice-Evans C. Antioxidant activity applying an improved ABTS radical cation decolorization assay. Free Radic. Biol. Med. 1999;26(9–10):1231–1237.
159. Kumari S, Deori M, Elancheran R, Kotoky J, Devi R. *In vitro* and *In vivo* Antioxidant, Anti-hyperlipidemic Properties and Chemical Characterization of *Centella asiatica* (L.) Extract.

Front Pharmacol. 2016;7:400.

160. Prieto P, Pineda M, Aguilar M. Spectrophotometric quantitation of antioxidant capacity through the formation of a phosphomolybdenum complex: specific application to the determination of vitamin E. Anal Biochem. 1999;269(2):337-41.
161. Ebrahimzadeh MA, Pourmorad F, Hafezi S. Antioxidant activities of Iranian corn silk. Turk. J. Biol. 2008;32:43–49.
162. Köse LP, Gülcin I, Gören AC, Namiesnik J, Martinez-Ayala AL, Gorinstein S. LC–MS/MS analysis, antioxidant and anticholinergic properties of galanga (Alpinia officinarum Hance) rhizomes. Ind Crops Prod. 2015;74:712–721.
163. Kumari S, Elancheran R, Kotoky J, Devi R. Rapid screening and identification of phenolic antioxidants in *Hydrocotyle sibthorpioides* Lam. by UPLC-ESI-MS/MS. Food Chem. 2016;203:521-529.
164. Chattopadhyay RR, Sarkar SK, Ganguly S, Banerjee RN, Basu TK. Effect of leaves of Vinca rosea Linn, on glucose utilization and glycogen deposition by isolated rat hemidiaphragm. Indian J Physiol Pharmacol. 1992;36:137–8.
165. Devi K, Khanam S, Rabbani S. Protective role of glibenclamide against nicotinamide-streptozotocin induced nuclear damage in diabetic Wistar rats. J Pharmacol Pharmacother. 2010;1(1):18.
166. Nugroho AE, Andrie M, Warditiani NK, Siswanto E, Pramono S, Lukitaningsih E. Antidiabetic and antihiperlipidemic effect of *Andrographis paniculata* (Burm. f.) Nees and andrographolide in high-fructose-fat-fed rats. Indian J Pharmacol. 2012;44(3):377-81.
167. Kumar R, Patel DK, Prasad SK, Sairam K, Hemalatha S. Antidiabetic activity of alcoholic root extract of *Caesalpinia digyna* in streptozotocin-nicotinamide induced diabetic rats. Asian

Pac J Trop Biomed. 2012;2(2):S934–40

168. Nair J, Velpandian T, Das US, Sharma P, Nag T, Mathur SR, Mathur R. Molecular and Metabolic Markers of Fructose Induced Hepatic Insulin Resistance in Developing and Adult Rats are Distinct and *Aegle marmelos* is an Effective Modulator. Sci Rep. 2018;8(1):15950.
169. Seifter S, Dayton S. The estimation of glycogen with the anthrone reagent. Arch Biochem 1950;25(1):191–200.
170. Brandstrup N, Kirk JE, Bruni C. The hexokinase and phosphoglucoisomerase activities of aortic and pulmonary artery tissue in individuals of various ages. J Gerontol 1957;12(2):166–71.
171. Pari L, Srinivasan S. Antihyperglycemic effect of diosmin on hepatic key enzymes of carbohydrate metabolism in streptozotocin-nicotinamide-induced diabetic rats. Biomed Pharmacother. 2010;64(7):477–81.
172. King J. A routine method for the estimation of lactic dehydrogenase activity. J Med Lab Technol. 1959;16:265-272.
173. Claiborne A. Catalase activity. In: Greenwald RA. CRC hand book of methods for oxygen radical research. Boca Raton: CRC Press; 1985: 283–4.
174. Sedlak J, Lindsay RH. Estimation of total, protein-bound, and nonprotein sulfhydryl groups in tissue with Ellman's reagent. Anal Biochem 1968;25(1):192–205.
175. Nandi A, Chatterjee IB. Scavenging of superoxide radical by ascorbic acid. J Biosci 1987;11(1– 4):435–41.
176. Ohkawa H, Ohishi N, Yagi K. Assay for lipid peroxides in animal tissues by thiobarbituric acid reaction. Anal Biochem. 1979;95(2):351–8.
177. Oguntibeju OO. Type 2 diabetes mellitus, oxidative stress and inflammation: examining the

links. Int J Physiol Pathophysiol Pharmacol. 2019;11(3):45-63.

178. Obanda DN, Cefalu WT. Modulation of cellular insulin signaling and PTP1B effects by lipid metabolites in skeletal muscle cells. J Nutr Biochem. 2013;24(8):1529-37.
179. Fernandez-Ruiz R, Vieira E, Garcia-Roves PM, Gomis R. Protein tyrosine phosphatase-1B modulates pancreatic β-cell mass. PLoS One. 2014;9(2):e90344.
180. Zhang W, Hong D, Zhou Y, Zhang Y, Shen Q, Li JY, Hu LH, Li J. Ursolic acid and its derivative inhibit protein tyrosine phosphatase 1B, enhancing insulin receptor phosphorylation and stimulating glucose uptake. Biochim Biophys Acta. 2006;1760(10):1505-12.
181. Long YC, Zierath JR. AMP-activated protein kinase signaling in metabolic regulation. J Clin Invest. 2006;116(7):1776-83.
182. Grygiel-Górniak B. Peroxisome proliferator-activated receptors and their ligands: nutritional and clinical implications - a review. Nutr J. 2014;13:17
183. Huang X, Liu G, Guo J, Su Z. The PI3K/AKT pathway in obesity and type 2 diabetes. Int J Biol Sci. 2018;14(11):1483-1496.
184. Ravichandran LV, Chen H, Li Y, Quon MJ. Phosphorylation of PTP1B at Ser(50) by Akt impairs its ability to dephosphorylate the insulin receptor. Mol Endocrinol. 2001;15(10):1768-80.
185. Cura AJ, Carruthers A. Role of monosaccharide transport proteins in carbohydrate assimilation, distribution, metabolism, and homeostasis. Compr Physiol. 2012;2(2):863-914.
186. Amin A, Tuenter E, Foubert K, Iqbal J, Cos P, Maes L, Exarchou V, Apers S, Pieters L. In Vitro and In Silico Antidiabetic and Antimicrobial Evaluation of Constituents from *Kickxia ramosissima* (*Nanorrhinum ramosissimum*). Front Pharmacol. 2017;8:232.
187. Laville M, Auboeuf D, Khalfallah Y, Vega N, Riou JP, Vidal H. Acute regulation by insulin

of phosphatidylinositol-3-kinase, Rad, Glut 4, and lipoprotein lipase mRNA levels in human muscle. J Clin Invest. 1996;98(1):43-9.

188. Tabatabaie T, Vasquez-Weldon A, Moore DR, Kotake Y. Free Radicals and the Pathogenesis of Type 1 Diabetes. Diabetes. 2003;52(8):1994-1999.
189. Cnop M, Welsh N, Jonas JC, Jörns A, Lenzen S, Eizirik DL. Mechanisms of pancreatic beta-cell death in type 1 and type 2 diabetes: many differences, few similarities. Diabetes. 2005;54(Suppl 2):S97-107.
190. Fu YY, Kang KJ, Ahn JM, Kim HR, Na KY, Chae DW, Kim S, Chin HJ. Hyperbilirubinemia reduces the streptozotocin-induced pancreatic damage through attenuating the oxidative stress in the Gunn rat. Tohoku J Exp Med. 2010;222(4):265-73.
191. Fornaini G, Dachà M, Stocchi V, Canestrari F, Serafini G, Chiarantini L, Magnani M. Role of hexokinase in the regulation of glucose metabolism in human erythrocytes. Ital J Biochem. 1986;35(5):316-20.
192. Mariappan MM, Prasad S, D'Silva K, Cedillo E, Sataranatarajan K, Barnes JL, Choudhury GG, Kasinath BS. Activation of glycogen synthase kinase 3β ameliorates diabetes-induced kidney injury. J Biol Chem. 2014;289(51):35363-75.
193. Lukens FD. Insulin and protein metabolism. Diabetes. 1964;13(5):451-61.
194. Almdal TP. Importance of glucagon for nitrogen loss in diabetes--via an accelerated hepatic conversion of amino nitrogen to urea nitrogen. Dan Med Bull. 1991;38(2):113-20. PMID: 2060319.
195. Dimitriadis G, Mitrou P, Lambadiari V, Maratou E, Raptis SA. Insulin effects in muscle and adipose tissue. Diabetes Res Clin Pract. 2011;93(S1):S52-9.
196. Bouskila M, Hirshman MF, Jensen J, Goodyear LJ, Sakamoto K. Insulin promotes glycogen

synthesis in the absence of GSK3 phosphorylation in skeletal muscle. Am J Physiol Endocrinol Metab. 2008;294(1):E28-35.

197. Caton PW, Nayuni NK, Khan NQ, Wood EG, Corder R. Fructose induces gluconeogenesis and lipogenesis through a SIRT1-dependent mechanism. J Endocrinol. 2011;208(3):273-83.
198. Wallace TM, Levy JC, Matthews DR. Use and abuse of HOMA modeling. Diabetes Care. 2004;27(6):1487-95.
199. Reaven GM. What do we learn from measurements of HOMA-IR? Diabetologia. 2013;56(8):1867-8.
200. Ginsberg HN, Zhang YL, Hernandez-Ono A. Regulation of plasma triglycerides in insulin resistance and diabetes. Arch Med Res. 2005;36(3):232-40.
201. Hurrle S, Hsu WH. The etiology of oxidative stress in insulin resistance. Biomed J. 2017;40(5):257-262.
202. Klok MD, Jakobsdottir S, Drent ML. The role of leptin and ghrelin in the regulation of food intake and body weight in humans: a review. Obes Rev. 2007;8(1):21-34.
203. Gruzdeva O, Borodkina D, Uchasova E, Dyleva Y, Barbarash O. Leptin resistance: underlying mechanisms and diagnosis. Diabetes Metab Syndr Obes. 2019;12:191-198.
204. D'souza AM, Neumann UH, Glavas MM, Kieffer TJ. The glucoregulatory actions of leptin. Mol Metab. 2017;6(9):1052-1065.
205. Burchell A, Hume R. The glucose-6-phosphatase system in human development. Histol Histopathol. 1995;10(4):979-93
206. Hers HG. The control of glycolysis and gluconeogenesis by protein phosphorylation. Philos Trans R Soc Lond B Biol Sci. 1983;302(1108):27-32.
207. Pessler D, Rudich A, Bashan N. Oxidative stress impairs nuclear proteins binding to the

insulin responsive element in the GLUT4 promoter. Diabetologia. 2001;44(12):2156-64.

208. Hamberg O, Vilstrup H. Effects of insulin and glucose on urea synthesis in normal man, independent of pancreatic hormone secretion. J Hepatol. 1994;21(3):381-7.
209. da Silva RP, Nissim I, Brosnan ME, Brosnan JT. Creatine synthesis: hepatic metabolism of guanidinoacetate and creatine in the rat *in vitro* and *in vivo*. Am J Physiol Endocrinol Metab. 2009;296(2):E256-61.
210. Utzschneider KM, Kahn SE. The role of insulin resistance in nonalcoholic fatty liver disease. J. Clin. Endocrinol. Metab. 2006;91(12):4753-61.
211. Jegatheesan P, De Bandt JP. Fructose and NAFLD: The Multifaceted Aspects of Fructose Metabolism. Nutrients. 2017;9(3):230.
212. Dharmalingam M, Yamasandhi PG. Nonalcoholic Fatty Liver Disease and Type 2 Diabetes Mellitus. Indian J Endocrinol Metab. 2018;22(3):421-428.
213. Marušić M, Paić M, Knobloch M, Liberati Pršo AM. NAFLD, Insulin Resistance, and Diabetes Mellitus Type 2. Can J Gastroenterol Hepatol. 2021;2021:6613827.

ANNEXURE

- ***Certificate of plants authentication***

  ***Ficus benghalensis* L. (Moraceae)** and ***Duranta repens* L. (Verbenaceae)** were authenticated at Indian Council of Medical Research-National Institute of Traditional Medicine (ICMR-NITM) Belagavi-590010, India; Herbarium was deposited for both plants for future reference; **RMRC-1405** (*Ficus benghalensis*) and **RMRC-1406** (*Duranta repens*).

राष्ट्रीय पारम्परिक चिकित्साविज्ञान संस्थान
ICMR-NATIONAL INSTITUTE OF TRADITIONAL MEDICINE
(भूतपूर्व क्षेत्रीय आयुर्विज्ञान अनुसंधान केन्द्र Formerly Regional Medical Research Centre)
Nehru Nagar, Belagavi-590 090

Dr. Harsha Hegde
Scientist-D
harshah@icmr.gov.in

भारतीय आयुर्विज्ञान अनुसंधान परिषद
INDIAN COUNCIL OF MEDICAL RESEARCH
स्वास्थ्य अनुसंधान विभाग, स्वास्थ्य और परिवार कल्याण मंत्रालय, भारत सरकार
Department of Health Research,
Ministry of Health & Family Welfare, Govt. of India

Date: 30-01-2019

AUTHENTICATION

This is to authenticate that the plants submitted by Mr. Pukar Khanal, Research Scholar, KLE's College of Pharmacy, KAHER, Belagavi are identified as ***Ficus benghalensis* L. (Moraceae)** and ***Duranta repens* L. (Verbenaceae)**. The voucher specimens of the same have been deposited in our herbaria with accession numbers RMRC-1405 and 1406 respectively.

Harsha Hegde
Scientist 'D'

डॉ. हर्ष वी. हेगडे वैज्ञानिक-डी
Dr. HARSHA V. HEGDE Scientist - 'D'
आयुर्वेदाचार्य-राष्ट्रीय पारम्परिक चिकित्साविज्ञान संस्थान
ICMR-NATIONAL INSTITUTE OF TRADITIONAL MEDICINE
नेहरु नगर, बेलगावी - ५९००१० कर्नाटक
Nehru Nagar, Belagavi 590010, Karnataka

- ***Ethical approval for animal studies***

  This animal study performed in the present study was performed after receiving the ethical clearance from Institutional Animal Ethics Committee (IAEC) of KLE College of Pharmacy Belagavi; resolution number KLECOP/CPCSEA, Reg. No. 221/Po/Re/S/ 2000/ CPCSEA,Res.28-12/10/2019.

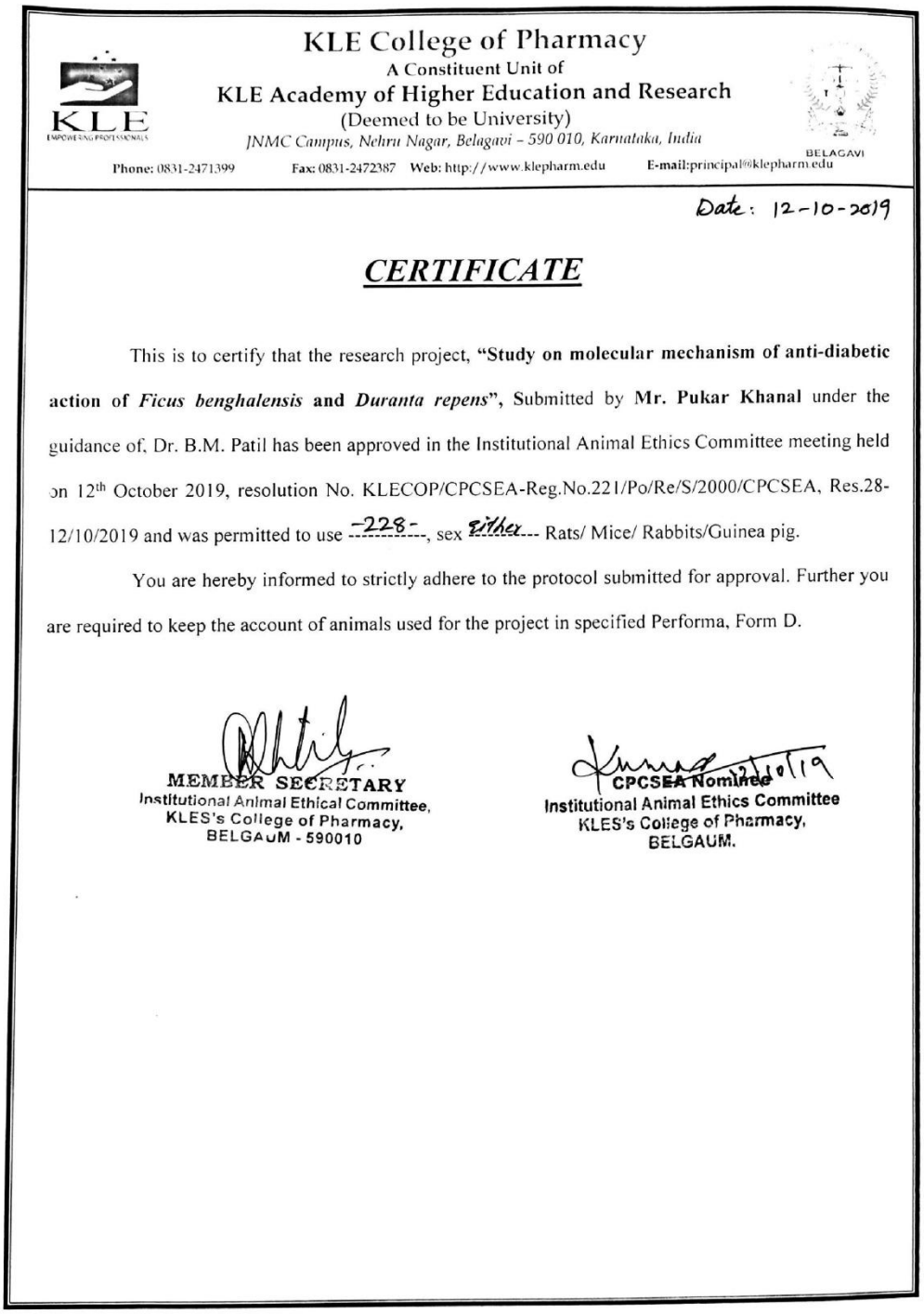

KLE College of Pharmacy
A Constituent Unit of
KLE Academy of Higher Education and Research
(Deemed to be University)
JNMC Campus, Nehru Nagar, Belagavi - 590 010, Karnataka, India
Phone: 0831-2471399 Fax: 0831-2472387 Web: http://www.klepharm.edu E-mail:principal@klepharm.edu

Date: 12-10-2019

CERTIFICATE

This is to certify that the research project, **"Study on molecular mechanism of anti-diabetic action of *Ficus benghalensis* and *Duranta repens*"**, Submitted by **Mr. Pukar Khanal** under the guidance of, Dr. B.M. Patil has been approved in the Institutional Animal Ethics Committee meeting held on 12th October 2019, resolution No. KLECOP/CPCSEA-Reg.No.221/Po/Re/S/2000/CPCSEA, Res.28-12/10/2019 and was permitted to use -228-, sex Either Rats/ Mice/ Rabbits/Guinea pig.

You are hereby informed to strictly adhere to the protocol submitted for approval. Further you are required to keep the account of animals used for the project in specified Performa, Form D.

MEMBER SECRETARY
Institutional Animal Ethical Committee,
KLES's College of Pharmacy,
BELGAUM - 590010

CPCSEA Nominee
Institutional Animal Ethics Committee
KLES's College of Pharmacy,
BELGAUM.

- ***List of publications***

1. **Khanal P**, **Patil BM**. Reversal of insulin resistance by *Ficus benghalensis* bark in fructose-induced insulin-resistant rats. ***J Ethnopharmacol.*** 2022;284:114761. **Impact factor: 4.3**, **Cite score: 6.0**
2. **Khanal P**, **Patil BM**. Integration of network and experimental pharmacology to decipher the antidiabetic action of *Duranta repens* L. ***J Integr Med.*** 2021;19(1):66-77. **Impact factor: 3.03**, **Cite score: 4.7**
3. **Khanal P**, **Patil BM**. Gene ontology enrichment analysis of α-amylase inhibitors from *Duranta repens* in diabetes mellitus. ***J Diabetes Metab Disord***. 2020;19(2):735-747. **Cite score: 2.1**
4. **Khanal P**, **Patil BM**. Consolidation of network and experimental pharmacology to divulge the antidiabetic action of *Ficus benghalensis* L. bark. ***3 Biotech***. 2021;11(5):238. **Impact factor: 2.40**, **Cite score: 3.5**
5. **Khanal P**, **Patil BM.** Integration of *in silico, in vitro* and *ex vivo* pharmacology to decode the anti-diabetic action of *Ficus benghalensis* L. bark. ***J Diabetes Metab Disord.*** 2020;19(2):1325-1337. **Cite score: 2.1**
6. **Khanal P**, **Patil BM**. Gene set enrichment analysis of alpha-glucosidase inhibitors from *Ficus benghalensis*. ***Asian Pac J Trop Biomed.*** 2019;9:263-70. **Impact factor: 1.54**, **Cite score: 4.8**
7. **Khanal P**, **Patil BM.** α-Glucosidase inhibitors from *Duranta repens* modulate p53 signaling pathway in diabetes mellitus. ***Adv Tradit Med.*** 2020;20:427–438. **Cite score: 1.8**
8. **Khanal P**, **Patil BM**. *In vitro* and *in silico* anti-oxidant, cytotoxicity and biological activities of *Ficus benghalensis* and *Duranta repens*. ***Chin. Herb. Med.*** 2020;12(4):406-413. **Cite score: 0.1**.

(*Front page of articles are attached*)

Note: The above mentioned impact factor and cite score of the journal are based on the Web of Science and Scopus data respectively are during the year of thesis submission (2022).

- ***List of presentations***

1. **Pukar Khanal**, **BM Patil**. *In silico* and *in vitro* α-amylase and α-glucosidase inhibitory activities of hydroalcoholic extract and fractions of *Ficus benghalensis* (bark). International Conference on "**Emerging Trends in Delivery of Phytoconstituents and Ethnopharmacology-Validation of Traditional Medicine-II**" Organized by Poona College of Pharmacy Bharati Vidyapeeth (Deemed to be University), Pune, India in association with All India Council for Technical Education (AICTE) and Society for Ethinopharmacology India-Pune Chapter.
2. **Pukar Khanal**, **BM Patil**. Network and experimental pharmacology of *Ficus benghalensis* L in diabetes mellitus organized by School of Pharmaceutical Technology, Adamas University held during 5^{th} -6^{th} April, 2021 in Oral presentation category in the 1st International e-conference on "**Changing Waves in Healthcare Research: Focus on Post-Covid Era**"

(*Certificates are attached*)

ERRATUM